

# **For Reference**

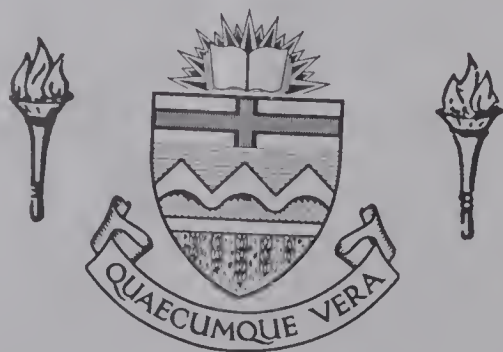
---

**NOT TO BE TAKEN FROM THIS ROOM**

# For Reference

NOT TO BE TAKEN FROM THIS ROOM

## Ex LIBRIS UNIVERSITATIS ALBERTAENSIS













THE UNIVERSITY OF ALBERTA

A STUDY OF BED-MATERIAL TRANSPORT BASED ON THE  
ANALYSIS OF FLUME EXPERIMENTS

BY



RICHARD HAMILTON COOPER

A THESIS

SUBMITTED TO THE FACULTY OF GRADUATE STUDIES  
IN PARTIAL FULFILMENT OF THE REQUIREMENTS FOR THE DEGREE OF  
DOCTOR OF PHILOSOPHY

DEPARTMENT OF CIVIL ENGINEERING

EDMONTON, ALBERTA

SPRING, 1970



Thesis  
1970  
10D

UNIVERSITY OF ALBERTA  
FACULTY OF GRADUATE STUDIES

The undersigned certify that they have read, and recommend to the Faculty of Graduate Studies for acceptance, a thesis entitled, A STUDY OF BED-MATERIAL TRANSPORT BASED ON THE ANALYSIS OF FLUME EXPERIMENTS, submitted by Richard Hamilton Cooper in partial fulfilment of the requirements for the degree of Doctor of Philosophy.



## ABSTRACT

The behavior of flow in alluvial channels was studied by analyzing the majority of the available experimental flume data. This analysis resulted in two graphical relationships that can be used for predicting flow variables. In the first of these relationships, a densimetric form of the Froude number was related to the concentration of bed-material discharge and the ratio between average depth of flow and median diameter of the bed-material particles; slope replaced the densimetric Froude number in the second relationship. These two sets of parameters were also used in criteria that were developed for predicting the type of bed-form that develops for given flow conditions.

The above relationships were based on the results of experiments on bed-materials having natural specific gravities approximately equal to 2.65. To account for variation in specific gravity, coefficients were developed to adjust the parameters contained in the relationships. These coefficients were based on the analysis of data in which the specific gravity varied from 1.05 to 4.22.

Finally, results describing the scope of available experimental conditions were presented. These results determine the range of application of the above relationships and provide a basis for determining future experimental requirements.





## ACKNOWLEDGEMENTS

The author is indebted to his supervisor, Professor A.W. Peterson, for his suggestions and guidance provided throughout the course of the work.

In the initial stages Dr. T. Blench and Dr. M.S. Yalin provided numerous research suggestions which were instrumental in developing the framework of the study.

Finally the author wishes to express his appreciation for financial assistance received from the National Research Council.



## TABLE OF CONTENTS

CHAPTER	PAGE
Title Page	i
Approval Sheet	ii
Abstract	iii
Acknowledgements	iv
Table of Contents	v
List of Tables	viii
List of Figures	ix
I. INTRODUCTION	1
Flow in Alluvial Channels	1
Classification of Existing Knowledge	3
Purpose and Scope	6
II. INFORMATION REVIEW	9
General	9
The Role of Bed-Forms in Alluvial Channels	10
The Resistance to Flow in Alluvial Channels	18
Sediment Transport	26
The Beginning of Bed-Material Movement	30
Review of Bed-Material Transport Theories	32
III. THE MATHEMATICAL MODEL	39
Dimensional Analysis	39
The Role of the Alluvial Bed-Material	41
The Laboratory Flume Problem	44
Modification of the Mathematic Model for Canals and Natural Channels	49



CHAPTER	PAGE
IV. SUMMARY OF AVAILABLE EXPERIMENTAL DATA	51
General	51
Types of Data	52
Laboratory Flume Data	55
Properties of the Experimental Bed-	
Materials	56
Experimental Equipment	60
Experimental Procedure	68
V. THE SCOPE OF EXPERIMENTAL CONDITIONS	78
Requirements for Empirical Analysis	78
Variables	80
Range and Distribution of Parameters	81
The Joint Distribution and Experimental	
Correlation Between Parameters	85
VI. PRESENTATION AND DISCUSSION OF RESULTS	90
General	90
Method of Analysis	91
The Relationship Between $Fr'$ , $C_{th}$ , and	
$h/D_{50}$	93
The Relationship Between $S$ , $C_{th}$ and $h/D_{50}$	130
VII. SUMMARY, CONCLUSIONS AND RECOMMENDATIONS	157
Summary and Conclusions	157
Recommendations	161
LIST OF REFERENCES	163



CHAPTER	PAGE
APPENDIX A: Summary of Computer Programs	
used in the Analysis	A1
APPENDIX B: Scope of Experimental	
Conditions for Individual Bed-	
Materials and Data Collections	B1
APPENDIX C: Joint Distribution Between	
Experimental Values of Pairs of	
the Parameters in the	
Mathematical Model	C1
APPENDIX D: Scatter Diagrams	D1







## LIST OF TABLES

TABLE	PAGE
4-1 Characteristics of the Different Types of Alluvial Channel Data	53
4-2 General Summary of Experimental Studies on Sediment Transport	57
4-3 Summary of the Experimental Bed-Material Properties	61
4-4 Summary of Experimental Equipment	69
4-5 Summary of the Experimental Operating Procedures	74
5-1 Distribution of Experimental Values of Observed and Computed Quantities for Existing Flume Experiments	82
5-2 Experimental Correlation and Joint Distribution Between Experimental Values of Pairs of Parameters	86
B-1 Distribution of Experimental Values of Observed and Computed Parameters for Individual Bed-Materials and Data Collections	B2
B-2 Distribution of Experimental Values of Computed Parameters for Individual Bed- Materials and Data Collections	B12



## LIST OF FIGURES

FIGURE	PAGE
1-1    Classification of Bed-Forms	2
2-1    The Liu Criteria for the Predication of Bed-Forms	16
2-2    The Simons and Richardson Criteria for the Prediction of Bed-Forms	17
2-3    The Einstein and Barbarossa Relationship for the Prediction of the Form Roughness Coefficient	21
2-4    The Graphical Relationship of Alam, Cheyer, and Kennedy (1966) for Predicting Friction due to Form Roughness	25
2-5    Variation of the Friction Factor with Reynolds Number ( $VR/\nu$ ) and Relative Particle Roughness ( $R/D_{50}$ ) for a Plane Alluvial Bed	27
2-6    Shields Relation for the Beginning of Bed- Material Movement	31
2-7    The Einstein $\phi$ - $\psi$ Relationship	36
5-1 $Z=f(M,N)$ for a Hypothetical Natural Phenomenon	79
5-2 $Z=f(M,N)$ for Experimental Conditions	79
6-1    Variation of $C_{tb}$ with $Fr'$ at Different Levels of $h/D_{50}$	94
6-2    Variation of $C_{tb}$ with $h/D_{50}$ at Different Levels of $Fr'$	96



FIGURE	PAGE
6-3 Variation of $h/D_{50}$ with $Fr'$ at Different Levels of $C_{tb}$	98
6-4 Variation of $C_{tb}$ with $Fr'$ and $Vi$ at Different Levels of $h/D_{50}$	102
6-5 Variation of $C_{tb}$ with $Fr'$ and $b/h$ at Different Levels of $h/D_{50}$	104
6-6 Relationship Between $b/h$ and the Ratio of Unit Discharge at Mid-Channel Computed from a Velocity Profile to $Q/b$ - Colorado State University Experiments	106
6-7 Variation of $C_{tb}$ with $Fr'$ and $\sigma_b$ at Different Levels of $h/D_{50}$	108
6-8 Location of Bed-Form Regions on the $Fr' - C_{tb}$ Plane	112
6-9 Location of Bed-Form Regions on the $h/D_{50} - C_{tb}$ Plane	114
6-10 Location of Bed-Form Regions on the $Fr' - h/D_{50}$ Plane	116
6-11 Relationship Between $Fr'$ , $C_{tb}$ , and $h/D_{50}$ on the $Fr' - C_{tb}$ Plane	120
6-12 Relationship Between $Fr'$ , $C_{tb}$ , and $h/D_{50}$ on the $h/D_{50} - C_{tb}$ Plane	121
6-13 Relationship Between $Fr'$ , $C_{tb}$ , and $h/D_{50}$ on the $Fr' - h/D_{50}$ Plane	122
6-14 Perspective View of the Solution Surface for the $Fr' - C_{tb} - h/D_{50}$ Relationship	123





FIGURE	PAGE
6-15 Variation of $2.65C_{tb}(\rho_f/\rho_b)$ with $Fr'$ and $h/D_{50}$ for Experimental Data on Heavy and Light Weight Bed-Materials	125
6-16 Comparison of the Relationship Between $Fr'$ , $C_{tb}$ , and $h/D_{50}$ with Natural Channel Observations	128
6-17 Variation of $C_{tb}$ with $S$ at Different Levels of $h/D_{50}$	131
6-18 Variation of $C_{tb}$ with $h/D_{50}$ at Different Levels of $S$	133
6-19 Variation of $h/D_{50}$ with $S$ at Different Levels of $C_{tb}$	135
6-20 Variation of $C_{tb}$ with $S$ and $Vi$ at Different Levels of $h/D_{50}$	138
6-21 Variation of $C_{tb}$ with $S$ and $b/h$ at Different Levels of $h/D_{50}$	140
6-22 Variation of $C_{tb}$ with $S$ and $\sigma_b$ at Different Levels of $h/D_{50}$	141
6-23 Location of Bed-Form Regions on the $S - C_{tb}$ Plane	142
6-24 Location of Bed-Form Regions on the $S - h/D_{50}$ Plane	144
6-25 Relationship Between $S$ , $C_{tb}$ , and $h/D_{50}$ on the $S - C_{tb}$ Plane	147
6-26 Relationship Between $S$ , $C_{tb}$ , and $h/D_{50}$ on the $h/D_{50} - C_{tb}$ Plane	148





FIGURE	PAGE
6-27 Relationship Between $S$ , $C_{tb}$ , and $h/D_{50}$ on the $S - h/D_{50}$ Plane	149
6-28 Perspective View of the Solution Surface for the $S - C_{tb} - h/D_{50}$ Relationship	150
6-29 Variation of $2.65 C_{tb} (\rho_f/\rho_b)$ with $1.65S/(\rho_b/\rho_f - 1)$ and $h/D_{50}$ for Experimental Data on Light and Heavy Weight Bed-Materials	151
6-30 The $Fr' - C_{tb} - h/D_{50}$ Relationship Compared with Regime Theory and Beginning of Movement Criteria	154
6-31 The $S - C_{tb} - h/D_{50}$ Relationship Compared with Regime Theory and Beginning of Move- ment Criteria	155
C-1 Joint Distribution Between Experimental Values of $Fr'$ and $S$	C2
C-2 Joint Distribution Between Experimental Values of $Fr'$ and $h/D_{50}$	C2
C-3 Joint Distribution Between Experimental Values of $Fr'$ and $C_{tb}$	C3
C-4 Joint Distribution Between Experimental Values of $Fr'$ and $b/h$	C4
C-5 Joint Distribution Between Experimental Values of $Fr'$ and $V_i$	C4
C-6 Joint Distribution Between Experimental Values of $S$ and $C_{tb}$	C5



FIGURE	PAGE
C-7 Joint Distribution Between Experimental Values of $S$ and $h/D_{50}$	C6
C-8 Joint Distribution Between Experimental Values of $S$ and $b/h$	C6
C-9 Joint Distribution Between Experimental Values of $S$ and $V_i$	C7
C-10 Joint Distribution Between Experimental Values of $h/D_{50}$ and $b/h$	C7
C-11 Joint Distribution Between Experimental Values of $h/D_{50}$ and $V_i$	C8
C-12 Joint Distribution Between Experimental Values of $V_i$ and $b/h$	C8
C-13 Joint Distribution Between Experimental Values of $V_i$ and $C_{tb}$	C9
C-14 Joint Distribution Between Experimental Values of $C_{tb}$ and $h/D_{50}$	C10
C-15 Joint Distribution Between Experimental Values of $C_{tb}$ and $b/h$	C11
D-1 Variation of $C_{tb}$ with $Fr'$ at Different Levels of $h/D_{50}$	D2
D-2 Variation of $C_{tb}$ with $h/D_{50}$ at Different Levels of $Fr'$	D4
D-3 Variation of $h/D_{50}$ with $Fr'$ at Different Levels of $C_{tb}$	D8



FIGURE	PAGE
D-4 Variation of $C_{tb}$ with $S$ at Different Levels of $h/D_{50}$	D11
D-5 Variation of $C_{tb}$ with $h/D_{50}$ at Different Levels of $S$	D14
D-6 Variation of $h/D_{50}$ with $S$ at Different Levels of $C_{tb}$	D17





## SYMBOLS

$A_1, A_2$	Terms used to represent sets of parameters.
$b$	Channel breadth (ft).
$C_{tb}$	Concentration of bed-material discharge by weight of total discharge (parts per hundred thousand, ppht).
$C_s$	Concentration of suspended fine sediment by weight of total discharge (ppht).
$\bar{C}/\sqrt{g}$	The dimensionless Chezy discharge coefficient.
$\bar{C}'/\sqrt{g}$	The dimensionless Chezy discharge coefficient for an equivalent plane bed flow.
$d$	The characteristic length for a particular flow (ft).
$D$	Particle size of a uniform sized granular material (mm or ft).
$D_i$	The particle size corresponding to the $i^{th}$ percentile on the particle size distribution curve for a bed-material (mm or ft).
$D_m$	The mean particle size (ft or mm).
$E$	A correction coefficient in the logarithmic formula for mean velocity used by Einstein and Barbarossa (1952).
$f, f', f''$	The Darcy-Wiesbach resistance coefficients for the total flow, the equivalent plane bed flow and the form roughness respectively.
$Fr'$	A densimetric form of Froude Number $Fr' = (\rho_f/\gamma_b')V^2/h$
$g$	Acceleration of gravity (ft/sec <sup>2</sup> )





$G_{tb}$	Rate of transport of bed-material (lb/sec).
$G'_{tb}$	Rate of transport of bed-material per unit breadth (lb/sec/ft).
$h$	Average depth of flow (ft).
$K_s$	Roughness height of the boundary (ft).
$K_1, K_2$ $K_b, K_b'$	Constants in various equations. Coefficients in the Meyer-Peter formula for bed-load transport.
$q_{tb}$	Volumetric rate of transport of bed-material per unit breadth (ft <sup>2</sup> /sec).
$Q$	Discharge of water sediment mixture (ft <sup>3</sup> /sec).
$R, R', R''$	Hydraulic radius corresponding to the total flow, the equivalent plane bed flow, and the form roughness respectively (ft).
$S$	Slope of the energy-grade line equal to the slope of the water surface or the bed for an equilibrium flow.
$V$	Average velocity based on the continuity principle (ft/sec).
$V_m$	Average velocity based on integration of a measured vertical velocity profile.
$V_*$	Shear velocity $V_* = \sqrt{\tau_o/\rho_f} = \sqrt{gdS}$ (ft/sec).
$Vi$	Dimensionless parameter $Vi = \sqrt[3]{vg} D_{50}/\nu$ .
$\alpha_b$	Dimensionless measure or set of measures describing the shape of bed material particles.
$\gamma'_b$	The buoyant unit weight of the bed material (lb/ft <sup>3</sup> ) $\gamma'_b = g(\rho_b - \rho_f)$ .



- $\epsilon_s$  Roughness height of the flume sides (ft).
- $\mu$  Dynamic viscosity of water sediment mixture (lb sec/ft<sup>2</sup>).
- $\nu$  Kinematic viscosity of water sediment mixture (ft<sup>2</sup>/sec).
- $\phi$  Parameter in the Einstein bed-load function
- $$\phi = \frac{G'_{tb}}{\rho_b g} \left( \frac{\rho_b - \rho_f}{\rho_b - \rho_f} \frac{1}{g D^3} \right)^{1/2}$$
- $\rho_b$  Mass density of bed material particles (slugs/ft<sup>3</sup>).
- $\rho_f$  Mass density of the fluid (slugs/ft<sup>3</sup>).
- $\sigma_b$  Gradation of the bed-material
- $$\sigma_b = 0.5(D_{84}/D_{50} + D_{50}/D_{16})$$
- $\tau_o$  Shear stress acting on the bed (lb/ft<sup>2</sup>).
- $\tau_c$  Critical shear stress acting on the bed for the beginning of movement of bed-material (lb/ft<sup>2</sup>).
- $\psi$  Parameter in the Einstein bed-load function
- $$\psi = \frac{\rho_b - \rho_f}{\rho_f} \frac{D}{R^* S}$$
- $\omega$  Fall velocity of bed-material particles (ft/sec).



## CHAPTER I

### INTRODUCTION

#### 1-1 Flow in Alluvial Channels

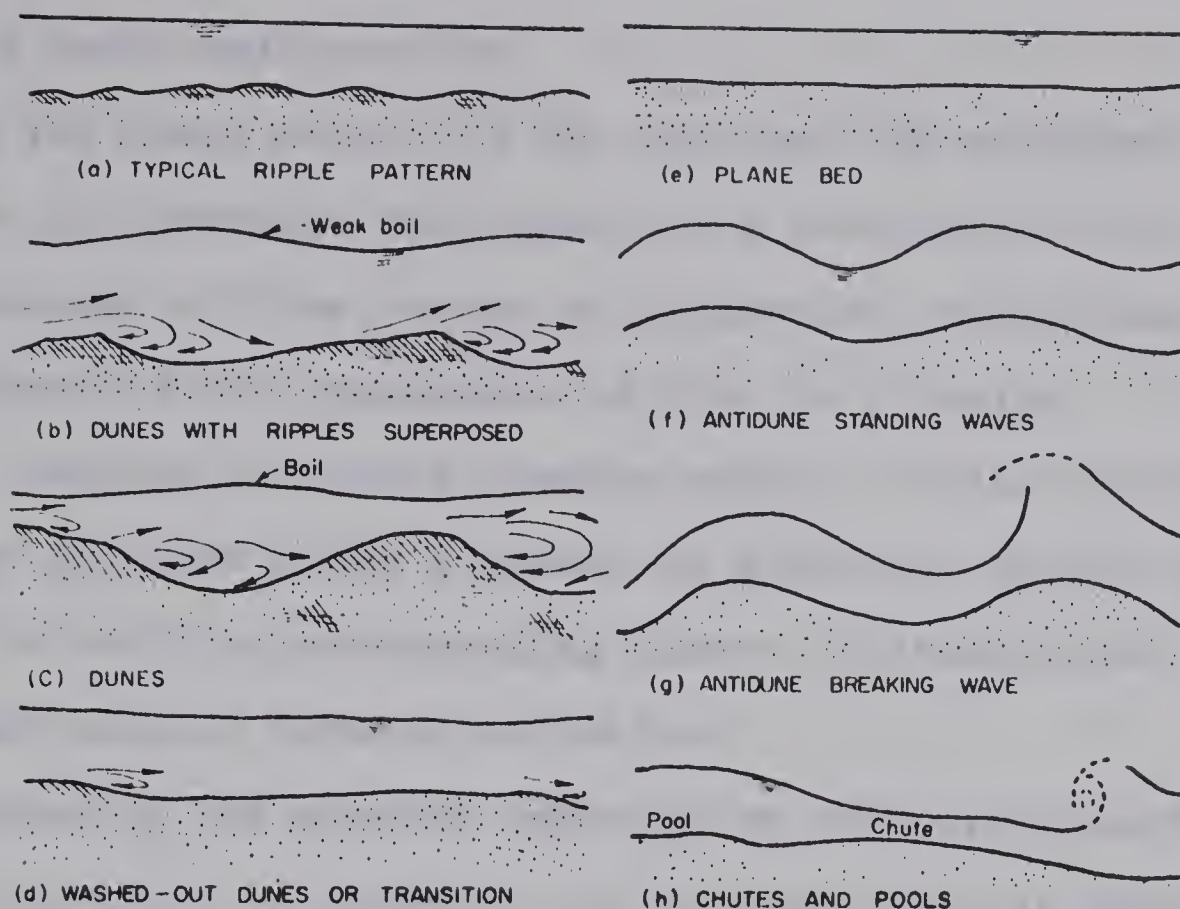
The majority of natural rivers and streams as well as many man made canals have mobile beds consisting of non-cohesive granular materials that are capable of being eroded, transported, and deposited by the flow. In the present study channels of this type are referred to as alluvial channels. By means of the above mechanisms, the geometry of an alluvial channel bed can be altered by the flow and tends to adjust to a configuration that is in equilibrium with the flow. A channel that has attained such a state of equilibrium is often referred to as a regime or stable channel.

Flow in an alluvial channel is a two phase motion consisting of the combined movement of water and bed-material. In this two phase motion, individual bed-material particles are transported either by rolling or sliding along the bed, by making intermittent hops through the fluid, or by being transported in suspension by the fluid.

Observations both in natural channels and in laboratory flumes have shown the bed of an alluvial channel to be capable of developing into a distinct pattern of bed-forms. A number of different bed-form configurations are possible; these are illustrated in Figure 1-1 along with the type of flow that







Flow regime	Bed form	Bed Material concentrations (ppm)	Mode of sediment transport	Type of roughness	Phase relation between bed and water surface
Lower regime	Ripples	10-200	Discrete steps	Form roughness predominates	Out of phase
	Ripples on dunes	100-1,200			
	Dunes	200-2,000			
Transition	Washed out dunes	1,000-3,000		Variable	
Upper regime	Plane beds	2,000-6,000	Continuous	Grain roughness predominates	In phase
	Antidunes	2,000→			
	Chutes and pools	2,000→			

Figure 1-1. Classification of Bed-Forms (Simons and Richardson, 1963)





occurs with each configuration.

The two phase nature of the flow and the existence of a number of different bed-forms, each associated with a different type of flow, serve to illustrate the extremely complex nature of the phenomenon of flow in alluvial channels. Arising from this complex nature, is the distinct possibility of there being a number of different phases of flow behavior with a corresponding number of transitions in the relationships between variables.

Because of the present emphasis on the development of water resources, it is essential to develop reliable theories for the solution of problems such as the prediction of consequences resulting from channel modification, the design of stable alluvial channels, and the prediction of the future behavior of existing natural alluvial channels. Although a large number of theories now exist, there is a general lack of confidence concerning their ability to produce reliable solutions to the above type of engineering problem.

## 1-2 Classification of Existing Knowledge

Engineers and geologists have been studying the problem of flow in alluvial channels since the start of the present century (DuBoys, 1879; Gilbert, 1914). Because of the varied interests of this group of investigators, numerous different approaches have been followed in the development of theories describing the various aspects of the phenomenon. The majority



of these studies can be categorized into one of the following general classifications: (1) studies on the geomorphic aspects of flow in alluvial channels, (2) detailed studies on the dynamics of flow in alluvial channels, and (3) studies intended to determine the relationships between the variables that describe the sediment properties, the fluid properties, the channel geometry, and the characteristics of the flow.

The first type of study involves the qualitative investigation of the behavior of natural channels. The approach has been to organize and report observations in a manner that results in a qualitative description of the various physical processes and their consequences. Although some simple correlations between the more pertinent variables have been made (Leopold, Wolman, and Miller, 1964), there has been no real attempt to develop relationships suitable for making accurate design predictions. The main value of the results from this type of study has been to provide a better qualitative understanding of the behavior of flow in alluvial channels.

The second of the above classifications includes both theoretical and experimental investigations that examine in detail some narrow aspect of the flow phenomenon. A typical example would be the study of the various forces acting on a sediment particle either in motion or at rest on the boundary. The purpose of these investigations has been to gain an understanding of the physical laws governing the dynamics of the phenomenon and to develop mathematical models describing





the various processes involved. Although such knowledge is necessary to develop a complete analytical solution to the problem, the results, at present, are of somewhat limited value for solving engineering problems.

The type of study depicted in the third classification deals with such topics as sediment transport and the resistance to flow in alluvial channels and has resulted in the majority of theories now in use in engineering practice. Because of the complex nature of the phenomenon, the derivation of completely analytical theories has not been possible. Consequently, the approach has usually involved the development of a mathematical model followed by an empirical evaluation of the model to test its validity, to determine numerical coefficients, and in some cases to determine the mathematical form of the relations.

The present study has evolved from a need to improve on the reliability of the existing theories. It is not unusual to obtain predictions from two different theories that differ, to an unacceptable degree, both with each other and with the truth. Some of the more obvious causes of this lack of reliability are the following:

- (1) Flow in an alluvial channel is an extremely complex phenomenon whose detailed mechanisms are not well understood.

- (2) Many of the existing theories have been based on mathematical models that are either invalid or incomplete.



(3) These theories are often based on experimental results that cover an insufficient range of experimental conditions. Consequently, the application of such a theory may require extrapolation into a region where it is likely to be invalid.

(4) Because of the use of a limited number of experimental results and because of the failure to consider all of the relevant variables, theories often consist of relationships describing the experimental design rather than a natural physical law.

### 1-3 Purpose and Scope

The purpose of the present study has been to investigate the behavior of flow in alluvial channels through the analysis of all available experimental data. The primary objective was to extend and improve the existing knowledge concerning the relationships between variables by considering as many of the possibly relevant variables as possible and by utilizing the entire available body of experimental data. Specific objectives were: (1) to compile, for the purpose of analysis, the majority of available experimental data, (2) to determine the existing scope of experimental conditions so that future experimental requirements could be accurately determined, and (3) to determine which of the variables are relevant to the behavior of the phenomenon and the manner in which these variables affect the phenomenon.

The relationships between variables have been





investigated by evaluating a mathematical model consisting of functional equations developed through the use of dimensional analysis. Since this approach tended to minimize the number of necessary simplifying assumptions, the effects of the majority of variables likely to be relevant to the behavior of the phenomenon could be examined.

The investigation has been limited to the development of relationships that would be suitable for use in solving engineering problems related to channel design and analysis. These relationships should be capable of predicting variables such as the rate of transport of bed-material, the equilibrium slope of the channel, the depth of flow, or the mean velocity of flow. Because the empirical analysis has been based primarily on the results of laboratory flume experiments for channels with rigid and vertical sides, there has been no attempt to develop relationships capable of describing the self-adjustment of channel breadth or the development of meander patterns in channels having natural sides.

For the empirical portion of the investigation, data from experimental flumes and from natural alluvial channels have been considered. However, the results have been based mainly on the laboratory flume experiments where an attempt was made to compile and utilize all available data. A limited number of the existing natural channel data were used



primarily to test the validity of the relationships developed from the analysis of experimental flume data.

In the past there has been considerable duplication of effort in experimental studies on flow in alluvial channels. Consequently, a part of the present study has been devoted to determining the scope of conditions covered by the available experimental data. These data have been analyzed to determine the distribution of experimental values of both observed and computed variables and the joint distribution between pairs of the parameters contained in the mathematical model. The purpose of this portion of the study has been to demonstrate the required extent of future experimental requirements and to determine the range of conditions for which the relationships based on experimental results are applicable.





## CHAPTER II

### INFORMATION REVIEW

#### 2-1 General

In the study of flow in alluvial channels numerous attempts have been made to formulate the relationships that are required for the solution of engineering problems. These efforts have resulted in the development of a multitude of theories describing the various aspects of the phenomenon.

The majority of theories can be classified into one of two categories. The first of these categories covers the sediment transport theories that relate the rate of transport of bed-material to the variables describing the properties of the bed-material and the flow. These theories are also used to predict unknown flow properties in terms of known rates of transport of bed-material and known flow and bed-material properties. In the second category fall the theories describing the resistance to flow in alluvial channels. They generally give the relationship between the channel slope, the mean velocity, the depth or hydraulic radius of the flow, and the variables describing the properties of the bed-material.

In order to solve engineering problems dealing with natural alluvial channels and canals, additional relationships not included in the above two categories are required to describe the self-adjustment of channel breadth and the development and behavior of meanders. These two aspects have





been studied in regime theory (Blench, 1969a) and in numerous geomorphic investigations (see Leopold, Wolman, and Miller, 1964), and a number of simple correlations between variables have been developed from the analysis of both canal and natural alluvial channel observations.

In the present chapter the more popular theories dealing with sediment transport and resistance to flow in alluvial channels are reviewed. In the process of discussing these theories, a qualitative description of the physical behavior of the phenomenon is given and some fundamental terms are defined.

## 2-2 The Role of Bed-Forms in Alluvial Channels

The experiments of Gilbert (1914) demonstrated the flow in an alluvial channel to be capable of molding the bed into a number of different configurations whose elements are commonly referred to as bed-forms. These bed-forms tend to migrate along the bed of the channel although the direction of migration can vary between the different types as can the size and shape of the bed-forms and the type of flow that is associated with them.

The existence of several different bed-form configurations, each associated with a distinct type of flow, emphasizes the complex nature of the phenomenon and suggests the possibility that it can operate in a number of distinct phases of behavior. These phases of behavior are likely to be associated with transitions in the various relationships between variables.



A general classification of bed-forms and their associated flows that has gained recent widespread acceptance was presented by Simons and Richardson (1963) and is illustrated in Figure 1-1. This classification has a tranquil lower flow regime and a rapid upper flow regime with both encompassing several different types of bed-forms. In order of their occurrence with increasing flow intensity, these bed-forms are ripples and dunes of the lower flow regime and plane bed, antidunes, and chutes and pools of the upper flow regime.

Both ripples and dunes are triangularly shaped bed-forms with gently sloping upstream faces and with downstream faces that slope steeply at approximately the angle of repose of the submerged bed-material. Dunes are generally much larger than ripples and under some conditions can have a ripple pattern develop on their upstream faces.

Along the upstream face of both ripples and dunes bed-material particles become detached and are transported by rolling, sliding, or jumping in a series of discrete steps until they reach the crest of the bed-form. At this point the particles either roll down and become deposited on the steep downstream face of the bed-form or are carried into the zone of a separation immediately downstream of the crest. Of the particles entering the zone of separation, some may be deposited in the trough between bed-forms, some may be carried back by reverse flow and deposited on the





downstream face, and some may be carried through the zone of separation onto the upstream face of the next bed-form where they begin a new cycle of transport. The particles deposited in the trough can be transported in either direction by turbulent eddies in the zone of separation. With both ripples and dunes there is a net erosion of particles from the upstream face and a net deposit of particles on the steep downstream face which results in the migration of the bed-form in a downstream direction.

Yalin (1964) reported ripples to be essentially a small scale feature whose size depends on the particle diameter but not on the depth of flow. Dunes, on the other hand, develop to a size that appears to be independent of particle diameter but varies roughly as the depth of flow. Yalin also suggests that the transition between ripples and dunes is likely to be abrupt with an absence of stable transitional bed-forms.

The flows that are associated with ripples and dunes are usually distinguishable by the appearance of the respective water surfaces. Whereas the separation zones of the ripple configuration cause little if any disturbance on the water surface, the much larger separation zones of a dune configuration result in the appearance of surface boils slightly downstream from the crest of each dune. As would be expected of the tranquil flows associated with a dune configuration, the water surface undulations and the



bed-forms are out of phase with each other.

The plane bed configuration is distinguishable by an absence of bed surface irregularities that are larger than the maximum particle diameter of the bed-material. Again the bed-material particles are transported by rolling, sliding or hopping in a series of discrete steps along the bed. However, at the higher rates of transport the upper layer or layers of the bed appear to be in a continual state of movement that is commonly referred to as sheet flow.

There is some question whether the plane bed configuration is limited only to the upper flow regime and its corresponding high levels of bed-material transport. Liu (1957) reported a stable plane bed for values of shear between the beginning of bed-material movement and the point at which dunes begin to form. This is contrary to the findings of Simons and Richardson (1966) who reported the formation of either ripples or dunes immediately upon the start of movement of the bed-material. However, since these two results are based on independent collections of experimental data, there is a possibility of both being correct within their respective ranges of experimental conditions.

The antidune bed-form configuration consists of a series of symmetrical bed waves that appear in phase with similarly shaped waves on the water surface. These waves





have been observed by Guy, Simons and Richardson (1966) to either remain stationary or to propagate in either direction along the channel depending on the balance between erosion and deposition on the alternate faces of the bed-form. The waves tend to grow in size and subsequently subside or grow until they attain a critical state at which time they become transformed into breaking waves.

The final bed-form configuration consists of alternate chutes and pools in which the flow accelerates rapidly throughout a long steeply sloping chute; it then passes through a form of hydraulic jump that is followed by a long pool through which a tranquil but accelerating flow exists. This type of bed-form and flow is associated with extremely high values of slope and bed-material transport rates.

Between the upper and lower flow regimes it is possible to have several types of transitional bed-forms. These bed-forms often appear as washed out dunes that are generally both longer and lower than regular dunes. However, in this region the bed configuration can also oscillate between dunes and a plane bed with neither bed-form remaining stable for any length of time. Furthermore the type of bed-form that develops can depend on the flow conditions that prevailed prior to entering the transitional region.

The type of flow and bed-form that exists in an



alluvial channel undoubtedly influences to a large extent the relationships describing resistance to flow and bed-material transport. Consequently, it has been necessary to develop criteria that could be used to predict the type of bed-form that will develop for a given set of flow conditions.

Liu (1957) related the particle size Reynolds number ( $V_*D/\nu$ ) to the ratio between shear velocity and fall velocity ( $V_*/\omega$ ) for the conditions where ripples form. Simons, Richardson, and Albertson (1961) extended this criterion to cover the transitions between the different bed-forms. The results of this latter work, shown in Figure 2-1, indicate the absence of ripples for particle sizes greater than about 2.0 mm and of dunes for particle sizes in excess of about 5.0 mm. The latter of these results is contrary to numerous field observations where bed-forms that resemble dunes have been observed for particle sizes much larger than 5.0 mm.

Simons and Richardson (1963) proposed the criterion shown in Figure 2-2 by which bed-forms can be predicted in terms of the stream power ( $\tau_0 V$ ) and the median diameter of the bed-material. In this criterion ripples cannot form for bed-materials having median diameters greater than about 0.65 mm. Unfortunately, the plot is limited to a maximum median diameter of about 1.0 mm and does not resolve the question of the existence of dunes for particle sizes greater than 5.0 mm.





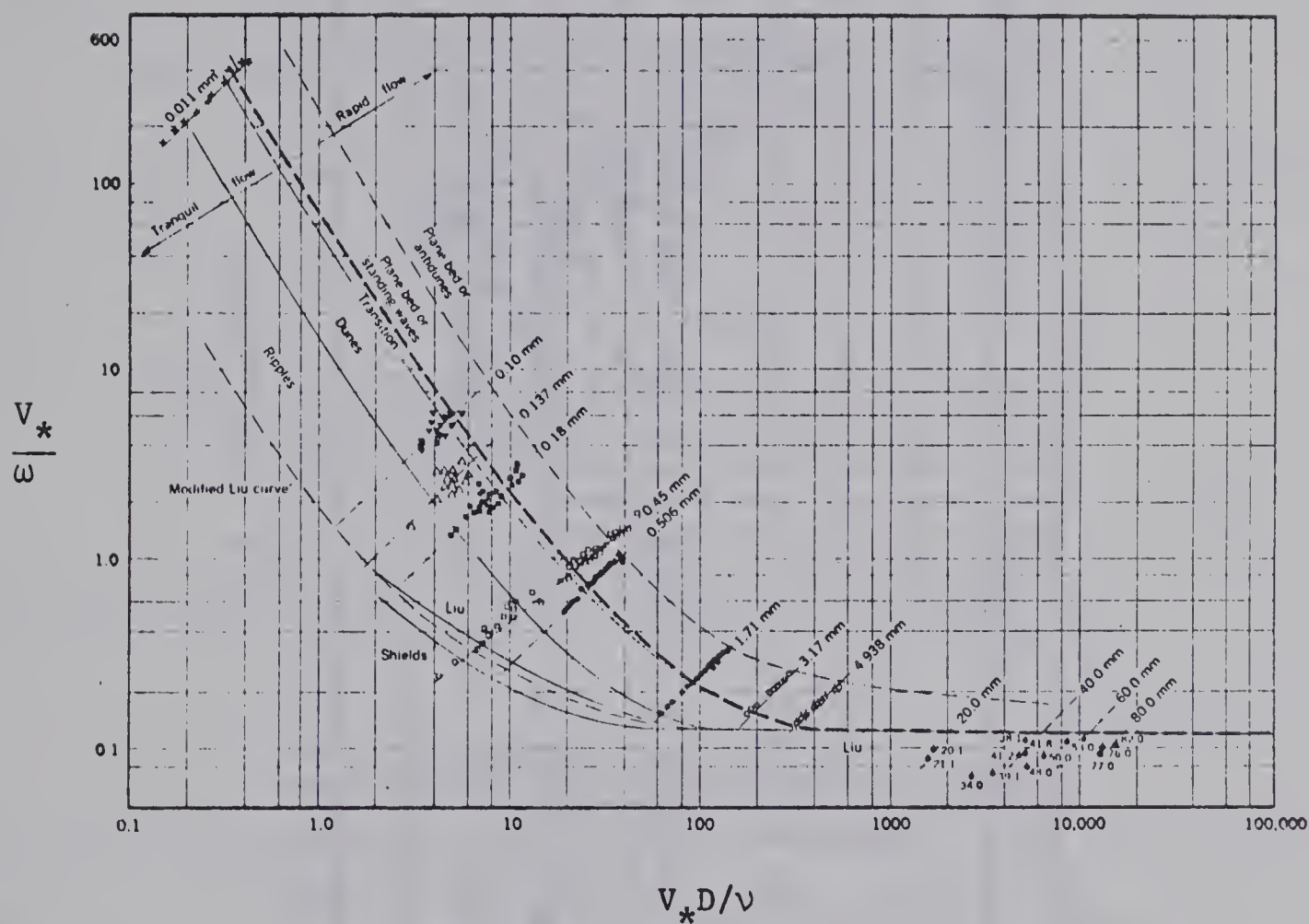


Figure 2-1. The Liu Criterion for the Prediction of Bed-Forms  
(Simons, Richardson, and Albertson, 1961)





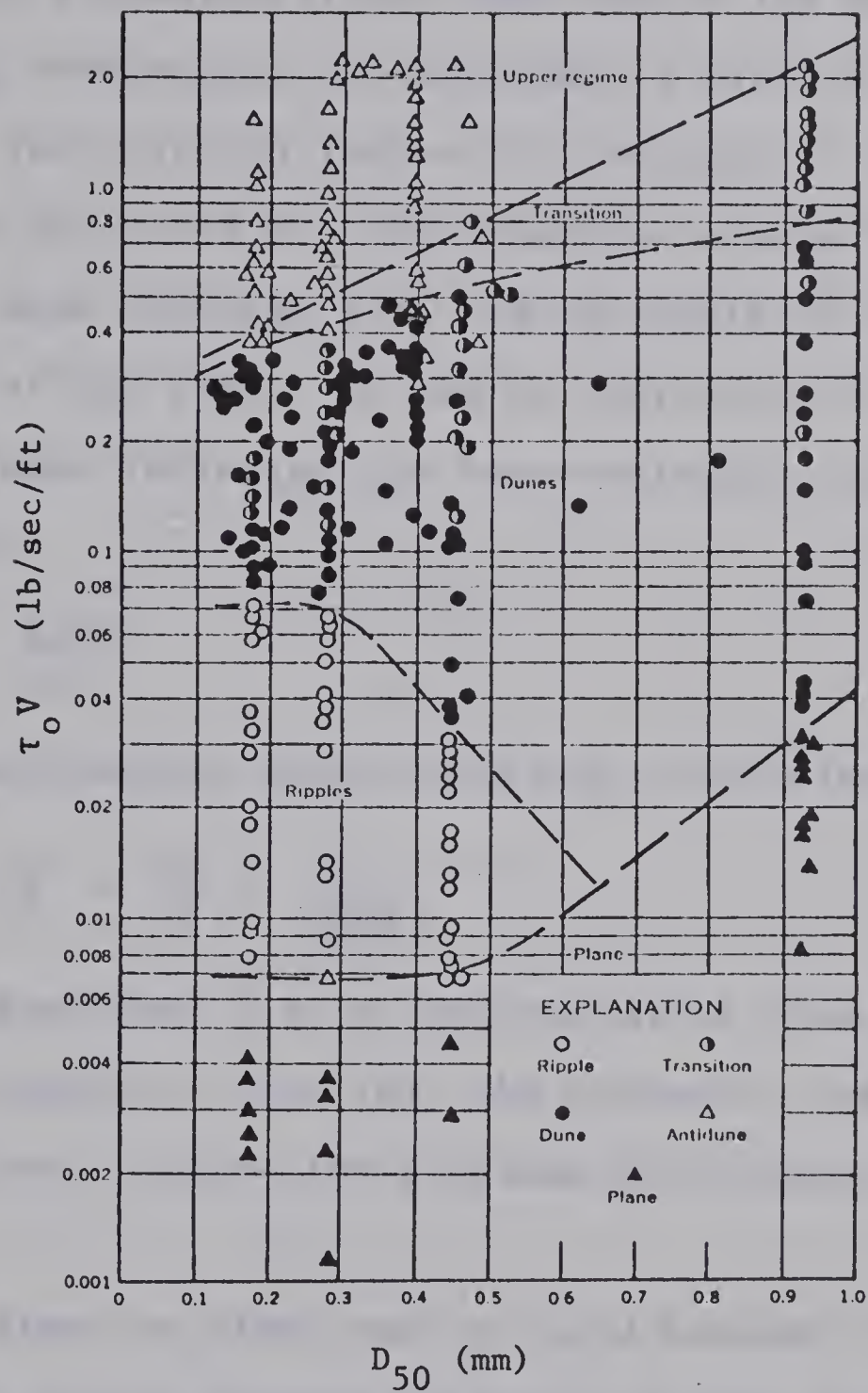


Figure 2-2. The Simons and Richardson Criteria for the Prediction of Bed-Forms (Simons and Richardson, 1966)



### 2-3 The Resistance to Flow in Alluvial Channels

Prediction of the friction factor for a given flow over a given bed-material has been one of the major problems confronting researchers in the study of flow in alluvial channels. The friction factor is a measure of the resistance to the flow and gives the relationship between channel slope (S), mean velocity (V), and the depth (h) or hydraulic radius (R) of the flow. It can be expressed in a number of different forms including the Darcy-Weisbach resistance coefficient

$$f = \frac{8gdS}{V^2} \quad (2-1)$$

and the dimensionless Chezy discharge coefficient

$$C / \sqrt{g} = \frac{\sqrt{8}}{f} = \frac{V}{\sqrt{gdS}} \quad (2-2)$$

In these expressions d is a representative flow dimension such as the depth of flow (h), the hydraulic radius (R), or in the case of pipe flow problems the diameter of the pipe.

For flows in pipes and in rigid boundary open channels the friction factor depends primarily on the relative roughness ( $K_s/d$ ) in the hydraulically rough regime, on the Reynolds number of the flow ( $Vd/\nu$ ) in the hydraulically smooth regime, and on both these parameters when the flow is transitional between the two regimes. However, it also depends to a lesser extent on factors such as the shape of the flow cross-section and the shape, spacing, and





orientation of the boundary roughness elements.

In an alluvial channel the resistance to flow is complicated by the presence of bed-forms whose geometry can vary with changing flow conditions and by the presence of varying levels of particle concentration in the flow adjacent to the bed. In addition to these factors the alluvial channel boundary has a particle roughness that is analogous to the type of roughness found in most rigid boundary situations.

A popular approach to the problem has been to separate the friction factor into one component that accounts for resistance due to the particle roughness of the boundary and another component that accounts for resistance due to bed-form roughness and other factors. This has usually been accomplished by considering an equivalent flow over a plane bed having the same particle roughness but with either hydraulic radius or slope different to account for the absence of bed-forms and other factors found in the actual flow. Relationships adopted from rigid boundary hydraulics are then used to determine the friction factor of the equivalent plane bed flow, and relationships are developed from alluvial channel data for determining the component of friction factor that can be attributed to resistance factors common only to the actual alluvial channel flow.

In one of the first applications of this approach Einstein and Barbarossa (1952) proposed the division of hydraulic radius ( $R$ ) into a component  $R'$  corresponding to an





equivalent plane bed flow having the particle roughness, velocity, and slope of the actual flow, and an additive component  $R''$  accounting for the effects of bed-form roughness. The total friction factor is then given by

$$f = f' + f'' = \frac{8gS}{V^2} (R' + R'') = 8 \left( \frac{V'_*}{V^2} + \frac{V''_*}{V^2} \right) \quad (2-3)$$

For the prediction of the friction factor of the equivalent plane bed flow, the Einstein-Barbarossa method uses the logarithmic formula for mean velocity

$$\frac{V}{V'_*} = 5.75 \log \left( 12.27 \frac{R'}{K_s} E \right) \quad (2-4)$$

in which  $K_s$  is equal to  $D_{65}$  and  $E$  is a parameter that accounts for transitional flows between the hydraulically smooth and the hydraulically rough regimes. On the other hand, the bed-form roughness component of friction factor is determined from a graphical relationship between  $V/V''_*$  and the parameter

$$\psi = \frac{\rho_b - \rho_f}{\rho_f} \frac{D_{35}}{R'S} \quad (2-5)$$

taken from the Einstein bed-load function. Figure 2-3 shows the empirical relation proposed by Einstein and Barbarossa and identifies the alluvial channel data that were used to obtain this relation.

Simons and Richardson (1966) used the results of their flume experiments to demonstrate the relationship between  $V/V''_*$  and  $\psi'$  to be multivalued over a range of conditions



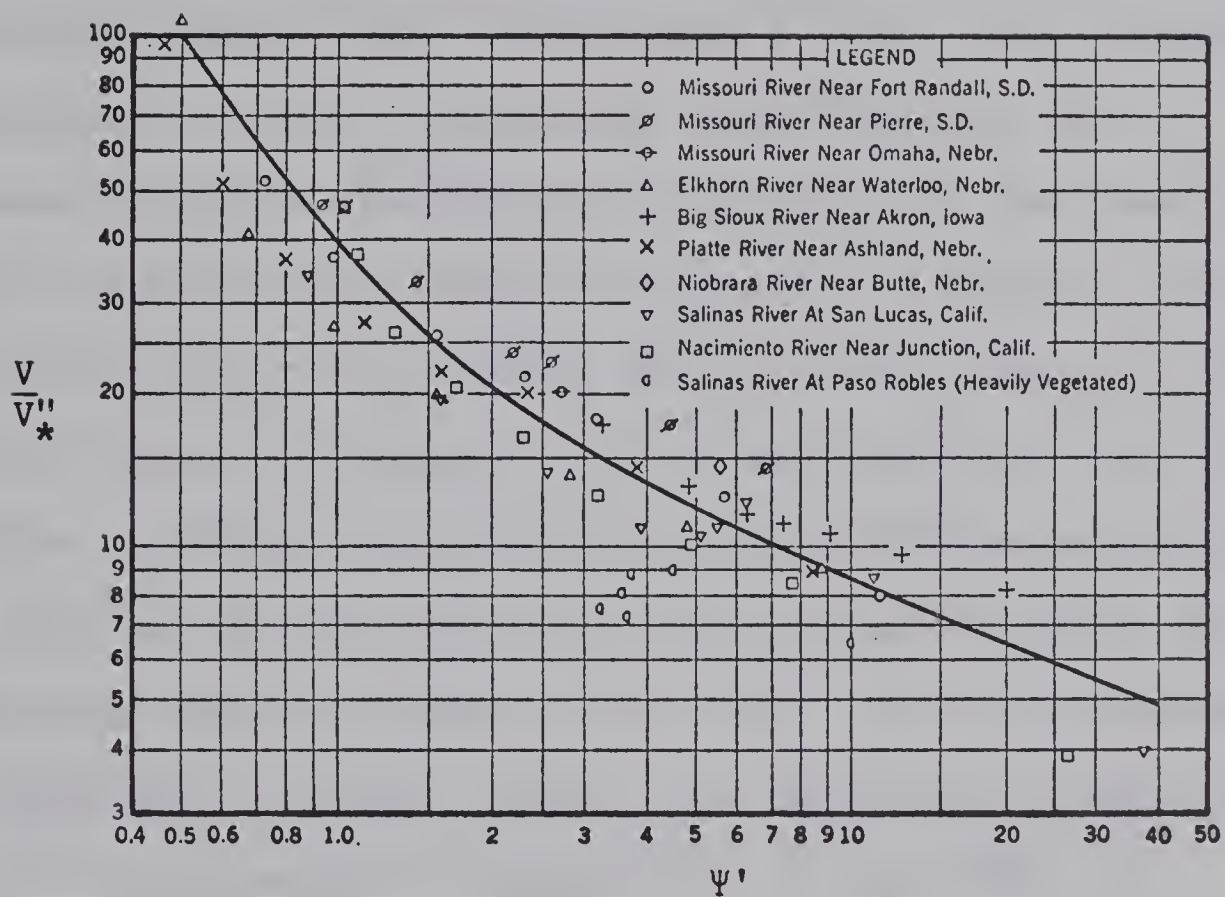


Figure 2-3. The Einstein and Barbarossa Relationship for the Prediction of Form Roughness Coefficient (Einstein and Barbarossa, 1952)





covering all possible bed-forms. This is in agreement with the earlier findings of Brooks (1958) who first suggested the possibility of relationships involving these variables being multivalued.

The resistance to flow problem has been approached in a similar manner both by Engelund (1966) and by Simons and Richardson (1966). Engelund, like Einstein and Barbarossa, divided the hydraulic radius into two components and used a logarithmic velocity formula, in which  $K_s$  was made equal to  $2D_{65}$ , to compute the friction factor of the equivalent plane bed flow. He also developed an empirical expression relating the hydraulic radius of the equivalent plane bed-flow to the properties of the bed-material and the slope and depth of the actual flow. For wide channels where depth and hydraulic radius are equivalent, Engelund's empirical relationship is equivalent to the  $V/V_*' - \psi'$  relationship of the Einstein and Barbarossa method.

Simons and Richardson (1966) developed three different methods for predicting friction factors in alluvial channels. All involved the consideration of an equivalent plane bed flow, but the methods differed in the type of flow that was considered and in the choice of variables to be adjusted in order to attain this flow. One of the methods involved the adjustment of channel slope to a plane bed flow having the same velocity, depth, and particle roughness as the actual flow. The other two methods involved the adjustment of velocity and either depth or hydraulic radius to a plane



bed flow having the same discharge and slope but with an equivalent particle roughness in one case and a hydraulically smooth boundary in the other.

Expressions from rigid boundary hydraulics were used to predict the friction factor of the equivalent flow in both the method of slope adjustment and the method of depth adjustment to a hydraulically smooth boundary. The results of flume experiments with plane alluvial beds have been used both to modify the logarithmic formula that was adopted for the slope adjustment method and to develop a relationship between  $\bar{C}'/\sqrt{g}$  and  $D_{50}$  for use in the method of depth adjustment to an equivalent particle roughness.

Finally, Simons and Richardson have provided, for each method, a number of equations and graphs for predicting the difference between the actual value and the equivalent flow value of the adjusted variable. These empirical relationships involve the type of bed-form, the median diameter of the bed-material, the channel slope, and the depth of flow; they are based on data from flume experiments (Guy, Simons and Richardson, 1966) and in some cases on canal observations.

Alam, Cheyer, and Kennedy (1966) presented yet another method in which an equivalent plane bed flow was considered. They separated channel slope and therefore the Darcy-Weisbach resistance coefficient into two additive components. The component  $f'$  corresponding to the particle roughness was determined from the Moody pipe friction diagram as





$$f' = \text{fn}\left(\frac{V4R}{v}, \frac{D_{50}}{4R}\right) \quad (2-6)$$

in which  $K_s$  was made equal to  $D_{50}$  of the bed-material and  $4R$  was used in place of the pipe diameter.

The form roughness component  $f''$ , on the other hand, was determined by evaluating the functional expression

$$f'' = \text{fn}\left(\frac{R}{D_{50}}, \sqrt{\frac{V}{gD_{50}}}\right) \quad (2-7)$$

which was obtained from dimensional analysis and from the consideration of theories describing the behavior of bed-forms. Subsequent empirical evaluation of this expression yielded the graphical relationship shown in Figure 2-4. As indicated in this figure, a comprehensive collection of data from flume experiments and natural channel observations were used in the evaluation.

Alam, Cheyer, and Kennedy recognized the possibility of differences existing between the friction factors predicted from theories adopted from rigid boundary hydraulics and the actual friction factors that would occur for the equivalent flow over a plane alluvial bed. However, they argued that such differences could be accounted for in the empirical development of the relationship describing the variation of the form resistance coefficient  $f''$ . This problem was also recognized by Simons and Richardson who based their predictions of friction factors for the equivalent plane bed flow partly on the results of flume experiments with plane alluvial beds.





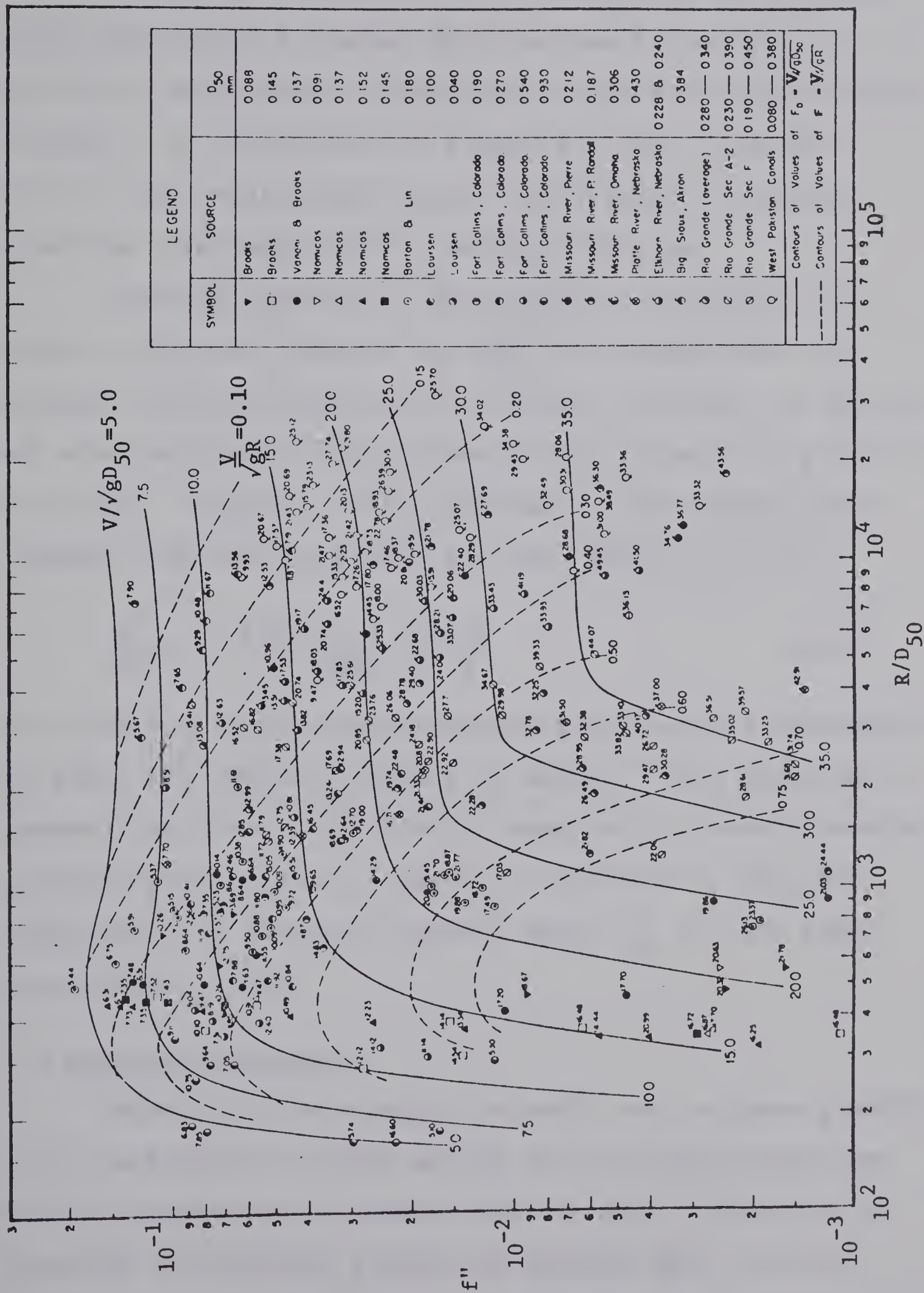


Figure 2-4. The Graphical Relationship of Alam, Cheyer, and Kennedy (1966) for Predicting Friction due to Form Roughness



In a recent study, Lovera and Kennedy (1969) used plane bed alluvial channel observations to develop a graphical relationship comparable to the Moody pipe friction diagram. As illustrated in Figure 2-5 they found the form of the relationship to be significantly different from the form suggested by the Moody diagram.

Another approach to the problem of resistance to flow in alluvial channels has been to consider only the overall friction factor and to develop, through the analysis of alluvial channel data, relationships capable of predicting its value. Typical of this approach is the regime slope formula suggested by Blench and Erb (1957)

$$\frac{v^2}{ghS} = 3.63 \left( 1 + \frac{C_{tb}}{233} \right) \left( \frac{V_b}{v} \right)^{\frac{1}{4}} \quad (2-8)$$

in which  $C_{tb}$  is the concentration of transported bed-material in parts per hundred thousand by weight. This equation is a generalized form of the Blasius equation for smooth boundary circular pipes and was originally developed by King for application to alluvial channels where  $C_{tb}$  is very small (see Blench, 1969a).

#### 2-4 Sediment Transport

When the flow velocity is small over a plane granular bed, the hydraulic forces acting on the surface particles may be insufficient to cause their movement. However, as velocity is increased a point is reached where certain





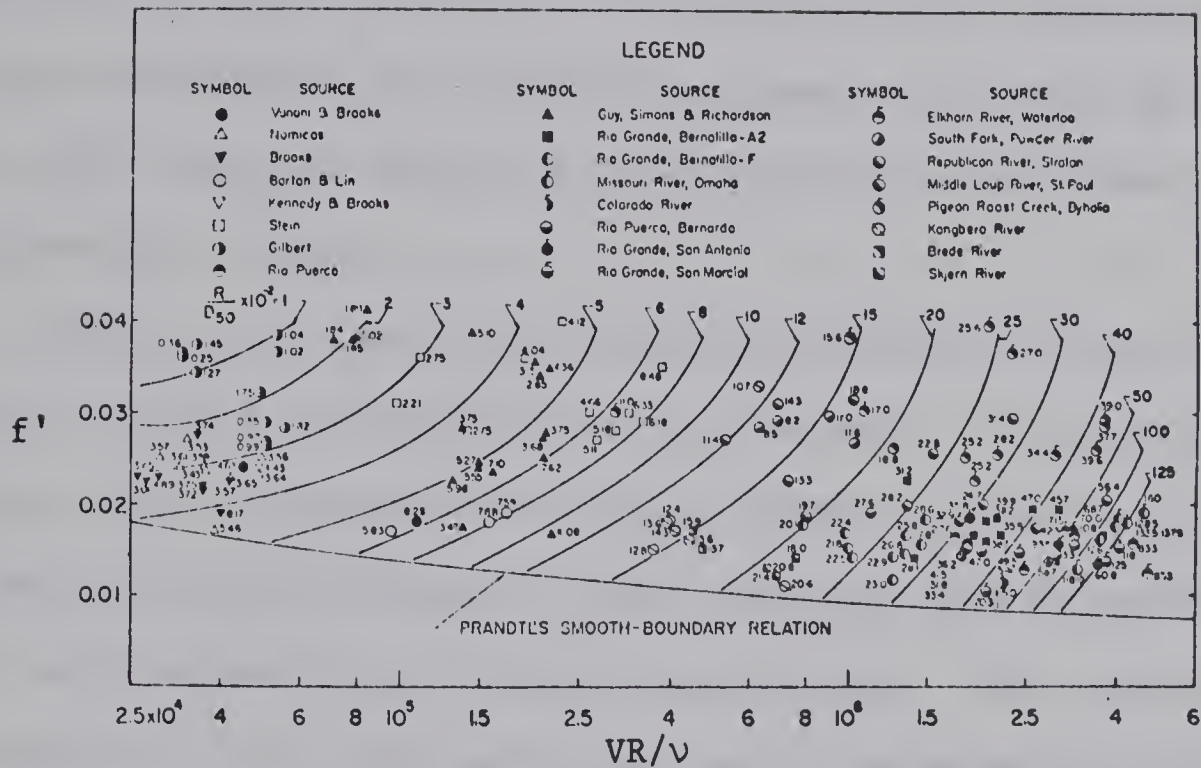


Figure 2-5. Variation of the Friction Factor with Reynolds Number ( $VR/\nu$ ) and Relative Particle Roughness ( $R/D_{50}$ ) for a Plane Alluvial-Bed (Lovera and Kennedy, 1969)



particles become detached from their positions on the bed and move a short distance along it. The detachment of such particles depends on their physical properties and their orientation, on the nature of the bed in the vicinity of the particle in question, and on the instantaneous flow velocities in this vicinity. The forces that determine particle detachment are the hydrodynamic lift and drag forces, the buoyant weight of the particle, and the various intergranular forces.

Once a given particle becomes detached it can move by rolling, sliding or hopping along the bed. This movement continues until the particle again comes to rest at a location on the bed where at that instant the hydrodynamic forces are incapable of sustaining motion. The particle then remains at its new position until detachment conditions are again reached. The movement of particles in this manner is an intermittent process in which a given particle can remain at rest on the bed for relatively long periods of time between periods of movement.

As flow velocity near the bed is further increased, the frequency of particle detachment increases as does the velocity of movement of these particles. Furthermore, the detachment, movement, and redeposition of particles affects the susceptibility for detachment of other particles by modifying both the shielding of these particles and the intergranular forces acting on them.

Transported particles that are supported for most of





the time by physical contact with the bed are considered to constitute the bed-load. These particles generally move within a layer, several particle diameters in thickness, that is referred to as the bed-layer.

A certain number of detached particles, because of their physical properties, their initial velocity, or the hydrodynamic forces acting on them, can be carried to a level above the bed-layer. Of these, some immediately settle back through the bed-layer and are transported essentially as bed-load, but others can be supported at these upper levels by turbulence and can be transported over large distances in suspension. Sediment that is transported in this fashion constitutes the suspended sediment load. The total suspended sediment load can be made up partly of suspended bed-material and partly of suspended fine sediment which does not originate from the bed and which remains in suspension at all practical stages of flow. The suspended fine sediment usually contains silt sizes and smaller and has been observed (Simons, Richardson, and Haushild, 1963) to have an appreciable effect on the physical properties of the water-sediment mixture.

Finally, the sum of the rate of bed-load transport and the rate of suspended bed-material transport equals the rate of total bed-material transport ( $G_{tb}$ ).

The concept of separating the total bed-material load into a bed-load and a suspended bed-material load is somewhat inexact. Although the transport mechanism may be different





for each type, there does not appear to be a sharp distinction between the two types. In the first place there is a continual exchange of bed-material particles across the upper surface of the bed layer. This implies that many of these particles are being transported part of the time as bed-load and part of the time as suspended load. Secondly, the thickness of the bed-layer is at best arbitrary, for there is likely a finite region near the top of the hypothetical bed-layer where significant concentrations of both bed-load and suspended load occur.

The various modes of bed-material transport have been defined for flow over a plane alluvial bed. However, with little modification these terms seem to be equally applicable to the various bed-form configurations found in alluvial channels. One possible modification would be to include as part of the bed-layer the zone of separation between adjacent ripples or dunes since the majority of bed-material that is moved as bed-load along the upstream face of these bed-forms is deposited in this region.

## 2-5 The Beginning of Bed-Material Movement

Several criteria have been proposed for predicting the critical flow conditions at which particles begin to move on a plane alluvial bed. Most of these criteria have been based on the results of flume experiments on uniform granular bed-materials.

The well known Shields criterion (see Yalin, 1969)



relating  $V_{*cr} D/\nu$  to  $\rho_f V_{*cr}^2 / (\gamma_b' D)$  is shown in Figure 2-6. In this relationship,  $\rho_f V_{*cr}^2 / (\gamma_b' D)$  is proportional to  $1/(V_{*cr} D/\nu)$  for values of  $V_{*cr} D/\nu$  less than about 5.0 where the flow is hydraulically smooth and critical conditions are likely not dependent on  $D$ . On the other hand,  $\rho_f V_{*cr}^2 / (\gamma_b' D)$  is a constant equal to about 0.05 for  $V_{*cr} D/\nu$  values greater than about 70 where the flow is hydraulically rough and critical conditions are likely independent of  $\nu$ .

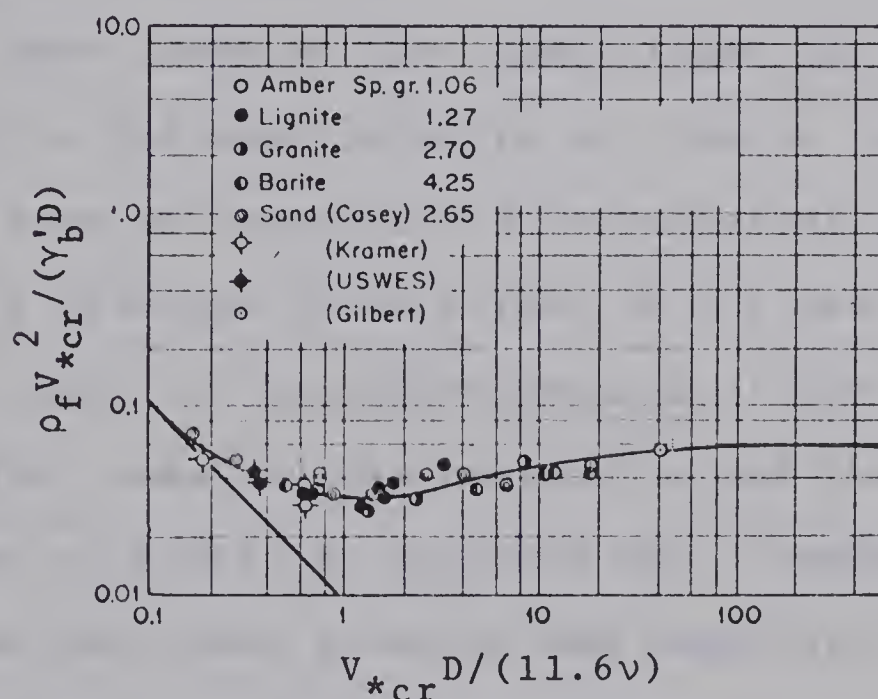


Figure 2-6. Shields Relation for the Beginning of Bed-Material Movement





## 2-6 Review of Bed-Material Transport Theories

Many theories have been proposed for the prediction of the rate of bed-load transport and the rate of total bed-material transport in alluvial channels. These theories have been based partly on mathematical models describing the transport phenomenon and partly the analysis of data obtained in most cases from flume experiments. Unfortunately, many of the theories have utilized only a small portion of the available experimental results and, as a consequence, have suffered from the corresponding limited range of experimental conditions.

Most theories have used either the shear stress on the bed or the mean velocity of flow as the main predictor of the rate of transport of bed-material. From a theoretical point of view the shear stress on the bed is likely the better choice of variables because of the obvious cause and effect relationship between it and the detachment and movement of particles near the bed. However, the consideration of both mean velocity and depth of flow is equivalent to the consideration of shear stress even if the relationship between them is not fully understood. Furthermore the mean velocity and depth are easier to measure and have been determined with a greater degree of accuracy in the existing flume experiments on which the bed-material transport theories are based.

One of the first formulas for the prediction of bed-material transport was developed by DuBoys in 1879 (see



Leliavsky, 1966). This formula was derived from theoretical considerations and can be written in the form

$$q_{tb} = K_1 \tau_o (\tau_o - \tau_c) \quad (2-9)$$

where  $q_{tb}$  is the volumetric rate of discharge of bed-material per unit breadth,  $\tau_o$  and  $\tau_c$  are respectively the shear stresses acting on the bed at the flow in question and at the critical conditions for which bed-material particles begin to move, and  $K_1$  is a coefficient depending on the properties of the bed-material. Although the validity of the physical model used in DuBoys' derivation has since been questioned, the equation has been found to agree reasonably well with laboratory observations (Leliavsky, 1966). Perhaps for this reason, numerous subsequent investigators have retained the basic form of DuBoys' equation for evaluation in empirical studies. The concept of relating  $q_{tb}$  to the excess shear stress acting on the bed ( $\tau_o - \tau_c$ ) has been modified by a number of investigators who preferred to relate  $q_{tb}$  to either the excess value of mean velocity ( $V - V_c$ ) or the excess value of discharge intensity ( $q - q_c$ ).

In 1934 Schoklitsch developed a bed-material transport formula of this latter type (Schulits, 1935); it can be expressed as

$$G'_{tb} = \frac{86.7}{\sqrt{D_{50}}} S^{3/2} (q - q_c) \quad (2-10)$$

where





$$q_c = 0.00532 \frac{n_{50}}{s^{4/3}} \quad (2-11)$$

This formula was based primarily on the results of the Gilbert experiments with uniform sized bed-materials.

Meyer-Peter and Müller (1948) used the results of their own flume experiments to develop a bed-load transport formula that has since gained widespread acceptance in practice. For two dimensional flow this formula is

$$\rho_f \left( \frac{K_b}{K'_b} \right)^{3/2} hS = K_3 (\rho_b - \rho_f) D_m + K_4 \frac{\rho_f^{1/3}}{g} \left( \frac{\rho_b - \rho_f}{\rho_f} \right)^{2/3} q_b^{2/3} \quad (2-12)$$

The coefficients  $K_3$  and  $K_4$  depend only on the properties of the bed-material, and the parameter  $K_b/K'_b$  is the ratio of the roughness coefficient of the actual flow to the roughness coefficient corresponding to a plane bed having the same particle roughness.

A different approach to the problem of bed-material transport was taken by Einstein (1942, 1950). From the consideration of the probability of a particle on the bed being detached and transported, he derived a mathematical expression describing the bed-load transport phenomenon and used it to develop a procedure for computing the rate of bed-load transport and the rate of total bed-material transport. For a uniform bed-material the equations involved in the Einstein procedure are

$$\phi = \left( \frac{q_b}{\rho_b g} \frac{\rho_f}{\rho_b - \rho_f} \frac{1}{g D^3} \right)^{1/2} \quad (2-13)$$





$$\psi = \frac{\rho_b - \rho_f}{\rho_f} \frac{D}{R'S} \quad (2-14)$$

and

$$\phi = \text{fn}(\psi) \quad (2-15)$$

In his original work Einstein (1942) used the results of the experiments of Meyer-Peter and Müller (1948) and of Gilbert (1914) to determine the form of Equation 2-15 as

$$0.465 \phi = e^{-0.391\psi} \quad (2-16)$$

which provided a reasonable fit to the data for all but the very high values of  $\phi$ . Brown (1949) proposed the alternative empirical solution

$$\phi = 40 \left( \frac{1}{\psi} \right)^3 \quad (2-17)$$

which is plotted in Figure 2-7 along with Equation 2-16 and the experimental data used by Einstein.

In 1950 Einstein extended the theory to apply to bed-material mixtures and derived analytically the  $\phi - \psi$  relationship in the form of an integral equation. However, it remained necessary to use experimental data to determine the values of three numerical constants in this equation. In the same study Einstein presented an empirical expression relating the rate of bed-load transport to the average concentration of bed-material particles in the bed-layer. Given this bed-material concentration at the lower level of suspension, the rate of suspended bed-material transport can be computed from the theory of suspension. Finally, Einstein provided a step by step procedure incorporating



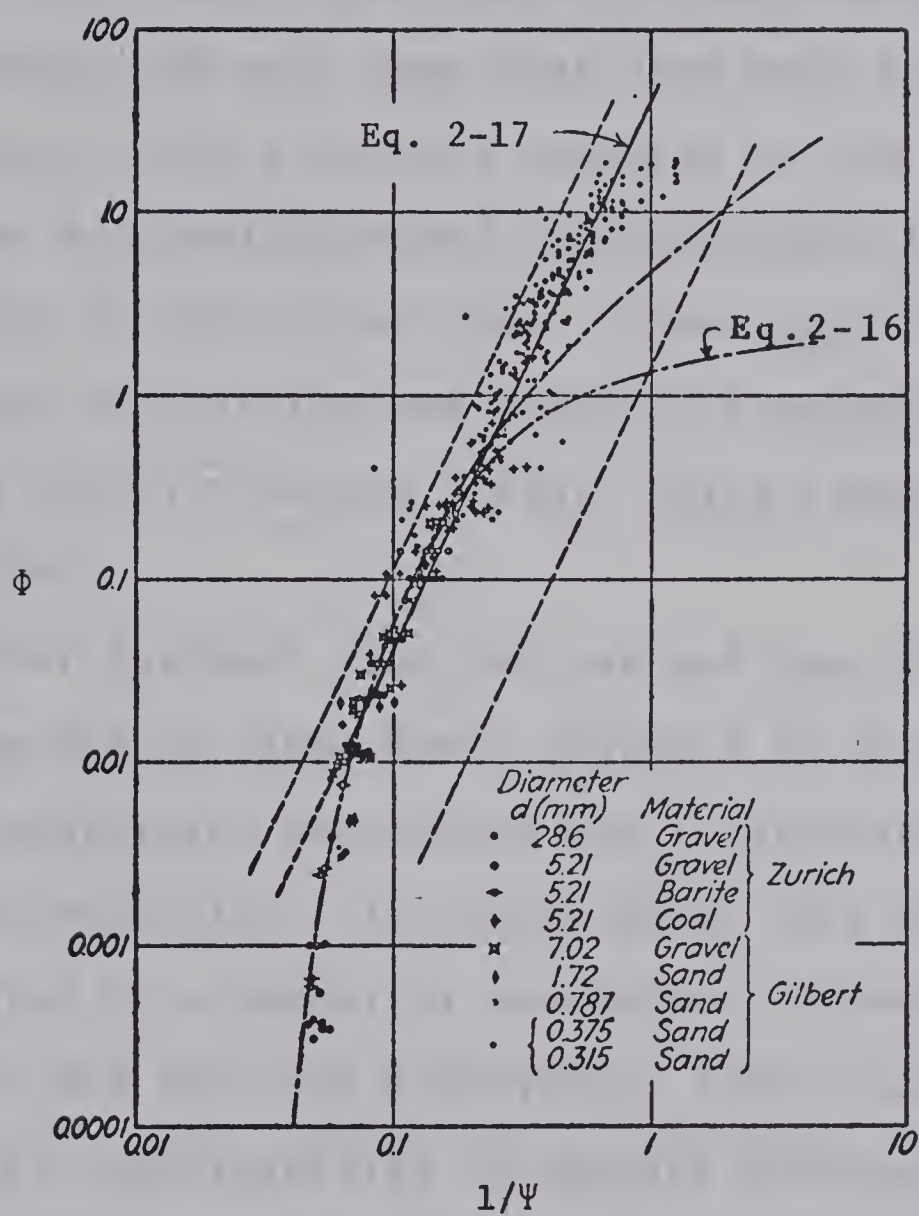


Figure 2-7. The Einstein  $\Phi$ - $\Psi$  Relationship





numerous equations and graphs for predicting both the rate of bed-load transport and the rate of suspended bed-material transport in natural alluvial channels.

The above methods of computing bed-material transport are by no means the only ones that have been developed to date. However, they provide a sampling of the numerous methods that are available and the approaches that have been followed in developing them. Other significant contributions include the bed-material transport formulas of Kalinske (1947), Laursen (1958), Yalin (1963), and Bagnold (1956).

Another approach that has not yet been discussed involves the use of dimensional analysis to formulate a functional expression describing the relationship between the relevant variables. In recent years this approach has been advocated by a number of researchers (Blench, 1969b; Yalin, 1969; and Barr and Herbertson, 1968), possibly because of its applicability to complex problems for which complete analytical solutions are not possible without making numerous simplifying assumptions. This approach, based on dimensional analysis, has the advantage of permitting the consideration of a large number of possibly relevant variables without requiring knowledge or assumption on how such variables enter into the relationships.

Rottner (1959) used dimensional analysis to formulate the expression



$$G'_{tb} = \text{fn} (Q, h, D_{50}, \rho_b, \rho_f, g, \nu) \quad (2-18)$$

Although the subsequent steps of the analysis contain a number of typographical errors, as pointed out by Yalin (1969), the final functional relationship that was evaluated by Rottner appears to be valid and can be written as

$$0 = \text{fn} \left( \frac{V}{\sqrt{gh(\rho_b - \rho_f)/\rho_f}}, \frac{G'_{tb}}{\rho_b g \sqrt{gh^3(\rho_b - \rho_f)/\rho_f}}, \frac{h}{D_{50}} \right) \quad (2-19)$$

In his evaluation of this relationship, Rottner utilized the comprehensive collection of experimental flume data that had been compiled by Johnson (1943) and obtained the following bed-material transport formula:

$$\begin{aligned} & \left( \frac{G'_{tb}}{\rho_b g \sqrt{(\rho_b - \rho_f)/\rho} \sqrt{gh^3}} \right)^{1/3} \\ &= 0.667 \left( \frac{D_{50}}{h} \right)^{2/3} Fr'^2 - 0.778 \left( \frac{D_{50}}{h} \right)^{2/3} \end{aligned} \quad (2-20)$$

Dimensional analysis was also used by Barr and Herbertson (1968) who proposed the functional relationship

$$0 = \text{fn} \left( \frac{G'_{tb}}{\rho_b g Q}, \frac{Q g^{1/3}}{\nu^{5/3}}, \frac{g^{1/2} D_{50}^{3/2}}{\nu}, \frac{D_{50}}{R} \right) \quad (2-21)$$

which they subsequently tested with selected data from the experiments of Brooks (1958), Stein (1965), Guy and others (1966), and Gilbert (1914). Although the results appear promising they were unfortunately not unified into either a mathematical or graphical form that would be suitable for engineering use.





## CHAPTER III

### THE MATHEMATICAL MODEL

In this chapter a dimensional analysis is applied to the problem of flow in alluvial channels. The purpose of the analysis was to develop a mathematic model that could be used as the basis for a subsequent empirical evaluation.

#### 3-1 Dimensional Analysis

Huntley (1967) in an historical account of dimensional analysis stated one of its main uses to be "in obtaining partial solutions of problems too complex for ordinary mathematical analysis." In this role, dimensional analysis has been a valuable tool in the development of hydraulics and has been used extensively by numerous investigators in the study of flow in alluvial channels.

The objective of dimensional analysis used in this manner is to express the behavior of a phenomenon in the form of functional equations relating non-dimensional parameters. These equations can then be evaluated empirically to determine the relative importance of individual parameters and to formulate the relationships between these parameters.

A complete dimensional analysis of a problem consists of the following steps:

- (1) The specification of limitations in the scope of the problem being investigated.





(2) The selection of a set of "characteristic quantities" whose specification is necessary and sufficient to completely determine the behavior of the phenomenon. These quantities should be mutually independent and are often referred to as the independent variables. Their selection requires physical understanding of the phenomenon, but it does not require a complete knowledge of the physical laws governing that behavior of the phenomenon.

(3) The selection of a number of pertinent dependent variables to be related to the independent variables to form a set of functional equations.

(4) Application of the theory of dimensions (Huntley, 1967; and Blench, 1969b), to replace the original variables with non-dimensional groups, thereby automatically reducing the number of independent variables in the functional equations.

By far, the most important and difficult requirement in dimensional analysis is the complete specification of the problem in terms of the interrelated variables (Steps 1 to 3 above). Only when this has been achieved can the functional equations in non-dimensional form be of any value to the development of meaningful relations between the variables.

Finally, dimensional analysis reduces the experimental requirements both by minimizing the number of independent variables requiring experimental variation and by enabling,



in many cases, scaled experiments to cover the same range of the non-dimensional groups as would full scale experiments.

### 3-2 Role of the Alluvial Bed-Material

The bed-material properties influence the following aspects of the flow phenomenon: (1) the resistance that is exerted on the flow due to particle roughness and (2) the forces acting on bed-material particles that are either in motion or at rest on the bed. The particle properties that are involved include the size, shape, orientation, surface roughness, and density.

The resistance to flow is affected by the size, shape, orientation, and the surface roughness of individual particles on the surface of the bed. It also depends to a large extent on the distribution of these properties over this surface. Of course, resistance to flow is also closely associated with the different bed-forms, and it can be expressed in terms of both bed-form and bed-material properties in addition to a necessary number of other independent variables.

The initiation of motion of a particle and its movement by rolling or sliding along the bed are influenced by essentially the same set of bed-material properties. Here particle weight and intergranular forces tend to oppose motion while the hydrodynamic forces of lift and drag tend to cause and maintain motion. Consequently, particle density







becomes important for its contribution to both weight and momentum. On the other hand, the distribution over the surface of the bed of particle shape, size, orientation, and surface roughness affect both the hydrodynamic and the intergranular forces.

The situation differs somewhat for a particle being transported through the fluid either by hopping or in suspension. Here the individual particle properties become more important because of their contribution to fall velocity and to the lift and drag forces, and the properties describing the surface of the bed become somewhat less important although they do contribute to the structure of the flow. The distributions of bed-material properties should again be considered, but they should be considered from the point of view of the whole bed-material rather than its surface.

The foregoing discussion points out the importance of the shape, size, surface roughness, and density of particles as well as their orientation on the surface of the bed. It also suggests that the distribution of these properties should be considered both for the surface layer and for the bed-material as a whole.

Unfortunately, the only observations available for most experimental bed-materials are the average particle density, the distribution of particle sizes, and in a few cases a qualitative assessment of average particle shape.



Because of these limitations in the experimental data, it is necessary to make some assumptions in order to describe the bed-materials in terms of properties that have been measured.

Since observations on the surface roughness of particles and their orientation in the bed are generally lacking, it is necessary to assume that the effect of these properties and of their distributions is either negligible or is constant for both natural and experimental bed-materials. The effect of particle density can likely be adequately represented by specifying an average value ( $\rho_b$ ) for the entire bed-material since this property remains relatively constant throughout most natural bed-materials. By assuming that the effect of particle shape can be accounted for by a single average measure  $\alpha_b$  and by assuming that the distribution of particle sizes can be described by specifying the median diameter ( $D_{50}$ ) and a single measure of gradation  $\sigma_b$  where

$$\sigma_b = \frac{1}{2} \left( \frac{D_{84}}{D_{50}} + \frac{D_{50}}{D_{16}} \right) \quad (3.1)$$

then the properties describing the effect of the bed-material on flow in alluvial channels are

$$(D_{50}, \sigma_b, \rho_b, \alpha_b)$$

This is by no means the only set of variables that can be used to describe the properties of the bed-material.





Simons and Richardson (1960) argued that fall velocity ( $\omega$ ) is the major factor determining the interaction between water and sediment and that it can be used to replace  $\rho_b$  and  $\alpha_b$ . However, it is questionable whether  $\omega$  by itself is capable of characterizing the role of the bed-material in either the formation of hydrodynamic lift forces where  $\alpha_b$  is important or the unsteady motion of a particle where  $\rho_b$  is important.

### 3-3 The Laboratory Flume Problem

The majority of flume experiments on flow in alluvial channels have been carried out in straight rectangular flumes containing alluvial beds and having rigid vertical sides. In most cases the flows have been steady and uniform, and sediment transport has consisted entirely of transported bed-material.

Under these conditions, the flow phenomenon becomes completely defined when the following physical properties are specified:

- (1) The breadth ( $b$ ) and the side roughness height ( $\epsilon_s$ ) of the flume.
- (2) The mass density ( $\rho_f$ ) of the fluid and its viscosity ( $\mu$ ).
- (3) The constant of gravitational acceleration ( $g$ ).
- (4) The physical properties that are necessary to describe the effect of the bed material, namely  $D_{50}$ ,  $\sigma_b$ ,  $\rho_b$ , and  $\alpha_b$ .





- (5) Any two of the flow properties chosen from mean velocity ( $V$ ), depth ( $h$ ), slope ( $S$ ), and the total rate of transport of bed-material ( $G_{tb}$ ).

These properties form the set of characteristic quantities

$$(b, \epsilon_s, \rho_f, \mu, g, D_{50}, \sigma_b, \rho_b, \alpha_b, h, G_{tb})$$

in which  $h$  and  $G_{tb}$  have been selected as the flow properties to be imposed on the phenomenon. When this set is imposed then all other variables including the remaining two flow properties ( $V$  and  $S$ ) become dependent and will adjust to a state of equilibrium. The relationship between the dependent variables ( $V$  and  $S$ ) and the set of characteristic quantities can be expressed in functional form as

$$V, S = \text{fn}(b, \epsilon_s, \rho_f, \mu, g, D_{50}, \sigma_b, \rho_b, \alpha_b, h, G_{tb}) \quad (3-2)$$

Although the present study has been limited to an investigation of the relationships suggested in Equation 3-2, it would also be possible to consider additional dependent variables such as those describing the geometry of bed-forms, for example.

Application of the standard techniques of dimensional analysis (see Huntley, 1967; and Blench, 1969b) can be used to reduce the above equations to the non-dimensional form

$$Fr', S = \text{fn} \left( \frac{h}{D_{50}}, C_{tb}, Vi, \frac{b}{h}, \sigma_b, \alpha_b, \frac{\rho_b}{\rho_f}, \frac{\epsilon_s}{b} \right) \quad (3-3)$$



in which

$$\begin{aligned} \gamma'_b &= g(\rho_b - \rho_f), \quad \nu = \frac{\mu}{\rho_f}, \quad C_{tb} = \frac{G_{tb}}{Q\rho_f g}, \\ Fr' &= \frac{\rho_f V^2}{\gamma'_b h}, \quad Vi = \frac{\sqrt[3]{\nu g} D_{50}}{\nu} \end{aligned} \quad (3-4)$$

At this point, because of the large number of parameters contained in Equation 3-3 and because of known deficiencies in the experimental data (see Chapter IV), it is necessary to make a number of assumptions in order to simplify the above mathematical model. In the existing flume experiments observations have not been made on either the shape of bed material particles ( $\alpha_b$ ) or the roughness height of the flume sides ( $\epsilon_s$ ). Consequently, it is necessary to assume that the effect of  $\alpha_b$  is either negligible or relatively constant over the range of values found in the different experimental and natural bed-materials. It is also necessary to assume that the  $\epsilon_s/b$  ratio has a negligible effect on the phenomenon due to  $\epsilon_s$  being small enough to result in a hydraulically smooth flow along the sides of the flume.

Finally, since  $\rho_b/\rho_f$  remains essentially constant for both natural bed-materials and the majority of experimental bed-materials, it can be eliminated from the equation. For the few available experiments where  $\rho_b/\rho_f$  has differed significantly from 2.65, an attempt has been made in the empirical portion of the analysis to account for its effect





by modifying other parameters in the functional equations.

As a result of the above simplifying assumptions, Equations 3-3 can be reduced to

$$0 = fn_i(Fr', C_{tb}, \frac{h}{\bar{D}_{50}}, Vi, \frac{b}{\bar{h}}, \sigma_b) \quad (3-5)$$

and

$$0 = fn_i(S, C_{tb}, \frac{h}{\bar{D}_{50}}, Vi, \frac{b}{\bar{h}}, \sigma_b) \quad (3-6)$$

which together form the basic mathematical model of a steady and uniform flow in a flume containing an alluvial bed.

The parameters contained in Equations 3-5 and 3-6 bear a close resemblance to the parameters used in "regime theory" (Blench, 1969a), but they are by no means the only possible set of parameters that can be formed from the variables in Equation 3-2. A large number of investigators prefer to incorporate the shear velocity

$$V_* = \sqrt{ghS} \quad (3-7)$$

into forms of both the Froude number and the Reynolds number. Unfortunately, the reliability of experimental values of  $V_*$  is questionable because of the difficulty that has been experienced in obtaining accurate measurements of equilibrium slope in flume experiments. For this reason it was considered advantageous to isolate slope as a separate and unmodified dimensionless parameter. Also, there is considerable support for the use of mean velocity ( $V_m$ ) in relationships involving the rate of transport of bed-material. This has been



advocated by a number of investigators including Colby (1964), Brooks (1958), and Maddock (1966).

The choice of dependent and independent variables is a subject that has been discussed at length without being completely resolved. The problem appears to depend on the single or multi-valued nature of the relations suggested by Equations 3-5 and 3-6 over the entire region of operating conditions and over the region of conditions corresponding to any one particular bed-form configuration. If the solutions to these equations are not unique, then the choice of independent variables could conceivably affect the relationships obtained from the results of flume experiments.

Brooks (1958) found a number of multi-valued relations to exist between the variables. However, these results were based on flume experiments carried out in or near the transitional region between the upper and lower flow regimes. Simons and Richardson (1966) clarified this result by finding the relations to be unique for any given bed-form but possibly non-unique over the entire spectrum of bed-forms. This later hypothesis has been supported by the recent work of Guy, Rathbun, and Richardson (1968) who compared results from a sediment injection system and a sediment recirculating system each of which had a different set of independent variables imposed. They found no significant differences to exist between results from the two different systems.





Accepting for the present the hypothesis that the relationships between variables are unique for any particular bed-form configuration, the choice of dependent and independent variables becomes arbitrary, and the implicit representation in Equations 3-5 and 3-6 where the subscript  $i$  refers to a particular bed configuration is, therefore, justified.

### 3-4 Modification of the Mathematical Model for Canals and Natural Channels

In the case of a man-made canal there is an additional degree of freedom for the self-adjustment of channel breadth that is not present in the laboratory flume with its rigid sides. Consequently, breadth ( $b$ ) should be transposed as an additional dependent variable to the LHS of Equation 3-2. Although man made canals are usually prevented by means of channel maintenance from developing natural meander patterns, this is an important aspect to the behavior of natural alluvial channels. However, where meandering takes place the quantities that describe its geometry can be considered as dependent variables in Equation 3-2 as modified in the present section.

Since the properties of the alluvial material that is found in the sides of both natural channels and canals can be considerably different than the properties of the bed-material, these properties must be included as separate independent variables that are imposed on the phenomenon.





They are likely to play an important role in both the adjustment of channel breadth and the development of meander patterns. Unfortunately, the erosion and deposition of the cohesive sediments usually found in channel sides is rather poorly understood. The ASCE Task Committee on Erosion of Cohesive Materials (1968) in recognizing this problem considered that "a major research effort must be undertaken to define those properties, whether chemical, physical, or environmental, that determine the resistance of a cohesive sediment to flowing water."



## CHAPTER IV

### SUMMARY OF AVAILABLE EXPERIMENTAL DATA

#### 4-1 General

Most theories on the behavior of flow in alluvial channels have been based to some extent on experimental studies. However, the degree of dependence on experimental results varies considerably between the different theories. In some the relationships are entirely empirical with little or no theoretical background while in others empiricism has been used only to evaluate numerical constants for otherwise analytically derived mathematical expressions.

Unfortunately, many theories have been based on only a portion of the available experimental data. This has generally limited their scope and has necessitated extrapolation into regions where they may not be valid. There is even a possibility of some theories describing the experimental design of a particular collection of data rather than the operation of the actual physical laws defining the phenomenon.

However, both of these dangers can be minimized by using all available experimental data during the empirical portion of the development of a theory. For this reason one of the objectives of the present study was to compile, for the purpose of analysis, the majority of available experimental data pertaining to flow in alluvial channels. The results of this compilation have been reported by





Cooper and Peterson (1969) and are summarized in the present chapter.

#### 4-2 Types of Data

Three different types of channels have provided data that are suitable for the study of flow in alluvial channels. These are laboratory flumes, artificial alluvial channels or canals, and natural alluvial channels. For a given type of analysis, the suitability of the data from each system depends on factors such as the steadiness and uniformity of the flow, the range of conditions encountered, and the ease and accuracy with which observations can be made. In Table 4-1, some of the characteristics found in the data from each system have been summarized.

Because of the degree of control available to the experimenter, the vast majority of flume experiments have had both steady and uniform flow conditions. The flumes have been straight in plan and have had rigid sides that in most cases were both smooth and vertical. Consequently, the flow in most laboratory flume experiments has been considerably less complex than the flow in natural channels. Furthermore the controlled laboratory conditions and the scale of the experiments have facilitated the observation of the rate of transport of bed-material which is an extremely difficult task in the field. Because of these factors, the results of laboratory flume experiments are valuable for the study of the transport of bed-material, as well as aspects



TABLE 4-1

## CHARACTERISTICS OF THE DIFFERENT TYPES OF ALLUVIAL CHANNEL DATA

FLUME DATA	CANAL DATA	RIVER DATA
<p>Rates of sediment transport observed. Data useful for studies on both resistance to flow and sediment transport.</p> <p>Channel usually straight with smooth and rigid vertical sides.</p>	<p>Rates of sediment transport usually not observed. Data useful for resistance to flow, but not sediment transport studies.</p> <p>Channel normally straight but with natural sides.</p>	<p>Rates of sediment transport usually not observed.</p>
<p>Breadth fixed.</p>	<p>Breadth variable, will adjust to equilibrium value.</p>	<p>Channel has natural sides and tends to develop a natural meander pattern. Data useful for development of relations for predicting meander geometry.</p>
<p>Small range in: V, Q, <math>D_{50}</math>, b, and h.</p>	<p>Small range in: <math>C_{tb}</math>, S, and <math>D_{50}</math>.</p>	<p>Breadth variable, will adjust to equilibrium value.</p>
<p>Large range in: S and <math>C_{tb}</math></p>	<p>Relatively large range in Q</p>	<p>Large range in all basic variables.</p>
<p>Data available for all phases of flow.</p>	<p>Data available only for the ripple and dune phases.</p>	<p>Data available for all phases of flow.</p>





such as the resistance to flow and the development of the different bed-form configurations. On the other hand, flume results are of little value in the development of relationships describing either the self-adjustment of channel breadth or the formation of meander patterns.

In a large number of canal systems, channel discharge has been maintained at a steady level, channel sides have consisted of natural alluvial material and have been capable of being formed by the flow, and longitudinal channel configuration has been maintained artificially by the use of channel training techniques. Reliable observations are generally available for discharge, slope, channel geometry, and bed-material properties. Unfortunately, the rate of transport of bed-material has seldom been accurately measured although it has usually been minimized in the design of the canal. Because of these characteristics, canal observations can be used in studies of the resistance to flow and the equilibrium adjustment of channel breadth, but they are of limited value to studies dealing with the rate of transport of bed-material or the development of meander patterns.

The flow phenomenon that occurs in a natural alluvial channel is extremely complex in comparison to flows normally found in either man-made canals or laboratory flume experiments. To begin with, most natural channels are formed from material that is neither homogeneous or isotropic; channel sides are usually formed from alluvial material that is considerably





different than the material found on the bed; meandering, which cannot occur in a rigid sided flume and which is usually prevented from occurring in man-made canals, is an important aspect in the behavior of a natural alluvial channel; and, finally, both discharge rates and rates of input of bed-material are invariably unsteady.

In spite of the complexities, reliable observations from natural channels can be used for testing the validity and extending the scope of theories that have been based primarily on the results of flume experiments. They are also valuable in studies of meander formation since the natural channel is the only system where this aspect of the phenomenon occurs. Unfortunately, there are few cases where natural channel data are suitable for the development of relationships involving the rate of transport of bed-material because this quantity has seldom been observed accurately in the field.

#### 4-3 Laboratory Flume Data

Beginning with the classic experiments of Gilbert (1914), the behavior of flow in alluvial channels has been the subject of numerous laboratory investigations. At present, observations from approximately four thousand different experiments are available. In the majority of these experiments observations have been made on basic quantities such as discharge, depth, slope, and the rate of transportation of bed-material for a flow that has attained a state of equilibrium



in a specified flume containing a specified bed-material. A small number of experimental studies have also considered the effect of factors such as bed-form geometry, suspended fine sediment, temperature, and bed-material gradation.

Table 4-2 contains a general summary of the different experimental studies from which data have been compiled for use in the present investigation. The table includes a brief description of the types of experiments that were performed and lists the number of bed-materials tested and the number of runs made in each study.

#### 4-3-1 Properties of the Experimental Bed-Materials

The bed-material properties that are likely to be relevant to the behavior of the flow (see Section 3-2) are the size, shape, orientation, surface roughness, and density of the particles as well as the surface and volumetric distributions where these properties show any appreciable variation throughout the bed-material.

Unfortunately, with the experimental bed-materials, the only properties that have been quantitatively observed are the average density of particles and the distribution of particle sizes. The effects of particle orientation on the bed and of particle surface roughness have usually been overlooked, and observations of these properties have not been made. Although the possible effects of particle shape have usually been recognized and although quantitative measures of this quantity are available (Alger and Simons, 1968), observations for the experimental bed-materials have,







TABLE 4-2

GENERAL SUMMARY OF EXPERIMENTAL STUDIES ON SEDIMENT TRANSPORT

Number	Data Source	Date of Study	Plot Symbol	Number of		Type of Test
				Materials	Tests	
1	Colorado State University 8.0 ft. flume -----	1956-61	□	6	239	General, <sup>1</sup> and the effect of viscosity variation caused by varying the concentration of fine sediment.
2	Colorado State University 2.0 ft. flume -----	1956-61	□	4	100	Effect of gradation, and the effect of viscosity variation resulting from the variation of either temperature or turbidity.
3	C.H. MacDougall -----	1933	+	3	74	General.
4	S.D. Chyn -----	1935	+	3	32	General, and the effect of gradation.
5	A.L. Jorissen -----	1938	+	2	26	Effects of gradation and compaction.
6	U.S.W.E.S. (Sands 1-9) --	1935	×	9	335	General.
7	U.S.W.E.S. (Sand 10) ----	1936	×	1	102	Effect of rising and falling stages. (Series 1, 3, 5 - rising stage. Series 2, 4, 6 - falling stage).
8	U.S.W.E.S. (Synthetic sands) -----	1936	×	18	313	Attempt to find synthetic mixture that would not form ripples.
9	U.S.W.E.S. (Turbidity tests) -----	1935	×	1	217	Effect of turbidity.
10	T.Y. LIU -----	1937	◇	6	310	General.

<sup>1</sup>General, refers to experiments designed to study the interrelationship between hydraulic parameters rate of sediment transport, and sediment properties.



TABLE 4-2 (Continued)

Number	Data Source	Date of Study	Plot Symbol	Number of Materials	Number of Tests	Type of Test
11	M.P. O'Brien -----	1936	4	1	83	General.
12	H.J. Casey -----	1935	4	2	92	General, and the effect of gradation. Data from only 2 of 17 materials tested are available.
13	Ho, Pang-Yung -----	1939	X	6	80	The effect of particle shape and general gravel studies.
14	G. Nominco -----	1957	Z	5	25	The effect of form roughness, bed-load, and suspended load on the resistance to flow.
15	V.A. Vanoni & N.H. Brooks	1957	Z	1	16	General.
16	N.H. Brooks-----	1957	Z	2	23	General.
17	R.A. Stein -----	1965	Y	1	57	General, and the properties of bed forms.
18	Kalinske & Hsia -----	1945	X	1	9	Transport of very fine sediment.
19	Barton & Lin -----	1955	X	1	31	General.
20	E.M. Laursen -----	1958	X	2	24	General.



TABLE 4-2 (Continued)

Number	Data Source	Date of Study	Plot Symbol	Number of Materials	Number of Tests	Type of Test
21	Gilbert -----	1914	⊙	9	892	General.
22	Meyer-Peter -----	1948	△	10	120	General.
23	Bogardi and Yen -----	1939	⬆	3	48	General.
24	L.G. Straub -----	1954	Y	1	18	General.
25	Einstein (Mtn. & Goose Creeks) -----	1944	*	2	88	Transport study in natural alluvial channels
26	B. Singh -----	1960	Σ	1	305	General
				101	3659	
<u>Unnatural Weight Material</u>						
1	U.S.W.E.S. -----	1936		19	298	General. Study the suitability of various light weight materials for use as a bed material.
2	Meyer - Peter -----	1948		2	20	General.





at most, been limited to a qualitative classification (U.S. Army Corps of Engineers, 1935) of the average shape of particles contained in the material.

The distributions of particle sizes have been reported in the form of cumulative frequency curves plotting either sieve diameter, measured intermediate diameter, or fall diameter. All of these measures of particle size are dependent to some extent on particle shape, with fall diameter depending also on both particle density and surface roughness.

The particle size distribution curves for the experimental bed-materials are contained in the data report of Cooper and Peterson (1969). These curves have been summarized in Table 4-3 where, for each of the experimental bed-materials, the median diameter ( $D_{50}$ ), and the gradation ( $\sigma_b$ ) are listed along with the type and origin of the mixture and the average specific gravity of the particles.

#### 4-3-2 Experimental Equipment

The characteristics of the experimental equipment can be a major factor affecting both the reliability of the experimental results and the range of the experimental conditions. These characteristics include the type and size of the flume system, the quantity and method of placement of the bed-material, and the instrumentation and observational techniques.

The flume length should be adequate to permit the



TABLE 4-3  
SUMMARY OF THE EXPERIMENTAL BED-MATERIAL PROPERTIES

Number	Data Source	Author's Designation	Series Number	Specific Gravity	Median Diameter (mm)	Classification of Particle Shape	Classification of Mixture	Type and Origin of the Material
1	Colorado State Univ. (b=8.0 ft.).....	.19 mm .27 mm .28 mm .45 mm .93 mm .47 mm	1 2 3 4 5 6	--- --- --- --- --- ---	0.19 0.27 0.28 0.45 0.93 0.47	Well-rounded Rounded Rounded Sub-angular to sub-rounded -do.- -do.-	Clay binder removed Natural, D < 2mm Natural, unprocessed Natural, #8 >D > #200 sieve Natural, #4 >D > #16 sieve Similar to 0.45mm sand	Decomposed sandstone River sand -do.- -do.- -do.- -do.-
2	Colorado State Univ. (b=2.0 ft.).....	.32 mm .33(U) mm .33(G) mm .54 mm	1 2 3 4	--- --- --- ---	0.32 0.33 0.33 0.54	Rounded -do.- Sub-rounded Sub-angular	Similar to 0.27mm sand Uniform, #40 > D > #60 sieve Synthetic, gradation large Similar to 0.45mm sand	River sand Commercial silica sand -do.- River sand
3	C.H. MacDougall	I II III	1 2 3	2.69 2.69 2.69	0.64 0.93 1.22	Rounded -do.- -do.-	Synthetic mixture -do.- -do.-	Beach sand -do.- -do.-
4	S.D. Chyn	1 2 3	1 2 3	2.69 2.69 2.69	0.77 0.83 0.58	--- --- ---	Synthetic mixture -do.- -do.-	"Plum Island sand" -do.- -do.-
5	A.L. Jarissen	I II	1 2	2.67 2.67	0.60 0.87	--- ---	Synthetic mixture -do.-	-do.- -do.-
6	USWES (Sands 1-9)	1 2 3 4 5 6 7 8 9	1 2 3 4 5 6 7 8 9	2.65 2.65 2.65 2.65 2.65 2.65 2.65 2.65 2.65	0.397 0.450 0.476 0.436 0.400 0.326 0.283 0.181 4.10	Sub-angular to sub-rounded -do.- Sub-rounded to rounded Angular to sub-rounded Sub-angular to angular Sub-rounded to sub-angular -do.- Sub-angular to angular Sub-rounded to sub-angular	Natural mixture -do.- -do.- -do.- -do.- -do.- -do.- -do.- -do.-	River sand -do.- -do.- -do.- -do.- -do.- -do.- -do.- -do.-

\* In this study, if the specific gravity was not reported, it was assumed equal to 2.65.





TABLE 4-3 (Continued)

Number	Data Source	Author's Designation	Series Number	Specific Gravity	Median Diameter (mm)	Gradation	Classification of Particle Shape	Classification of Mixture	Type and Origin of the Material
7	USWES (Sand 10)	10	1-6	2.65	0.95	1.39	Sub-angular to angular	Synthetic mixture	See USWES sand 5 above
8	USWES (Synthetic sands)	U589	1	2.65	0.67	1.10	-do.-	Uniform	River sand
		U853	2	2.65	0.94	1.11	-do.-	-do.-	-do.-
		U293	3	2.65	0.36	1.15	-do.-	-do.-	-do.-
		A	4	2.65	0.77	1.21	-do.-	Synthetic mixture	-do.-
		B	5	2.65	0.66	1.30	-do.-	-do.-	-do.-
		C	6	2.65	0.72	1.49	-do.-	-do.-	-do.-
		D	7	2.65	1.03	1.14	-do.-	-do.-	-do.-
		E	8	2.65	0.88	1.08	-do.-	-do.-	-do.-
		F	9	2.65	1.08	1.44	-do.-	-do.-	-do.-
		G	10	2.65	0.90	1.33	-do.-	-do.-	-do.-
		H	11	2.65	0.96	1.55	-do.-	-do.-	-do.-
		I	12	2.65	0.94	1.68	-do.-	-do.-	-do.-
		U417	13	2.65	0.48	1.10	-do.-	-do.-	-do.-
		J	14	2.65	0.90	1.75	-do.-	-do.-	-do.-
		K	15	2.65	0.725	1.30	-do.-	-do.-	-do.-
		L	16	2.65	0.63	1.56	-do.-	-do.-	-do.-
		M	17	2.65	0.69	1.62	-do.-	-do.-	-do.-
		J(r)	18	See sand J					
		E(r)	19	See sand E					
		Filter	20	2.65	0.45	1.81	-do.-	Natural mixture	-do.-
		H(r)	21	See sand H					
9	USWES (Turbidity tests)	Turb.	1	2.65	0.486	1.86	-do.-	Natural mixture	---
10.	T.Y. Liu	I	1	2.66	4.30	1.16	Rounded	Synthetic mixture	River sand
		II	2	2.66	3.25	1.10	-do.-	-do.-	-do.-
		III	3	2.66	2.26	1.13	-do.-	-do.-	-do.-
		IV	4	2.66	1.48	1.22	-do.-	-do.-	-do.-
		V	5	2.66	3.60	1.21	-do.-	-do.-	-do.-
		VI	6	2.66	1.70	1.35	-do.-	-do.-	-do.-



TABLE 4-3 (Continued)

Number	Data Source	Author's Designation	Series Number	Specific Gravity	Median Diameter (mm)	Classification of Particle Shape	Classification of Mixture	Type and Origin of the Material
11	M.P. O'Brien	Columbia River Sand	1	2.57	0.360	Sub-angular	Natural mixture	Columbia River
12	H.J. Casey	h III a	1 2	--- ---	2.26 1.20	Sub-angular to rounded -do.-	Uniform Synthetic mixture	---
13	Ho, Pang-Yung	I II III IV V VI	1 2 3 4 5 6	2.58 2.58 2.58 2.58 2.58 ---	3.0 4.3 6.1 1.3 6.0 1.45	Flat -do.- -do.- -do.- -do.- Rounded	Synthetic mixture -do.- -do.- -do.- -do.- -do.-	Sand and gravel from Ruhr River -do.- -do.- -do.- -do.- -do.-
14	G. Nomieos	6 7 3 4 5	1 2 3 4 5	2.65 2.65 --- --- ---	.091 .147 .145 .137 .152	Well-rounded -do.- Sub-rounded -do.- -do.-	Synthetic mixture -do.- Unprocessed -do.- -do.-	Commercial silica sand -do.- Commercial quartz sand -do.- -do.-
15	V.A. Vanoni & N.H. Brooks	4	1	---	.137	-do.-	-do.-	-do.-
16	N.H. Brooks	1 2	1 2	--- ---	.143 .088	-do.- -do.-	-do.- -do.-	-do.- -do.-
17	R.A. Stein	---	1	---	0.4	---	Natural mixture	River sand
18	Kalinske & Hsia	---	1	2.67	.012	Spherical	Unprocessed	Commercial silica concrete admixture
19	Barton & Lin	---	1	---	.18	Well-rounded with flat mica flakes	---	50% quartz, 40% mica
20	E.M. Laursen	1 2	1 2	--- ---	.04 .11	--- ---	---	Ottawa silica sand -do.-



TABLE 4-3 (Continued)

Number	Data Source	Author's Designation	Series Number	Specific Gravity	Median Diameter (mm)	Gradation	Classification of Particle Shape	Classification of Mixture	Type and Origin of the Material
22	G.K. Gilbert	A B C D E F G H I	1	2.69	.305	---	Sub-angular	Uniform	River Sand
			1	2.69	.375	---	-do.-	-do.-	-do.-
			1	2.69	.506	---	-do.-	-do.-	-do.-
			1	2.69	.786	---	-do.-	-do.-	-do.-
			1	2.69	1.710	---	Sub-rounded	-do.-	-do.-
			1	2.69	3.170	---	-do.-	-do.-	-do.-
			1	2.69	4.938	---	-do.-	-do.-	-do.-
			1	2.69	7.010	---	-do.-	-do.-	-do.-
			1	2.69	.506	---	-do.-	-do.-	-do.-
23	Meyer-Peter	---	1	2.68	28.65	---	Well-rounded	Uniform	---
			2	2.68	5.21	---	-do.-	-do.-	---
			3	2.68	4.5	D <sub>90</sub> = 12.3mm	---	Mixture	---
			4	2.68	2.74	---	---	-do.-	---
			5	2.68	1.7-2.0	D <sub>95</sub> = 4.5mm	---	-do.-	---
			6	2.68	1.4-1.6	D <sub>95</sub> = 3.0mm	---	-do.-	---
			7	2.68	1.4	-do.-	---	-do.-	---
			8	2.68	1.3-1.5	-do.-	---	-do.-	---
			9	2.68	1.0	D <sub>95</sub> = 1.4mm	---	-do.-	---
24	Bogardi & Yen	-I II III	10	2.68	0.4	D <sub>95</sub> = 0.7mm	---	-do.-	---
			1	2.63	10.0	---	Well-rounded	Uniform	Natural river mtl., sieved into 3 uniform grades
			2	2.61	6.8	---	-do.-	-do.-	
			3	2.64	15.0	---	-do.-	-do.-	
25	L.G. Straub	---	1	---	0.185	1.40	---	Natural mixture	Missouri river sand





TABLE 4-3 (Continued)

Number	Data Source	Author's Designation	Series Number	Specific Gravity	Median Diameter (mm)	Gradation	Classification of Particle Shape	Classification of Mixture	Type and Origin of the Material
26	Einstein Mtn. Ck.	---	1	2.65	.90	1.84	---	Natural mixture	River sand-Mtn.Ck.
27	Einstein Goose Ck.	---	1	2.65	.286	1.47	---	Natural mixture	River sand-Goose Ck.
28	B. Singh		1	2.64	.62	1.13	Well rounded	Uniform	Beach sand
1	USWES(Lt.Wt.Mtl.)	H1	1	1.85	.98	1.89	Angular	Commercial mixture	Haydite
		H2	2	1.85	.92	1.88	-do.-	-do.-	-do.-
		H3	3	1.74	1.2	2.12	-do.-	-do.-	-do.-
		C1	4	1.35	3.2	1.76	-do.-	Mixture from crushing	Coal
		C2	5	1.35	1.0	2.11	-do.-	-do.-	-do.-
		C3	6	1.32	3.0	1.65	-do.-	-do.-	-do.-
		C4	7	1.32	1.5	1.47	-do.-	-do.-	-do.-
		C5	8	1.31	2.15	2.33	-do.-	-do.-	-do.-
		C6	9	1.31	1.08	1.88	-do.-	-do.-	-do.-
		C7	10	1.26	4.3	1.59	-do.-	-do.-	-do.-
		C8	11	1.26	1.12	2.03	-do.-	-do.-	Flake pitch
		R1	12	1.11	2.5	2.26	-do.-	-do.-	-do.-
		R2	13	1.11	1.3	1.82	-do.-	-do.-	Rosin
		G1	14	1.07	3.4	1.82	-do.-	-do.-	Gilsonite
		G2	15	1.07	.84	1.98	-do.-	-do.-	-do.-
		G3	16	1.05	3.4	2.01	-do.-	-do.-	-do.-
		G4	17	1.05	1.2	1.49	-do.-	-do.-	-do.-
		G5	18	1.03	3.0	2.57	-do.-	-do.-	-do.-
		G6	19	1.03	1.1	1.72	-do.-	-do.-	-do.-
2	Meyer-Peter (lignite)		1	1.25	.521	---	-do.-	---	---
3	Meyer-Peter (Baryta)		1	4.22	.521	---	-do.-	---	---



development and observation of a steady and uniform flow while allowing for entrance and exit transitions. Often the reliability of data has suffered in cases where, due to insufficient flume length, the region of observation has included part of these transition regions.

On the other hand, channel breadth is a major factor determining the effect of the channel sides in relation to the bed on the resistance to flow. For a given depth of flow, slope, and bed-material, the relative influence of the sides increases as breadth decreases. Eventually a limiting value of breadth is reached where the sides tend to influence the flow throughout the entire cross-section, and two-dimensional flow no longer exists. Consequently, if a two dimensional flow is to be simulated in a set of experiments, then the fixed breadth of a laboratory flume can have the effect of limiting the allowable experimental range of depth for a given slope and bed-material.

The bed-material should be placed in the flume to a thickness that exceeds half of the maximum bed-form height. Otherwise, local scour is capable of reaching the floor of the flume thereby inhibiting the complete and natural development of bed-forms. This, in turn, can alter the resistance to a given flow and reduce the reliability of the resulting data.

Two different types of systems have been used to handle the transported bed-material. First is the





recirculating system in which discharged sediment is directly recirculated to the upstream end of the flume. With this system the operator has no direct control over the rate of transport of bed-material since the rate of injection depends on the rate of bed-material discharge which, in turn, is dependent upon other imposed variables such as discharge and depth. In the other system sediment is injected at a controllable rate at the upstream end of the flume and independently collected upon discharge from the downstream end. Although the operator can directly impose the rate of transport of bed-material with this type of system, it has the disadvantage of being less suitable for experiments where large quantities of bed-material are transported.

Experimentation on flow in alluvial channels has suffered to some extent from a lack of standardization of the instrumentation and techniques that have been used in observing the phenomenon. Observations of depth of flow, slope, the measures of bed-form geometry, and the various rates of sediment transport have been particularly susceptible to variation caused by the method of observation.

Consider, for example, the measurement of bed-load and suspended load whose sum is equal to the total rate of transport of bed-material in experiments where there is no additional wash load. When the suspended load is measured by integrating the results of a number of point samples taken over a vertical profile that extends to a given



distance from the bed, the result is likely to include a number of particles which should normally be included as bed-load. On the other hand, in the measurement of bed-load by means of a bed-load trap, there is a distinct possibility of a portion of the saltating bed-load evading the trap and of a portion of the material moving in suspension being caught. In this case, the design of the sediment trap and point sampler, the portion of the water discharge that is drawn off through the sediment trap, and the distance from the bed at which point sampling is discontinued all have an effect on the resulting measurements.

Table 4-4 contains a brief description of the different experimental systems that have been used. For each system, it describes the geometry of the flume and the mobile bed, the type of sediment handling system, and the methods used in the measurement of sediment transport rates.

#### 4-3-3 Experimental Procedure

When conducting an experiment the values of certain controllable variables are imposed on the phenomenon by the experimenter while the values of other variables are imposed by the nature of the experimental system. These variables are often referred to as independent variables. As a result of their imposition, other dependent variables go through a process of adjustment until a state of equilibrium between the dependent and the independent variables is reached. Usually at this time, observations are made and the experiment





TABLE 4-4

## SUMMARY OF EXPERIMENTAL EQUIPMENT

No.	Source of Data	Flume System		Mobile Bed Thickness (ft.)	Type of Sediment Handling System	Sediment Transport Measurement		Remarks
		Type	Length Width (ft.) (ft.)			Total Load	Bed Susp. Load	
1	Colorado State Univ. 8.0 ft. flume -----	a, d	150.0	8.0	150.0	-	f	i - 0
2	Colorado State Univ. 2.0 ft. flume -----	a, d	60.0	2.0	60.0	-	f	i - 0
3	C.H. MacDougall ---	a, d	32.0	2.0	32.0	-	g	- n -
4	S.D. Chyn -----	a, d	32.0	2.0	32.0	-	g	- n -
5	A.L. Jorissen -----	a, d	32.0	2.0	32.0	-	g	- n -
6	USWES (Sands 1-9) -	a, d	48.0	2.30	42.0	0.167	g	- n -
7	USWES (Sand 10) ---	a, d	48.0	2.30	20.6	0.167	g	- n -

## LEGEND:

- Type of flume system
  - Recirculating, with external storage capacity. Depth is controlled by tailgate manipulation.
  - Recirculating, but with no external storage. Depth varies with quantity of water in the system.
  - Non-recirculating.
  - Variable slope.
  - Fixed slope.
- Type of sediment handling system
  - Sediment recirculated with the main flow.
  - Non-recirculating, with a manual or mechanical sand feed.
  - Non-recirculating, no feed.
- Sediment transport measurement
  - Total Load.
    - Breadth integrating slice sampler in over-flow nappe.
    - Sampling from return pipe.
    - Sampling in discharge sump
    - Point sampler in discharge nappe
    - Measurement of the rate of feed.
  - Bed Load.
    - Bed-load trap
    - Suspended Load
    - Point sampler





TABLE 4-4 (Continued)

No.	Source of Data	Flume System			Mobile Bed		Type of Sediment Handling System	Sediment Transport Measurement			Remarks
		Type	Length (ft.)	Width (ft.)	Length (ft.)	Thickness (ft.)		Total Load	Bed Load	Susp. Load	
8	USWES (Synthetic Sands) -----	a,d	25.0	1.0	25.0	-	h	-	n	-	
9	USWES (Turbidity) -	a,d	25.0	1.0	25.0	-	h	-	n	-	
10	T.Y. Liu. -----	a,d	32.0	2.67	9.8	0.167	h	-	n	-	The mobile bed was 2.0 ft. wide.
11	M.P. O'Brien -----	a,d	43.0	3.0	-	-	h	-	n	0	
12	H,J, Casey -----	-	46.0	1.31	-	-	g	-	n	-	
13	Ho, Pang-Yung -----	-	52.5	1.31	-	-	g	-	n	0	
14	G. Nominco -----	b,d	40.0	0.875	40.0	-	f	j	-	-	System contained heaters for temp.
15	Vanoni & Brooks ---	b,d	60.0	2.79	60.0	-	f	j	-	-	
16	N.H. Brooks -----	b,d	40.0	0.875	40.0	-	f	j	-	-	System contained heaters for temp.
17	R.A. Stein -----	b,d	100.0	4.0	100.0	-	f	j	-	-	
18	Kalinske & Hsia ---	a,d	80.0	2.25	-	-	f	i	-	0	
19	Barton & Lin -----	a,d	70.0	4.0	-	0.3	f	j	-	0	
20	E.M. Laursen -----	b,d	105.0	3.0	90	-	f	1	-	0	



TABLE 4-4 (Continued)

No.	Source of Data	Flume System			Mobile Bed		Type of Sediment Transport		Remarks
		Type	Length (ft.)	Width (ft.)	Length (ft.)	Thick- ness (ft.)	Hand- ling System	Measurement Total Bed Suspend Load	
22	G.K. Gilbert -----	a,d	31.5	1.96 (max.)	-	-	g	-	-
23	Meyer-Peter -----	b,e	165.0	6.57	92.0	-	g	-	- A number of smaller flumes were also used. However, their specifications are not available.
24	Bogardi & Yen -----	a,d	32.0 32.0	2.75 1.0	10.0 10.0	0.25 0.25	h	-	- Partitions were used to construct the narrow flume. In 2.75 ft. flume, bed width was 2.0 ft.
25	L.G. Straub -----	a,e	30.0	1.0	30.0	0.25	g	n	- Used for constant discharge tests.
		a,d	42.0	3.0	42.0	0.167	g	n	- Used for constant rate of transport tests.
26	Einstein (Mountain & Goose Creeks) -----	-	-	-	-	-	-	-	- Tests were performed in a natural channel which contained a bed load trap.
UNNATURAL WT. MATERIAL									
1	USWES -----	a,d	25.0	1.0	25.0	-	g	-	-
2	Meyer-Peter -----	-	-	1.16	-	-	-	-	-





is concluded.

The process of selecting and imposing one set of variables while permitting another set to adjust to a state of equilibrium constitutes the experimental procedure.

The relationship between the independent variables and two dependent variables for flow in a laboratory flume containing an alluvial bed is given by Equation 3-2 which can be combined with the continuity equation

$$Q = Vbh \quad (4-1)$$

to give

$$Q, S = \text{fn}(b, \epsilon_s, \rho_f, \mu, g, D_{50}, \sigma_b, \rho_b, \alpha_b, h, G_{tb}) \quad (4-2)$$

The variables on the RHS of this equation comprise a set of independent variables which could be imposed on the phenomenon thereby causing the dependent variables on the LHS to adjust to a state of equilibrium.

As discussed in Section 3-3 there is a distinct possibility of the relationships suggested by Equation 4-2 being multivalued. This implies that for a given set of imposed values of the independent variables the flow can adjust to one of several possible sets of equilibrium values of the dependent variables. However, this does not affect the validity of Equation 4-2 providing the multivalued nature of the relationships can be recognized in the analysis of experimental results.

Theoretically there can be a free interchange between dependent and independent variables providing all of a set of



independent variables remain truly independent of the others in the set and providing the number of independent variables remains invariant. However, in practice an independent variable is usually taken to be one that is either fixed by the nature of the experimental system or is directly controllable by the experimenter. On the other hand, a dependent variable should be one that has the freedom to self-adjust. These requirements obviously place certain limitations on the choice between dependent and independent variables.

In most of the experimental studies, the variables  $b$ ,  $\epsilon_s$ ,  $\rho_f$ ,  $\mu$ ,  $D_{50}$ ,  $\sigma_b$ ,  $\rho_b$ ,  $\alpha_b$ , and  $g$  have been fixed by the nature of the experimental system whereas  $Q$ ,  $G_{tb}$ ,  $h$ , and  $S$  have either been imposed or have been permitted to adjust as dependent variables.

Of these latter quantities, discharge ( $Q$ ) is directly controllable and is usually imposed on the phenomenon. In the case of a non-recirculating sediment injection system,  $G_{tb}$  is usually imposed as the other independent variable. The process of self-adjustment of depth and slope can then be assisted by setting an initial slope near the expected equilibrium value and by maintaining a uniform flow depth by means of tailgate manipulation. Conversely, either depth or slope must be imposed and the rate of transport of bed-material allowed to adjust in a recirculating sediment system.

Table 4-5 contains a summary of the experimental



TABLE 4-5

## SUMMARY OF THE EXPERIMENTAL OPERATING PROCEDURES

No.	Data Source	Independent Variables	Dependent Variables		Remarks
			Allowed to self-adjust	Controlled by Experimenter	
1.	Colorado State Univ. ( $b = 8.0$ ft.)	Q, S Q, h h, S	$G_{tb}$ $G_{tb}$ $G_{tb}$	h S Q	-These procedures were used interchangeably throughout the experiments in both flumes.
2.	Colorado State Univ. ( $b = 2.0$ ft.)				
3.	C. H. MacDougall	S, Q	h	$G_{tb}$	-Water surface slope adjusted by tailgate. -Sediment injected at a rate that maintained constant bed level.
4.	S. D. Chyn	Procedure same as that of MacDougall			
5.	A. L. Jorissen	Procedure same as that of MacDougall			
6.	USWES (sands 1-9)	S, Q	h	$G_{tb}$	-Sediment injection system, injection rate varied to equal transport rate. -Slope maintained at initial value by tailgate adjustment. -Several series of experiments at constant S, with Q incremented between tests.
7.	USWES (sand 10)	Procedure same as with sands (1-9), except experiments were carried through a falling stage in addition to the rising stage used in sands (1-9).			
8.	USWES (synthetic sands)	S, Q	h, $G_{tb}$		-Slope maintained constant by tailgate adjustment. -Sediment trap at D/S end, but sediment injection was not reported.
9.	USWES (turbidity tests)	Q, h, S, $C_w$	$G_{tb}$		-Turbidity varied by addition of a silt, wash load. -Sediment trap at D/S end, injection of sediment not reported.





TABLE 4-5 (Continued)

No.	Data Source	Independent Variables	Dependent Variables		Remarks
			Allowed to self-adjust	Controlled by Experimenter	
10.	T. Y. Liu	Q, S	$G_{tb}, h$		-Uniform flow maintained by tailgate adjustment. -Sediment trap at D/S end, Sediment injection was not reported.
11.	M. P. O'Brien				
12.	H. J. Casey				
13.	Ho, Pang-Yung				
14.	G. Nomicos	Q, h	$G_{tb}, S$		-Recirc. sediment system. -Depth controlled by vol. of water.
15.	V. A. Vanoni & N. H. Brooks	Procedure same as experiments by G. Nomicos			
16.	N. H. Brooks	Procedure same as experiments by G. Nomicos			
17.	R. A. Stein	Q, h	$G_{tb}, S$		-Recirc. sediment system. -Depth controlled by vol. of water.
18.	Kalinske & Hsia	S, h	$G_{tb}$	Q	-Recirc. sediment system. -Uniform depth by tailgate control.
19.	Barton & Lin	Q, S	$G_{tb}, h$		-Recirc. sediment system. -Water surface slope maintained by tailgate adjustment.
20.	E. M. Laursen	Q, h	$G_{tb}, S$		-Recirc. sediment system. -Depth controlled by vol. of water.
21.	West Bengal River Research Institute	Q, S	$G_{tb}, h$		-Uniform depth by tailgate control. -Sediment trap at D/S end. Injection of sediment at U/S end not reported.
22.	G. K. Gilbert	Q, $G_{tb}$	h, S		-Sediment injection system, with D/S trap.



TABLE 4-5 (Continued)

No.	Data Source	Independent Variables	Dependent Variables		Remarks
			Allowed to self-adjust	Controlled by Experimenter	
23.	Meyer Peter	$Q, h$	$S$	$G_{tb}$	-Depth controlled by vol. of water. -Sediment injection system with D/S trap.
24.	Bogardi & Yen	$Q, S$	$G_{tb}, h$		-Uniform flow maintained by tailgate adjustment. -D/S sediment trap, but no injection.
25.	L. G. Straub	$G_{tb}, Q$	$h, S$		-Injection elevator & sediment trap. - $G_{tb}$ const. for one series of tests, $Q$ for another.
27.	B. Singh	$S, Q$	$h$	$G_{tb}$	-Sediment injector and trap. -Uniform depth and transport rate were maintained.





procedures that have been followed in the different flume studies whose results have been utilized in the present investigation.



## CHAPTER V

### THE SCOPE OF EXPERIMENTAL CONDITIONS

#### 5-1 Requirements for Empirical Analysis

Ideally the experimental data that are used in the development of a theory should cover all combinations of conditions likely to be met in the subsequent use of the theory; otherwise, either serious extrapolation errors or invalid expressions describing only the experimental design can result. For this reason, any limitations in the scope of a set of experimental data should be noted, and the use of relationships based on such data should be limited within this scope.

To determine the effective scope of a set of experimental data it is necessary to consider: (1) the range and distribution of experimental values of each variable in a set of independent variables and (2) the joint distribution between pairs of these variables. To illustrate this requirement, let us consider a hypothetical phenomenon whose behaviour can be completely specified by the two independent variables  $M$  and  $N$ . Suppose that an experimental investigation is to be carried out to determine the form of the relationship

$$Z = f(M,N) \qquad (5-1)$$

where  $Z$  is a dependent variable. Also suppose that in the natural phenomenon the possible conditions of behaviour fall



within the region (R) in Figure 5-1 such that

$$M_1 < M < M_2 \quad \text{and} \quad N_1 < N < N_2$$

and that the true relationship of Equation 5-1 is shown by the curves of constant Z in Figure 5-1.

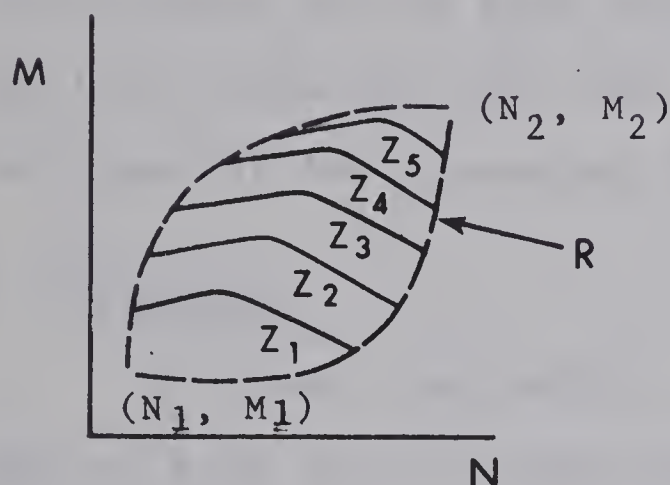


Figure 5-1

$Z=f(M,N)$  for  
Conditions in Natural  
Phenomenon

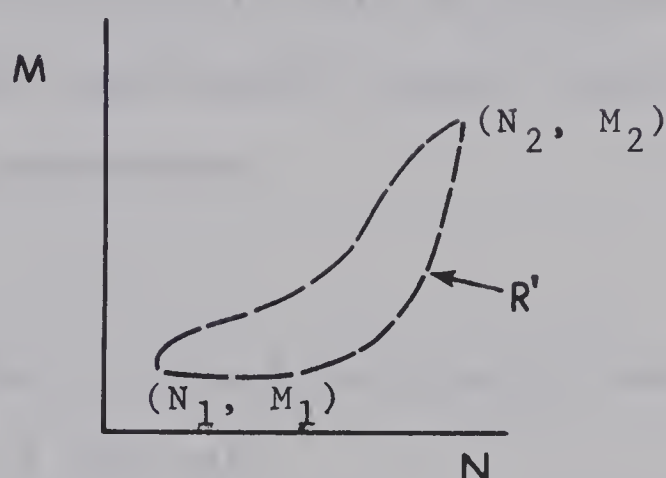


Figure 5-2

$Z=f(M,N)$  for  
Experimental Conditions

If Equation 5-1 is to be empirically evaluated, then the experiments should be designed so that experimental points are obtained throughout the entire region R. To illustrate, consider a set of experiments where all points fall within the region R' in Figure 5-2. Although the experimental range of the individual independent variables M and N is the same as in the natural phenomenon, there is a considerable portion of the region R (Figure 5-1) where there have been no experimental points obtained.

Consequently, an empirical analysis could not detect the existence of the transition in the relationship  $Z=f(M,N)$  or the form of the relationship for values of N above this





transition. Because of the nature of the relationship being studied and because of the nature of the experiments, which have been designed so that  $M$  is nearly a function of  $N$ , it would even be difficult to determine the true form of Equation 5-1 within the region  $R'$ . It is likely that a relationship of the form  $Z=f(M)$  or  $Z=f(N)$  would be reported, and this would describe only the experimental design and not the physical law governing the phenomenon.

## 5-2 Variables

In flume experiments, observations have usually been made on each of the quantities in the set

$$A_1 = (Q, b, h, S, C_{tb} \text{ (or } G_{tb}), D_{50}, \sigma_b) \quad (5-2)$$

The quantities  $\rho_f$  and  $\rho_b$  have not been included in this set since both have been relatively constant throughout the majority of flume experiments. Viscosity, on the other hand, has varied over a limited range due to variations in temperature and concentration of suspended fine sediment, but it has been omitted because of the scarcity of available measurements.

The existing theories on flow in alluvial channels are usually expressed in terms of parameters made up from the above basic quantities and the unmeasured viscosity which is usually given an assumed value. Some of the more common parameters are contained in the set



$$A_2 = (V, \frac{VD_{50}}{v}, \frac{V^2}{h}, \frac{V^2}{D_{50}}, h, S, \frac{V_* D_{50}}{v}, \frac{V^2}{h}, \frac{V_*^2}{D_{50}}, \frac{QS}{b}, \frac{\bar{C}}{\sqrt{g}}, f, n) \quad (5-3)$$

Additional parameters not included in this set can usually be formed either by the use of a constant or by combining two or more parameters.

### 5-3 Range and Distribution of Parameters

The experimental data summarized in Table 4-2 have been analyzed to determine the range and distribution of experimental values of each of the parameters contained in sets  $A_1$  and  $A_2$  (Equations 5-2 and 5-3). The results of this analysis are given in Table 5-1 where the distribution of experimental values has been approximately represented by listing, for each parameter, the mean, the standard deviation, the minimum, the maximum, and five intermediate percentiles (10%, 25%, 50%, 75%, and 90%).

These results demonstrate the effect that limitations in the experimental systems have had on the scope of experimental results. For example, in 90 per cent of the tests, discharges were less than 6.92 cfs, depths were less than 0.719 feet, and breadths were less than 6.56 feet. Because of these restrictions, there is a scarcity of data having large values of velocity ( $V$ ), large values of  $h/D_{50}$ , and small values of slope ( $S$ ). Ninety per cent of the experiments had slopes greater than or equal to 0.001 and  $h/D_{50}$





TABLE 5-1  
DISTRIBUTION OF EXPERIMENTAL VALUES OF OBSERVED AND COMPUTED  
QUANTITIES FOR EXISTING FLUME EXPERIMENTS

	Mean Value	Standard Deviation	Min Value	Percentiles					Maximum Value
				10%	25%	50%	75%	90%	
Q (cfs)	3.251	12.12	0.016	0.212	0.363	0.789	1.465	6.92	162.9
V (ft/sec)	2.073	1.081	0.344	1.115	1.352	1.723	2.563	3.403	9.448
h (ft)	0.355	0.309	0.030	0.102	0.168	0.255	0.500	0.719	3.583
b (ft)	2.52	2.70	0.230	0.830	1.00	1.96	2.69	6.56	8.0
C <sub>tb</sub> (ppht)	266.3	647.2	0.0	1.7	7.7	26.2	239.1	870.0	11,000.0
G <sub>tb</sub> (lb/sec/ft x10 <sup>2</sup> )	15.47	63.64	0.0	0.0339	0.1809	0.8785	9.022	31.58	1226.0
S (%)	0.462	0.518	0.005	0.10	0.10	0.225	0.610	1.18	3.10
hS (ft) x 10 <sup>3</sup>	1.188	1.841	0.031	0.243	0.427	0.675	1.274	2.427	28.58
D <sub>50</sub> (mm)	1.445	3.098	0.011	0.30	0.42	0.62	0.96	3.3	28.65
h/D <sub>50</sub>	247.7	760.7	4.816	20.07	51.52	117.0	264.4	489.4	18,330.
b/h	10.12	11.34	0.6319	2.000	3.704	6.936	12.31	21.37	89.60
QS/b (ft <sup>2</sup> /sec x10 <sup>2</sup> )	4.067	13.43	0.0107	0.2722	0.5861	1.177	3.278	7.762	270.0
V <sub>*</sub> D <sub>50</sub> /ν	143.8	654.1	0.1964	11.72	18.78	30.68	53.86	206.4	9012.
V D <sub>50</sub> /ν	1562.	6911.	3.027	136.6	225.3	380.3	687.4	2517.	88,810.
Chezy C/ √g	12.40	2.807	4.998	9.053	10.46	12.50	14.04	15.40	43.80
Darcy-Weisbach f	0.0603	0.0295	0.0042	0.0336	0.0405	0.0511	0.0730	0.0974	0.3198
Manning n (ft <sup>1/6</sup> )	0.0181	0.00518	0.00515	0.0127	0.0143	0.0170	0.0212	0.0357	0.0446
V <sub>*</sub> <sup>2</sup> /D <sub>50</sub> (ft/sec <sup>2</sup> )	17.77	27.63	0.4834	2.608	4.036	8.823	22.23	41.32	604.1
V <sup>2</sup> /D <sub>50</sub> (ft/sec <sup>2</sup> )	2999.	6404.	117.2	413.3	624.7	1070.	3002.	7278.	207,800.
V <sup>2</sup> /h (ft/sec <sup>2</sup> )	23.43	31.39	0.5854	2.577	5.685	11.12	31.11	57.87	402.7



values smaller than 489.4. Since values outside these limits commonly occur both in canals and in natural channels, there is a definite need to extend the experimental scope of both these parameters. Unfortunately, experiments capable of accomplishing this will require expensive, large scale experimental equipment.

Experimental values of  $b/h$  are in most cases considerably less than the values commonly found in nature. However, with the exception of values less than about 5.0 where the effect of channel sides may be significant, the  $b/h$  ratio probably has little influence on the behaviour of the phenomenon. In any event, since the effective range of this parameter is from about 2.0 to 20.0, there appears to be sufficient data to permit an evaluation of its influence.

Table 5-1 shows a rather narrow range of bed-material sizes in the existing flume experiments. The median diameter was less than 3.3 mm in 90 per cent of the tests and less than 0.96 mm in 75 per cent of the tests. Only about 10 per cent of the data had bed-materials having median diameters falling within the gravel range ( $D_{50} > 3\text{mm}$ ).

The distribution of gradation ( $\sigma_b$ ) for the experimental bed-materials is such that the majority of experiments have used either uniform sized materials or natural alluvial mixtures. Although this quantity is not included in Table 5-1, a close examination of the data revealed that 45.8 per cent of the experiments had approximately uniform bed-materials





having values of gradation less than 1.20, and 40.2 per cent had bed-materials with natural gradations falling between 1.20 and 1.70. Only 14 per cent of the experiments had bed-materials with gradations exceeding 1.70.

It is interesting to note that the variation in gradation ( $\sigma_b$ ) has been much greater for the experimental bed-materials than for the bed-materials usually found in natural channels. Consequently, the main reason for examining the effect of  $\sigma_b$  is to determine the validity of theories that have been based on experiments with unnaturally graded bed-materials.

One aspect of the phenomenon that appears to be fully covered in the flume experiments is the range of concentrations of transported bed-material where experimental values of  $C_{tb}$  range from 0.0 to 11,000 ppht. A full 10 per cent of the tests had  $C_{tb}$  values less than 1.7 ppht which covers the important region near the beginning of transport.

The distribution of experimental values of the parameters in sets  $A_1$  and  $A_2$  have also been determined for each bed-material that has been tested and for each source of flume data listed in Table 4-2. In Tables B-1 and B-2 of Appendix B these distributions have been approximated by listing the minimum and maximum values, the first and third quartiles, and the median value for each parameter.





#### 5-4 The Joint Distribution and Experimental Correlation Between Parameters

The flume data have also been analyzed to determine the joint distribution and the approximate experimental correlation between pairs of the parameters

$$\left( Fr', S, \frac{h}{D_{50}}, C_{tb}, V_i, \frac{b}{h} \right)$$

taken from the mathematic model developed in Chapter III. In this analysis the data were first grouped into intervals on one of a pair of these parameters. The data in each interval were then examined to determine the effective range of experimental values of the other parameter, and the results were presented by plotting, for each interval, the mean value of the first or grouped parameter against the median, the second, tenth, ninetieth, and ninety-eighth percentiles of the other parameter. The plots resulting from this analysis have been placed in Appendix C.

In these plots the bands formed by the second and ninety-eighth percentiles give the effective range of experimental values for this set of parameters and form the limiting boundaries for the application of the design method developed in the following chapter. On the other hand, the trend of these bands and of the median value curves indicates the level of experimental correlation existing between the various pairs of parameters. The results of these plots have been summarized in Table 5-2 where an assessment has been



TABLE 5-2

## EXPERIMENTAL CORRELATION AND JOINT DISTRIBUTION BETWEEN EXPERIMENTAL VALUES OF PAIRS OF PARAMETERS

Parameter <sup>1</sup> Pair	Level of Assoc.	Cause of Assoc.		Remarks	
		Natu- ral	Exp.	Correlation	Scope
Fr'-S (C-1)	high	x			
Fr'-h/D <sub>50</sub> (C-2)	high	x	x	Limited discharge capacity would result in large values of Fr' associated with small h/D <sub>50</sub> values.	General shortage of high h/D <sub>50</sub> values, particularly at high levels of Fr'.
Fr'-C <sub>tb</sub> (C-3)	high	x		Fr' is likely a good predictor of C <sub>tb</sub> .	Shortage of low C <sub>tb</sub> values at Fr' levels greater than about 0.5.
Fr'-b/h (C-4)	med.				A large amount of data are available with b/h values greater than 5.0 at all levels of Fr'.
Fr'-Vi (C-5)	low	x	x	It is necessary to increase Fr' as Vi increases to obtain given level of C <sub>tb</sub>	Shortage of high Vi values at levels of Fr' greater than about 0.8.
S-h/D <sub>50</sub> (C-7)	high	x	x	High values of slopes have resulted in small depths because of a limited discharge capacity.	Shortage of high h/D <sub>50</sub> values at the higher levels of slope.
S-C <sub>tb</sub> (C-6)	high	x		Slope, like Fr', is a good predictor of C <sub>tb</sub>	Deficiency in small C <sub>tb</sub> values at high slopes. This implies a deficiency of large D <sub>50</sub> values.

<sup>1</sup>Number in brackets refers to Figure number in Appendix C.





TABLE 5-2 (Continued)

Parameter Pair	Level of Assoc.	Cause of Assoc.			Remarks	
		Natural	Exp.	Spurious	Correlation	Scope
S-b/h (C-8)	none					
S-Vi (C-9)	low	x	x		Same as Fr'-Vi	
$h/D_{50}$ - $C_{tb}$ (C-14)	none					Deficiency in large values of $h/D_{50}$ at all levels of $C_{tb}$ .
$h/D_{50}$ -b/h (C-10)	med.			x		
$h/D_{50}$ -Vi (C-11)	high	x		x		Deficiency in high Vi values for $h/D_{50} > 50$
$C_{tb}$ -b/h (C-15)	none					
$C_{tb}$ -Vi (C-13)	very low	x			$C_{tb}$ naturally tends to be somewhat less for larger materials. Natural association may be higher than experimental association.	
b/h-Vi (C-12)	none					Deficiency in high Vi values for b/h levels exceeding 5.



made of the level of experimental correlation between pairs of parameters, the probable causes of this correlation, and any serious deficiencies or gaps in the available experimental data.

There appear to be three main causes of experimental correlation between pairs of parameters. First is a natural cause and effect relationship that might exist between the parameters. An example would be the natural correlation between  $Fr'$  and  $S$  that appears in observations on natural channels as well as in data from flume experiments. Other clear examples of pairs of parameters that appear to be correlated through a natural cause and effect relationship include  $Fr'$  and  $C_{tb}$  and  $S$  and  $C_{tb}$ .

Correlation between experimental values of parameters can also result from limitations in the experimental systems used. For example, the experimental data show a high level of correlation between  $S$  and  $h/D_{50}$ ; this can be attributed partly to limitations in discharge capacity which would result in a reduction of depth as slope increases; however, to a certain extent there is likely a cause and effect relationship that also contributes to the high degree of correlation found in the experimental values of these two parameters. The association between  $Fr'$  and  $h/D_{50}$ , between  $Fr'$  and  $Vi$ , and between  $S$  and  $Vi$  all appear to result partly from experimental limitations and partly from a cause and effect relationship.



Finally, a spurious correlation can exist between two parameters when the same variable is contained in both parameters. For example, a high level of correlation exists between the experimental values of  $h/D_{50}$  and  $V_i$  because of the presence of the variable  $D_{50}$  in each parameter. However, the form of the relation between these two parameters (see Figure C-11) suggests that  $h$  and  $D_{50}$ , the two variable quantities contained in the parameters, are actually unrelated.

An examination of the plots in Appendix C showed a number of deficiencies to exist in the existing body of experimental data. The more important of these have been listed in Table 5-2 and include a lack of high experimental values of  $h/D_{50}$  at all levels of  $C_{tb}$  and particularly at the higher levels of  $Fr'$ ,  $S$ , and  $V_i$ ; a shortage of high values of  $V_i$  corresponding to  $h/D_{50}$  values greater than about fifty; and a shortage of small values of  $C_{tb}$  at the higher levels of both  $S$  and  $Fr'$ . All of these deficiencies can generally be attributed to limitations in the experimental systems. Again, future experiments designed to provide data covering these conditions will require systems capable of handling extremely large discharges and bed-material sizes.





## CHAPTER VI

### PRESENTATION AND DISCUSSION OF RESULTS

#### 6-1 General

In Chapter III dimensional analysis was used to develop the functional equations

$$0 = \text{fn}(\text{Fr}', C_{tb}, \frac{h}{D_{50}}, V_i, \frac{b}{h}, \sigma_b) \quad (6-1)$$

and

$$0 = \text{fn}(S, C_{tb}, \frac{h}{D_{50}}, V_i, \frac{b}{h}, \sigma_b) \quad (6-2)$$

which together form a mathematic model of a steady and uniform flow in a rigid sided flume containing an alluvial bed. It was assumed that the specific gravity of the bed-material is approximately equal to 2.65, and that the effect of variation in shape, orientation, and surface roughness of particles is negligible.

Equations 6-1 and 6-2 can be combined to form

$$0 = \text{fn}(\text{Fr}', S, \frac{h}{D_{50}}, V_i, \frac{b}{h}, \sigma_b) \quad (6-3)$$

in which the concentration of transported bed-material has been eliminated. This latter equation describes the resistance to flow in an alluvial channel which is an aspect of the phenomenon that has been fully examined by Alam, Cheyer and Kennedy (1966) by a similar approach to that followed in the present study. Equations 6-1 and 6-2, on



the other hand, can be broadly classified as bed-material transport equations.

The present chapter is concerned with the presentation and discussion of the results of an empirical evaluation of Equations 6-1 and 6-2. This evaluation has primarily been based on data from the laboratory flume studies described in Chapter III. However, in the few cases where  $C_{tb}$  has been observed in natural channels, these observations have been used to test the results obtained from the analysis of flume data.

The analysis of data and the preparation of plots were carried out on the IBM model 360-67 computer and the CalComp model 770/663 plotter at the University of Alberta Computing Centre. Consequently much of the work has consisted of the preparation of data into a form suitable for analysis and the development of programs for performing this analysis. Appendix A contains abstracts of the different computer programs that were used.

## 6-2 Method of Analysis

The basic problem in the analysis was to determine the relationship between the six parameters contained in each of the two functional equations. Because of the large number of parameters involved, the equations were initially simplified to the form

$$0 = f_n(Fr', C_{tb}, \frac{h}{D_{50}}) \quad (6-4)$$





and

$$0 = \text{fn}(S, C_{tb}, \frac{h}{D_{50}}) \quad (6-5)$$

by assuming the effects of  $V_i$ , and  $\sigma_b$  to be negligible over the range of conditions considered in the analysis.

If these assumptions are valid, then the solution for each simplified equation can be represented by a surface in the three dimensional coordinate system formed from the parameters. Consequently, each relationship was investigated by plotting data on the plane formed by two of the parameters and by contouring the resulting plots for different levels of the third parameter. This process was repeated on each of the three possible coordinate planes in order to better define the solution surface.

The solution surfaces represented in this manner consisted of a family of curves with each curve relating two of the parameters at a constant level of the third parameter. However, since the third parameter was in most cases a continuous variable, the data plotted on each curve actually covered a selected range of values of this third parameter. Consequently the scatter exhibited by the plots could be attributed partly to variation of the third parameter within the selected interval, partly to experimental error, and partly to the possible effect of the parameters  $V_i$ ,  $b/h$ , and  $\sigma_b$  which was initially assumed to be negligible. The validity of these initial assumptions



was tested by examining the scatter in the above plots to determine if it could be attributed to variation in any of these three parameters. If values of the parameters appeared to vary randomly throughout the scatter plots then the assumptions were considered to be valid. On the other hand, a systematic variation would indicate that the parameter did have a significant effect on the phenomenon.

By analyzing data in which the type of bed-form had been observed, the role of bed-forms in each of the relationships was examined. The boundaries between the different bed-form regions were determined on each solution surface for the purpose of providing a method for the prediction of bed-forms.

### 6-3 The Relationship between $Fr'$ , $C_{tb}$ and $h/D_{50}$

The relationship suggested by Equation 6-4, is shown in Figures 6-1, 6-2, and 6-3. In Figure 6-1 the experimental data have been plotted on the  $Fr'$ - $C_{tb}$  plane with different plots corresponding to different levels of  $h/D_{50}$ . In each of these plots the range of values of  $h/D_{50}$  has been minimized in order to reduce the scatter attributable to variation in this parameter. Different plotting symbols have been used to identify the various sources of data as described in Table 4-2. Because the use of narrow and separated intervals of  $h/D_{50}$  has resulted in the exclusion of much of the data, similar but more comprehensive plots





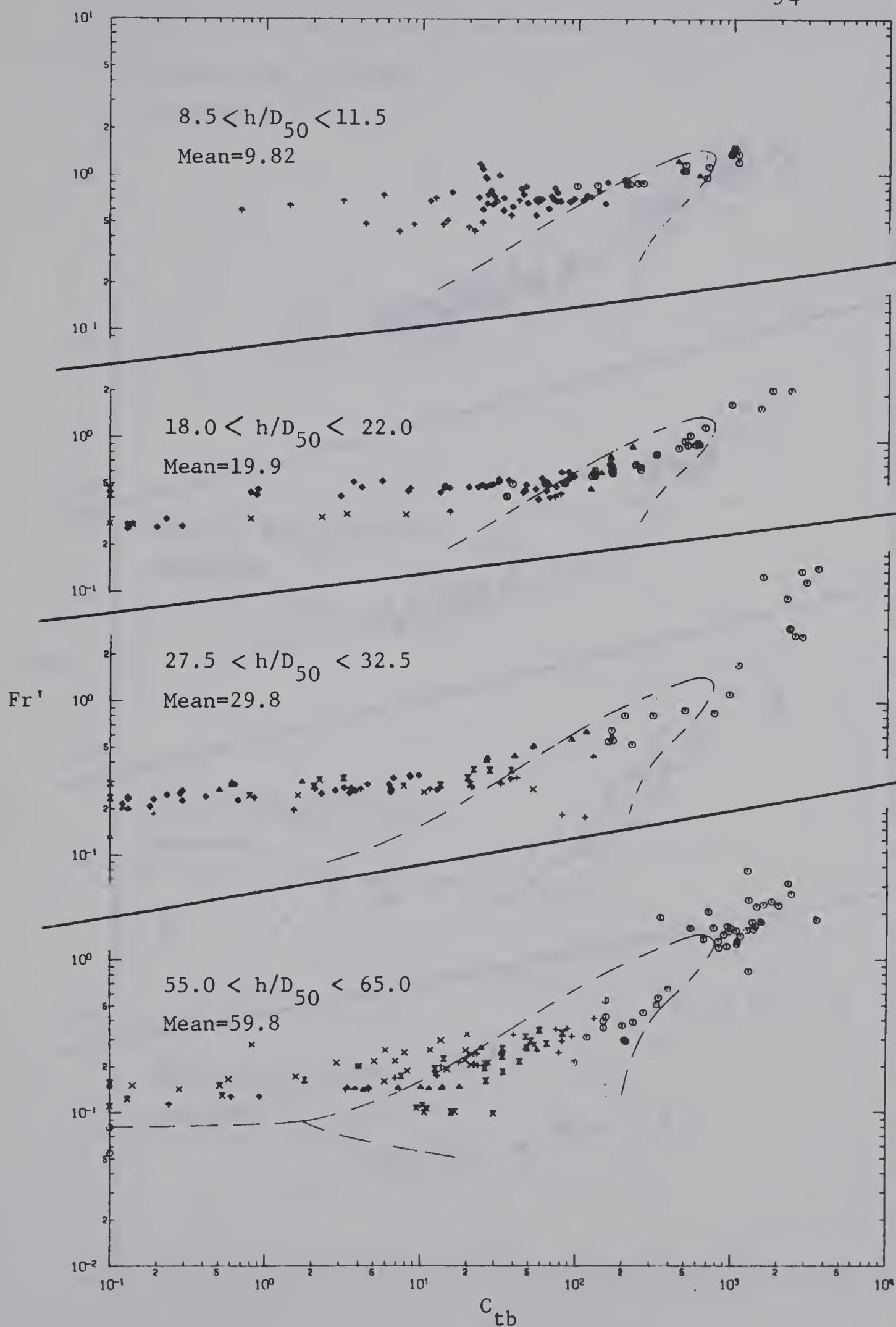


Figure 6-1. Variation of  $C_{tb}$  with  $Fr'$  at Different Levels of  $h/D_{50}$





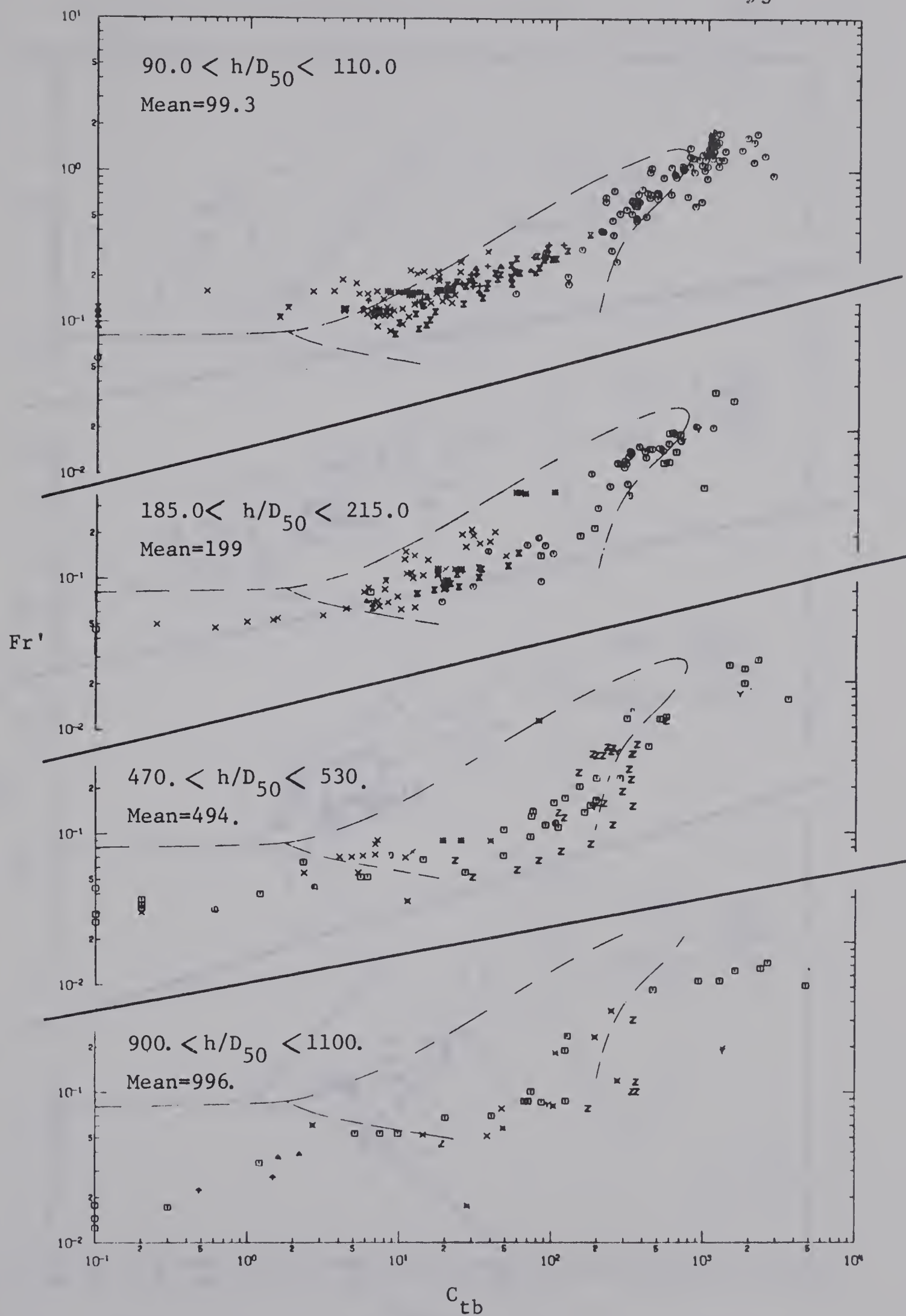


Figure 6-1. (Continued)



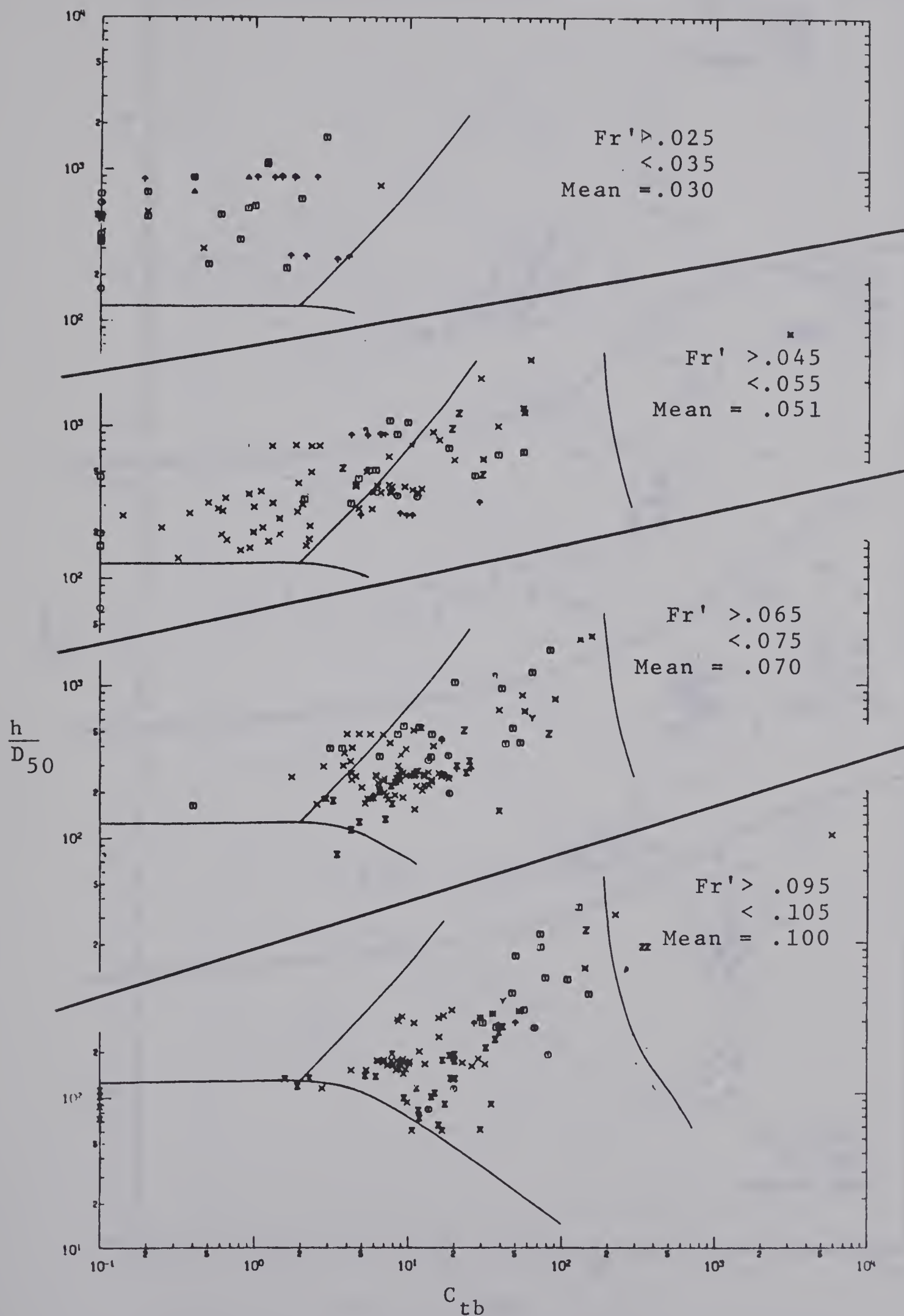


Figure 6-2. Variation of  $C_{tb}$  with  $h/D_{50}$  at Different Levels of  $Fr'$





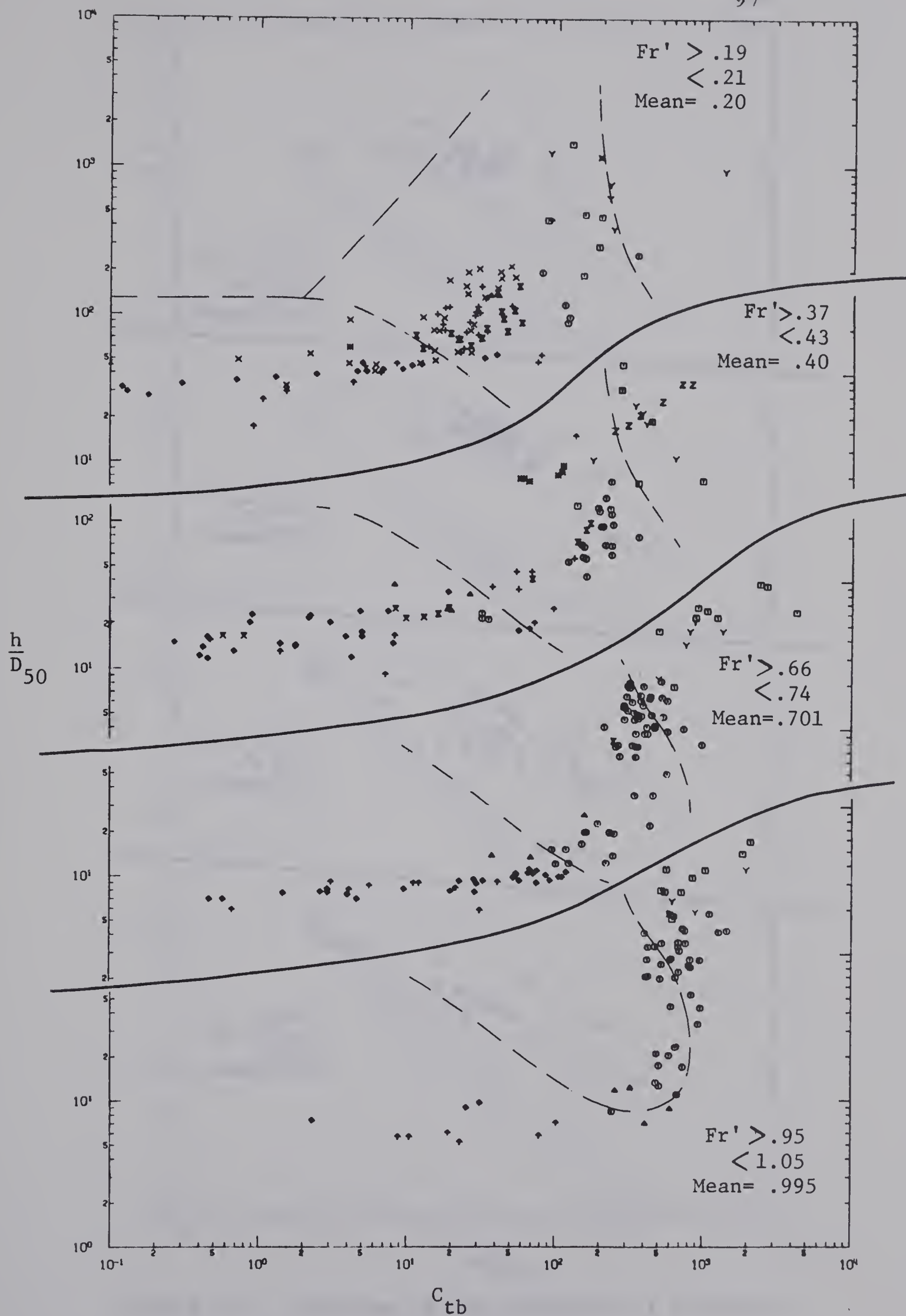


Figure 6-2 (Continued)



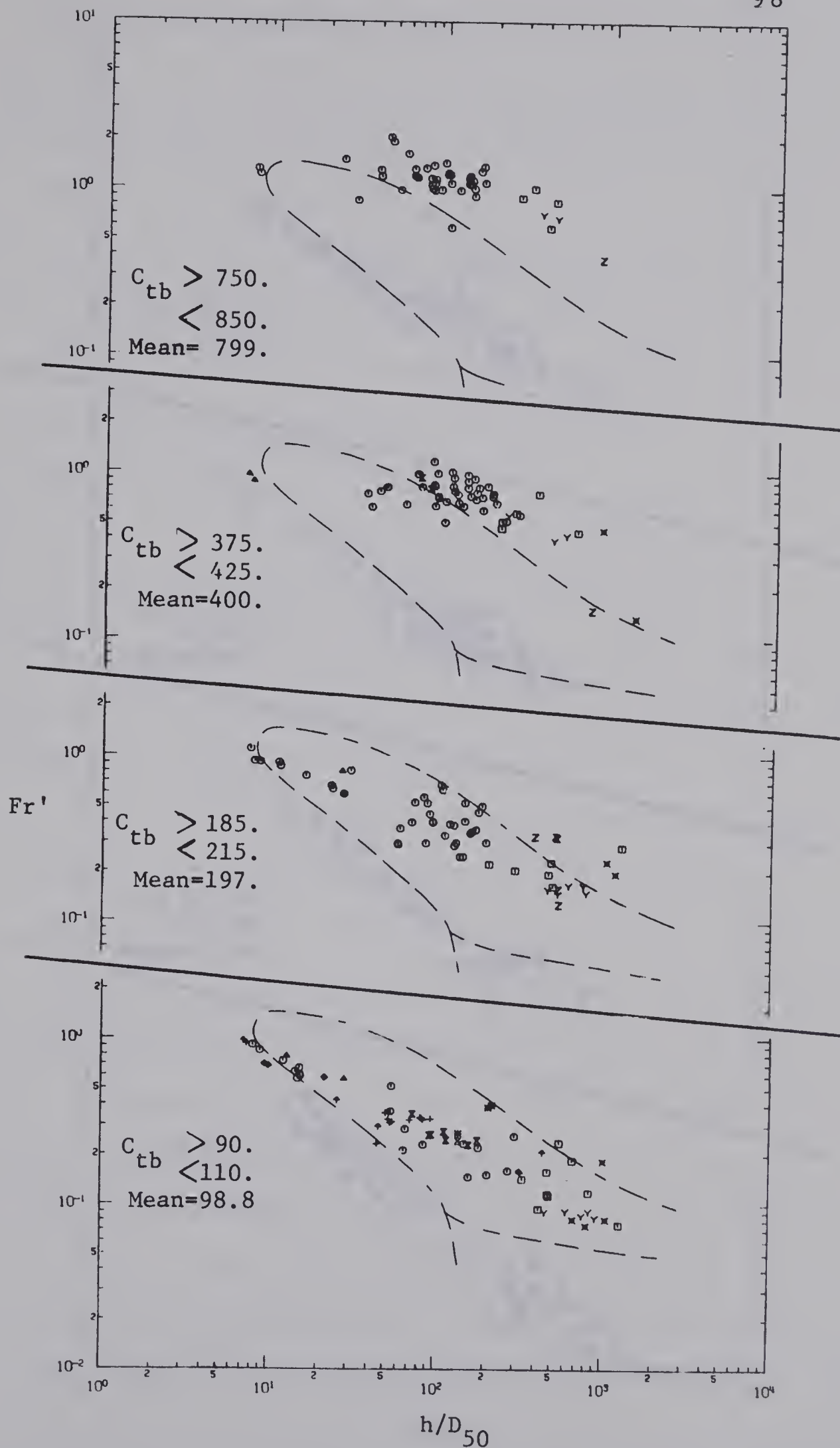


Figure 6-3. Variation of  $h/D_{50}$  with  $Fr'$  at Different Levels of  $C_{tb}$



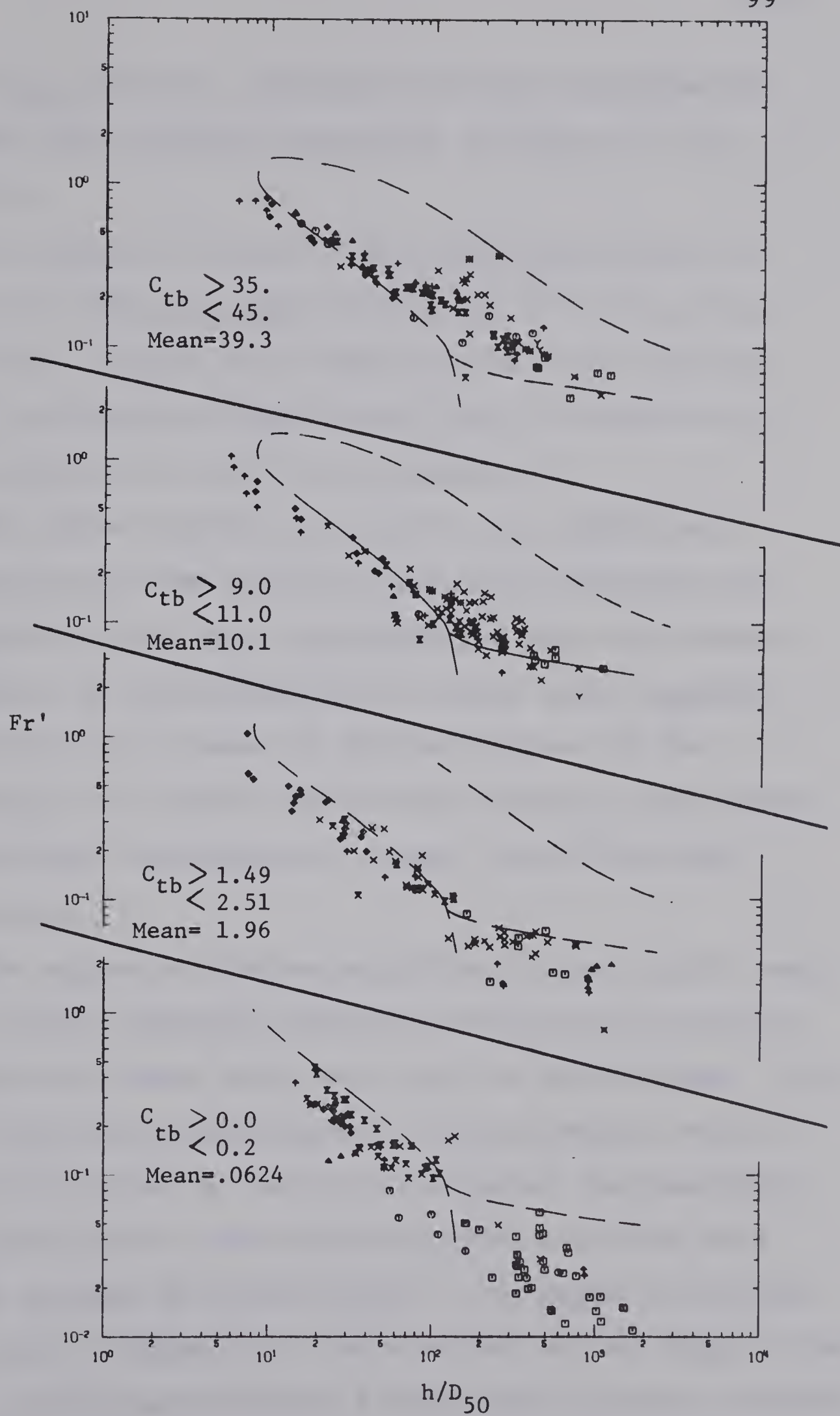


Figure 6-3 (Continued)





having  $h/D_{50}$  intervals covering the entire experimental range have been prepared and placed in Figure D-1 of Appendix D.

In Figures 6-2 and 6-3 the same relationship is shown on the  $h/D_{50}-C_{tb}$  plane and on the  $Fr'-h/D_{50}$  plane respectively. Again, more comprehensive plots covering the full experimental range of the third parameter are given in Figures D-2 and D-3 of Appendix D.

The above scatter plots give a two dimensional representation of the solution surface for Equation 6-4. It is apparent from this representation that the surface has a number of discontinuities in shape which suggests the existence of a number of distinct phases in the relationship. It remains to be seen whether or not these discontinuities correspond to changes in the bed-form configuration.

The degree of scatter exhibited in these plots tends to vary between different regions of the solution surface and between the three different views of this surface. This scatter can be attributed partly to experimental error, partly to variation in the third parameter, and possibly to the variation of other parameters whose effects were initially assumed to be negligible. The degree of scatter appears also to depend to a large extent on the shape of the solution surface particularly in the case of scatter caused by variation in the third parameter.



Earlier in this chapter it was assumed that variation in  $V_i$ ,  $b/h$ , and  $\sigma_b$  had a negligible effect on the relationship between  $Fr'$ ,  $C_{tb}$  and  $h/D_{50}$ . In the present section these assumptions were tested by examining individually the variation of each of these parameters within scatter plots of  $Fr'$  against  $C_{tb}$  for a number of levels of  $h/D_{50}$ .

In Figure 6-4 the effect of  $V_i$  is examined in four plots on the  $Fr'$ - $C_{tb}$  plane, each at a different level of  $h/D_{50}$ . For these plots, five different intervals of  $V_i$  were chosen, and the data falling in each interval were identified by the use of a different plotting symbol.

In plots (a), (b), and (c) of this figure, variation in  $V_i$  appears to have little or no effect on the relationship since the points at each level of  $V_i$  scatter at random throughout the overall scatter band. The plots cover an  $h/D_{50}$  range of 10.0 to 400.0; however, the maximum average value of  $V_i$  in each plot varies with  $h/D_{50}$ . At the  $h/D_{50}$  levels of about 15, 90, and 330 respectively, these maximum average values are 139.0, 53.4, and 20.6, and the corresponding maximum values of  $D_{50}$  are 6.2, 2.4, and 0.92 mm ( $D_{50} = 0.0445 V_i$  at  $v = 10^{-5}$ ). On the other hand, the minimum average value of  $V_i$  in each plot appears to be at least as small as values likely to be encountered in nature. In plot (d) which contains data having  $h/D_{50}$  values greater than 800.0, all of the data points correspond to the lowest  $V_i$  interval ( $V_i < 10.0$  or  $D_{50} < .445$  mm);





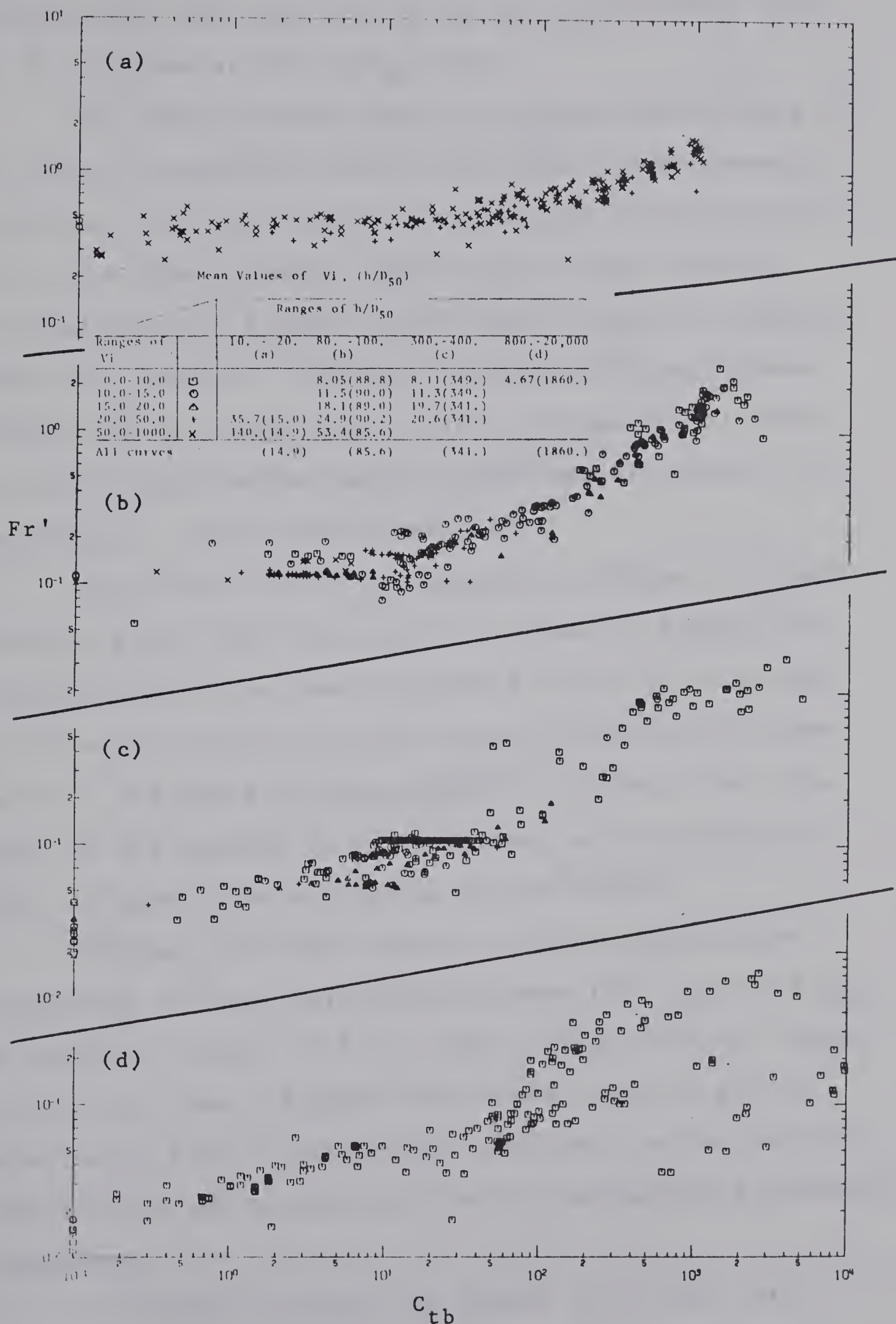


Figure 6-4. Variation of  $C_{tb}$  with  $Fr'$  and  $Vi$  at Different Levels of  $h/D_{50}$



consequently, the effect of  $V_i$  on the relationship could not be assessed at this  $h/D_{50}$  level.

The above results appear to verify the validity of the initial assumption within the scope of experimental conditions covered. However, because of limitations in this scope, the practical application of any results obtained from the present investigation should be limited within the range of conditions mentioned above. These limitations are shown more clearly in Figure C-11 where the joint distribution between experimental values of  $V_i$  and  $h/D_{50}$  is represented graphically.

The effect of  $b/h$  is examined in Figure 6-5 which contains plots that are similar to those in Figure 6-4 except the data have been separated into five intervals of  $b/h$  with the data in each interval identified by the use of a different plotting symbol. In these plots the range of  $b/h$  appears to be sufficient at all levels of  $h/D_{50}$  to permit the evaluation of its effect.

Fortunately there appears to be no significant difference in the relationship between  $Fr'$ ,  $C_{tb}$  and  $h/D_{50}$  at different levels of  $b/h$ . This is true even for values of  $b/h$  less than 3.0 where the channel sides might be expected to have a considerable influence on the velocity distribution and consequently on the bed-material transport phenomenon.

To further examine the effect of  $b/h$  the ratio



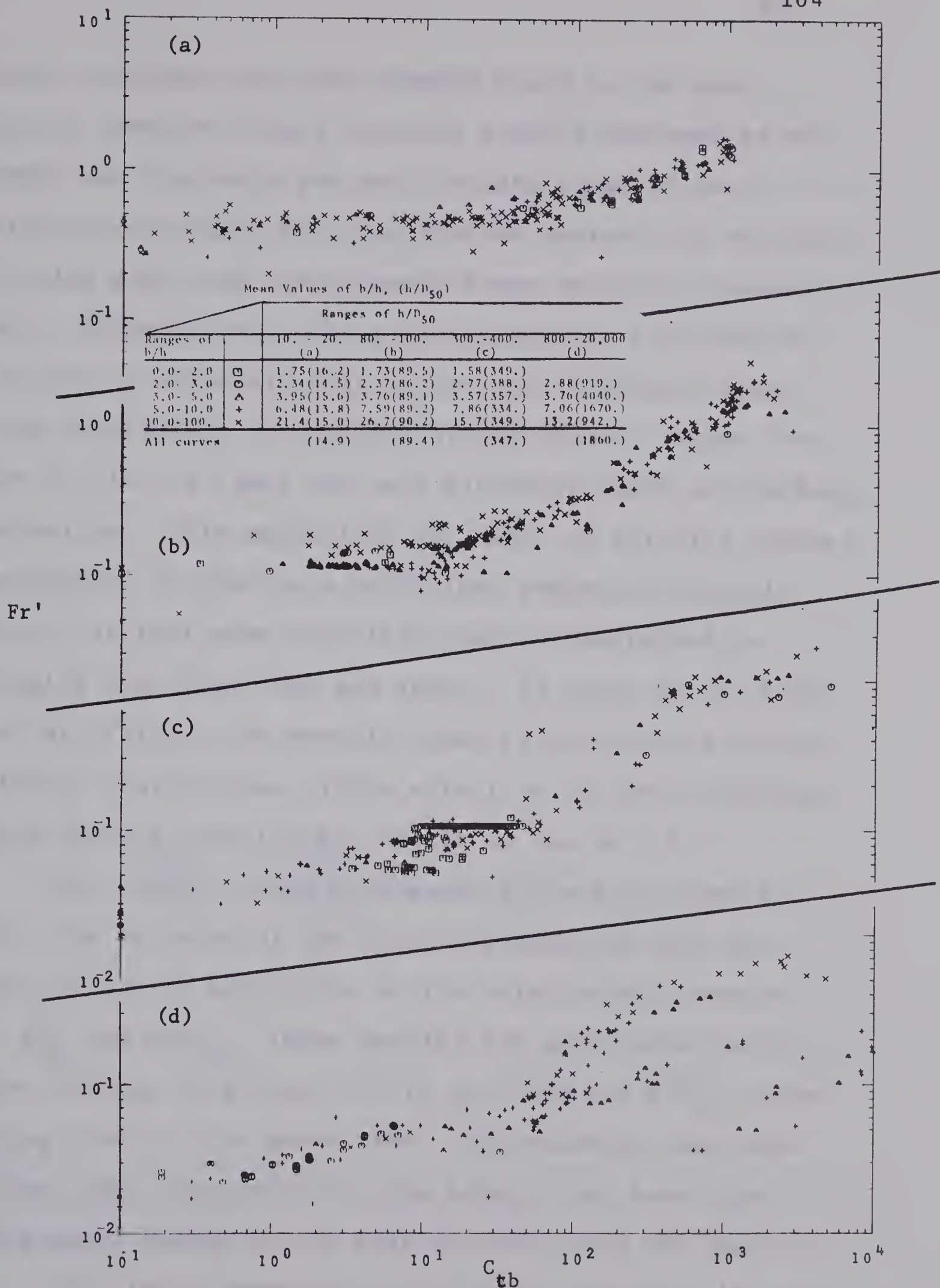


Figure 6-5. Variation of  $C_{tb}$  with  $Fr'$  and  $b/h$  at Different Levels of  $h/D_{50}$





between discharge per unit breadth based on the mean velocity computed from a velocity profile observed at mid-channel and discharge per unit breadth based on the continuity principle has been plotted against  $b/h$  in Figure 6-6 using data from the Colorado State University experiments. Unfortunately, the level of scatter exhibited by this plot is extremely high as the unit discharge based on the observation of velocity at mid-channel ranges from about 0.5 to 1.5 times the unit discharge based on discharge observation. This emphasizes the need, in alluvial channel experiments, to observe a sufficient number of velocity profiles so that mean velocities can be determined by averaging over both time and space. In spite of the high level of scatter, the overall trend of the plotted points indicates that  $b/h$  has little effect on the unit discharge at mid-channel even for  $b/h$  values as low as 2.5.

The results shown in Figures 6-5 and 6-6 tend to verify the validity of the initial assumption that the effect of  $b/h$  is negligible on the relationship between  $Fr'$ ,  $C_{tb}$  and  $h/D_{50}$ . These results are applicable for  $b/h$  values ranging from about 2.0 to 20.0 and for  $h/D_{50}$  values ranging from 15.0 to about 1800. Consequently, the data have not been corrected for side effects nor have data having small values of  $b/h$  been excluded from the analysis.

The final assumption to be tested involves the effect of the gradation ( $\sigma_b$ ) of the bed-material. Although this



quantity remains relatively constant in the bed-materials found in natural channels, a wide variation in gradation has existed between the different experimental bed-materials. For this reason it was necessary to examine the effect of  $\sigma_b$  in order to justify the use of experimental data having unnatural values of bed-material gradation.

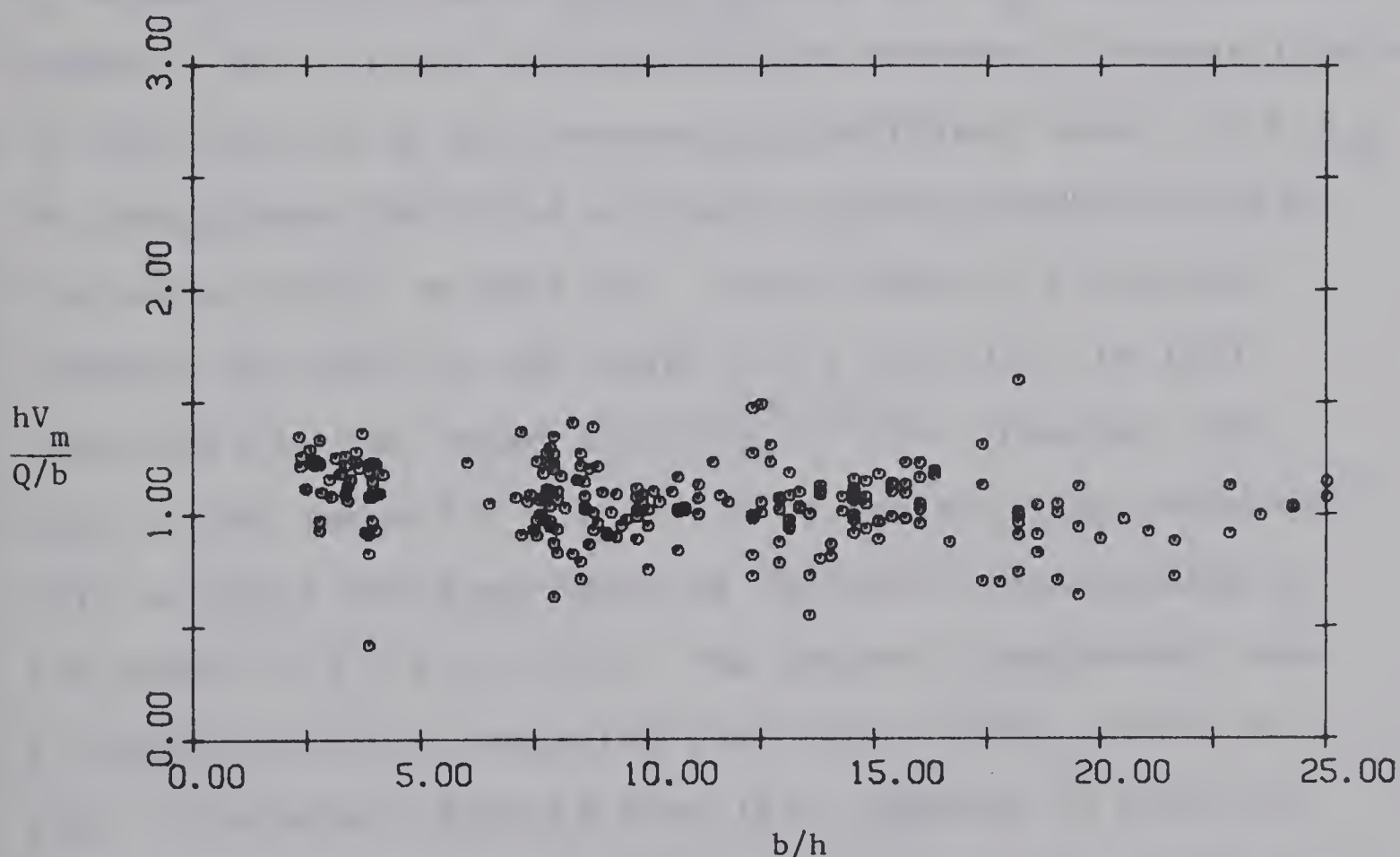


Figure 6-6. Relationship Between  $b/h$  and the Ratio of Unit Discharge at Mid-Channel Computed from a Velocity Profile to  $Q/b$  - Colorado State University Experiments





In Figure 6-7 the data have again been plotted on the  $Fr'-C_{tb}$  plane at different levels of  $h/D_{50}$ , but in this case they have been separated into five ranges of  $\sigma_b$ . The first of these ranges ( $1.0 < \sigma_b < 1.25$ ) covers the uniform bed-materials, the second two ( $1.25 < \sigma_b < 1.75$ ) cover the range of values found in natural bed-materials, and the last two ( $1.75 < \sigma_b < 5.0$ ) correspond to unnatural mixtures.

In three of these plots (a, b, and d) variation in  $\sigma_b$  appears to have some effect on the  $Fr'-C_{tb}$  relationship. However, this effect is inconsistent between different levels of variation in  $\sigma_b$  and between the different levels of  $h/D_{50}$ . To demonstrate the first of these inconsistencies consider the curves shown on plot (a). Here there is a definite tendency for data in the range  $1.0 < \sigma_b < 1.25$  to fall above data in the range  $1.25 < \sigma_b < 1.50$ . However, the data in the range  $2.0 < \sigma_b < 5.0$  go against this trend and fall on about the same curve as the data corresponding to the range  $1.25 < \sigma_b < 1.50$ . The second inconsistency can be demonstrated by comparing the trend of the curves in plot (a) against those in plot (b). Whereas in plot (a) there is a tendency for data having larger values of  $\sigma_b$  to fall on a curve beneath but approximately parallel to the curve formed by data having small  $\sigma_b$  values, this tendency is reversed in plot (b) where the data in the range  $1.75 < \sigma_b < 2.0$  definitely fall above the main scatter band



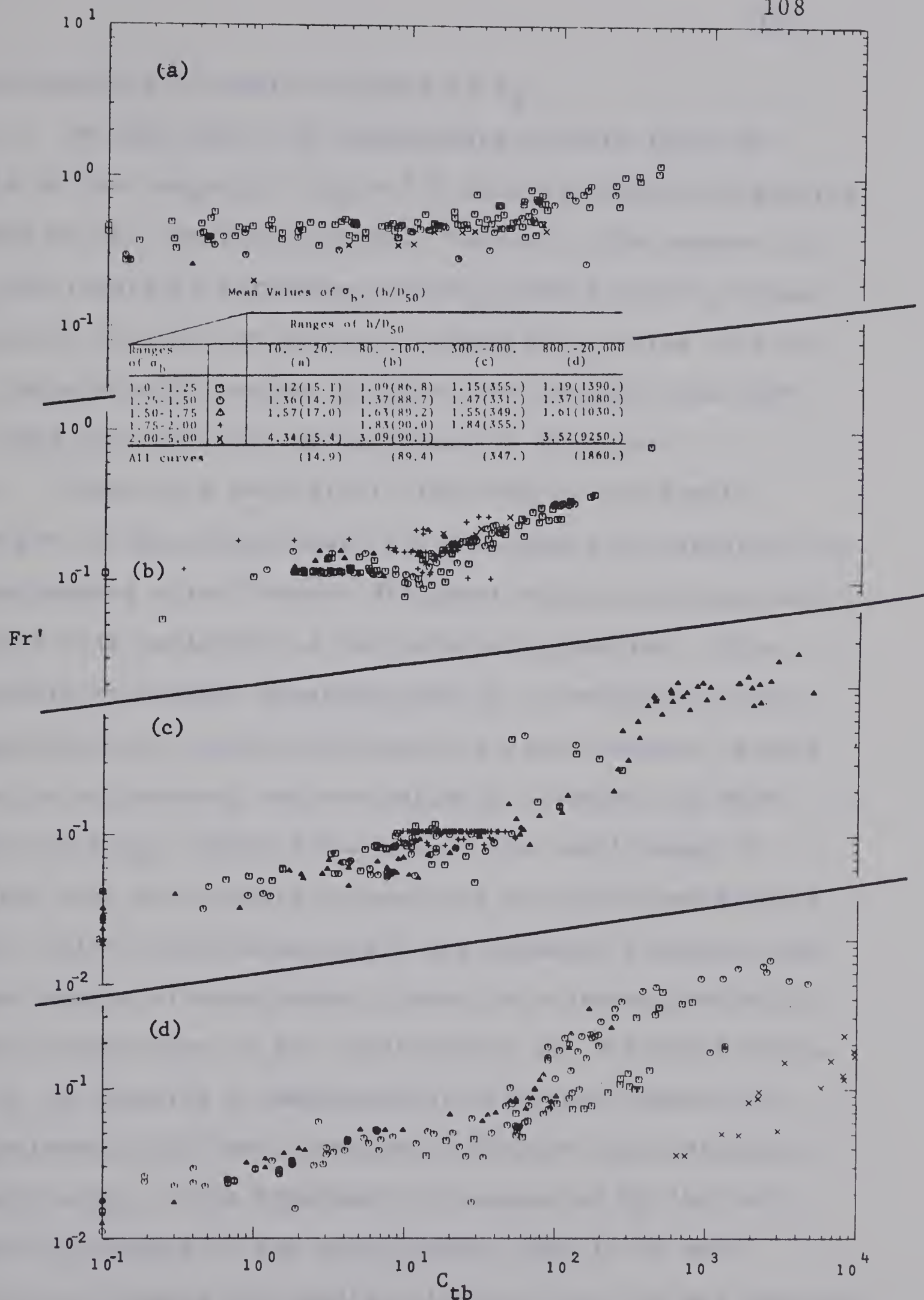


Figure 6-7. Variation of  $C_{tb}$  with  $Fr'$  and  $\sigma_b$  at Different Levels of  $h/D_{50}$





corresponding to smaller values of  $\sigma_b$ .

In plot (d) it is interesting to note that the data in the range  $2.0 < \sigma_b < 5.0$  fall far below the general trend of the remaining points. However, this appears to be the result of variation in  $h/D_{50}$  rather than  $\sigma_b$  since the data in question have an average  $h/D_{50}$  value of 9250 as compared with average  $h/D_{50}$  values ranging from 1030 to 1390 for the other three curves in the plot.

There is a possibility that these unsystematic changes in the relationship are the result of variation in experimental error between different sources of experiments rather than variation in bed-material gradation. This possibility becomes apparent when it is recognized that experiments on a given bed-material cannot appear in more than one  $\sigma_b$  interval and are unlikely to appear in more than one  $h/D_{50}$  interval because of the small range of depths that are usually covered for any given bed-material. Since only a few bed-materials are normally tested in any given source of experiments, there is a strong possibility that a comparison of the relationship for different levels of  $\sigma_b$  is actually a comparison of different sources of experiments with their inherent different types of experimental error. This hypothesis is supported by the fact that the changes in the relationship tend to be most prevalent between intermediate levels of  $\sigma_b$  and are generally not apparent between the extreme levels where they would be expected to be found.





Because of the inconsistent nature of the apparent effect of gradation and because of the possibility of this effect being the result of variation in experimental error between different sources of data, no cause is found for the rejection of the initial assumption as being invalid. However, the results are by no means conclusive, and there remains a possibility of bed-material gradation having a systematic effect on the relationship that is not apparent due to experimental error.

The transitions that occur in the relationship shown in Figures 6-1, 6-2, and 6-3 suggest the existence of a number of operating phases each of which may coincide with a particular bed-form configuration. If this is the case then each bed-form should occur within a specific region on the solution surface for Equation 6-4, and the boundaries between these regions should appear as curves on each of the three planes formed by pairs of the coordinate axes.

To determine the location and extent of these bed-form regions, the Colorado State University experiments, the Gilbert experiments, and the T.Y. Liu experiments have been analyzed. In the Colorado State University experiments, the bed-forms were classified according to the classification system proposed by Simons and Richardson (1963) which has been adopted for use in the present study.

Gilbert, on the other hand, did not use the ripple, standing wave, or chute and pool classifications, and he did



not distinguish between plane bed with sheet flow in the upper flow regime as opposed to the same configuration in the lower flow regime. There is a possibility that these bed forms did not occur in the Gilbert experiments or that ripples were classified as dunes while standing waves and chutes and pools were classified as antidunes.

Finally, in the T.Y. Liu experiments the bed-forms were classified as either plane bed with sheet flow, riffles, or dunes. Since the correspondence between riffles and the various bed-forms described in Figure 1-1 is not clear, there has been no attempt to define a region on the solution surface corresponding to this classification. The Liu experiments have been included in this portion of the analysis primarily for the purpose of defining the plane bed with sheet flow region of the lower flow regime.

The data from these three sources have been plotted on the three different coordinate planes in Figures 6-8, 6-9, and 6-10. In each of these figures the different types of bed-form have been identified by the use of different plotting symbols.

From these plots, four different bed-form regions have been identified and the boundaries between these regions have been drawn. The regions are: (1) ripples, (2) dunes, (3) plane bed with sheet flow in the lower flow regime, and (4) the bed-forms of the upper flow regime including plane bed with sheet flow, antidunes, standing waves, and chutes and pools. Since the plane bed with







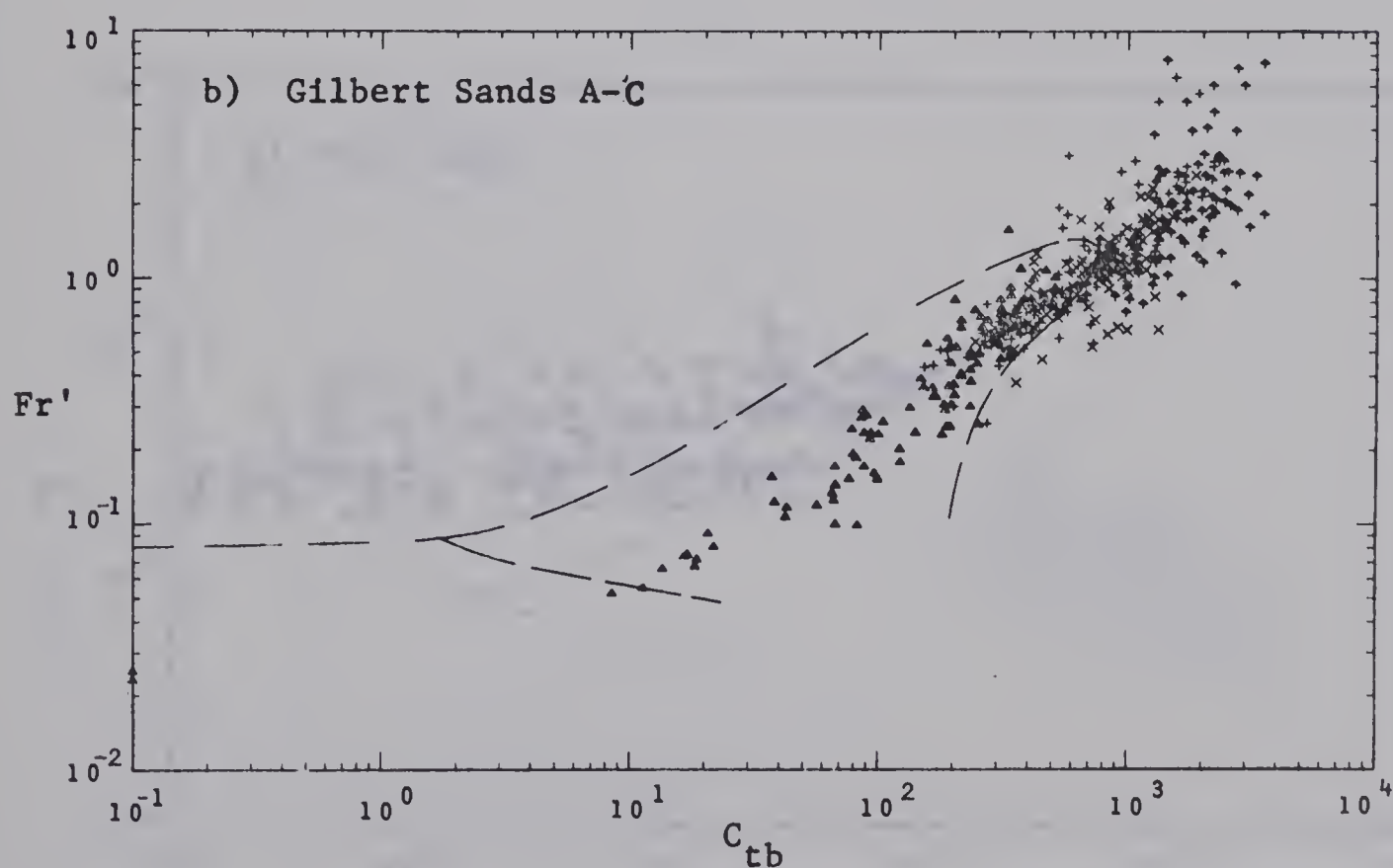
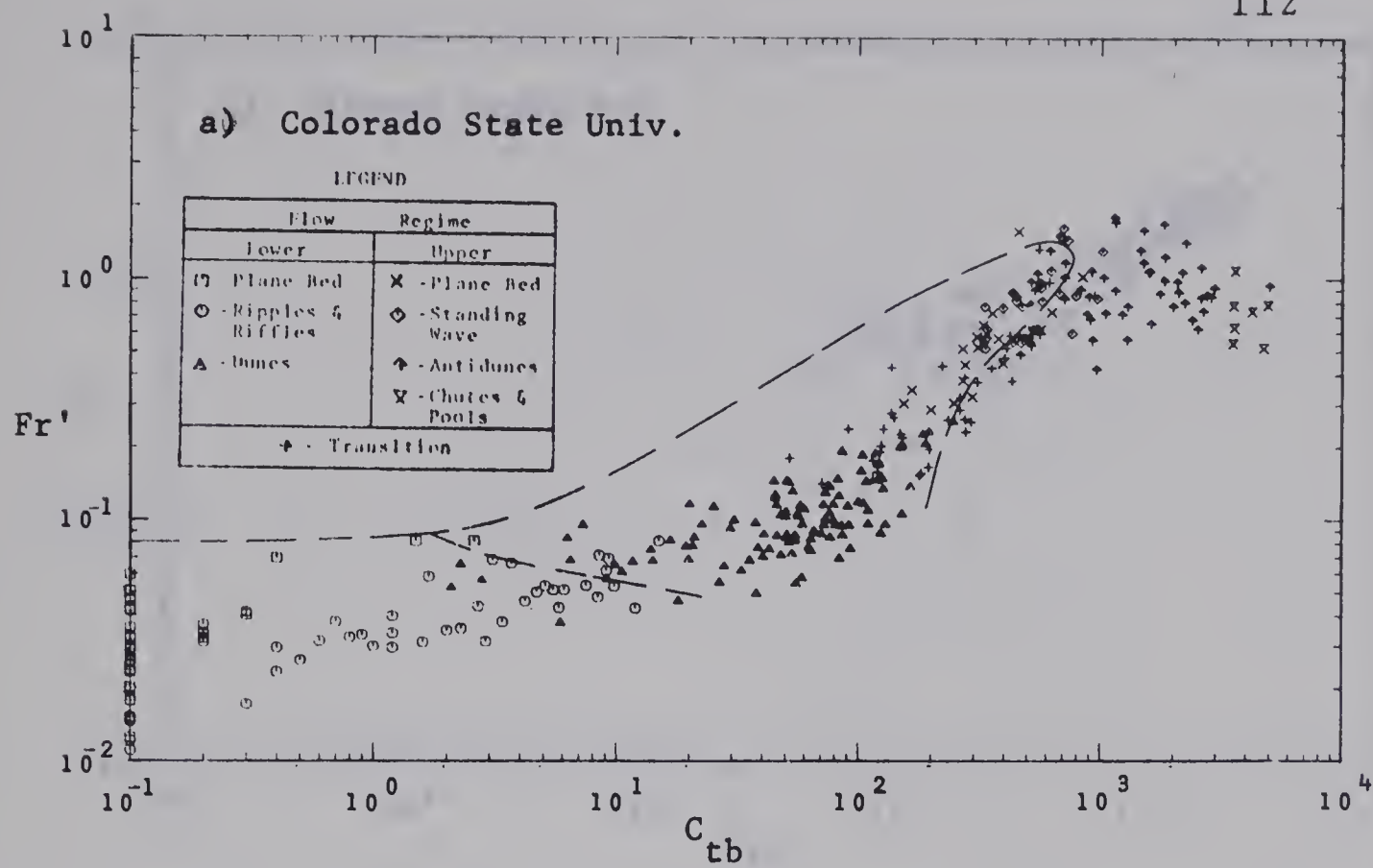


Figure 6-8. Location of Bed-Form Regions on the  $Fr'$  -  $C_{tb}$  Plane



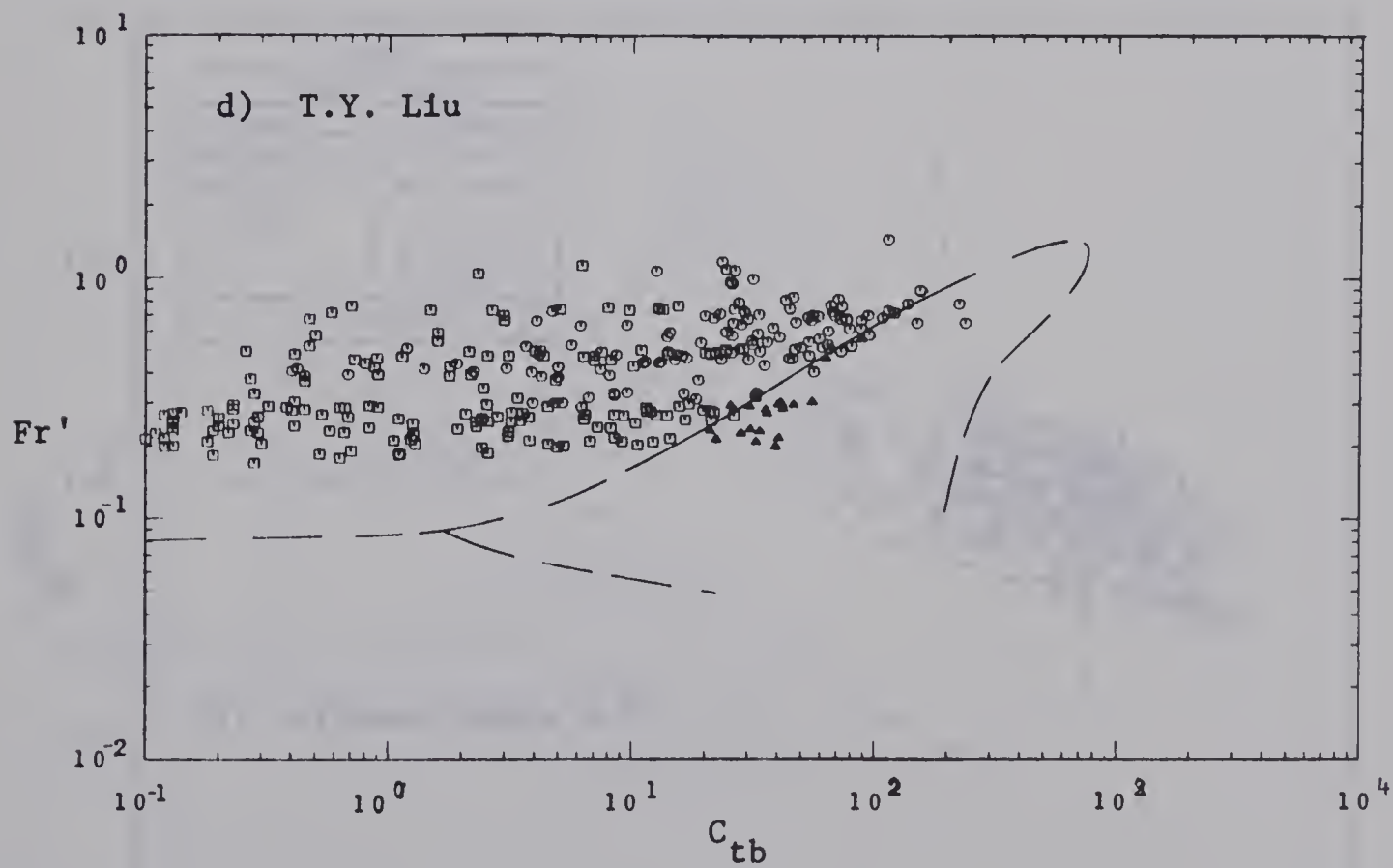
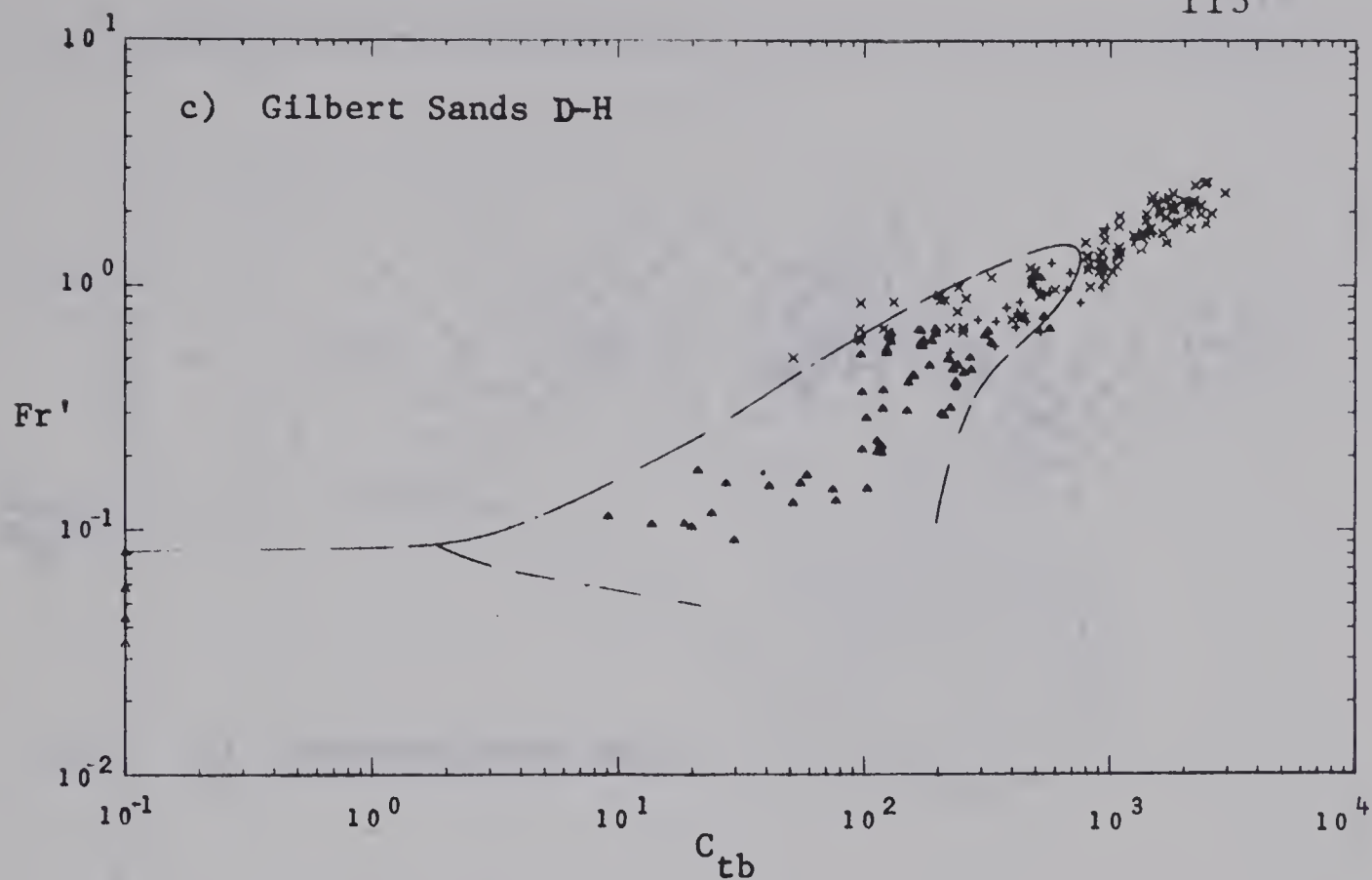


Figure 6-8 (Continued)



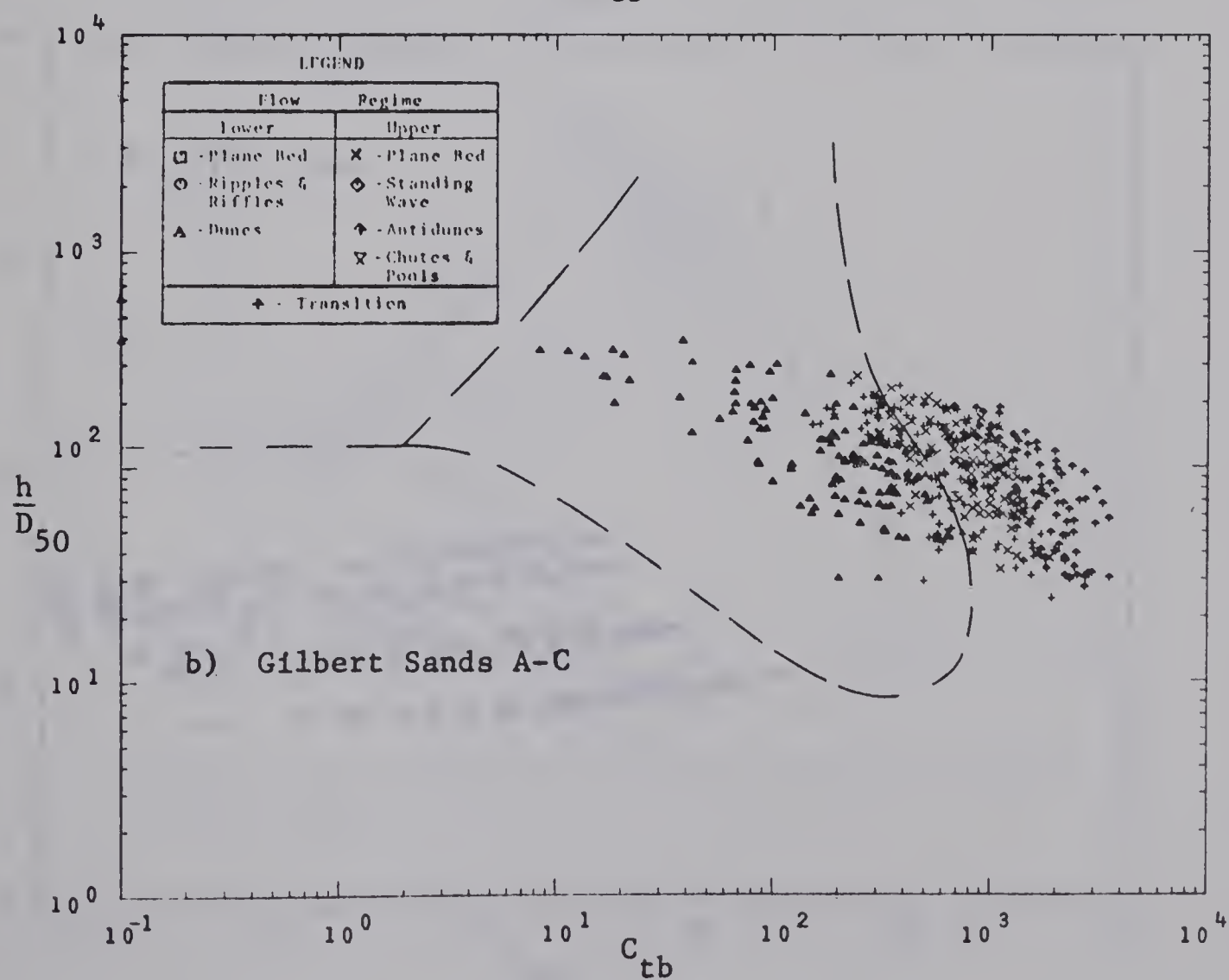
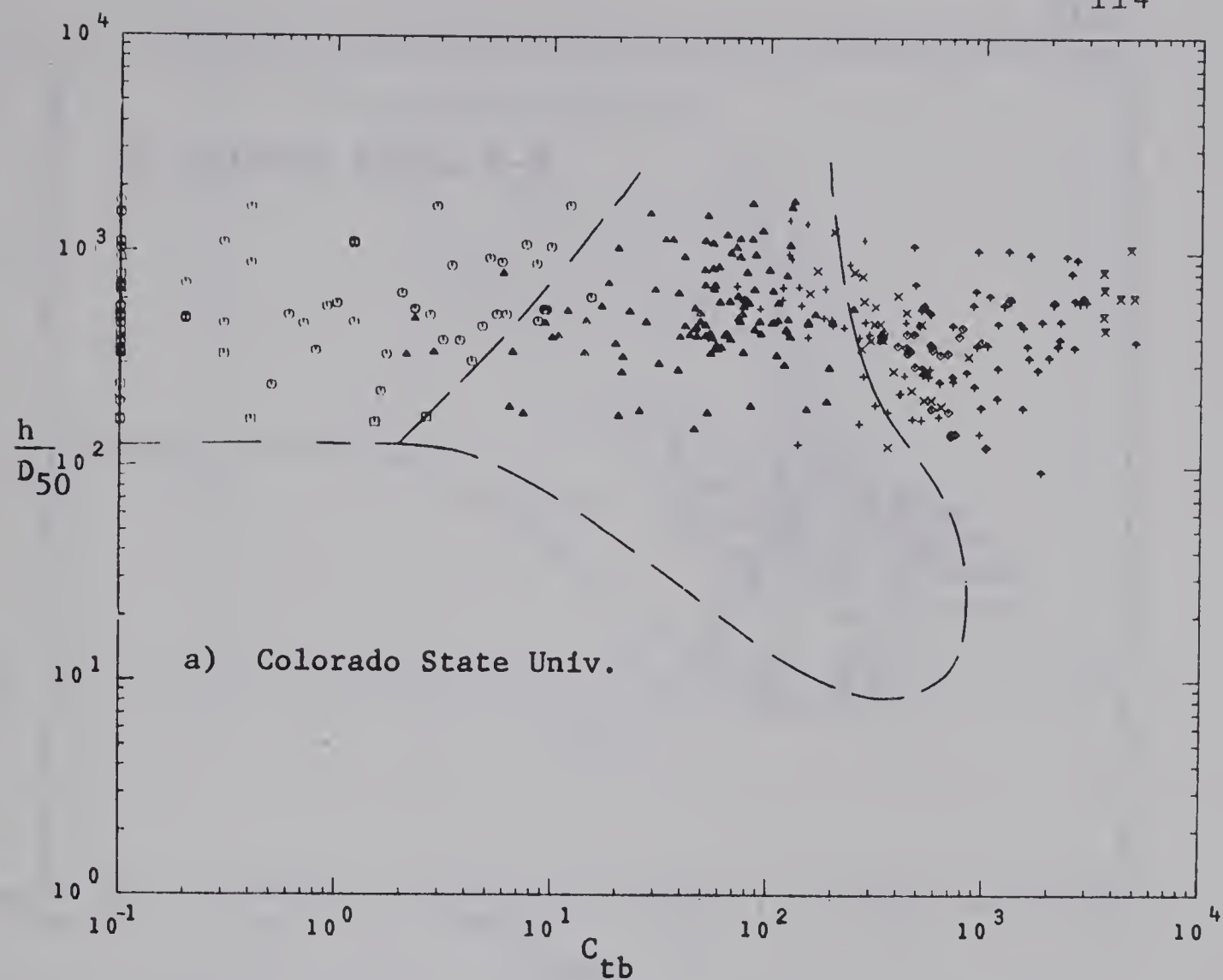


Figure 6-9. Location of Bed-Form Regions on the  $h/D_{50}-C_{tb}$  Plane





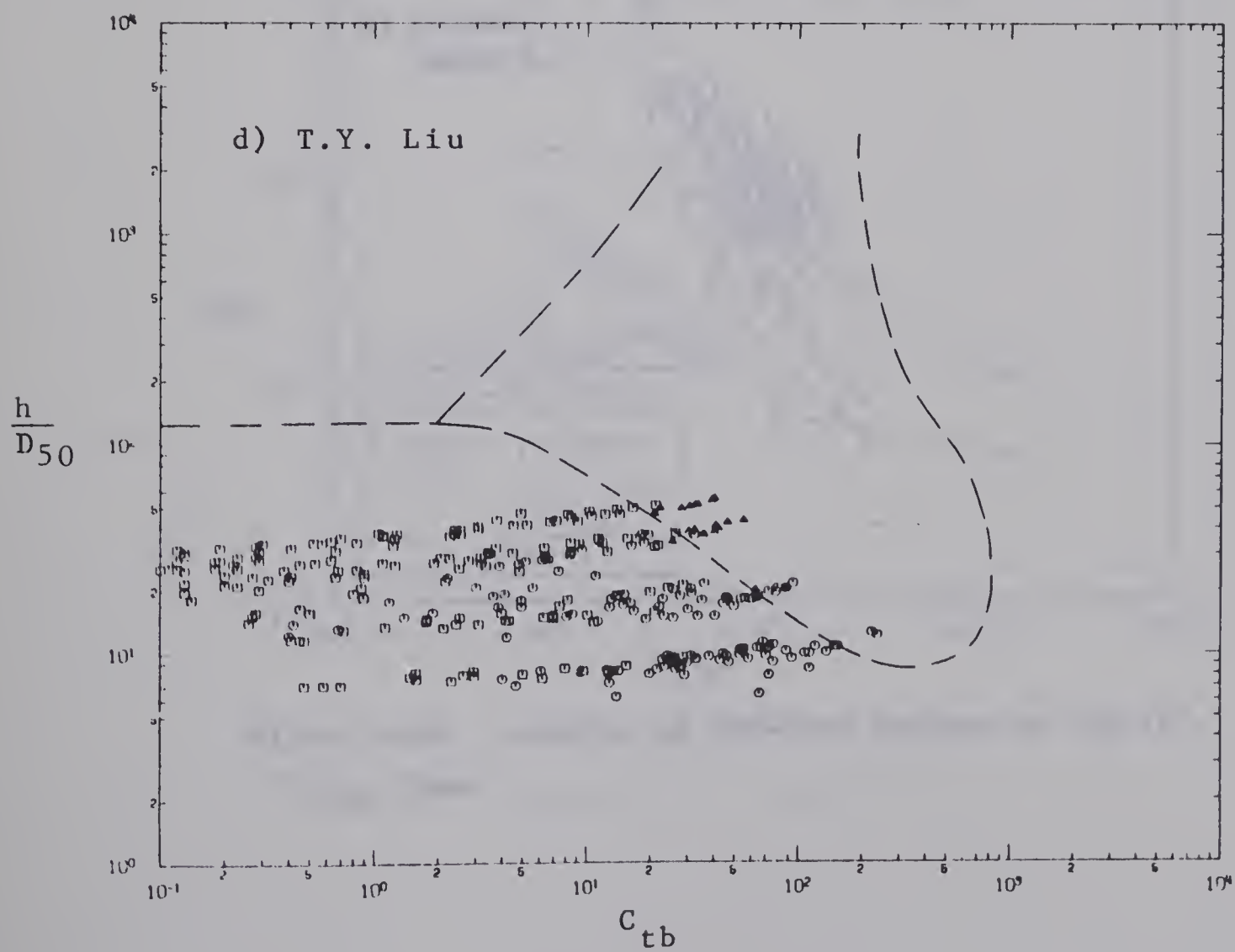
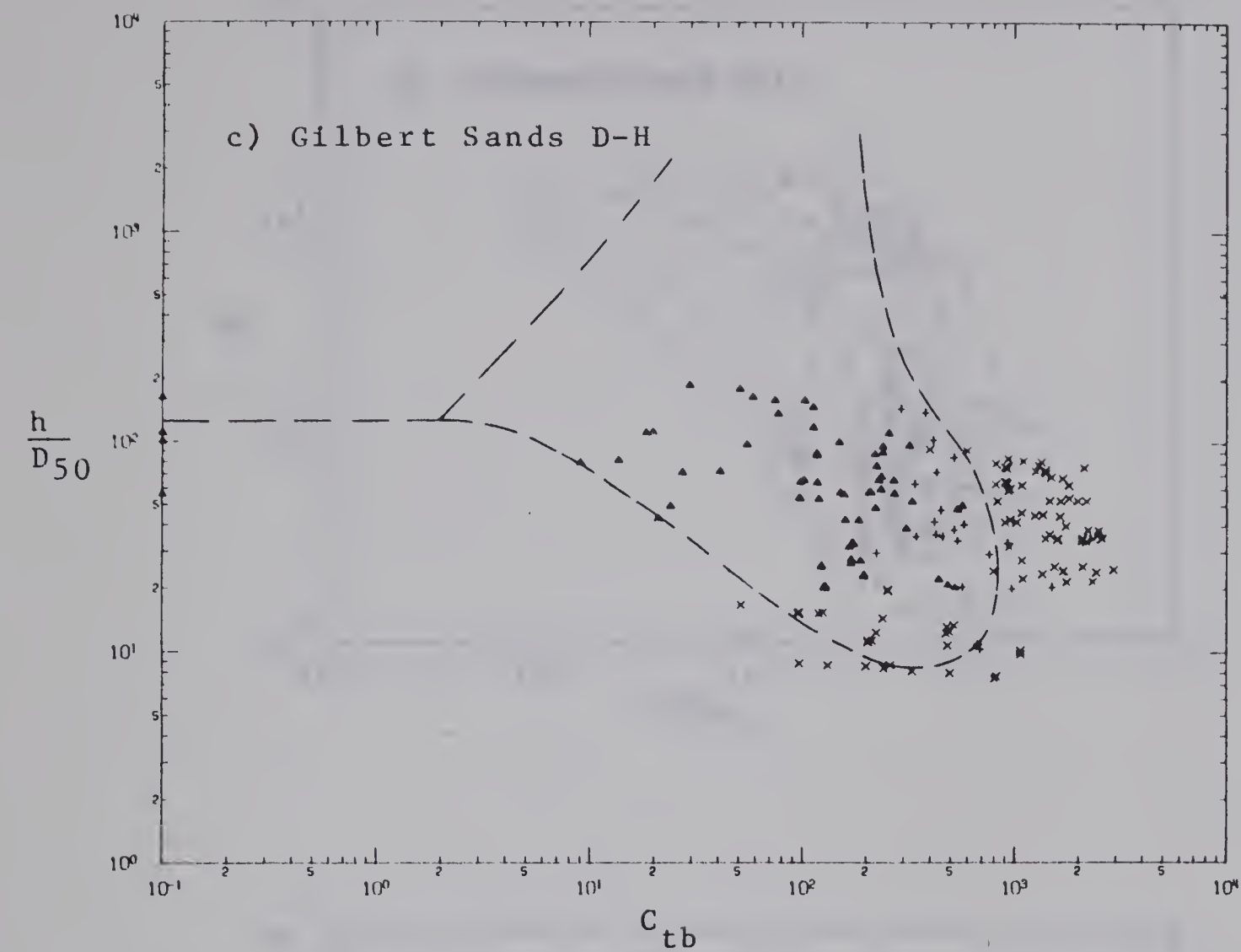


Figure 6-9 (Continued)



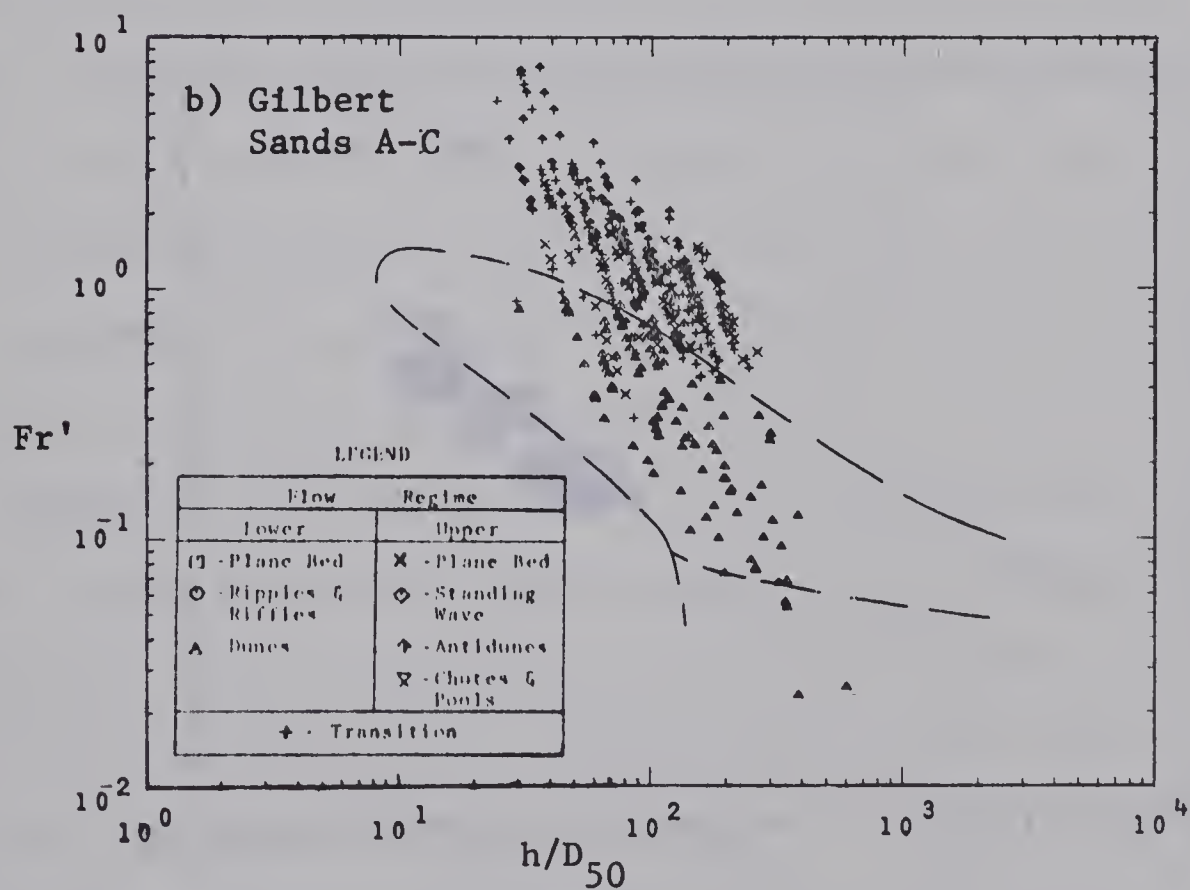
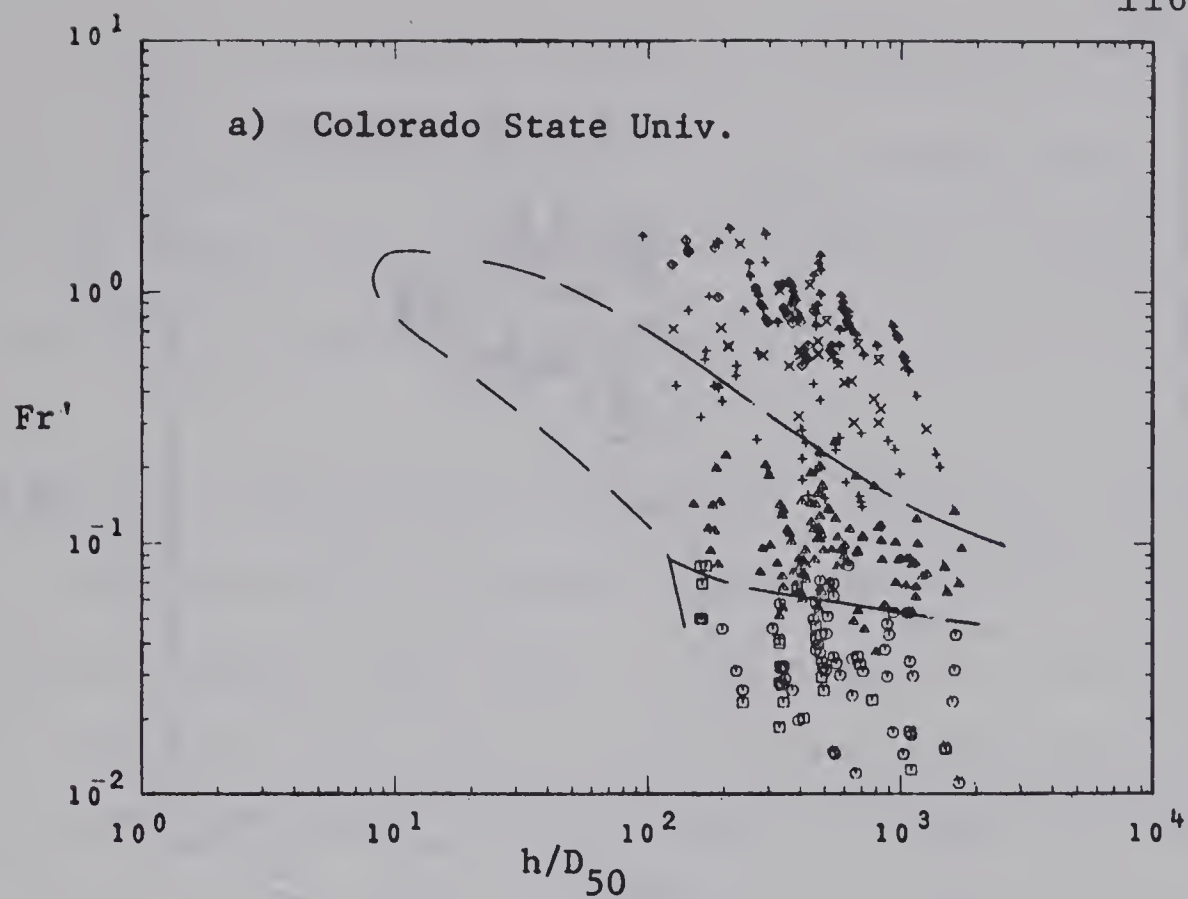


Figure 6-10. Location of Bed-Form Regions on the  $Fr'$ - $h/D_{50}$  Plane





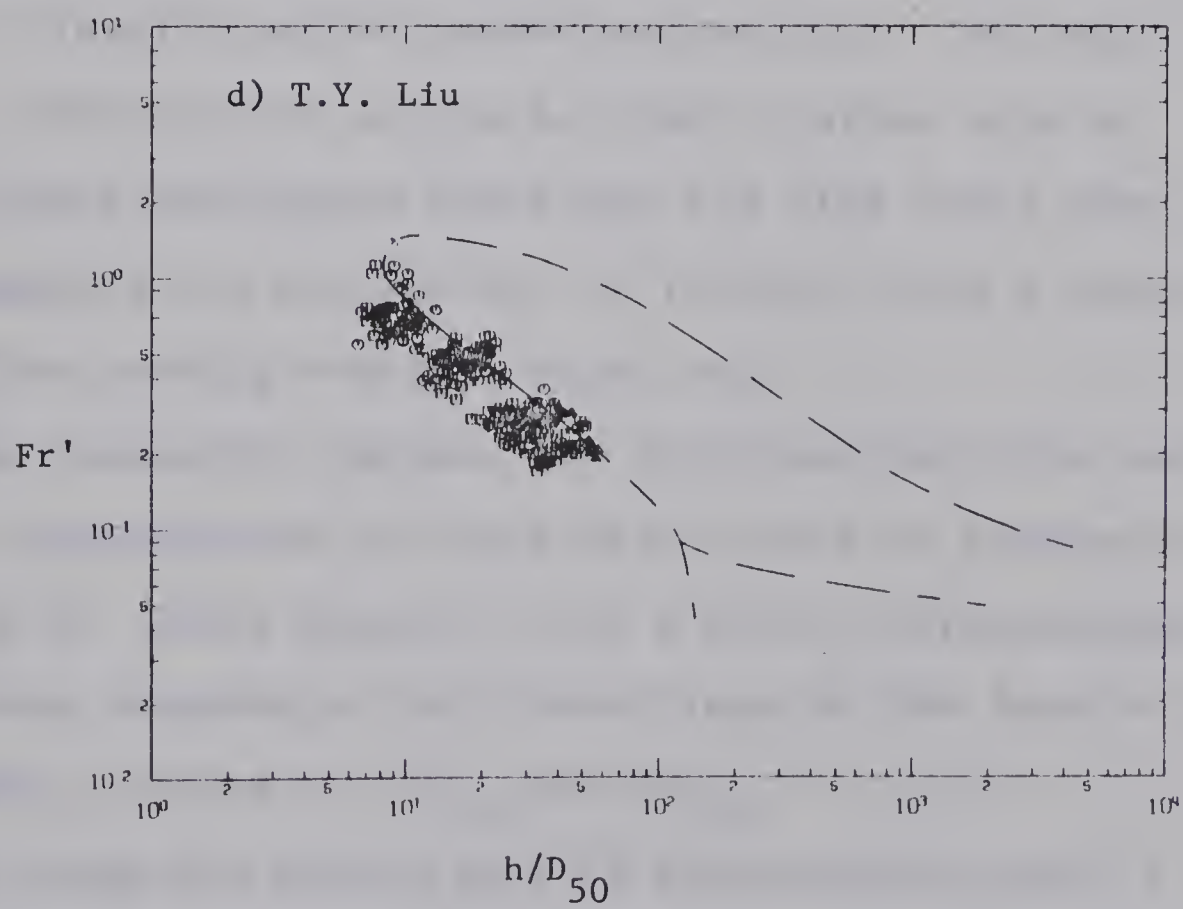
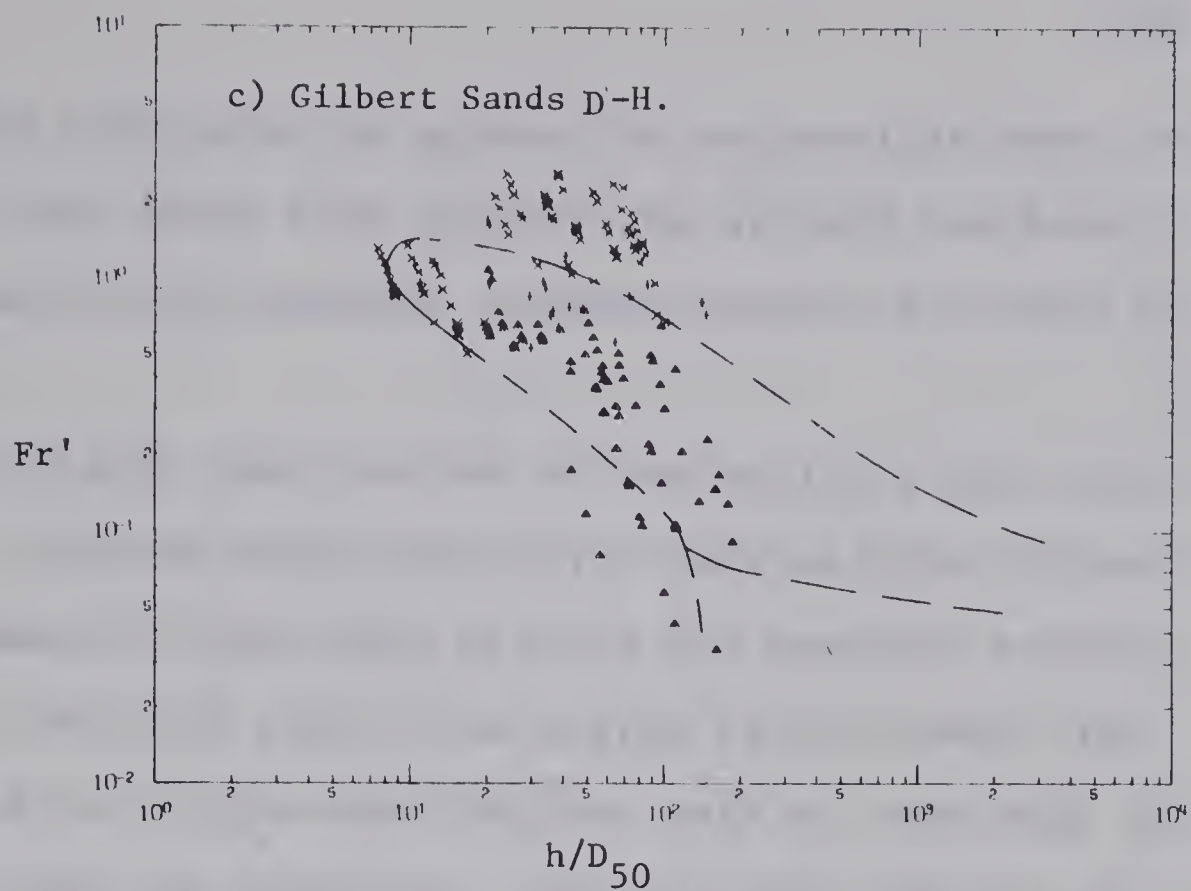


Figure 6-10. (Continued)



sheet flow configuration appears to be possible both in the upper and lower flow regimes, no attempt has been made to define the boundary between regions (3) and (4) above.

Initially this portion of the analysis made use of only the Colorado State University data and the Gilbert data. However, these data defined the boundary between the plane bed with sheet flow region of the lower flow regime and the ripple-dune regions only at very high and very low rates of transport. Consequently, the Liu data were introduced into the analysis for the sole purpose of better defining this boundary in spite of the somewhat different classification system used by Liu. The fact that the riffle points of the Liu data scatter more or less at random throughout the plane bed with sheet flow points suggests the possibility of riffles being a washed out bed-form tending toward a plane bed.

The boundaries between the different bed-form regions have been superimposed on the scatter plots in Figures 6-1, 6-2, and 6-3. There appears to be a close correspondence between these boundaries and transitions in the form of the relationship between  $Fr'$ ,  $C_{tb}$  and  $h/D_{50}$ .

By using the above plots of experimental data, a graphical representation of the solution surface for Equation 6-4 has been developed on each of the three possible coordinate planes. This representation is shown in Figures



6-11, 6-12, and 6-13 along with the curves separating the various different bed-form regions. Both regression analysis and data smoothing techniques were attempted in the development of this graphical solution. However, these methods produced results that appeared to be less suitable than when the solution curves were finally fitted to the experimental data by eye.

The form of the above graphical relationship varies considerably between the different bed-form regions. In the plane bed region of the lower flow regime, the concentration of transported bed-material has only a slight effect on the relationship between  $Fr'$  and  $h/D_{50}$ , and a slight variation in either of these parameters corresponds to a large variation in  $C_{tb}$ . Consequently this region appears to be somewhat unstable since a slight increase in channel discharge is sufficient to shift the behavior of the flow phenomenon from zero bed-material transport conditions through the plane bed region to the more stable dune region with its relatively high rates of bed-material transport.

In both the ripple and dune regions all three of the parameters in Equation 6-4 appear to be relevant in the relationship. However there is a definite transition in the form of the solution curves between the ripple and dune regions which suggests that each of these bed-forms corresponds to a distinct phase of behavior. In the ripple region the solution surface becomes nearly parallel to the  $h/D_{50}-C_{tb}$  plane; this partially accounts for the high level of scatter





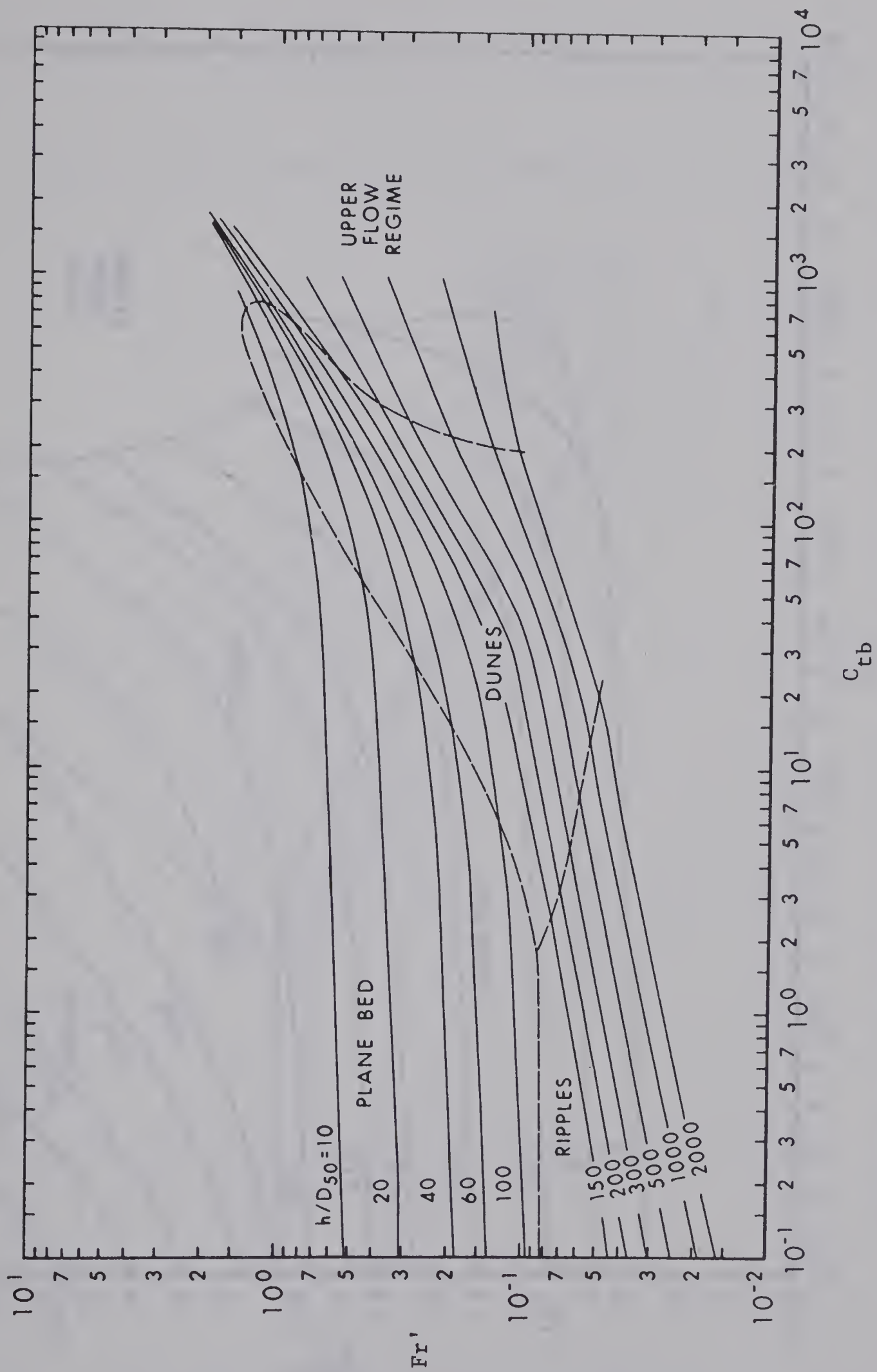


Figure 6-11. Relationship Between  $Fr'$ ,  $C_{tb}$ , and  $h/D_{50}$  on the  $Fr' - C_{tb}$  Plane



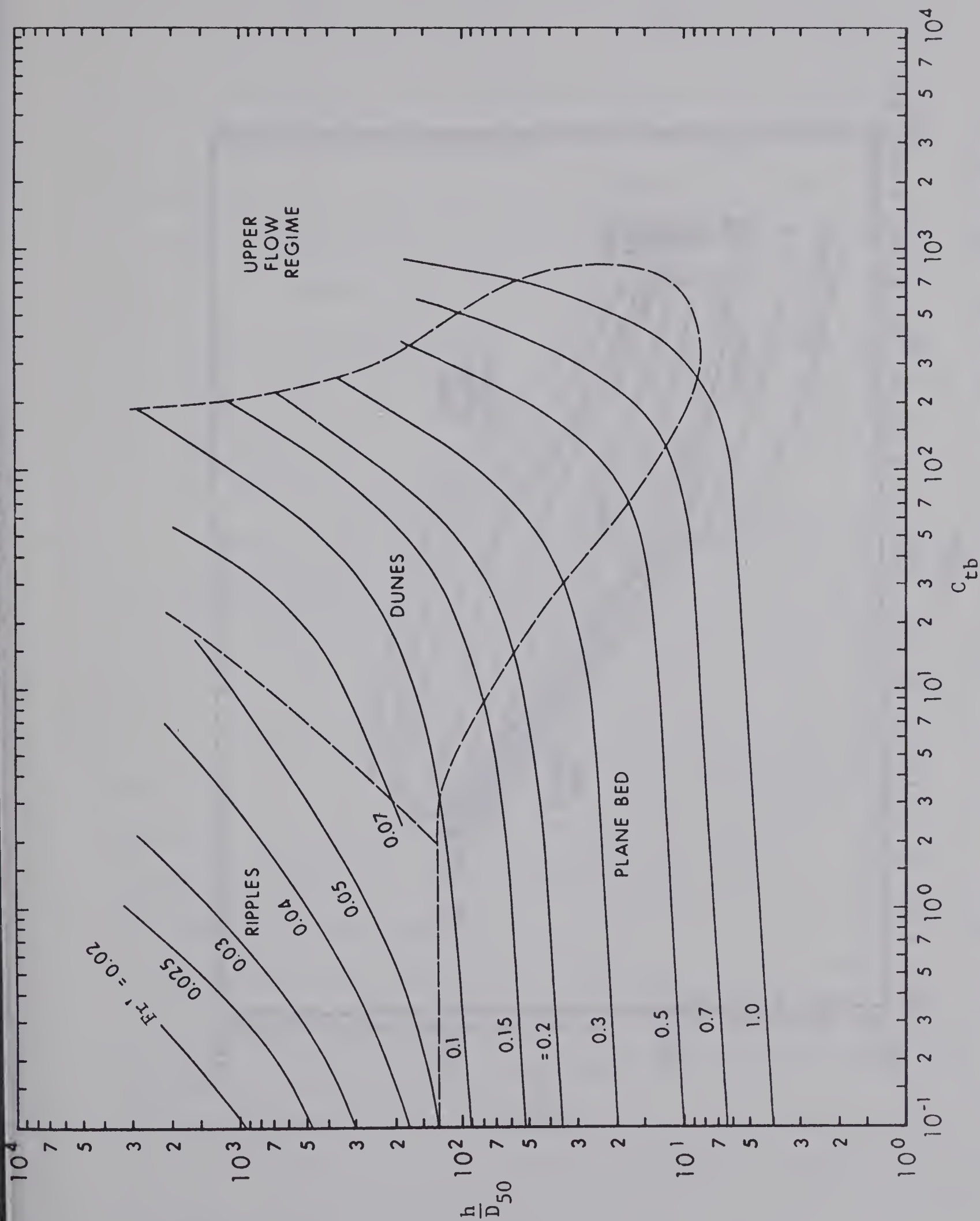


Figure 6-12. Relationship Between  $Fr'$ ,  $C_{tb}$ , and  $h/D_{50}$  on the  $h/D_{50} - C_{tb}$  Plane





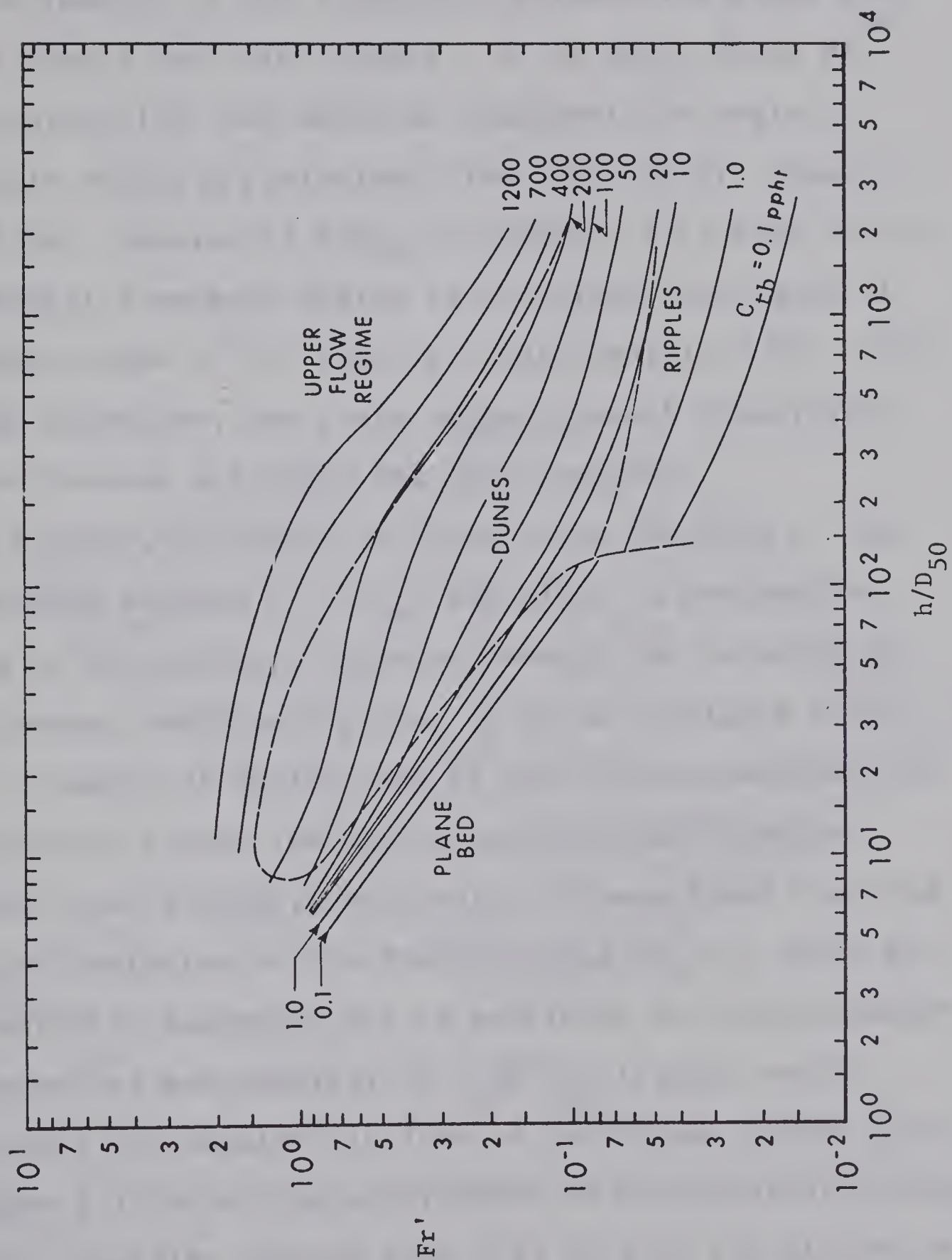


Figure 6-13. Relationship Between  $Fr'$ ,  $C_{tb}$ , and  $h/D_{50}$  on the  $Fr' - h/D_{50}$  Plane



exhibited by the plotted data in this region of Figure 6-2.

Figure 6-13 demonstrates an interesting feature of the relationship at the transition between the plane bed and the ripple bed-form regions. At an  $h/D_{50}$  value of approximately 150, bed-material transport can begin in the ripple region at a relatively low value of  $Fr'$  equal to about 0.04. However if  $h/D_{50}$  is slightly less than 150.0, bed-material transport begins in the plane bed region at the higher value of  $Fr'$  equal to approximately 0.08. With this one exception, the plots suggest smooth transitions to exist between all other bed-form regions.

Finally, to assist in visualizing the form of the relationship between  $Fr'$ ,  $C_{tb}$ , and  $h/D_{50}$ , a perspective drawing of the solution surface, showing the location of the different bed-form regions, is given in Figure 6-14.

A number of collections of data from experiments on bed-materials having specific gravities significantly different than 2.65 were available. It was found that the effect of variation in the density ratio ( $\rho_b/\rho_f$ ) could be satisfactorily accounted for by modifying the concentration of transported bed-material to  $2.65 C_{tb} (\rho_f/\rho_b)$  and by considering the densimetric form of the Froude number ( $Fr'$ ). In Figure 6-15 data from experiments on bed-materials having specific gravities ranging from 1.03 to 4.22 are plotted on the  $Fr' - 2.65 C_{tb} (\rho_f/\rho_b)$  plane at several different levels of  $h/D_{50}$ . These results appear to be in excellent agreement





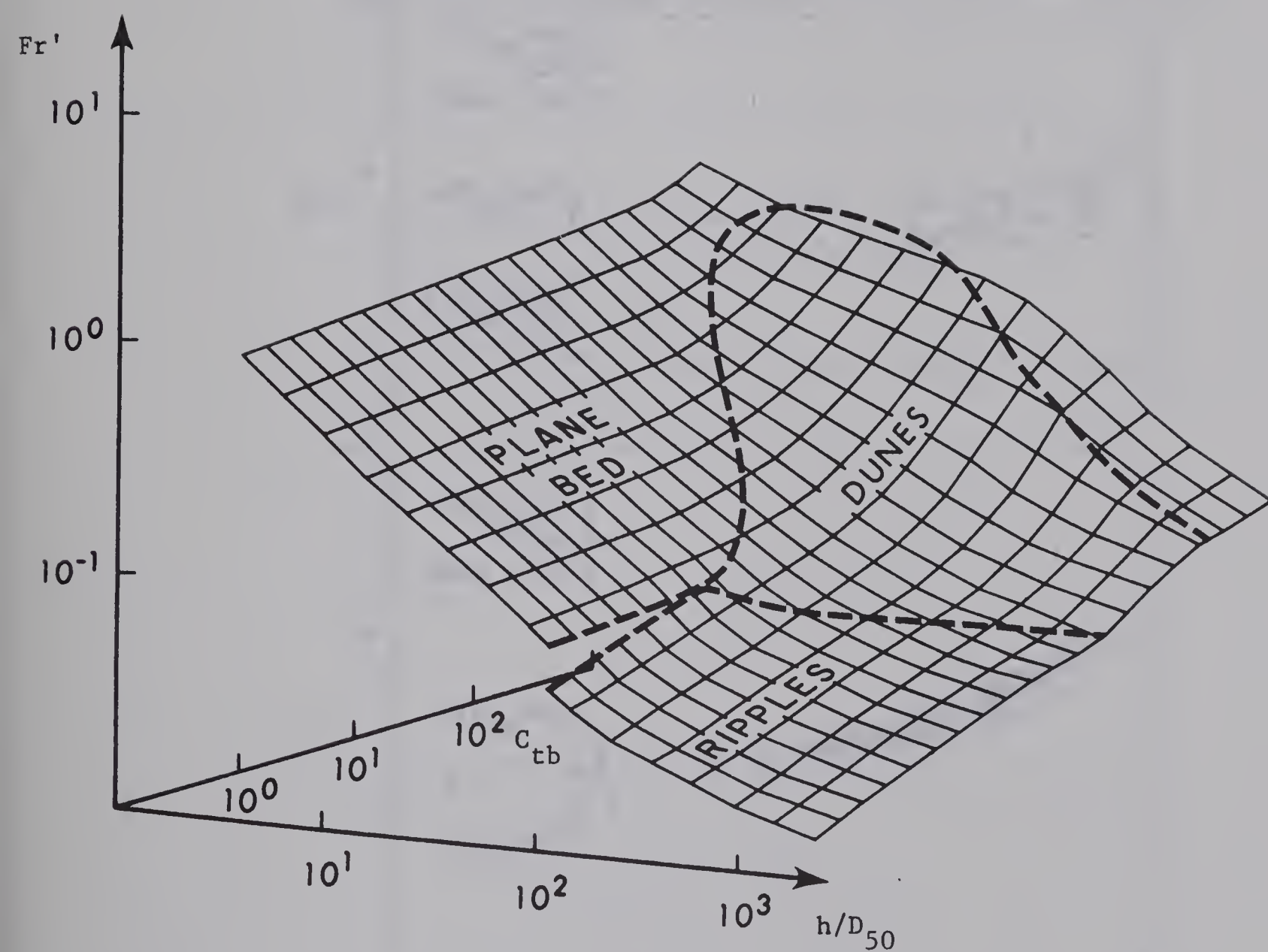


Figure 6-14. Perspective View of the Solution Surface for the Relationship Between  $Fr'$ ,  $C_{tb}$ , and  $h/D_{50}$





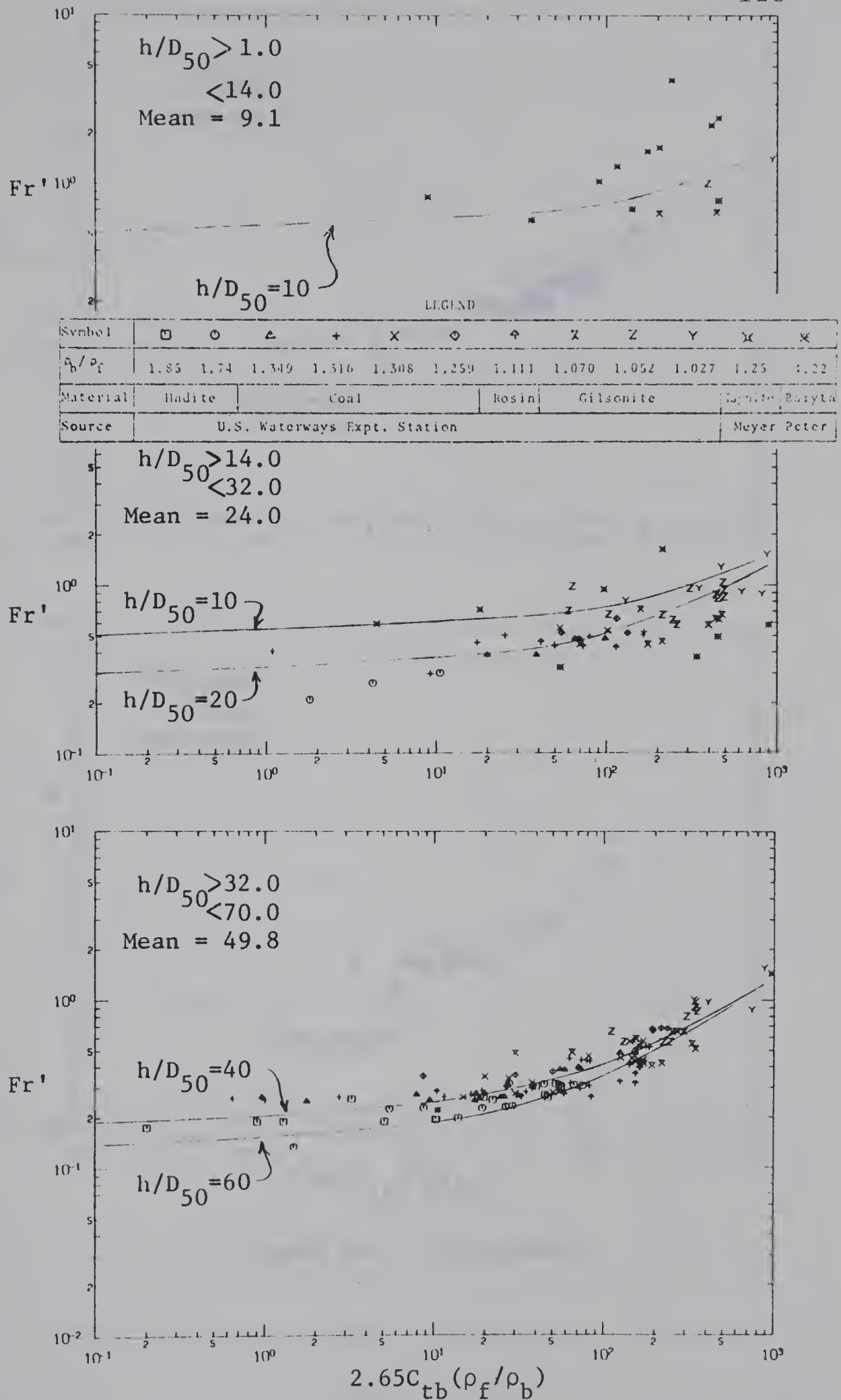


Figure 6-15. Variation of  $2.65C_{tb}(\rho_f/\rho_b)$  with  $Fr'$  and  $h/D_{50}$  for Experimental Data on Light and Heavy Weight Bed-Materials



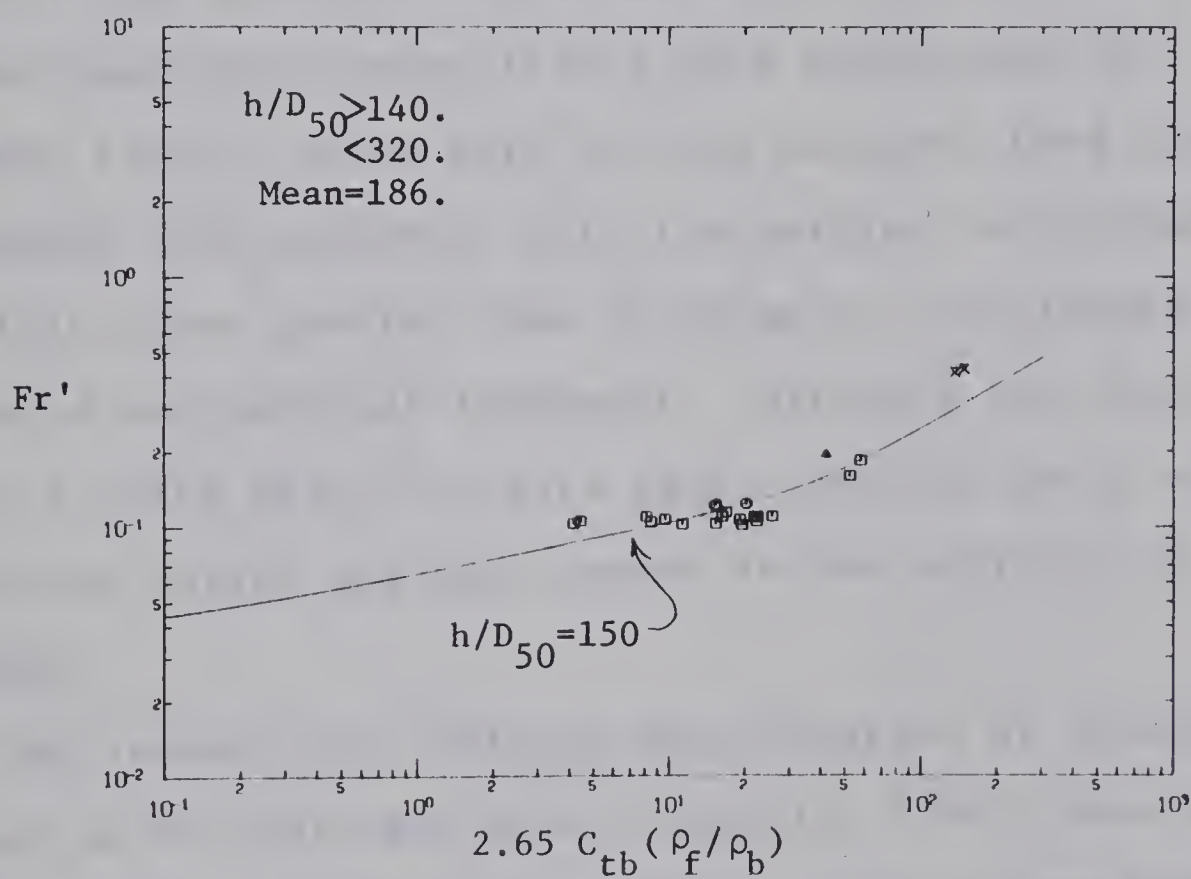
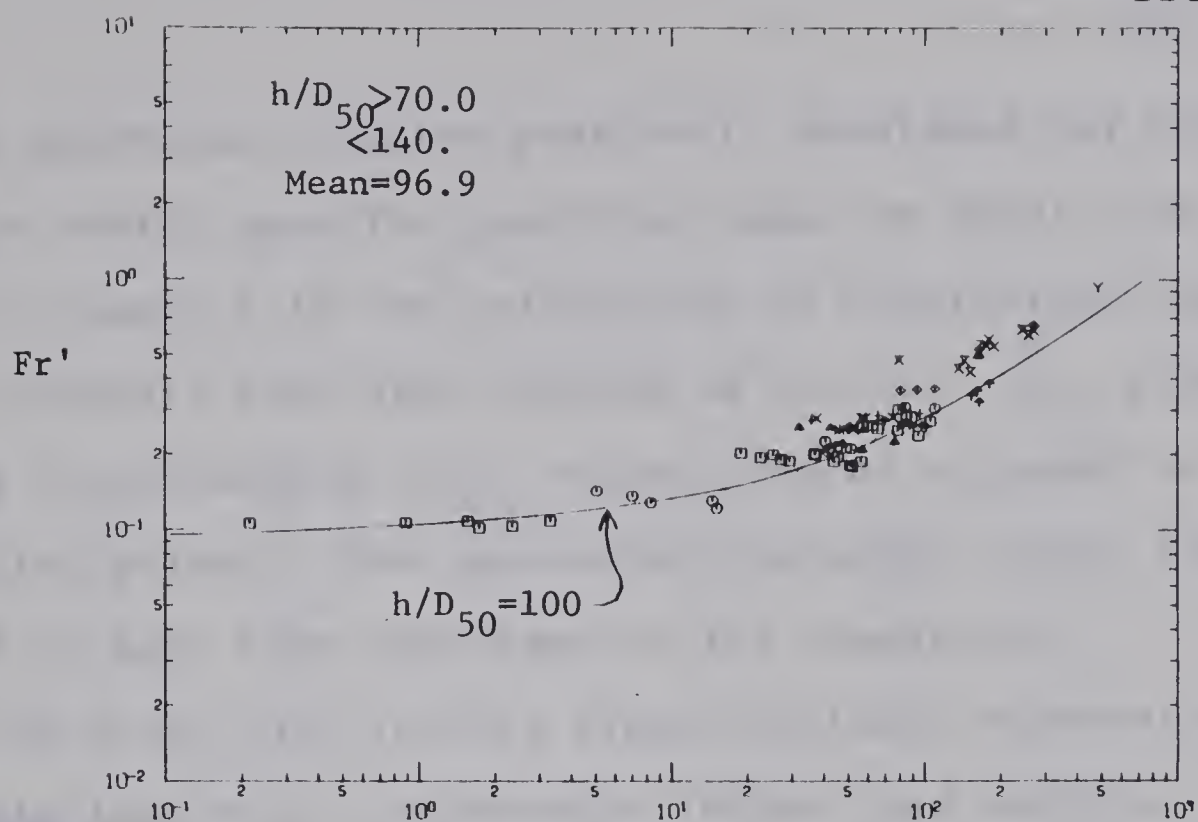


Figure 6-15. (Continued)





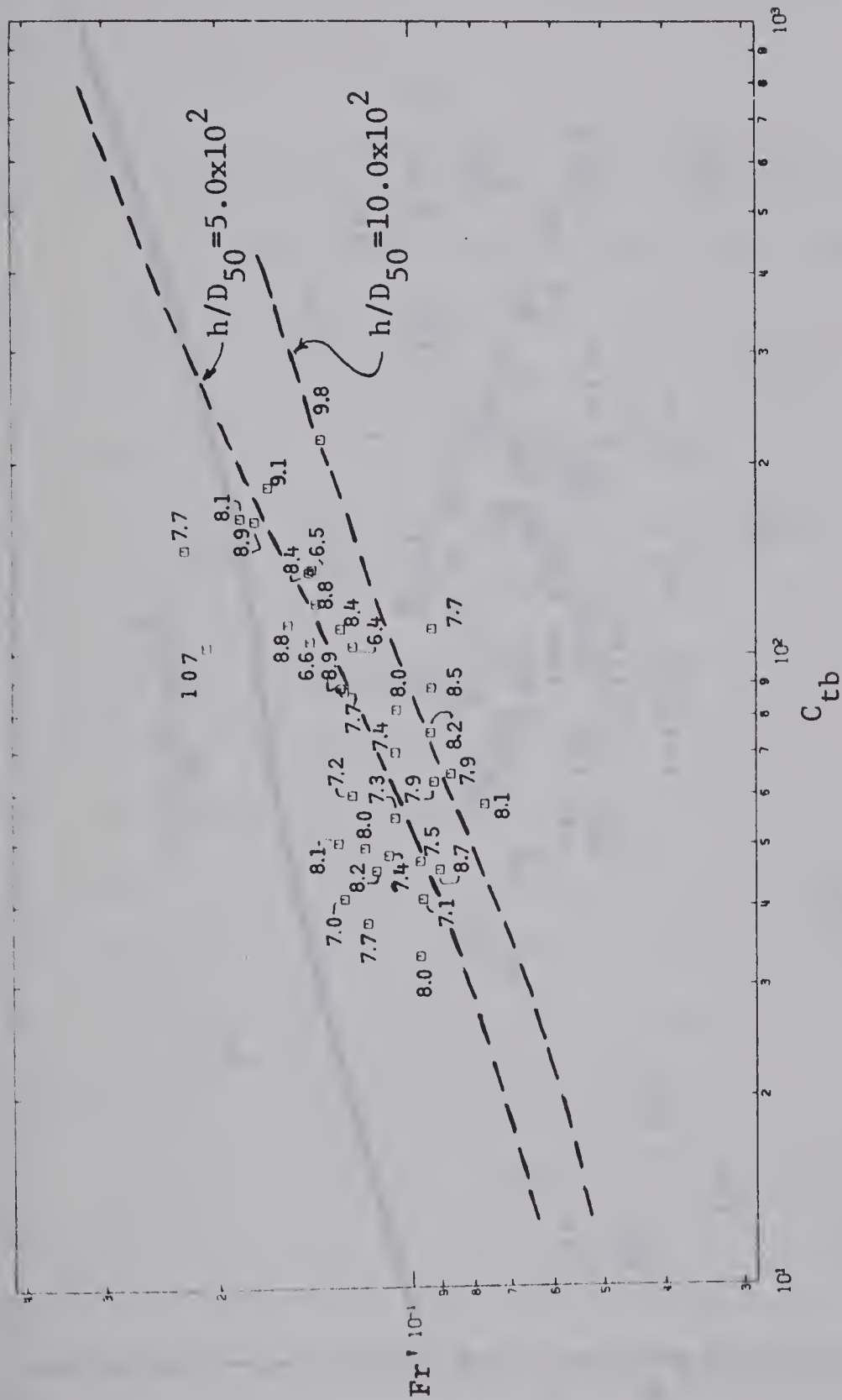
with the graphical solution previously developed for bed-materials having specific gravities equal to about 2.65.

In Figure 6-16 two collections of observations on natural channels have been plotted on the  $Fr' - C_{tb}$  plane with the corresponding  $h/D_{50}$  values printed adjacent to the plotted points. The appropriate solution curves from Figure 6-11 have been superimposed for comparison.

The first plot in this figure contains observations on **the Middle Loup** River in Nebraska (Hubbel and Matekja, 1959) where the transported bed-material was measured as suspended load after being lifted into suspension in a turbulence flume. Since part of this measured load consisted of suspended fine sediment, only the portion corresponding to particle sizes greater than 0.125 mm was considered as the rate of bed-material transport. Although the level of scatter is quite high, the data agree satisfactorily with the solution curves and add support to the validity of the method.

The second plot contains data observed at several locations on the Colorado River (Leopold, 1969); they were used because their high  $h/D_{50}$  values, ranging from 2300 to 23,200, could indicate the nature of the solution surface beyond the scope of experimental conditions. The measured suspended load of particles larger than 0.125 mm was taken as a rough estimate of the rate of bed-material transport. The data tend to follow the trend of the solution curve

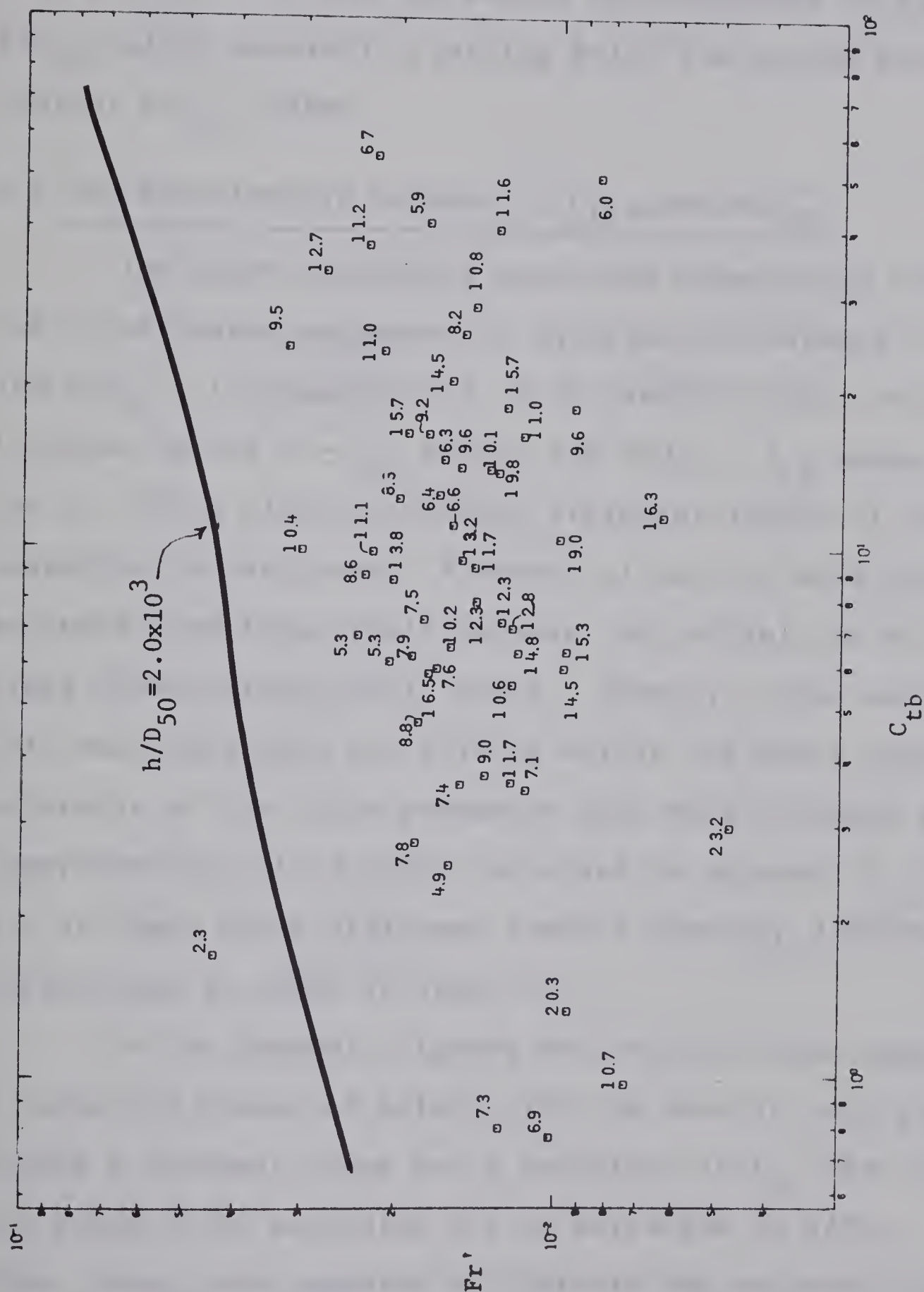




a) Middle Loup River. (Values of  $h/D_{50} \times 10^{-2}$  are printed adjacent to points)

Figure 6-16. Comparison of the Relationship Between  $Fr'$ ,  $C_{tb}$ , and  $h/D_{50}$  with Natural Channel Observations (Curves have been taken from Figure 6-11)









for  $h/D_{50} = 2000$  and, as expected, fall considerably below this curve with the points corresponding to higher  $h/D_{50}$  values generally plotting below the points having smaller  $h/D_{50}$  values.

#### 6-4 The Relationship between $S$ , $C_{tb}$ , and $h/D_{50}$

The above procedures have been repeated in evaluating the relationship suggested by Equation 6-5 between  $S$ ,  $C_{tb}$ , and  $h/D_{50}$ . In Figures 6-17, 6-18, and 6-19 this relationship is shown on the  $S - C_{tb}$  plane, the  $h/D_{50} - C_{tb}$  plane, and the  $S - h/D_{50}$  plane at several different levels of the third parameter in each case. A number of sets of data have been excluded from these plots because the reliability of their slope observations was in doubt. However, these excluded data and those data not falling within the above narrow intervals of the third parameter have been included in a more comprehensive set of plots contained in Appendix D. In all of these plots different symbols identify different data collections as shown in Table 4-2.

In the Appendix figures the rejected data appear as a number of groups of points with the data in each group having a constant slope but a variation in  $C_{tb}$  that seems too large to be accounted for by variation in  $h/D_{50}$ . At first these data appeared to indicate the existence of a non-unique relationship between the variables as suggested by Brooks (1958). However, the data in question exhibit these properties within each of the bed-form regions of the



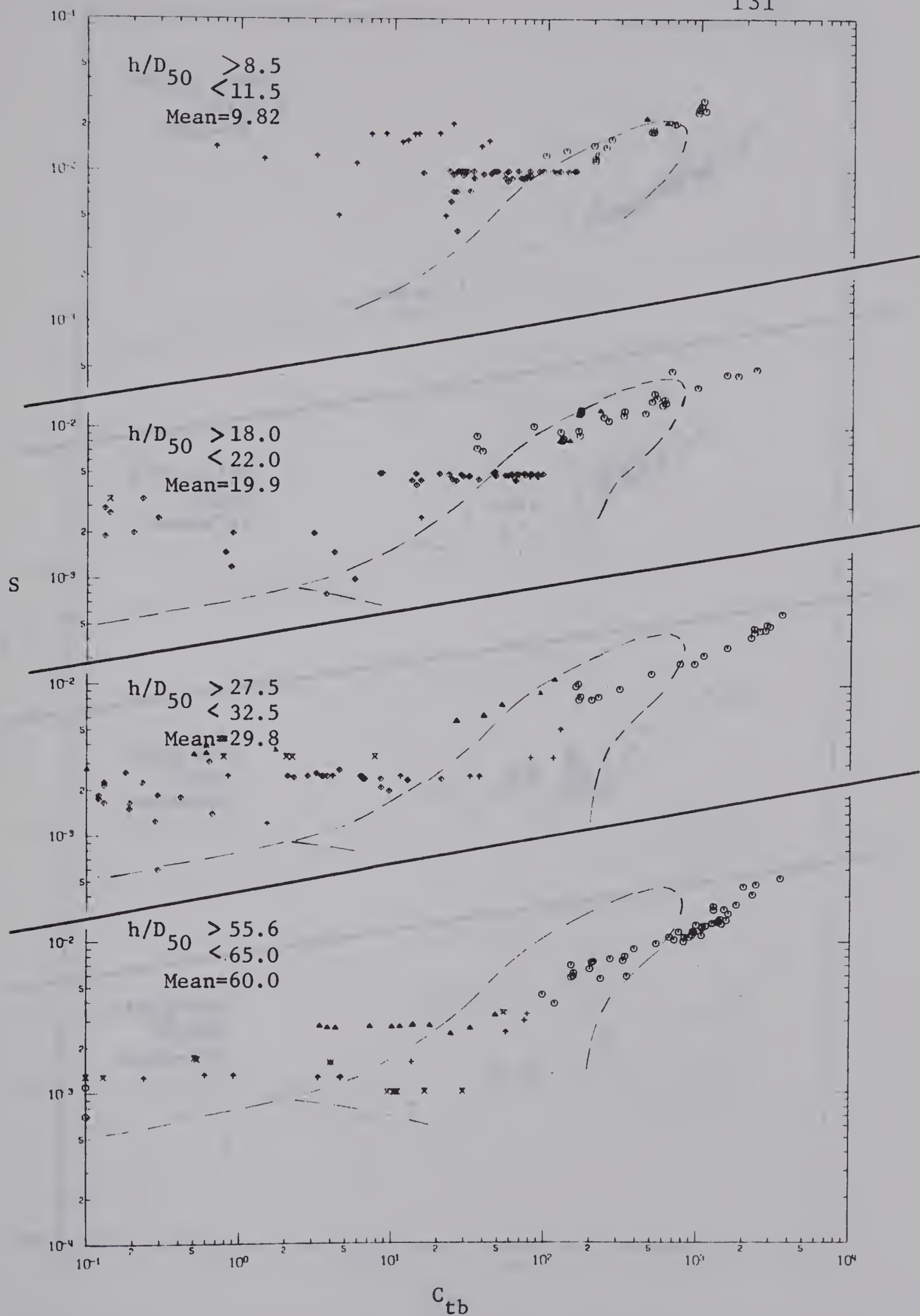


Figure 6-17. Variation of  $C_{tb}$  with  $S$  at Different Levels of  $h/D_{50}$





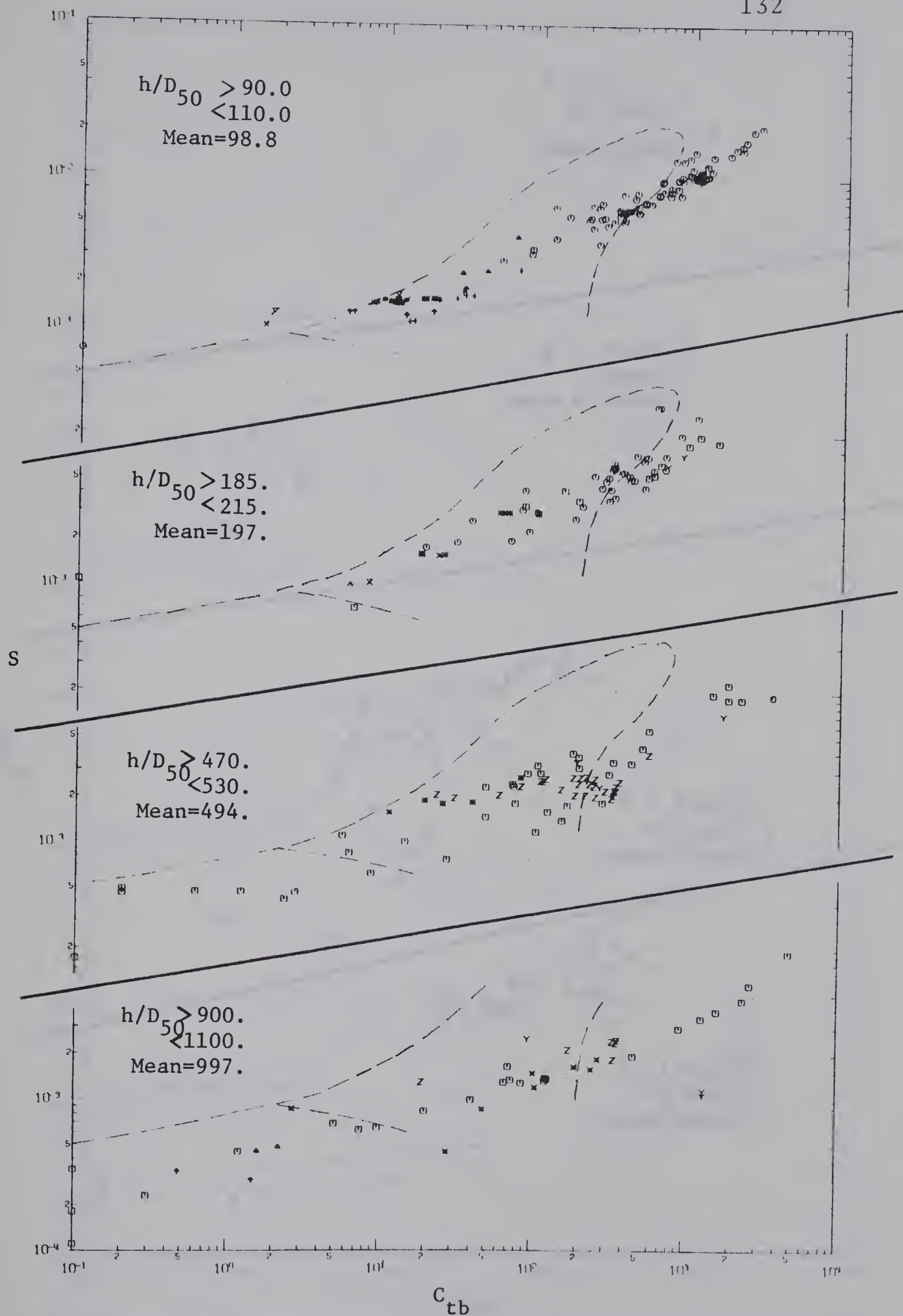


Figure 6-17 (Continued)



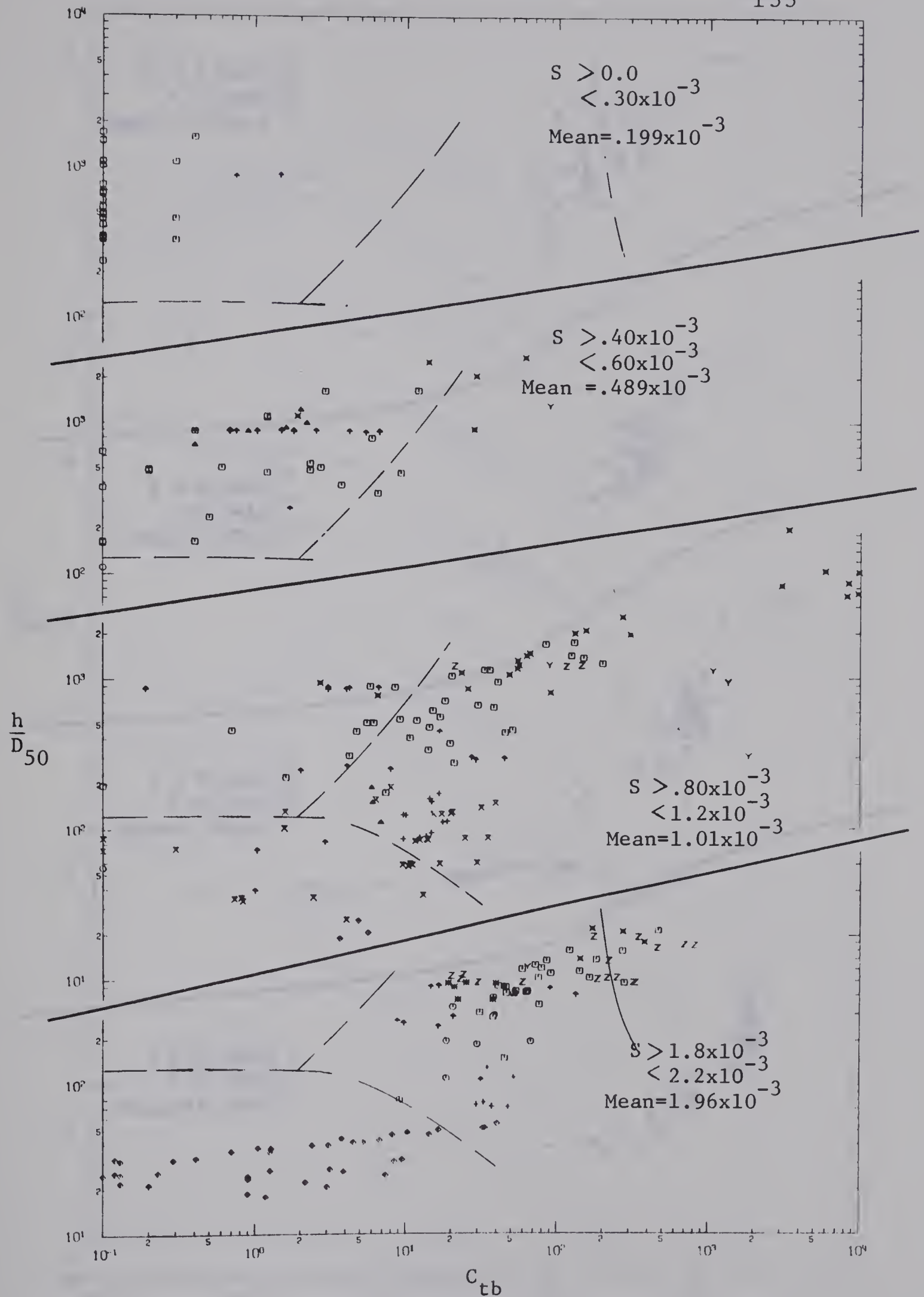


Figure 6-18. Variation of  $C_{tb}$  with  $h/D_{50}$  at Different Levels of  $S$



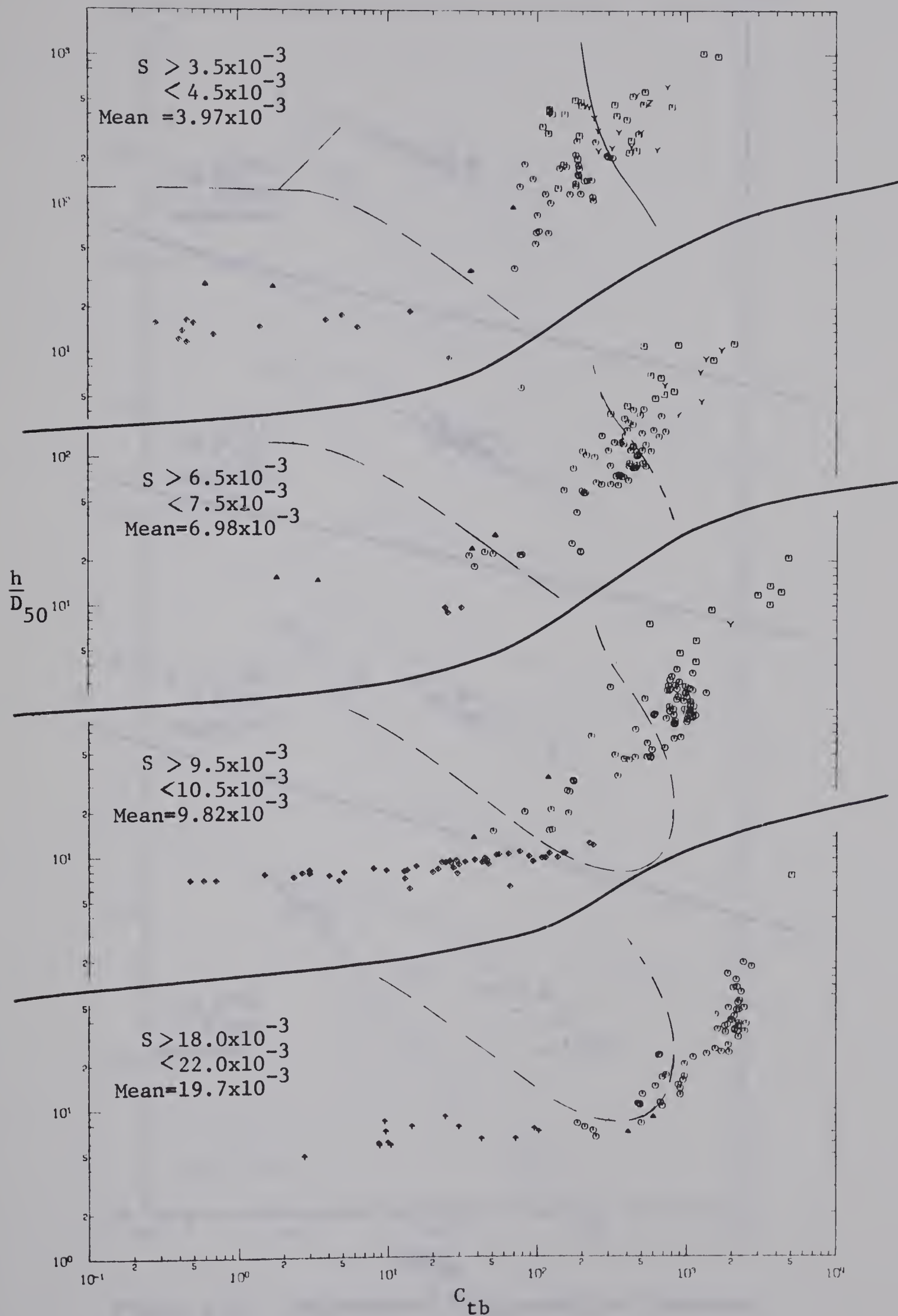


Figure 6-18 (Continued)





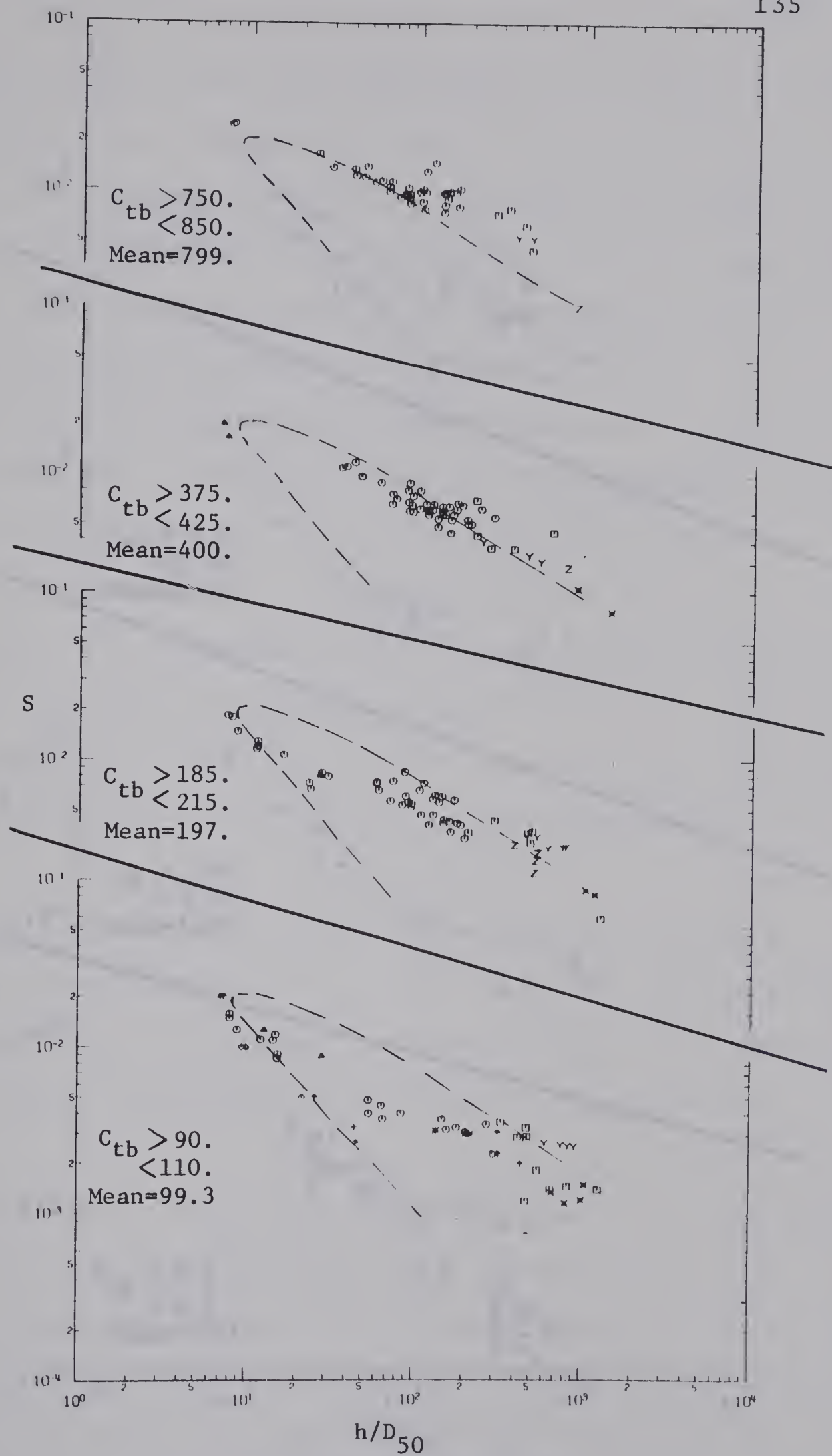


Figure 6-19. Variation of  $h/D_{50}$  with  $S$  at Different Levels of  $C_{tb}$



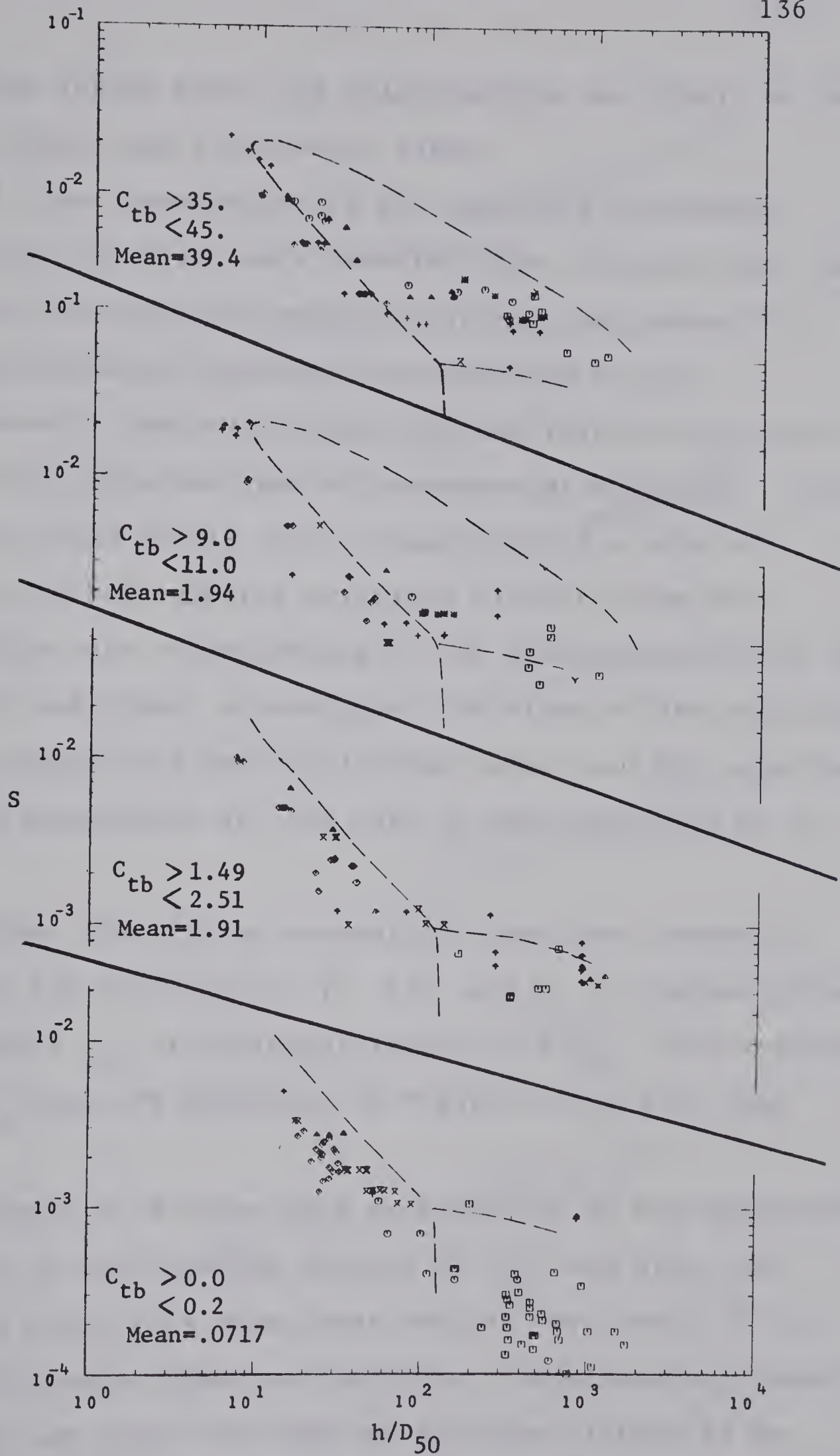


Figure 6-19. (Continued)





lower flow regime where the relationships are likely to be unique (Simons and Richardson, 1966).

A close examination of the operating procedures responsible for these data revealed that, in each case, the procedure consisted of imposing discharge and slope in a flume system where discharged bed-material was not recirculated. Instead bed-material was injected at a rate equal to the observed rate of bed-material discharge. This procedure could result in the imposition of a rate of transport of bed-material differing slightly from the equilibrium rate corresponding to the preselected values of discharge and slope; accordingly, the slope of the bed would tend to adjust to a new equilibrium value, and the reported initial slope values for the data in question would be in error.

Again the initial assumptions have been tested by examining the variation of  $V_i$ ,  $b/h$ , and  $\sigma_b$  in scatter plots of  $S$  against  $C_{tb}$  at different levels of  $h/D_{50}$ . The results of these tests are presented in Figures 6-20, 6-21, and 6-22.

Figure 6-20 shows that variation in  $V_i$  has apparently no effect on the relation between  $S$ ,  $C_{tb}$ , and  $h/D_{50}$  for values of  $h/D_{50}$  less than about 400 and for levels of  $V_i$  within the ranges shown on the plots. Unfortunately these ranges do not cover the range of  $V_i$  values likely to be encountered in nature. For example, at an  $h/D_{50}$  level of about 15 (plot a) the maximum average value of  $V_i$  is 139



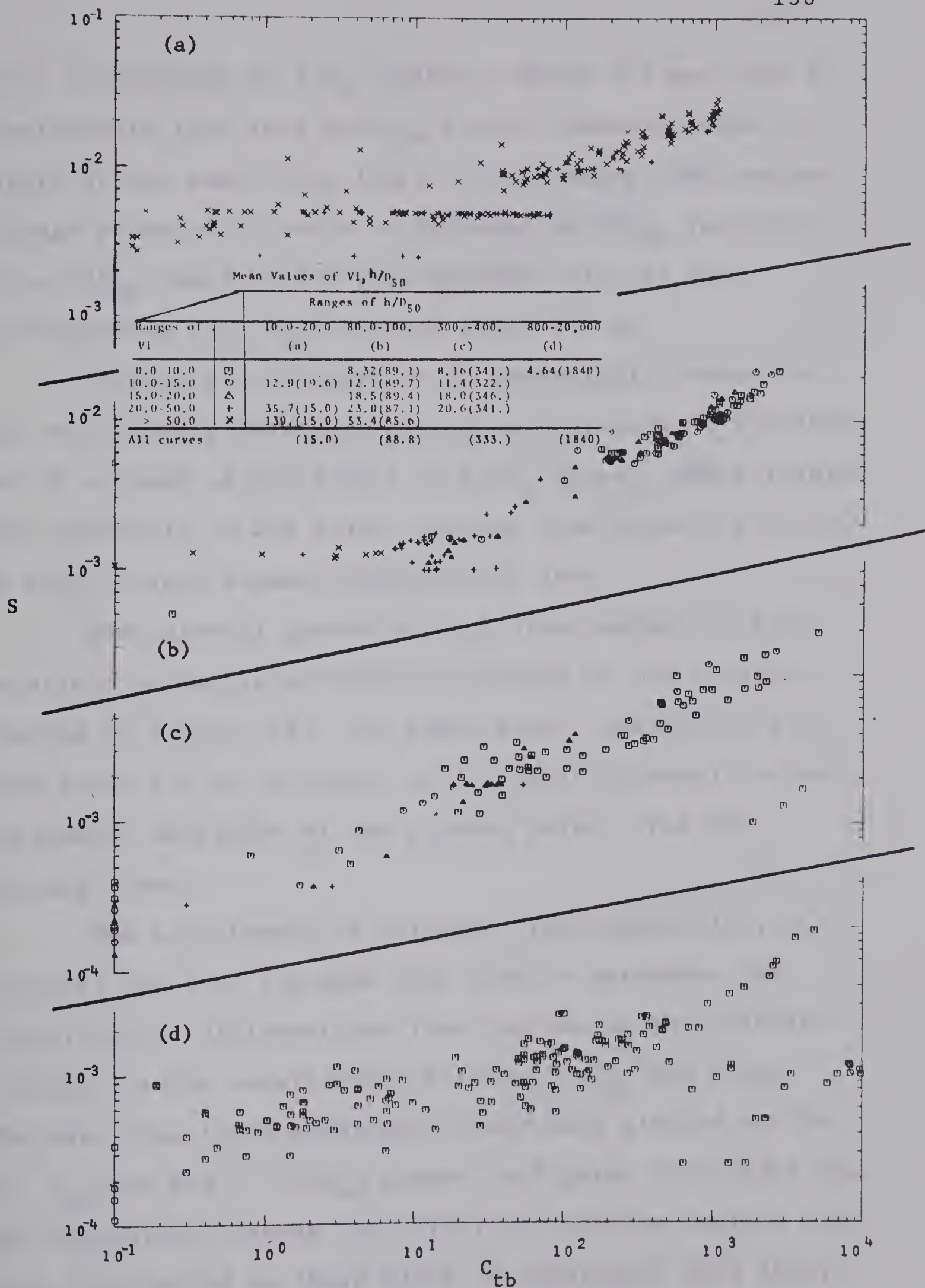


Figure 6-20. Variation of  $C_{tb}$  with  $S$  and  $V_i$  at Different Levels of  $h/D_{50}$





which corresponds to a  $D_{50}$  value of about 6.2 mm; this is considerably less than the  $D_{50}$  values commonly found in nature at the same  $h/D_{50}$  level. Furthermore, the maximum average value of  $V_i$  tends to decrease as  $h/D_{50}$  increases; at an  $h/D_{50}$  level of 347 this maximum value is 15.7 corresponding to a  $D_{50}$  value of about 0.7 mm.

In Figure 6-21 there is no appreciable change in the relationship between  $S$  and  $C_{tb}$  as a result of variation in  $b/h$  at each of the levels of  $h/D_{50}$  given. These results are applicable to  $b/h$  values ranging from about 2.0 to 20.0 at  $h/D_{50}$  values between about 15 and 1000.

Bed-material gradation ( $\sigma_b$ ) also appears to have no effect on the relationship according to the results plotted in Figure 6-22. In these plots, variation in  $\sigma_b$  from about 1.1 to in excess of 3.0 fails to result in any systematic deviation of the plotted points from the average trend.

The experiments of Colorado State University, G.K. Gilbert, and T.Y. Liu have been used to determine the extent of the different bed-form regions on the solution surface for the relationship between  $S$ ,  $C_{tb}$  and  $h/D_{50}$ . The data from these experiments have been plotted on the  $S - C_{tb}$  and the  $S - h/D_{50}$  planes in Figures 6-23 and 6-24. The boundaries between the different bed-form regions have been constructed in these plots in accordance with their representation on the  $h/D_{50} - C_{tb}$  plane given in Figure 6-9.





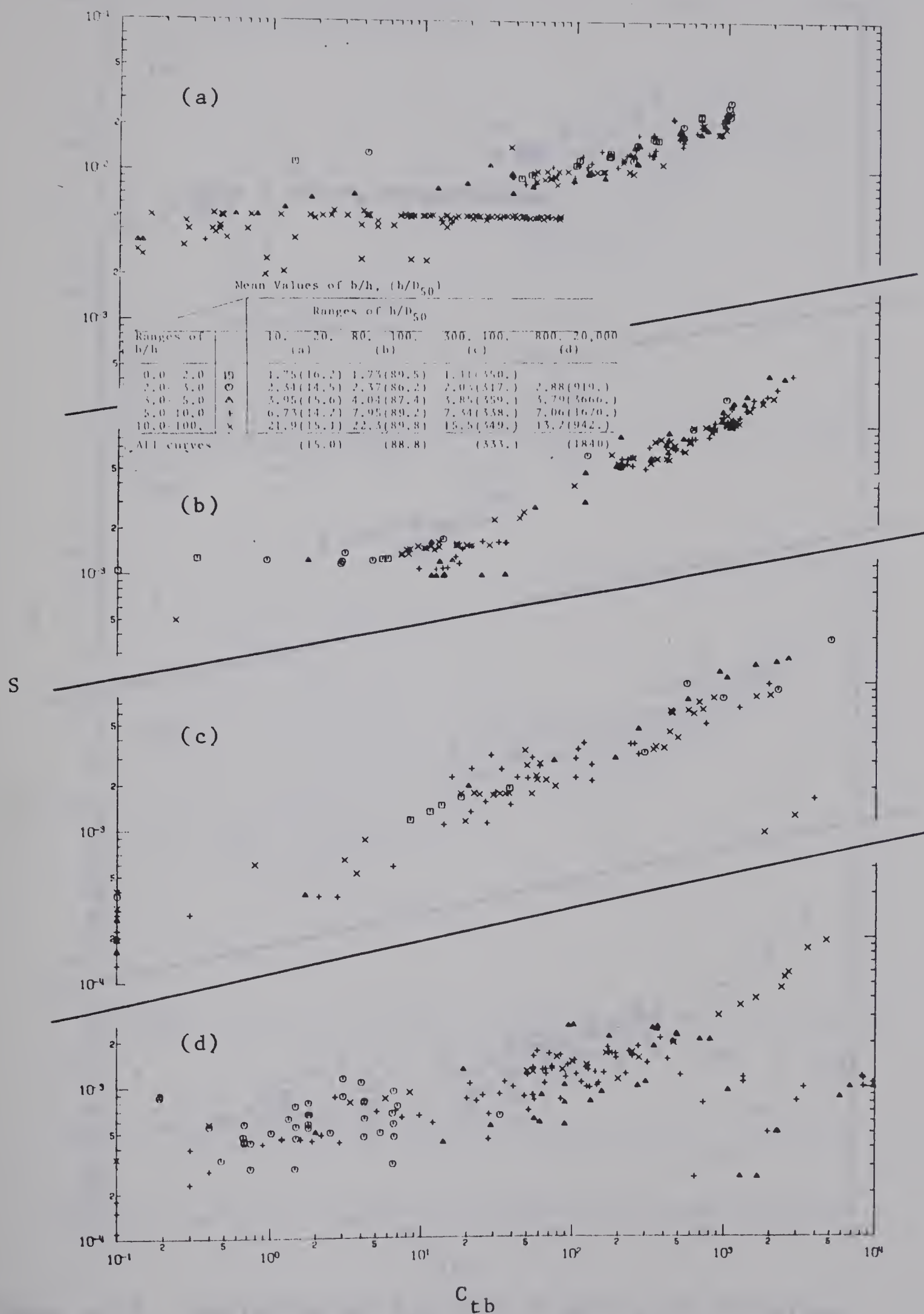


Figure 6-21. Variation of  $C_{tb}$  with  $S$  and  $b/h$  at Different Levels of  $h/D_{50}$



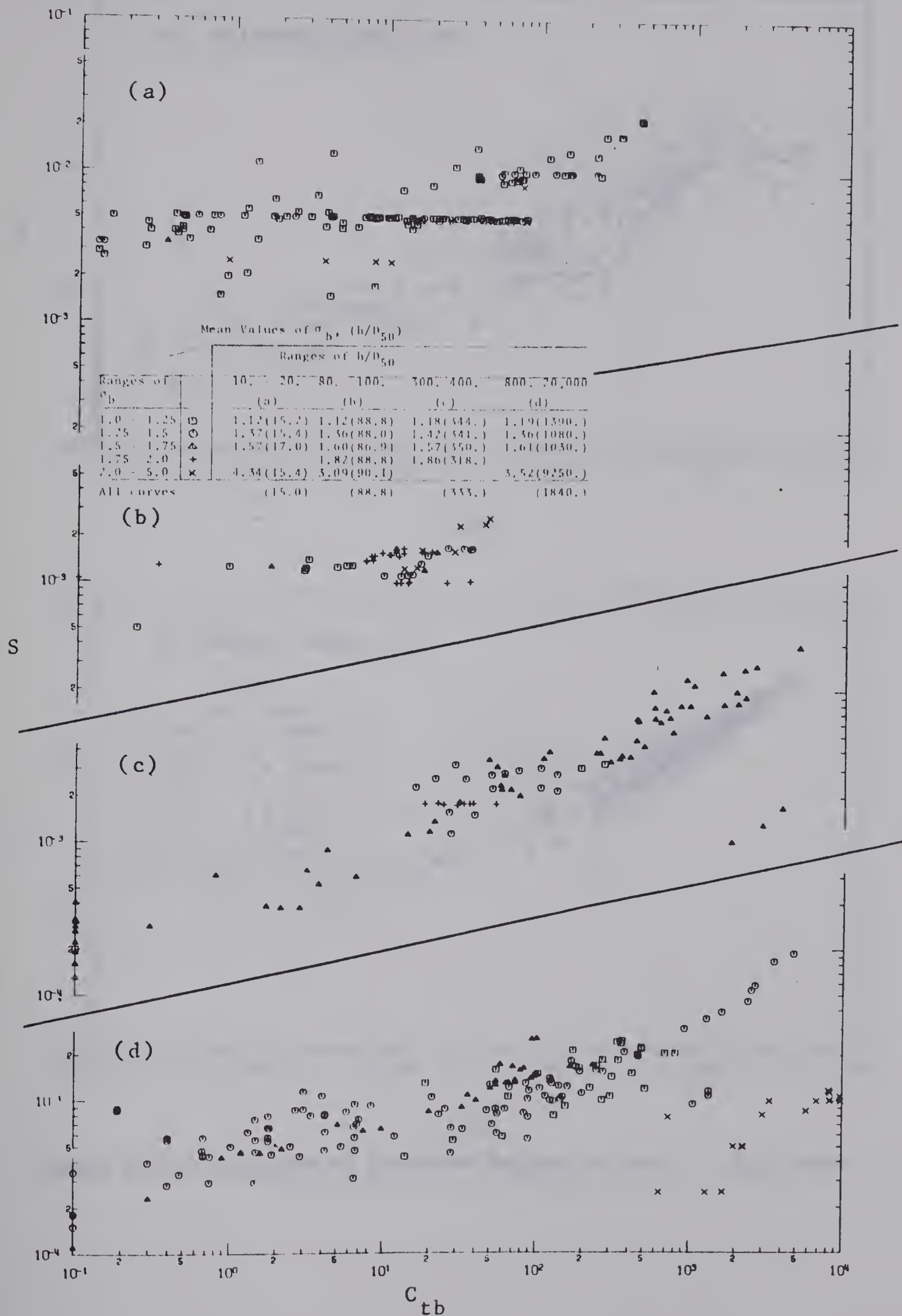


Figure 6-22. Variation of  $C_{tb}$  with  $S$  and  $\sigma_b$  at Different Levels of  $h/D_{50}$





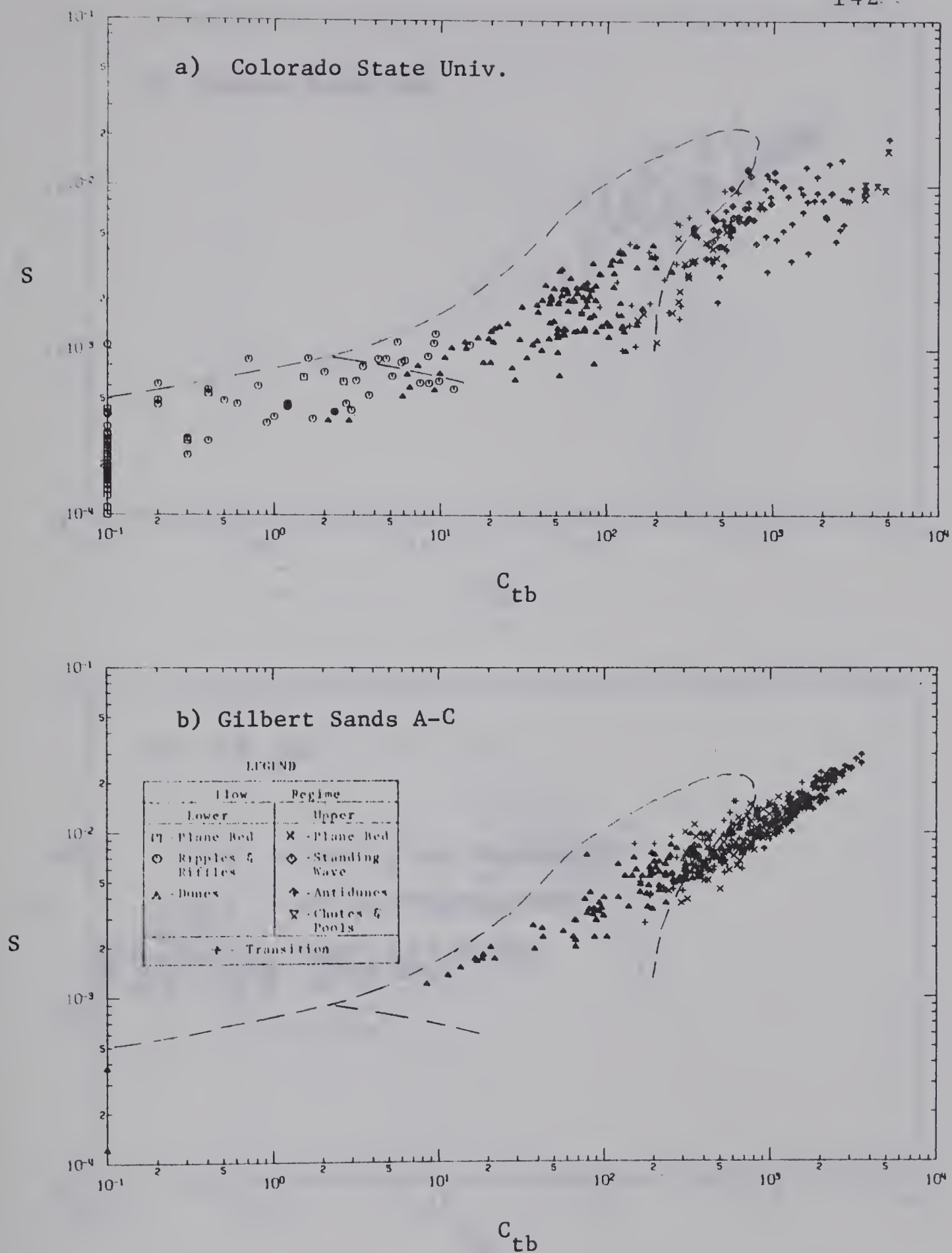


Figure 6-23. Location of Bed-Form Regions on the  $S - C_{tb}$  Plane



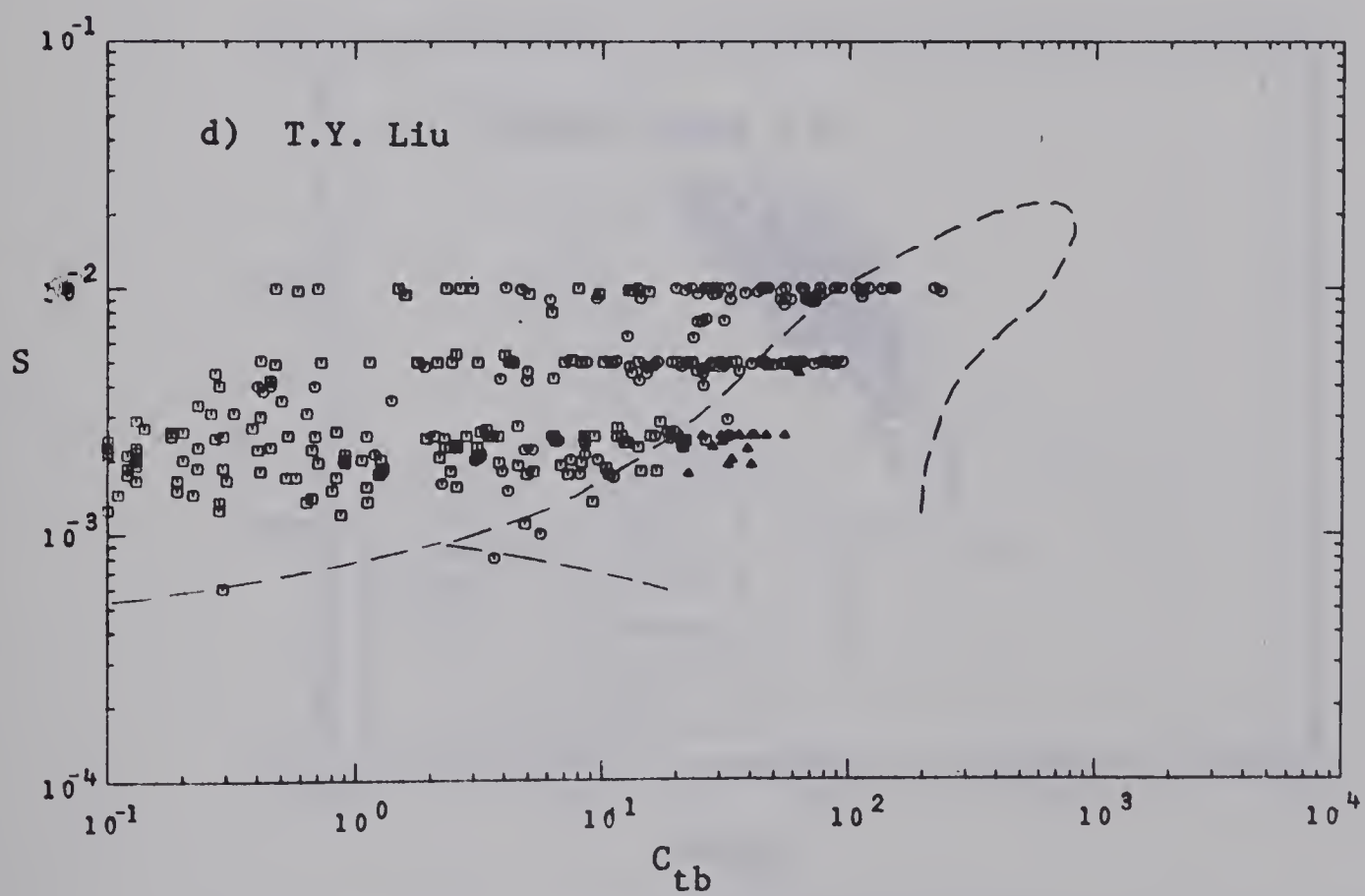
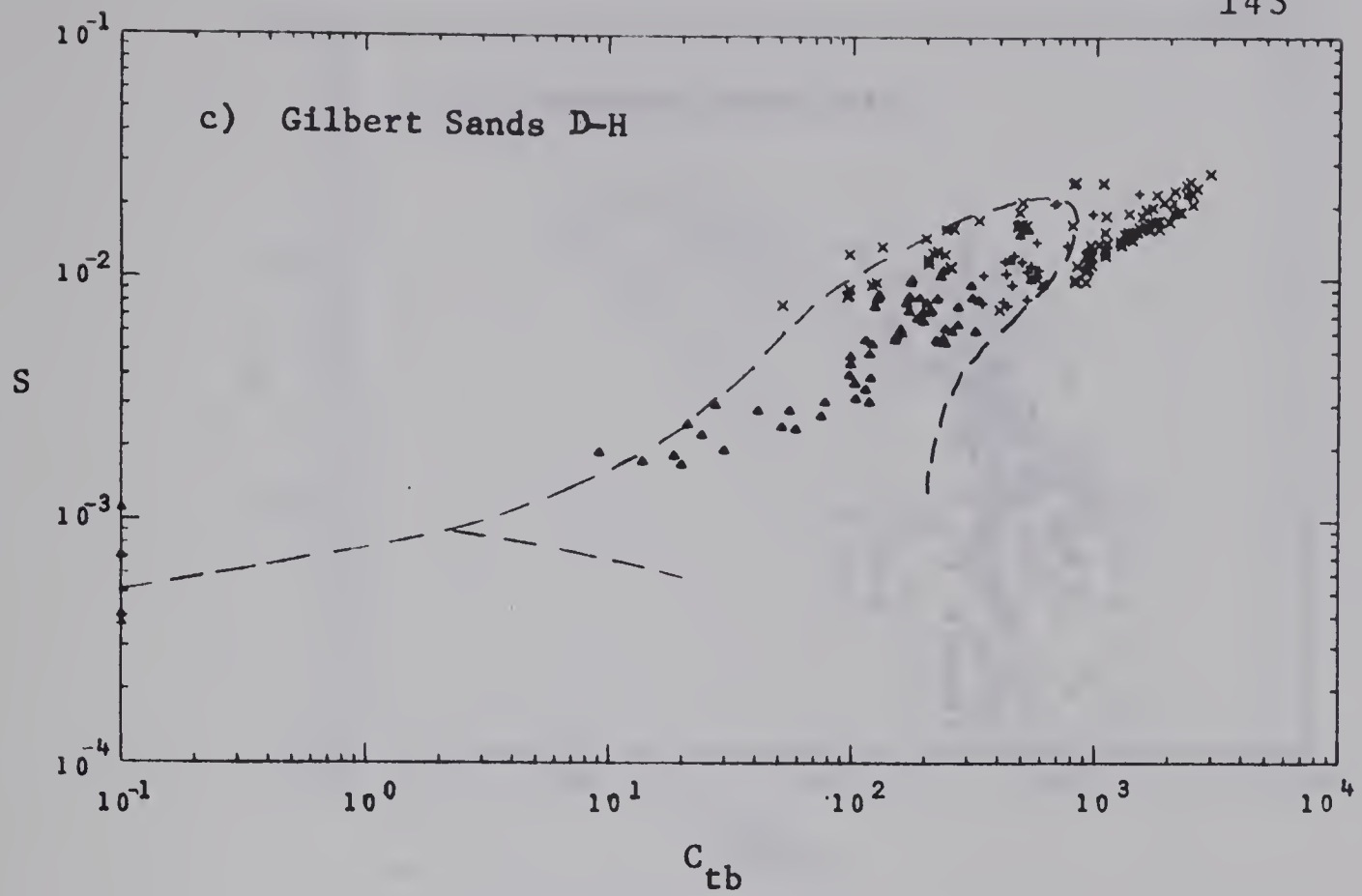


Figure 6-23. (Continued)



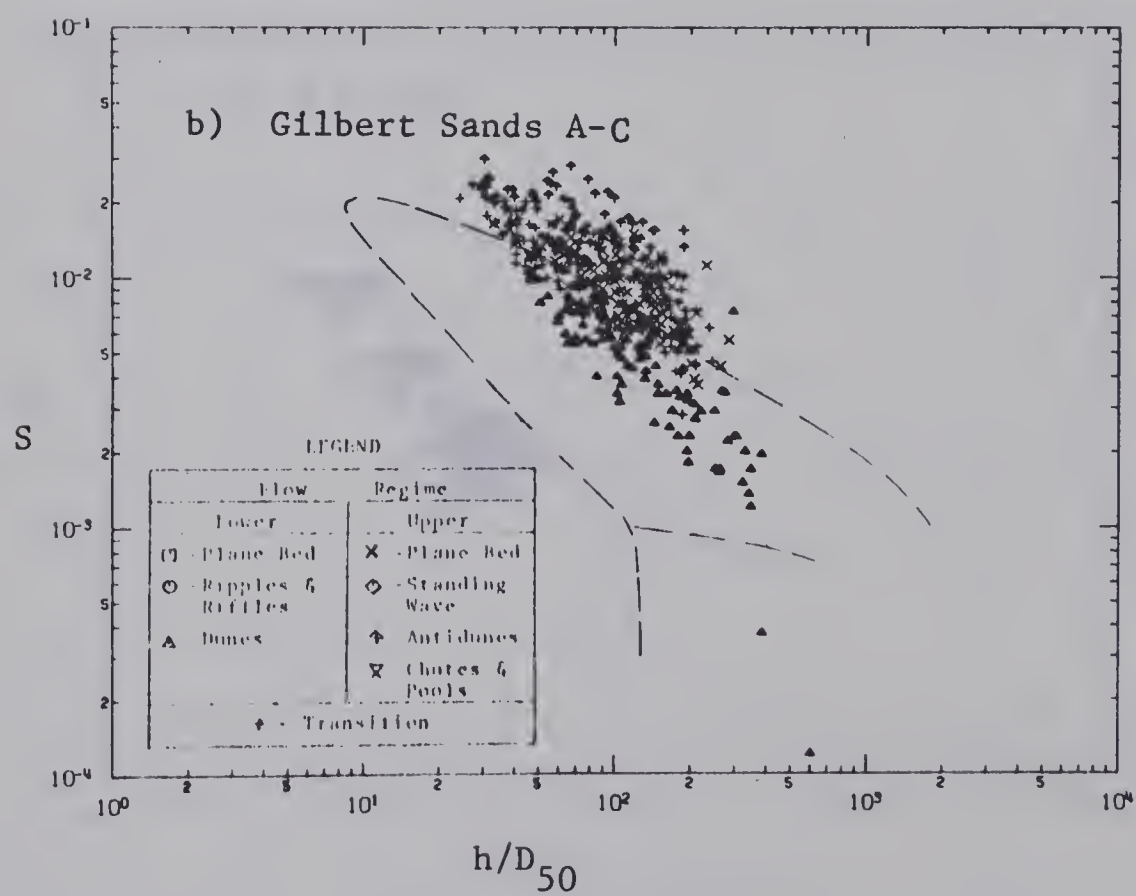
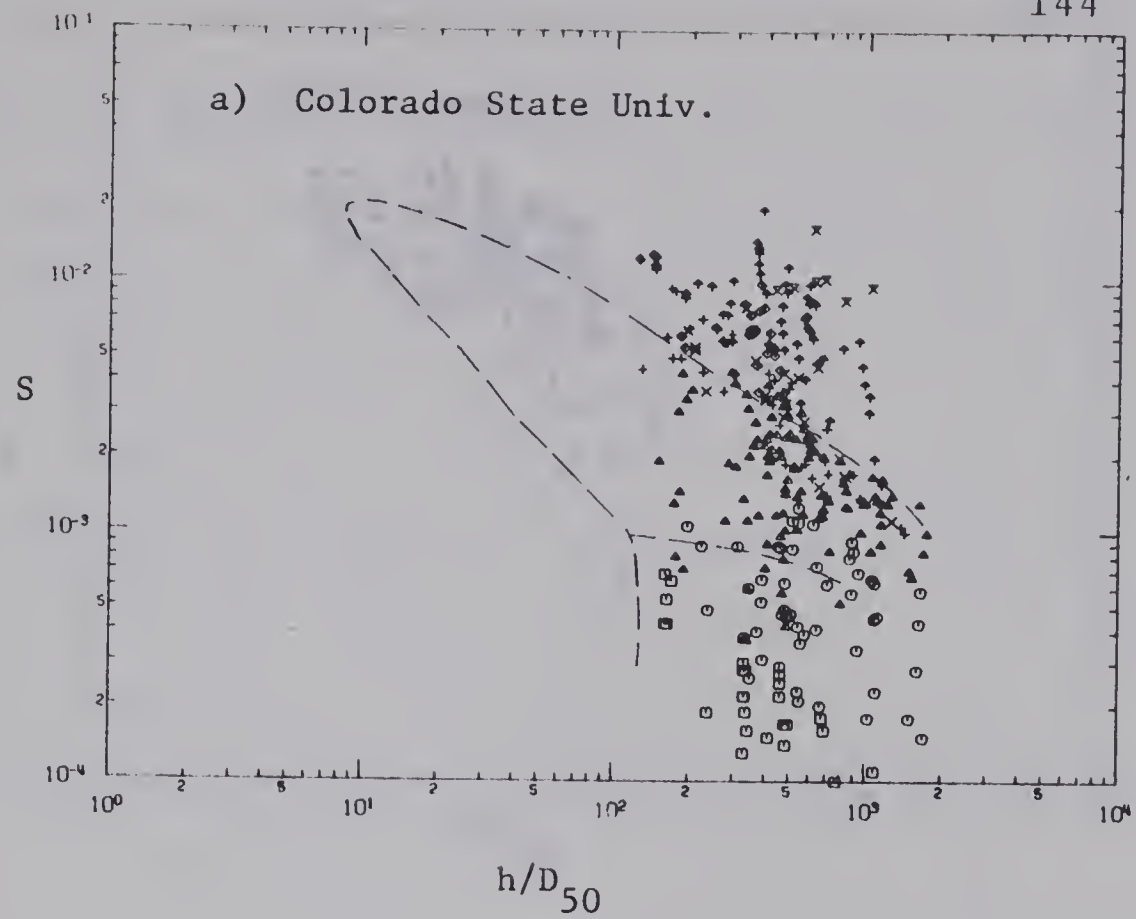


Figure 6-24. Location of Bed-Form Regions on the  $S$ - $h/D_{50}$  Plane





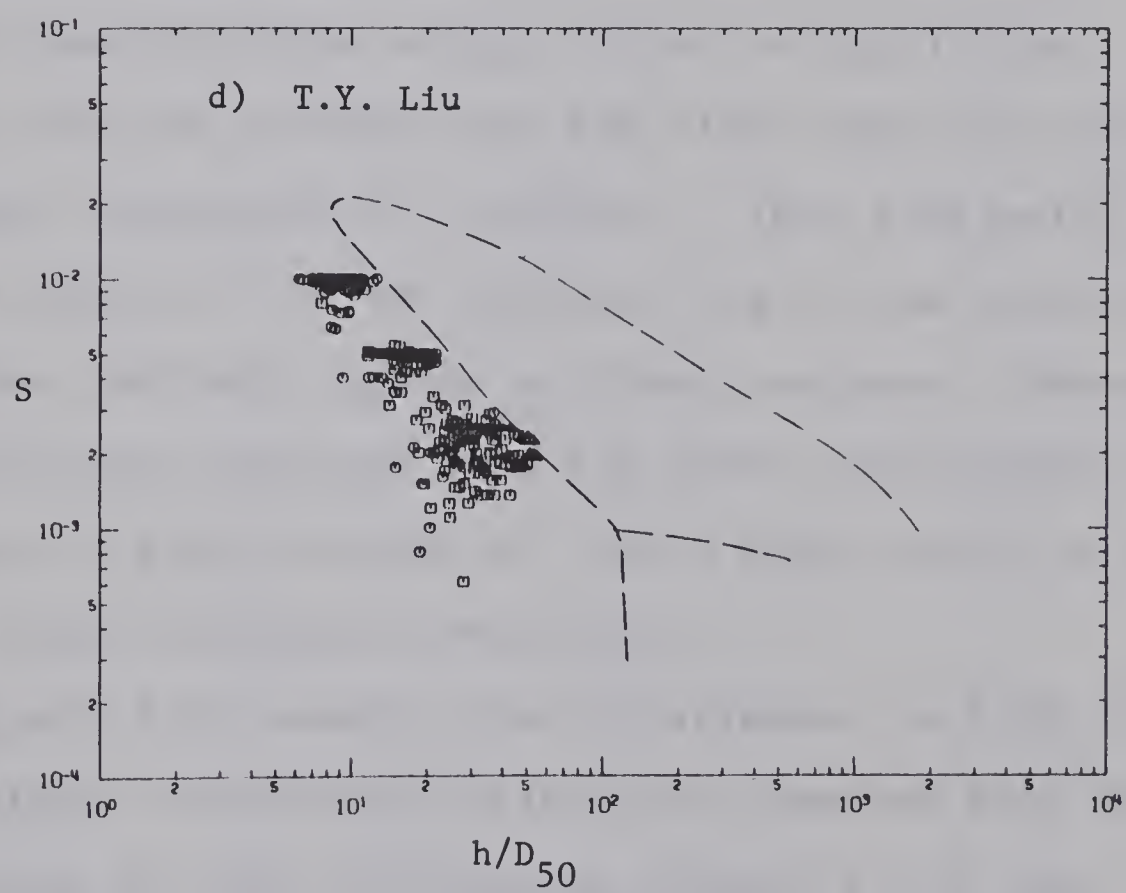
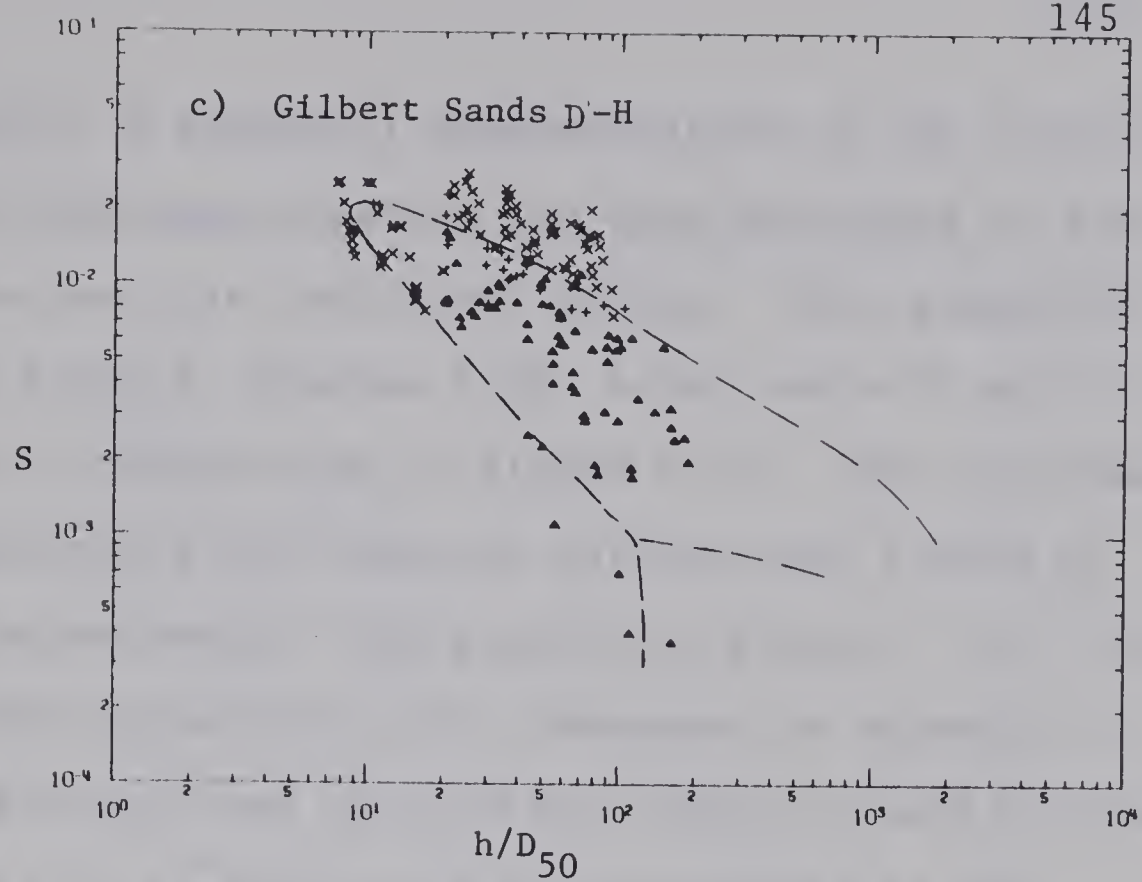


Figure 6-24 (Continued)



Finally, a graphical representation of the solution surface for the slope relation has been developed on each of the three possible coordinate planes. This graphical solution is given in Figures 6-25, 6-26, and 6-27 and is illustrated in perspective in Figure 6-28. The individual curves representing the solution surface were fitted by eye to the experimental data plotted in Figures 6-17, 6-18, 6-19, and the appropriate plots contained in Appendix D. Those data having slope observations whose reliability was considered to be in doubt were not considered in the construction of these curves.

There appears to be a high degree of similarity between the solution surfaces for the slope relation and the previously determined  $Fr'$  relation. This similarity is found in the shape of the two surfaces and in the location of the various bed-form regions on these surfaces. However, such similarity was expected from the close relationship that is known to exist between  $Fr'$  and  $S$  whose ratio is a form of the Chezy discharge coefficient.

In Figure 6-29 results from experiments on both light and heavy weight bed-materials have been compared with the solution curves for the relationship between  $S$ ,  $C_{tb}$  and  $h/D_{50}$ . It was found that the effects of variation in the density ratio ( $\rho_b/\rho_f$ ) could be accounted for by using  $1.65 S/(\rho_b/\rho_f - 1)$  and  $2.65 C_{tb} (\rho_f/\rho_b)$  instead of  $S$  and  $C_{tb}$ . These modified parameters had no effect on the solution





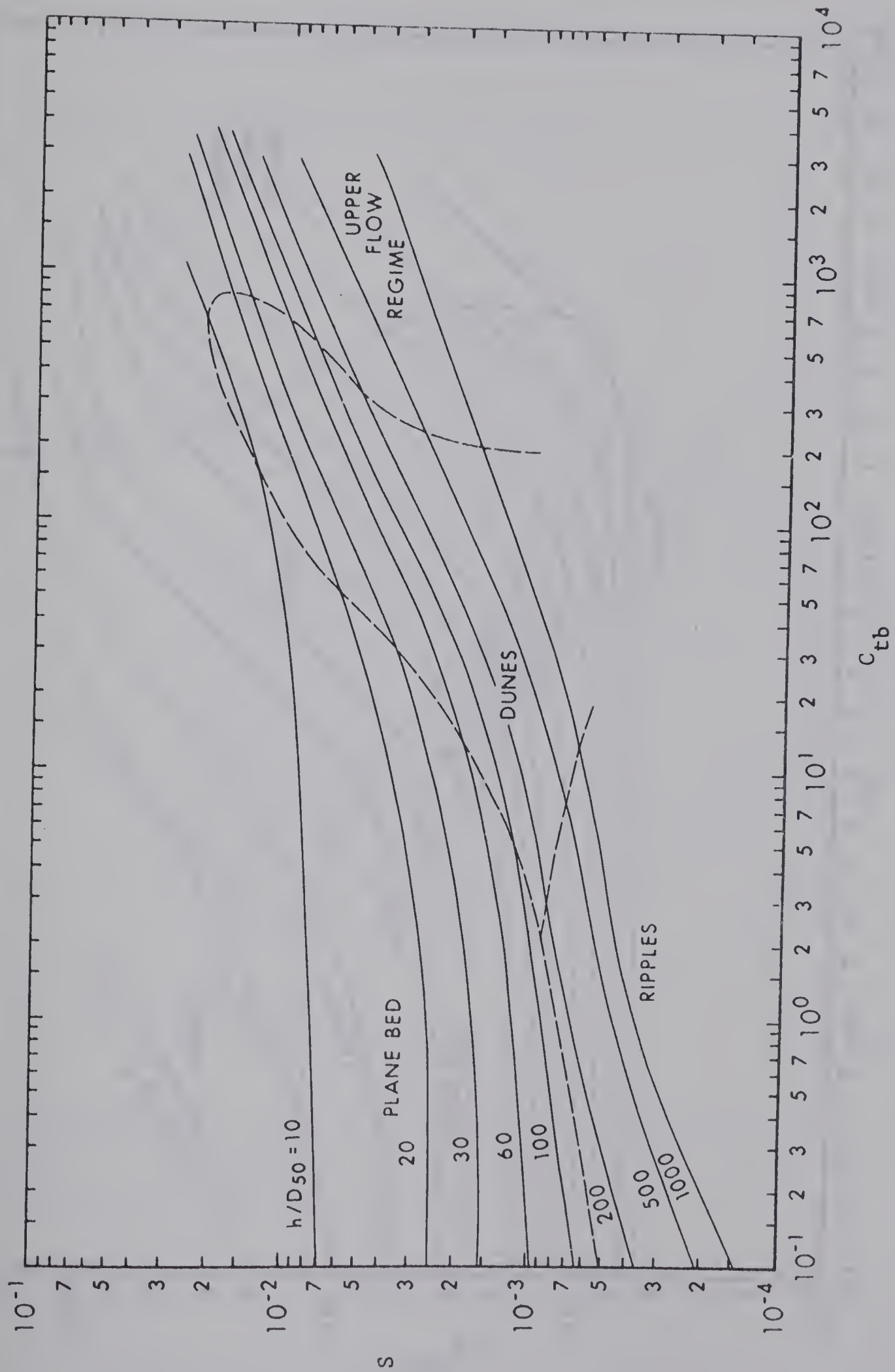


Figure 6-25. Relationship Between  $S$ ,  $C_{tb}$ , and  $h/D_{50}$  on the  $S - C_{tb}$  Plane



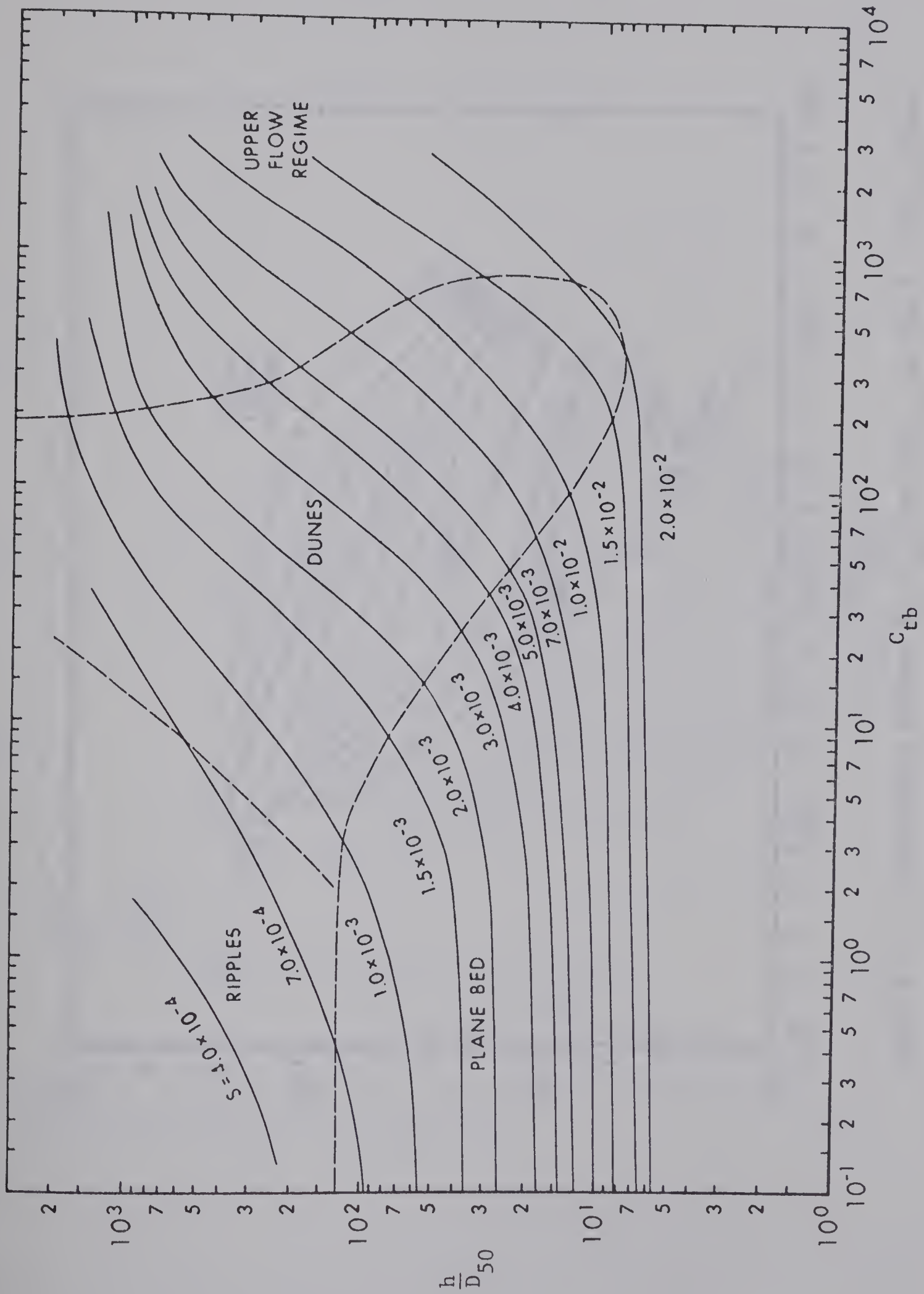


Figure 6-26. Relationship Between  $S$ ,  $C_{tb}$ , and  $h/D_{50}$  on the  $h/D_{50}$ - $C_{tb}$  Plane



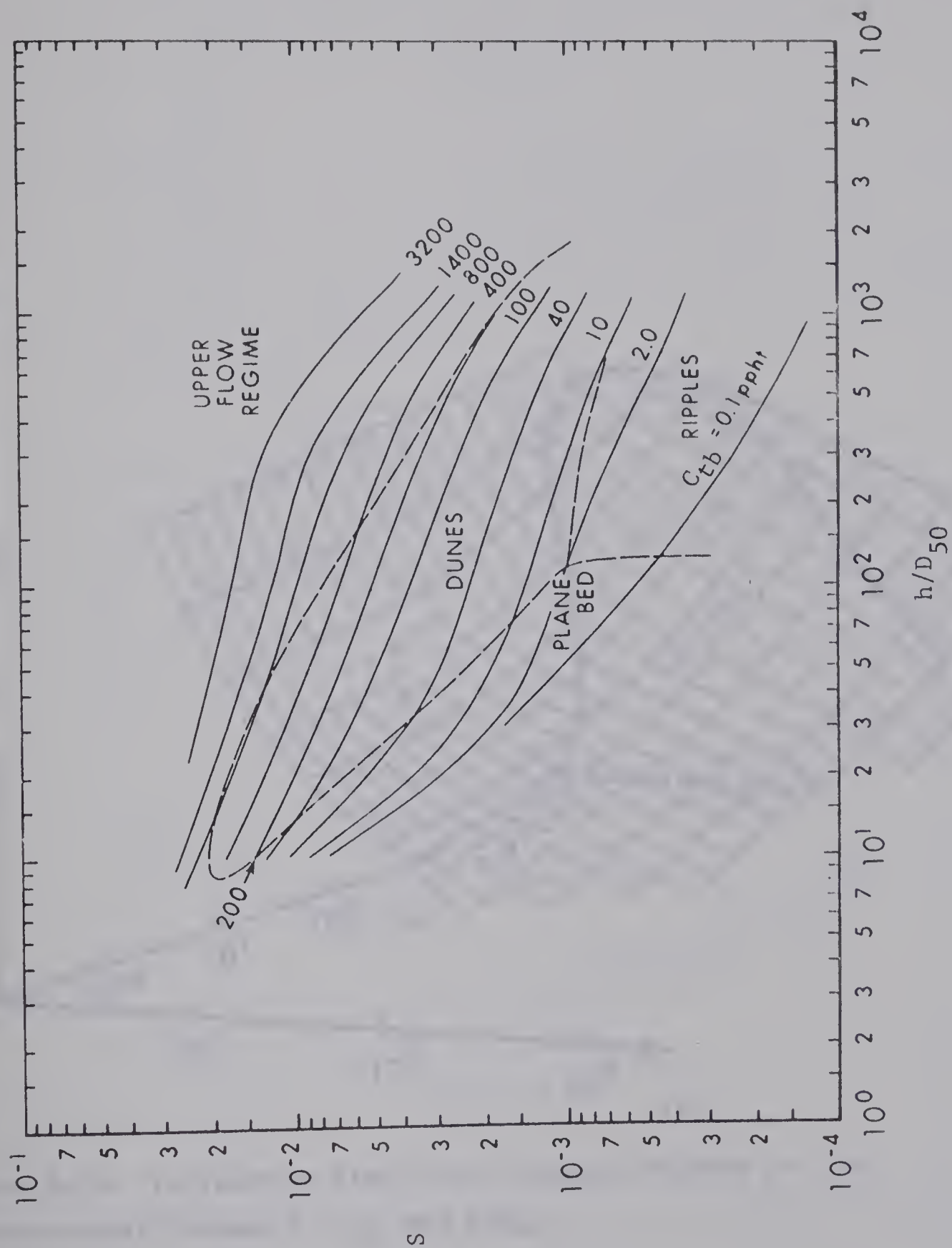


Figure 6-27. Relationship Between  $S$ ,  $C_{tb}$ , and  $h/D_{50}$ , on the  $S - h/D_{50}$  Plane





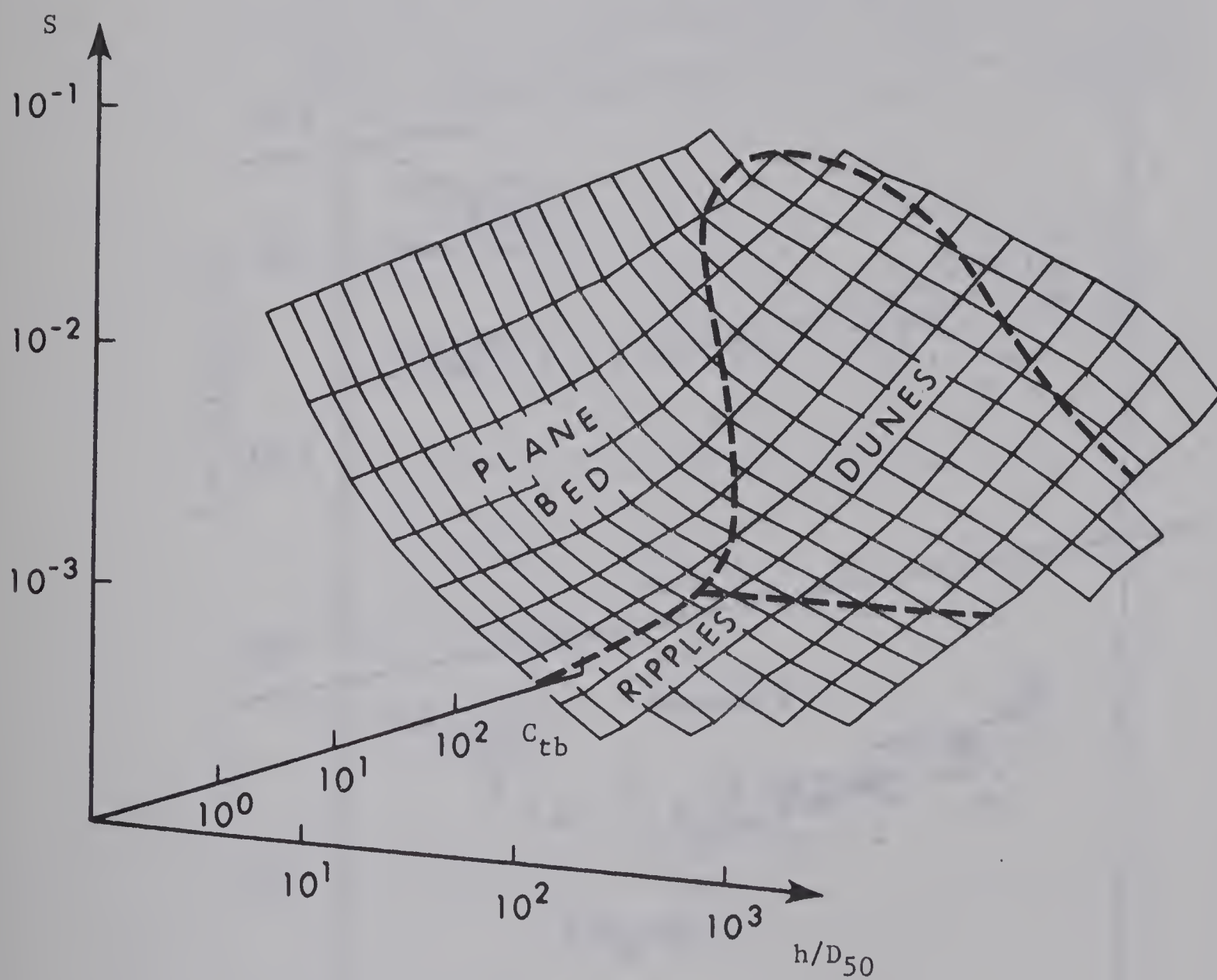


Figure 6-28. Perspective View of the Solution Surface for the Relationship Between  $S$ ,  $C_{tb}$ , and  $h/D_{50}$



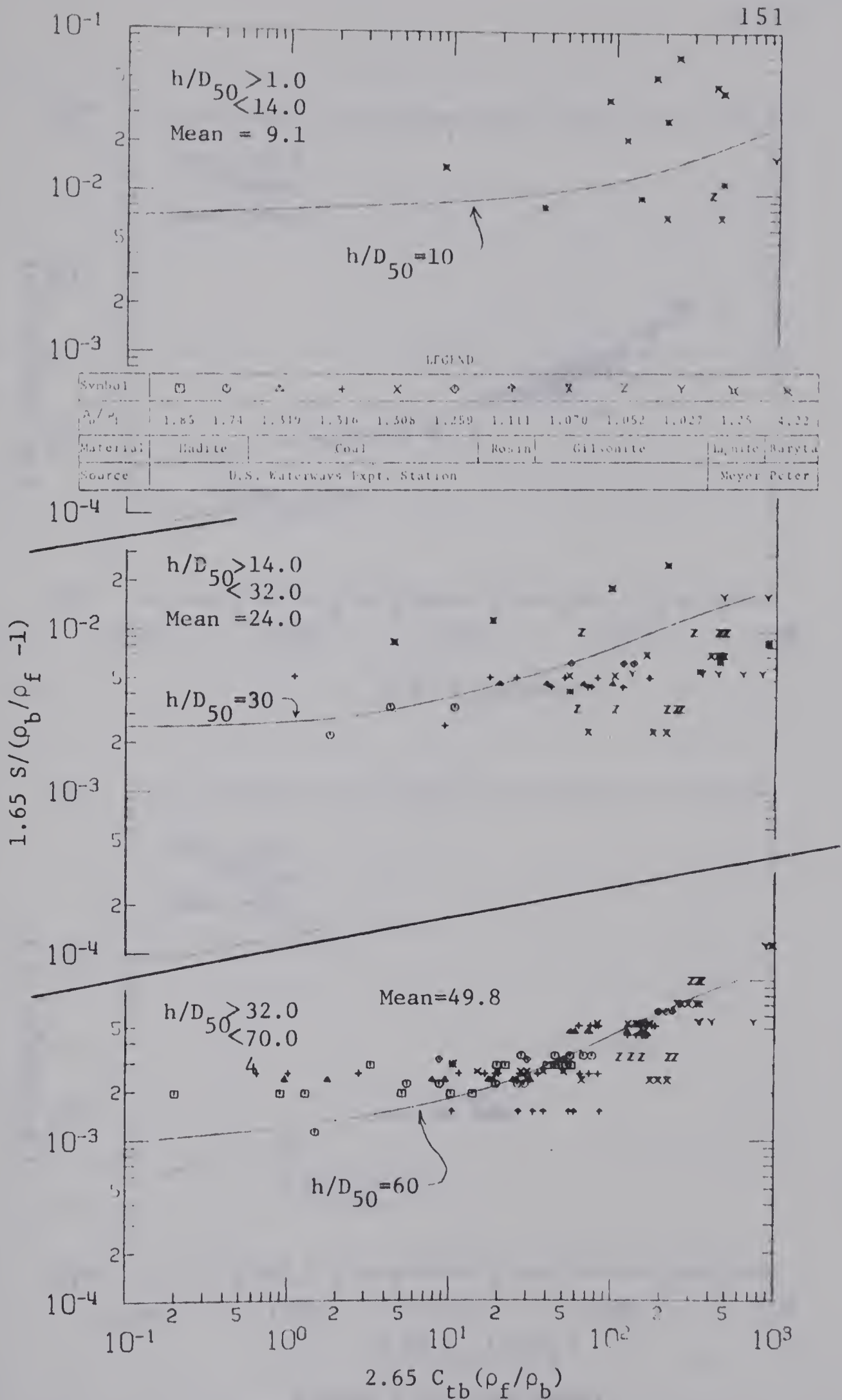


Figure 6-29. Variation of  $2.65 C_{th} (\rho_f / \rho_b)$  with  $1.65 S / (\rho_b / \rho_f - 1)$  and  $h/D_{50}$  for Experimental Data on Light and Heavy Weight Bed-Materials





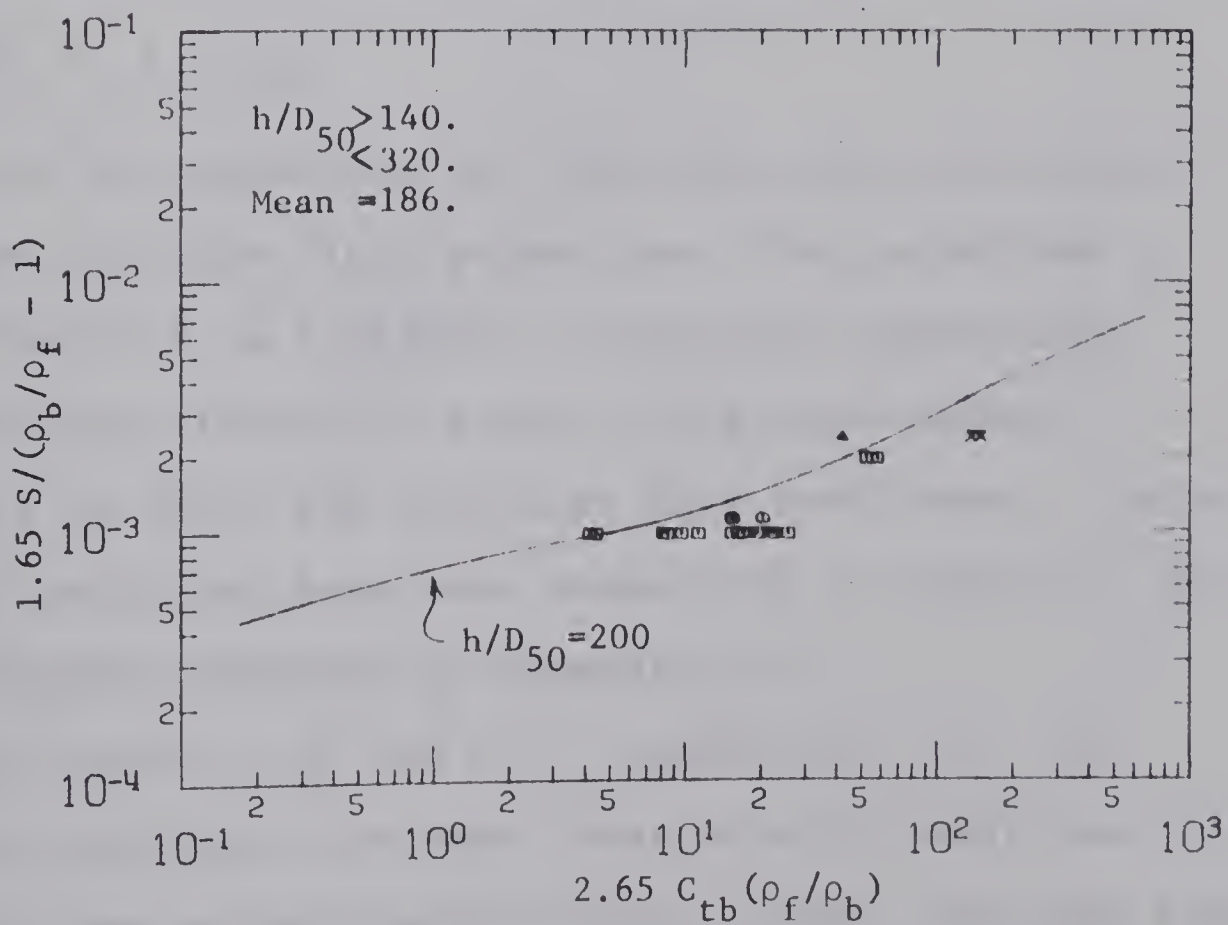
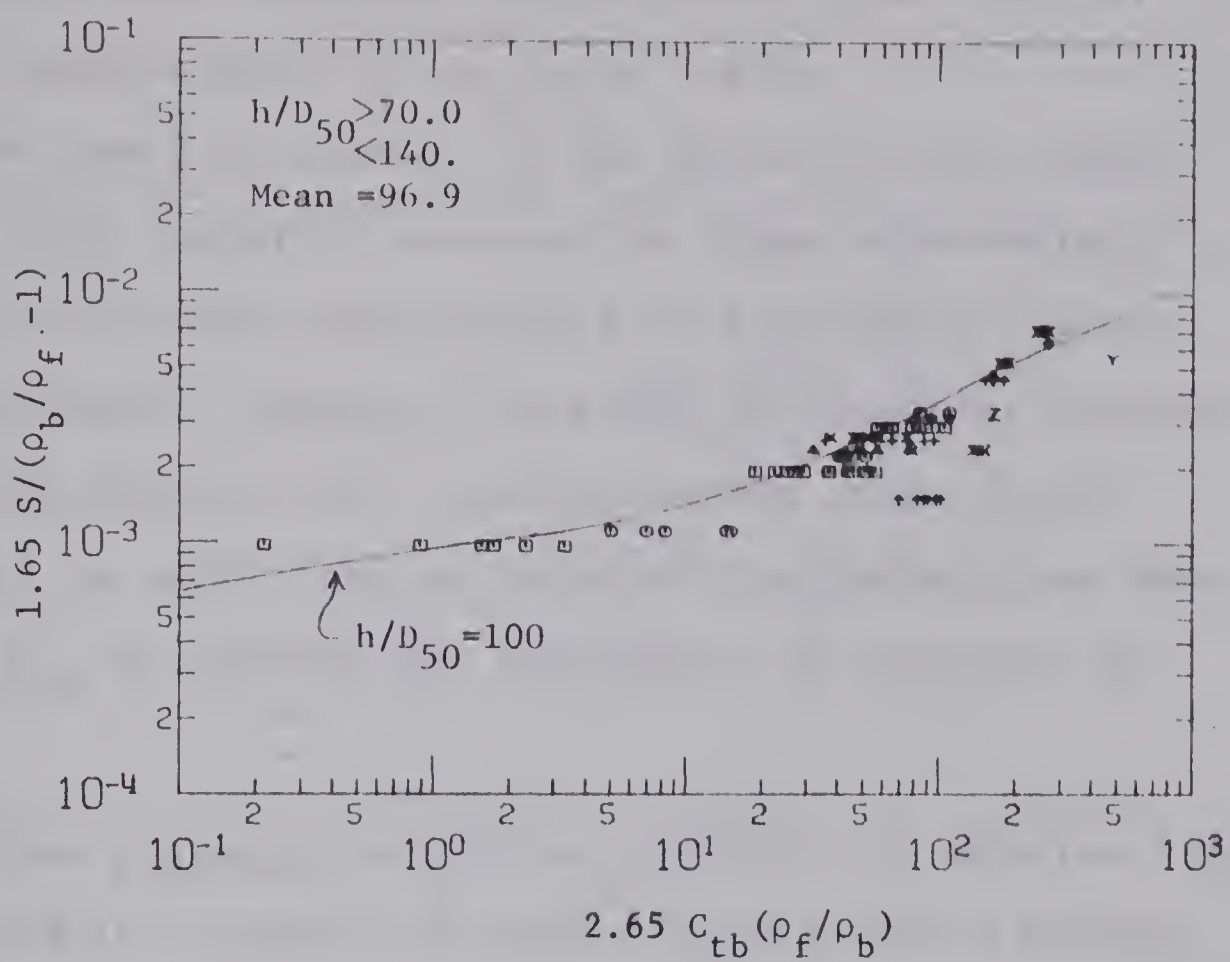


Figure 6-29 (Continued)



curves since both modifying coefficients equal one for a natural weight material ( $\rho_b/\rho_f = 2.65$ ).

The level of scatter in the plots of this figure is quite high, possibly because the slope observations for most of the data were subject to the type of error discussed above. However, the level of agreement between the plotted data and the solution curves seems to be sufficient to verify the validity of the corrections made to  $S$  and  $C_{tb}$  to account for the effect of variation in  $\rho_b/\rho_f$ .

The two graphical solutions presented in Figures 6-11 to 6-13 and in Figures 6-25 to 6-27 constitute a method that can be used for predicting any two of the variables

$$(V, h, S, C_{tb})$$

in terms of the remaining two variables, the bed-material properties, and the fluid properties. The solutions are applicable to a steady and uniform two dimensional flow operating within the scope of the experimental conditions on which the solutions have been based. These limiting conditions have been summarized in Chapter V and in the figures contained in Appendix C.

In Figures 6-30 and 6-31 respectively, the two graphical solutions have been compared with conditions predicted from regime theory (Blench, 1969a) for high levels of  $h/D_{50}$  and with criteria for the beginning of movement of particles from a plane alluvial bed.



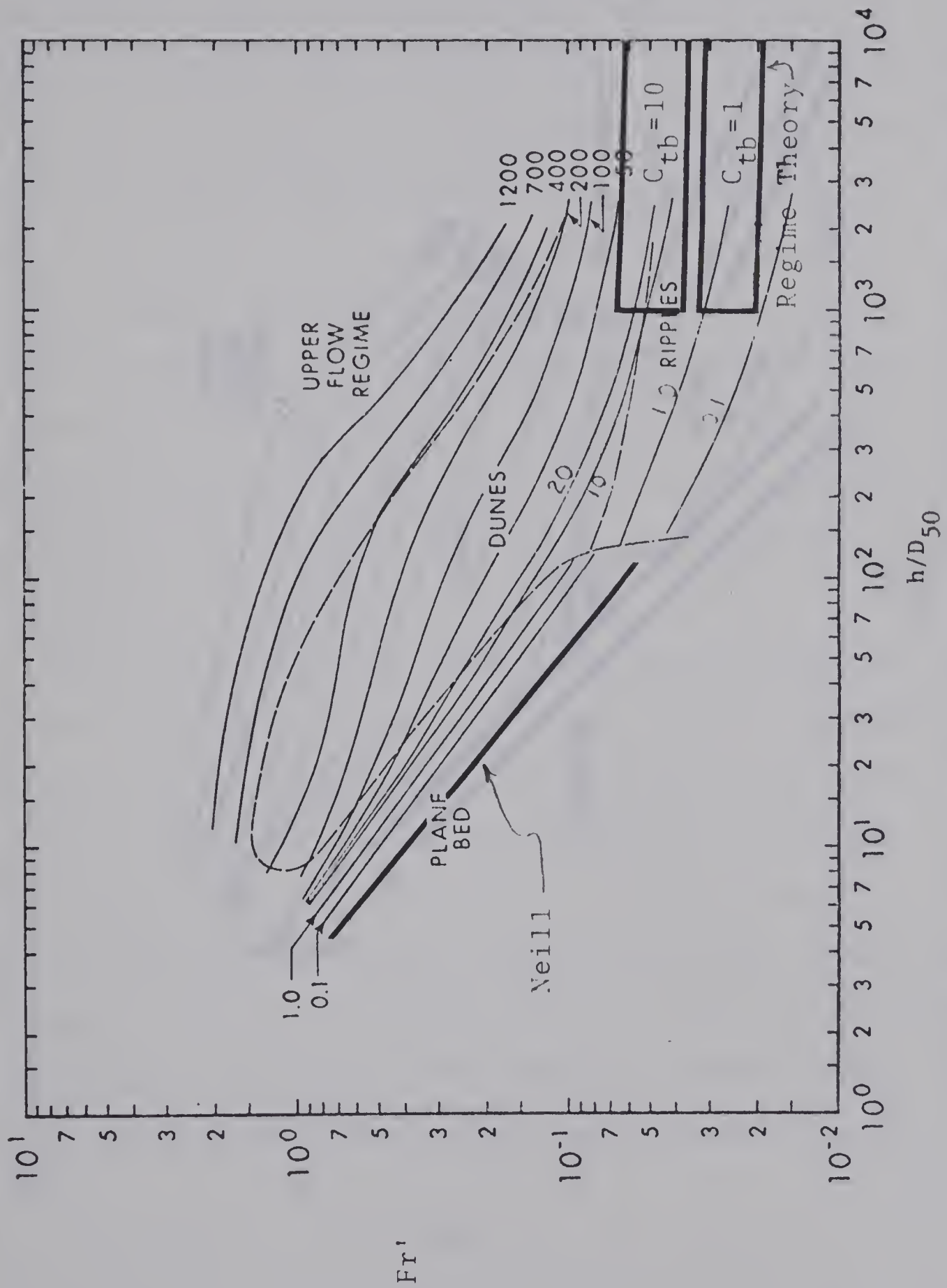


Figure 6-30. The  $Fr' - C_{tb} - h/D_{50}$  Relationship Compared with Regime Theory and Beginning of Movement Criteria





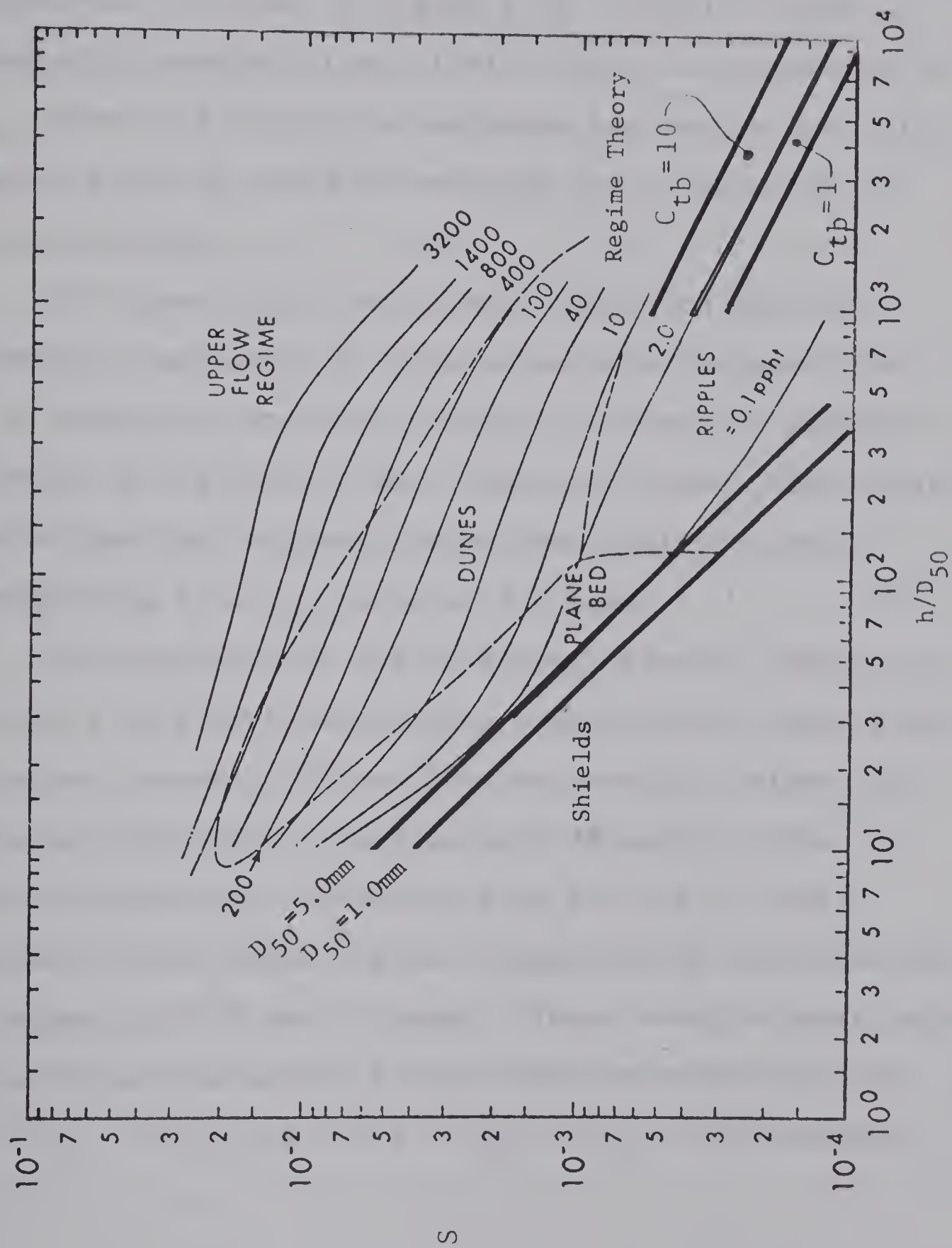


Figure 6-31. The  $S-C_{tb}-h/D_{50}$  Relationship Compared with Regime Theory and Beginning of Movement Criteria



The  $Fr' - h/D_{50}$  criterion developed by Neill (1967) for predicting the beginning of movement of coarse uniform bed-material is shown in Figure 6-30. Neill's curve essentially parallels the solution curve corresponding to a  $C_{tb}$  value of 0.1 ppht in the plane bed region and falls slightly below as could be expected for a beginning of motion criterion.

In Figure 6-31, the Shields criterion for the beginning of movement of uniform bed-material particles, in the form given by Yalin (1969), is shown for particle diameters of 1.0 and 5.0 mm. These two curves also closely parallel and fall slightly below the solution curve corresponding to a  $C_{tb}$  value of 0.1 ppht.

The equations of regime theory (Blench, 1969a) are applicable to flows having  $h/D_{50}$  values greater than 1000,  $D_{50}$  values between 0.10 and 0.60 mm, and  $C_{tb}$  values less than about 10.0 ppht. In Figures 6-30 and 6-31 the range of predictions resulting from the use of these equations within their region of application are shown for  $C_{tb}$  values of 10.0 and 1.0 ppht. These results agree quite well with extrapolations of the solution curves for the  $Fr' - C_{tb} - h/D_{50}$  and the  $S - C_{tb} - h/D_{50}$  relationships.





## CHAPTER VII

### SUMMARY, CONCLUSIONS AND RECOMMENDATIONS

#### 7-1 Summary and Conclusions

The present study has been undertaken for the purpose of developing relations that would be capable of adequately predicting the behavior of flow in alluvial channels. A review of the existing theories suggested the value of many of these theories to be somewhat restricted either because they have failed to take into consideration the effects of one or more possibly relevant variables or because they have been based on only a limited collection of experimental data and consequently are applicable to only a limited range of conditions. Accordingly, an attempt has been made in the present study to formulate a mathematical model involving all of the possibly relevant variables and to evaluate this model by analyzing the majority of available experimental data.

A major portion of the work has necessarily consisted of the compilation of many collections of experimental data and the preparation of these data for subsequent analysis on a computer. Data from over three thousand different experiments were included in the compilation and used in the analysis.

A mathematic model describing the behavior of flow in alluvial channels was developed by the method of dimensional analysis. Since this approach tended to minimize the required number of simplifying assumptions, it permitted consideration



of the majority of variables likely to have a relevant effect on the phenomenon. The final form of the mathematical model which was subjected to empirical evaluation consisted of the two functional expressions

$$0 = \text{fn}(\text{Fr}', C_{tb}, \frac{h}{D_{50}}, Vi, \frac{b}{h}, \sigma_b) \quad (7-1)$$

and

$$0 = \text{fn}(S, C_{tb}, \frac{h}{D_{50}}, Vi, \frac{b}{h}, \sigma_b) \quad (7-2)$$

The model was evaluated by plotting scatter diagrams of the relationship between the first three parameters in each expression and determining if the scatter in these plots could be attributed to variation in any of the remaining parameters.

The results showed the parameters  $Vi$  and  $b/h$  to have no significant effect on either relationship within the range of experimental conditions covered in the analysis. However, it must be emphasized that at all levels of  $h/D_{50}$ , the experimental range of  $Vi$  is significantly less than that found in nature.

Upon first examination, variation in the bed-material gradation ( $\sigma_b$ ) had no noticeable effect on the  $S-C_{tb}-h/D_{50}$  relationship but appeared to be the cause of some of the scatter in  $\text{Fr}'-C_{tb}-h/D_{50}$  relationship. However, the effects of this variation were unsystematic at each level of  $h/D_{50}$  and were inconsistent between the different levels of  $h/D_{50}$ . Because of these inconsistencies





and because variation in  $\sigma_b$  in many cases corresponded to a change in the source of experiments, there appears to be a strong possibility that the apparent effect of  $\sigma_b$  can be attributed to variation in the degree of experimental error.

By accepting this latter hypothesis and by limiting the scope of application to the effective experimental range of  $V_i$  at each level of  $h/D_{50}$ , the mathematical model was reduced to

$$0 = \text{fn}(\text{Fr}', C_{tb}, \frac{h}{D_{50}}) \quad (7-3)$$

and

$$0 = \text{fn}(S, C_{tb}, \frac{h}{D_{50}}) \quad (7-4)$$

It was found that the non-dimensional parameters contained in this mathematical model resulted in satisfactory data correlations that adequately described the phenomenon.

From the plots of experimental data, graphical representations of the solution surfaces for Equations 7-3 and 7-4 were constructed in the form of families of curves drawn on each of the possible coordinate planes. These solution curves can be used for the prediction of any two of the variables  $V$ ,  $S$ ,  $h$ , and  $C_{tb}$  in terms of known bed-material properties and known values of the remaining two variables.

Considerable attention was given to the role of the various possible bed-forms and the possibility of a different phase of behavior corresponding to each bed-form. Several





sets of experimental data in which bed-forms had been classified were used to determine, on each of the solution surfaces, the boundaries between the regions corresponding to the different bed-form configurations. A close correspondence was found to exist between the location of these boundaries and the locations of transitions in the form of the relationships between variables. The plots showing these boundaries can be used as criteria for predicting the type of bed-form configuration that will develop for a given set of flow conditions.

The above results were based on data from experiments on bed-materials having natural specific gravities approximately equal to 2.65. However, a number of collections of data were available from experiments on bed-materials having specific gravities ranging from 1.03 to 4.22. From an analysis of these data, it was found that variation in particle density could be satisfactorily accounted for by replacing  $C_{tb}$  with  $2.65 C_{tb}(\rho_f/\rho_b)$  and  $S$  with  $1.65 S/(\rho_b/\rho_f - 1)$ .

The graphical solution for Equation 7-3 was tested against a number of natural channel observations. The agreement between these two results supported the validity of the solution.

The experimental equipment, operating procedures, and properties of the bed-materials not considered in the analysis varied considerably between the different collections of data



on which the graphical solutions have been based. Variation in these factors could be expected to add to the already high level of experimental error generally associated with experiments on flow in alluvial channels. Because of the overall quality of the data used, the graphical solutions should, at best, be considered as approximations to the natural physical laws governing the phenomenon.

Another objective of the investigation was to examine the compiled experimental data for the purpose of determining the scope of available experimental conditions. Results were presented to describe the distribution of experimental values of a number of observed and computed variables in addition to the joint distribution between experimental values of pairs of the parameters contained in the mathematical model. These results define the allowable range of conditions to which the above graphical solutions can be safely applied. They are also valuable for eliminating unnecessary duplication of results in the design of future experiments.

The major deficiencies in the existing experimental data included a shortage of experiments having  $h/D_{50}$  values in the range above 500 and a shortage of experiments on gravel sized bed-materials ( $D_{50} > 3$  mm,  $V_i \lesssim 70$ ) for all but the very small values of  $h/D_{50}$ . Conditions in both of these regions commonly occur in natural channels.







## 7-2 Recommendations

From the results of the foregoing study the following recommendations can be made:

(1) Experiments should be carried out to test for the existence of a stable plane bed configuration at low rates of bed-material transport and to determine more precisely the location of the boundaries between the different bed-form regions and the extent of any transitional zones between these regions.

(2) Detailed experimental studies are needed to examine the role of the bed-material properties such as particle size gradation, particle shape and its distribution, the orientation of particles, and their surface roughness. The results of these studies could be used to either modify or verify the method presented herein.

(3) The results describing the scope of existing experimental conditions should be carefully considered in the design of future general experiments on bed-material transport. This will eliminate unnecessary duplication of experimental effort and will result in a worthwhile expansion of the experimental data.

(4) New experiments should be carried out in the range of  $h/D_{50}$  between five hundred and ten thousand, at all levels of bed-material transport. Furthermore, data should be obtained for bed-materials having median diameters falling in the gravel range ( $D_{50} > 3\text{mm}$  or  $V_i \geq 70$ ), over as large an



$h/D_{50}$  as possible. These were the two major deficiencies found in considering the scope of existing experimental conditions, and new data covering these regions would permit a valuable extension to the range of application of the method presented herein.



## LIST OF REFERENCES

- Alam, A.M.Z., Cheyer, T.F., and Kennedy, J.F., 1966, Friction factors for flow in sand bed channels: Report no. 78, Hydrodynamics Laboratory, Dept. of Civil Engineering, Massachusetts Institute of Technology.
- ASCE Task Committee on Erosion of Cohesive Materials, 1968, Erosion of cohesive sediments: Am. Soc. Civil Engineers Jour., v. 94, no. HY-4.
- Bagnold, R.A., 1956, The flow of cohesionless grains in fluid: Royal Soc. Philos. Trans., v. 249.
- Barr, D.I.H., and Herbertson, J.G., 1968, Similitude theory applied to correlation of flume sediment transport data: Am. Geophys. Union, Water Resources Research, v. 4, no. 2.
- Blench, T. and Erb, R.B., 1957, Regime analysis of laboratory data on bed-load transport: Lallouille Blanche, no. 2, p. 148-157.
- Blench, T., 1969a, Mobile-bed fluviology: University of Alberta Press, 2nd Edition.
- Blench, T., 1969b, Dimensional analysis and dynamical similarity for hydraulic engineers: University of Alberta Bookstore, Edmonton, Canada.
- Brooks, N.H., 1958, Mechanics of Streams with movable beds of fine sand: Am. Soc. Civil Engineers Trans., v. 123.
- Brown, C.B., 1950, Engineering hydraulics (Hunter Rouse, editor): John Wiley and Sons, New York.
- Chang, Y.L., 1939, Laboratory investigation of flume traction and transportation: Am. Soc. Civil Engineers Trans., v. 104.
- Colby, B.R., 1964, Discharge of sands and mean-velocity relationships in sand-bed streams: U.S. Geol. Survey Prof. Paper 462-A.
- Cooper, R.H., and Peterson, A.W., 1969, A review of data from sediment transport experiments: Dept. of Civil Engineering, University of Alberta, Report no. HY-ST2.
- Einstein, H.A., 1942, Formulas for the transportation of bed-load: Am. Soc. Civil Engineers Trans., v. 107.





- Einstein, H.A., 1950, The bed-load function for sediment transportation in open channel flows: U.S. Dept. of Agriculture Tech. Bull. 1026.
- Einstein, H.A., and Barbarossa, N.L., 1952, River channel roughness: Am. Soc. Civil Engineers Trans., v. 117.
- Engelund, F., 1966, Hydraulic resistance of alluvial streams: Am. Soc. Civil Engineers Jour., v. 92, no. HY-2.
- Gilbert, G.K., 1914, The transport of debris by running water: U.S. Geol. Survey Prof. Paper 86.
- Guy, H.P., Simons, D.B., and Richardson, E.V., 1966, Summary of alluvial channel data from flume experiments: U.S. Geol. Survey Prof. Paper 462-I.
- Guy, H.P., Rathbun, R.E., and Richardson, E.V., 1967, Recirculating and sand-feed type flume experiments: Am. Soc. Civil Engineers Jour., v. 93, no. HY-5.
- Hubbell, D.W., and Matekja, D.Q., 1959, Investigations of sediment transportation, Middle Loup River at Dunning Nebraska: U.S. Geol. Survey Water-Supply Paper 1476.
- Huntley, H.E., 1967, Dimensional analysis: Dover Publications, New York.
- Johnson, J.W., 1943, Laboratory investigations on bed-load transportation and bed roughness: U.S. Soil Conservation Service, No. SCS-TP-50.
- Kalinske, A.A., 1947, Movement of sediment as bed-load in rivers: Am. Geophys. Union Trans., v. 28.
- Laursen, E.M., 1958, The total sediment load of streams: Am. Soc. Civil Engineers Proc., v. 84, no. HY-1.
- Leliavsky, S., 1966, An introduction to fluvial hydraulics: Dover Publications, New York.
- Leopold, L.B., 1969, Personal correspondence.
- Leopold, L.B., Wolman, M.G., and Miller, J.P., 1964, Fluvial processes in geomorphology: W.H. Feeman & Co., San Francisco.
- Liu, H.K., 1957, Mechanics of Sediment ripple formation: Am. Soc. Civil Engineers Jour., v. 83, no. HY-2.
- Lovera, F., and Kennedy, J.F., 1969, Friction factors for flat-bed flows in sand channels: Am. Soc. Civil Engineers Jour., v. 95, no. HY-4.



- Maddock, T., 1966, The behavior of straight alluvial channels: Proc. of the Symposium of Hydrology and Water Resources, Ankara, Turkey, 1966.
- Meyer-Peter, E., and Müller, R., 1948, Formulas for bed-load transport: Internat. Assoc. for Hydraulic Structures Research, 2nd Meeting, Stockholm.
- Neill, C.R., 1967, Mean-velocity criterion for scour of coarse uniform bed-material: Internat. Assoc. for Hydraulic Research, Proc. of the XII Congress.
- Rottner, J., 1959, A formula for bed-load transportation: La Houille Blanche, no. 3.
- Schulits, S., 1935, The Schoklitsch bed-load formula: Engineering, v. 139.
- Simons, D.B., Richardson, E.V., and Albertson, M.L., 1961, Flume studies using medium sand (0.45 mm): U.S. Geol. Survey Water Supply Paper 1498-A.
- Simons, D.B., and Richardson, E.V., 1963, Form of bed-roughness in alluvial channels: Am. Soc. Civil Engineers Trans., v. 128.
- Simons, D.B., Richardson, E.V., and Haushild, W.R., 1963, Some effects of fine sediment on flow phenomenon: U.S. Geol. Survey Water Supply Paper 1498-G.
- Simons, D.B., and Richardson, E.V., 1966, Resistance to flow in alluvial channels: U.S. Geol. Survey Prof. Paper 422-J.
- Stein, R.A., 1965, Laboratory studies of total load and apparent bed-load: Am. Geophys. Union, Jour. of Geophysical Research. v.70, no. 8.
- Yalin, M.S., 1963, An expression for bed-load transportation: Am. Soc. Civil Engineers Jour., v. 89, no. HY-3.
- Yalin, M.S., 1964, Geometrical properties of sand waves: Am. Soc. Civil Engineers Jour., v. 90, no. HY-5.
- Yalin, M.S., 1969, Sediment transport, (A textbook in preparation).







## APPENDIX A

### SUMMARY OF COMPUTER PROGRAMS USED IN THE ANALYSIS



Program Name: GPL

Description: GPL is designed to simplify the preparation of two dimensional data plots for plotting on a CalComp plotter. It can be used with any Fortran IV calling program and has the following features and options:

(1) The ability to generate multiple plots (a plot consists of a single X-Y coordinate system and all data points plotted on that system) and to organize their placement on the plotting paper.

(2) The ability to handle multiple curves (a curve consists of a single set of X and Y values) on a given plot and to identify each curve with a different plotting symbol.

(3) The option of choosing from arithmetic, logarithmic, or probability scales for each axis on a given plot.

(4) The option of selecting the size of each axis and of having either specified or automatically determined origins and/or scales.

(5) The option of selecting the type of plotting, the permissible types include symbols only, symbols joined by either straight lines or smooth curves, straight lines or smooth curves only, and bar graphs.

(6) The option of having the value of a third parameter printed adjacent to each plotted point.



Output from GPL includes a plot tape for use on a CalComp plotter and a printed summary table describing each curve plotted.

GPL is fully documented and is operational on an IBM model 360-67 computer. It uses the standard CalComp package of subroutines.

Reference: Cooper, R.H., and Howells, R.F., 1969, Subroutine GPL - An autoplotting routine for use with the CalComp plotter: Department of Civil Engineering, University of Alberta.





Program Name: PL4P

Description: PL4P is a subroutine designed to plot four dimensional data into families of curves. The data are first sorted into groups corresponding to specified intervals of one of the four parameters with each group representing a family of curves. The data in each group are then sorted into sub-groups corresponding to specified intervals of a second parameter; each sub-group represents a curve within a particular family of curves. Finally, subroutine GPL is used to prepare plots of the remaining two parameters with one family of curves placed on each plot and with a unique plotting symbol used to identify each curve on a plot.

Output is in the form of a plot tape generated by GPL for use on a CalComp plotter, a printed plot summary also generated by GPL, and a table of average values of the grouped and sub-grouped parameters for each curve and family of curves. The intervals used to group the data are also printed.

The user must supply the main calling program in which the data is either read or generated. In addition, certain plotting control parameters and grouping intervals are supplied on input data cards. Automatic selection of grouping parameters is an option.

Reference: A source deck complete with users instructions is on file at the Hydraulics Laboratory, University of Alberta.



Program Name: DIST

Description: The function of this program is to prepare tables giving the approximate distribution of observations on each of up to ten parameters within each class interval of another parameter. Observations on as many as eleven parameters are grouped about the first parameter according to class intervals supplied by the user. Within each group, the number of observations and their frequency are determined along with the maximum, minimum, median, and the first and third quartiles for each of the remaining parameters. These values are printed in tabular form.

The user must supply a subroutine to read the data and a number of input cards containing program control information.

Reference: A source deck complete with users instructions is on file at the Hydraulics Laboratory, University of Alberta.





Program Name: JDIS

Description: The function of this program is to graphically represent the joint distribution between observations on two parameters. The data are grouped into a number of class intervals of one of the parameters. For each of these groups, the mean value of the grouped parameter is plotted as abscissa against the second, tenth, fiftieth, ninetieth, and ninety-eighth percentiles of the other parameter as ordinate. The process is then repeated with the data being grouped about the other parameter.

The user can specify the number of class intervals, whether they are to be determined on an arithmetic or logarithmic basis, and the type, size, scale and origin of the plot axes. Subroutine GPL is used to generate the plots.

Reference: A source deck complete with users instructions is on file at the Hydraulics Laboratory, University of Alberta.



## A P P E N D I X      B

### SCOPE OF EXPERIMENTAL CONDITIONS FOR INDIVIDUAL BED-MATERIALS AND DATA COLLECTIONS



TABLE B-1  
DISTRIBUTION OF EXPERIMENTAL VALUES OF OBSERVED AND COMPUTED  
VARIABLES FOR DIFFERENT BED MATERIALS AND DATA COLLECTIONS

Bed Material	No. of Tests		Q (cfs)	V (fps)	h (ft)	Total Bed-Material Transport		S x 10 <sup>2</sup>	hS (ft x 10 <sup>3</sup> )	h/D <sub>50</sub>	b/h
						C <sub>tb</sub> (ppht)	G <sub>tb</sub> (lb/sec/ft)				
Colorado State University - B = 8.0 ft											
All Mtls.	239	Min.	1.840	0.657	0.19	0.0	0.0	0.005	0.047	124.55	6.02
		25%	7.200	1.452	0.50	4.2	0.00240	0.065	0.432	291.83	8.99
		50%	12.010	2.036	0.61	66.2	0.06551	0.158	1.205	478.78	13.11
		75%	16.850	3.793	0.89	439.0	0.47490	0.437	2.301	834.67	16.00
		Max.	22.690	6.227	1.33	4730.0	8.05764	1.280	6.175	1749.60	42.11
.19 mm	40	Min.	2.000	0.737	0.30	0.0	0.0	0.005	0.047	481.54	7.34
		25%	6.450	1.039	0.52	0.4	0.00028	0.057	0.313	834.67	8.60
		50%	11.680	1.808	0.64	86.1	0.05995	0.100	0.793	1027.29	13.11
		75%	21.960	3.809	0.93	275.0	0.47490	0.194	1.313	1492.78	15.38
		Max.	22.330	4.741	1.09	4730.0	8.05764	0.950	6.175	1749.60	26.67
.27 mm	20	Min.	5.110	0.793	0.45	0.0	0.0	0.007	0.067	507.90	7.08
		25%	11.090	1.831	0.60	20.0	0.02125	0.108	0.781	677.20	8.33
		50%	15.680	2.085	0.91	75.3	0.08872	0.140	1.236	1027.09	9.52
		75%	21.690	4.281	0.99	476.0	0.80902	0.280	1.764	1117.38	13.56
		Max.	21.840	4.934	1.13	3580.0	5.96177	1.022	6.132	1275.39	17.78
.28 mm	37	Min.	4.160	0.818	0.30	0.0	0.0	0.007	0.071	326.44	7.48
		25%	9.900	1.682	0.57	29.8	0.02001	0.100	0.660	620.24	8.70
		50%	15.190	2.160	0.65	73.2	0.07920	0.136	1.185	707.29	12.31
		75%	17.230	3.573	0.92	276.0	0.40289	0.229	1.433	1001.09	14.04
		Max.	22.020	4.937	1.07	4240.0	7.07079	1.007	5.740	1164.31	26.67
.45 mm	45	Min.	1.840	0.657	0.19	0.0	0.0	0.015	0.066	128.73	8.00
		25%	4.540	1.060	0.33	1.0	0.00055	0.049	0.307	223.58	11.59
		50%	7.910	1.692	0.46	55.4	0.03592	0.193	1.107	311.65	17.39
		75%	13.340	3.768	0.69	458.0	0.41914	0.466	1.792	467.48	24.24
		Max.	21.620	6.227	1.00	1510.0	1.92137	1.010	4.343	677.51	42.11
.93 mm	43	Min.	4.490	0.998	0.38	0.0	0.0	0.013	0.131	124.55	7.21
		25%	7.640	1.468	0.50	0.4	0.00028	0.050	0.304	163.88	7.92
		50%	12.060	2.025	0.58	25.3	0.02422	0.145	1.165	190.10	13.79
		75%	20.440	3.117	1.01	262.0	0.32886	0.587	3.889	331.04	16.00
		Max.	22.690	6.070	1.11	1020.0	1.23557	1.280	5.544	363.81	21.05
.47 mm	54	Min.	6.920	1.138	0.30	0.2	0.00011	0.042	0.315	194.55	6.02
		25%	8.160	1.609	0.51	46.3	0.03066	0.180	1.221	330.74	10.67
		50%	15.260	2.122	0.62	76.5	0.09618	0.240	1.920	402.07	13.11
		75%	15.580	4.489	0.75	525.0	0.64802	0.578	2.451	486.38	15.69
		Max.	21.420	5.317	1.33	1770.0	2.67108	0.960	4.030	862.52	26.67
Colorado State University - B = 2.0 ft											
All Mtls.	100	Min.	0.880	0.846	0.48	0.0	0.0	0.014	0.071	332.96	2.25
		25%	2.110	1.880	0.52	46.0	0.03237	0.147	0.853	423.25	2.82
		50%	3.830	2.759	0.60	195.0	0.22685	0.339	2.335	470.91	3.33
		75%	6.040	4.750	0.71	560.0	1.03374	0.628	4.027	533.33	3.85
		Max.	7.890	6.212	0.89	5000.0	12.26159	1.928	13.110	704.76	4.17
.32 mm	31	Min.	0.880	0.846	0.51	0.0	0.0	0.014	0.071	485.71	2.70
		25%	1.880	1.679	0.56	22.6	0.01326	0.139	0.778	533.33	3.12
		50%	3.480	2.445	0.60	115.0	0.12486	0.210	1.397	571.43	3.33
		75%	5.320	4.417	0.64	560.0	0.86814	0.635	3.937	609.52	3.57
		Max.	6.820	5.590	0.74	4930.0	10.32104	1.620	10.530	704.76	3.92
.33(U) mm	14	Min.	1.000	1.000	0.49	0.0	0.0	0.025	0.125	452.45	3.85
		25%	1.410	1.356	0.50	14.2	0.00625	0.102	0.530	461.68	3.85
		50%	3.290	3.357	0.51	221.0	0.22685	0.290	1.479	470.91	4.00
		75%	4.420	4.420	0.52	499.0	0.68814	0.620	3.100	480.15	4.00
		Max.	6.040	5.808	0.52	1840.0	3.46744	1.140	5.928	480.15	4.08
.33(G) mm	17	Min.	1.050	1.039	0.48	0.0	0.0	0.022	0.110	443.21	3.77
		25%	1.460	1.404	0.50	8.5	0.00387	0.063	0.328	461.68	3.85
		50%	2.320	2.189	0.51	122.0	0.08831	0.143	0.744	470.91	3.92
		75%	4.000	3.922	0.52	510.0	0.63648	0.433	2.190	480.15	4.00
		Max.	6.460	6.212	0.53	2250.0	4.53492	0.980	4.998	489.38	4.17





TABLE B-1 (Continued)

Bed Material	No. of Tests	Q  (cfs)	V  (fps)	h  (ft)	Total Bed-Material Transport		S  x 10 <sup>2</sup>	hS  (ft x 10 <sup>3</sup> )	h/D <sub>50</sub>	b/h	
					C <sub>tb</sub>  (ppht)	G <sub>tb</sub>  (lb/sec/ft)					
Colorado State University - B = 2.0 ft (continued)											
.54 mm	38	Min.	1.060	0.869	0.59	0.0	0.0	0.0160	0.098	332.96	2.25
		25%	3.820	2.274	0.66	105.0	0.12514	0.2940	2.434	372.46	2.63
		50%	4.840	3.457	0.72	269.0	0.44698	0.4330	3.280	406.32	2.78
		75%	7.590	5.421	0.76	569.0	1.36631	0.7680	5.069	428.89	3.03
		Max.	7.890	6.125	0.89	5000.0	12.26159	1.9280	13.110	502.26	3.39
G.K. Gilbert											
All Mtls.	892	Min.	0.093	0.764	0.04	0.0	0.0	0.0120	0.089	5.74	0.63
		25%	0.363	2.292	0.11	248.0	0.06349	0.6100	0.988	40.36	3.89
		50%	0.545	2.774	0.17	490.0	0.13706	0.9700	1.366	82.53	6.86
		75%	0.734	3.244	0.23	1010.0	0.26255	1.3700	2.009	128.92	11.19
		Max.	1.119	5.076	0.74	3530.0	1.10268	3.1000	8.496	601.63	44.55
A	61	Min.	0.182	0.990	0.06	38.5	0.00900	0.1800	0.484	60.00	2.32
		25%	0.363	2.080	0.09	339.0	0.06350	0.5500	0.762	89.00	10.00
		50%	0.363	2.464	0.13	631.0	0.12098	0.7500	0.904	129.00	12.45
		75%	0.734	2.780	0.18	1240.0	0.22130	1.1000	1.170	180.00	16.61
		Max.	1.119	3.460	0.29	2750.0	0.38832	1.7700	1.795	293.00	29.25
B	207	Min.	0.093	0.764	0.04	0.1	0.00002	0.0120	0.089	30.08	0.63
		25%	0.182	2.198	0.09	265.0	0.05359	0.5600	0.792	72.36	4.15
		50%	0.363	2.694	0.15	574.0	0.12469	0.8500	1.095	118.70	7.76
		75%	0.545	3.046	0.20	1090.0	0.24501	1.3300	1.520	164.23	13.47
		Max.	1.119	4.209	0.74	3530.0	0.67336	2.9600	3.596	601.63	44.55
C	236	Min.	0.093	1.113	0.04	8.4	0.00385	0.1200	0.548	24.10	1.14
		25%	0.363	2.165	0.11	326.0	0.07141	0.6100	0.981	65.06	3.83
		50%	0.363	2.729	0.16	580.0	0.15746	0.8800	1.239	96.39	7.21
		75%	0.734	3.179	0.21	1080.0	0.26083	1.2200	1.610	126.51	12.17
		Max.	1.119	4.753	0.58	2810.0	0.81682	2.5200	3.580	348.79	33.00
D	116	Min.	0.093	0.868	0.06	0.0	0.0	0.0370	0.155	21.71	1.42
		25%	0.182	2.116	0.09	265.0	0.06133	0.6400	1.115	36.43	4.37
		50%	0.363	2.626	0.15	835.0	0.15651	1.1400	1.459	59.69	7.10
		75%	0.545	3.310	0.22	1480.0	0.36135	1.6500	1.897	84.11	10.00
		Max.	0.734	4.665	0.48	2950.0	1.10268	2.7500	3.881	186.82	16.13
E	52	Min.	0.182	1.017	0.08	0.1	0.00002	0.0400	0.247	13.73	1.17
		25%	0.363	1.957	0.13	98.0	0.03346	0.4800	1.043	22.99	3.07
		50%	0.734	2.398	0.22	223.0	0.09664	0.8350	1.702	39.75	4.16
		75%	0.734	2.808	0.36	470.0	0.14843	1.2700	2.386	63.64	5.99
		Max.	1.119	3.925	0.62	1500.0	0.33977	2.2800	4.218	110.16	13.61
F	36	Min.	0.182	2.022	0.08	95.0	0.01499	0.7400	1.224	7.50	1.91
		25%	0.363	2.412	0.12	170.0	0.04441	0.8500	1.849	11.35	3.88
		50%	0.363	2.704	0.18	223.0	0.09945	1.2900	2.305	16.92	6.21
		75%	0.734	3.125	0.26	525.0	0.12144	1.7000	2.650	25.48	7.69
		Max.	1.119	3.479	0.35	1070.0	0.25054	2.5300	3.400	33.27	12.82
G	69	Min.	0.363	2.391	0.09	31.5	0.01596	0.6200	1.722	5.74	1.18
		25%	0.363	2.865	0.17	125.0	0.05496	0.9800	2.405	10.80	2.79
		50%	0.734	3.143	0.24	260.0	0.11451	1.4400	3.112	15.12	4.03
		75%	1.119	3.686	0.32	652.0	0.32797	2.0400	4.266	19.88	6.60
		Max.	1.119	4.789	0.56	1070.0	0.71478	3.1000	8.496	34.44	14.19
H	27	Min.	0.363	2.989	0.17	31.5	0.03005	0.7400	2.742	7.26	1.29
		25%	0.734	3.224	0.25	93.0	0.03703	1.1000	3.663	10.87	1.51
		50%	0.734	3.475	0.34	185.0	0.17349	1.5100	4.681	14.78	1.94
		75%	1.119	4.260	0.44	500.0	0.34913	2.0200	6.350	19.00	2.64
		Max.	1.119	5.076	0.51	1040.0	0.72172	2.9200	7.949	22.17	3.95
I	88	Min.	0.734	2.344	0.12	205.1	0.07956	0.3900	0.897	70.48	3.21
		25%	0.734	2.676	0.16	297.5	0.10259	0.5700	1.147	96.99	5.97
		50%	1.021	3.266	0.20	388.4	0.21708	0.6300	1.425	121.69	7.92
		75%	1.119	3.694	0.23	1052.2	0.38748	1.0400	1.748	139.76	10.34
		Max.	1.119	4.319	0.31	1291.8	0.61057	1.2000	2.540	187.95	16.75



TABLE B-1 (Continued)

Bed Material	No. of Tests		Q (cfs)	V (fps)	h (ft)	Total Bed-Material Transport		S  x 10 <sup>2</sup>	hS (ft x 10 <sup>3</sup> )	h/D <sub>50</sub>	b/h
						C <sub>tb</sub> (ppht)	G <sub>tb</sub> (lb/sec/ft)				
Meyer-Peter											
All Mtls.	120	Min.	0.021	1.152	0.03	0.0	0.0	0.0400	0.374	6.37	1.42
		25%	2.066	2.086	0.37	5.5	0.00491	0.2712	1.255	22.93	2.51
		50%	4.944	2.737	0.61	26.1	0.02361	0.3520	2.128	35.52	4.57
		75%	57.951	6.439	1.31	68.4	0.18081	0.8190	10.437	60.51	10.08
		Max.	162.940	9.448	3.58	600.0	1.79048	2.2700	28.577	1225.61	66.56
28.65 mm	34	Min.	57.951	5.925	1.12	0.4	0.00549	0.3171	8.369	11.95	1.83
		25%	57.951	6.754	1.31	13.0	0.10474	0.5021	11.634	13.93	2.32
		50%	115.510	7.364	2.37	36.7	0.21333	0.7385	13.827	25.19	2.88
		75%	161.850	8.172	2.82	69.3	0.80429	0.9278	18.171	30.03	5.01
		Max.	162.940	9.448	3.58	324.2	1.79048	1.7690	28.577	38.12	5.84
5.2 mm	20	Min.	0.766	2.600	0.19	1.2	0.00139	0.3180	1.763	11.06	1.42
		25%	0.766	3.015	0.25	14.0	0.01545	0.5380	2.400	14.86	2.02
		50%	2.147	3.352	0.48	39.6	0.04574	0.7550	3.272	27.91	2.60
		75%	2.148	3.575	0.60	223.7	0.18081	1.2670	4.298	34.87	4.98
		Max.	2.899	4.193	0.81	556.0	0.45791	2.2700	5.859	47.68	6.14
4.5 mm	7	Min.	3.531	2.414	0.22	74.4	0.02499	0.8010	1.811	16.99	18.53
		25%	4.944	2.682	0.28	121.4	0.05709	0.8100	2.301	21.41	18.85
		50%	6.886	3.230	0.32	166.2	0.10886	0.8120	2.642	24.77	20.18
		75%	7.769	3.403	0.35	189.1	0.13975	0.8190	2.822	26.52	23.35
		Max.	8.829	3.867	0.35	199.2	0.16729	0.8270	2.836	26.98	29.42
3.4 mm	24	Min.	0.537	1.284	0.25	0.0	0.0	0.2659	0.703	23.55	2.05
		25%	1.522	1.923	0.48	0.9	0.00053	0.2721	1.284	42.58	2.51
		50%	2.144	2.154	0.60	4.3	0.00370	0.2745	1.639	55.79	2.72
		75%	2.394	2.232	0.66	13.7	0.01248	0.2765	1.804	60.51	3.56
		Max.	3.270	2.492	0.80	24.1	0.02921	0.2822	2.246	73.61	6.43
2 mm	17	Min.	2.472	2.037	0.18	5.6	0.00190	0.2250	0.479	37.59	9.68
		25%	5.297	2.142	0.37	23.9	0.00996	0.2404	0.882	74.58	10.11
		50%	7.946	2.467	0.49	35.5	0.02812	0.2450	1.188	99.78	13.36
		75%	11.654	2.655	0.65	43.6	0.04000	0.2590	1.620	131.88	17.87
		Max.	11.654	2.893	0.68	48.6	0.05388	0.2940	1.805	137.78	35.46
1 mm	18	Min.	0.021	1.152	0.03	0.4	0.00027	0.0400	0.374	6.37	4.08
		25%	0.512	1.398	0.17	2.2	0.00228	0.0500	0.512	44.02	5.68
		50%	2.066	1.546	0.37	18.6	0.00385	0.2672	0.629	95.43	10.34
		75%	7.063	1.779	0.93	68.4	0.01088	0.4066	0.763	712.65	13.15
		Max.	19.423	2.245	1.61	600.0	0.04140	2.0700	1.757	1225.61	66.56
C.H. MacDougall											
All Mtls.	74	Min.	0.134	1.047	0.06	6.9	0.00105	0.1110	0.210	30.48	3.83
		25%	0.546	1.517	0.17	18.2	0.00534	0.1110	0.366	56.96	5.95
		50%	0.792	1.717	0.22	29.9	0.00950	0.1670	0.480	82.27	9.05
		75%	1.190	1.856	0.34	78.4	0.01506	0.3330	0.579	105.42	11.49
		Max.	2.260	2.237	0.52	131.8	0.04195	0.3330	0.759	196.19	31.25
I	27	Min.	0.134	1.047	0.06	15.5	0.00172	0.1110	0.213	30.48	4.85
		25%	0.356	1.444	0.13	24.1	0.00470	0.1670	0.284	64.29	9.26
		50%	0.596	1.578	0.18	49.1	0.00972	0.3330	0.406	84.29	11.30
		75%	0.764	1.673	0.22	99.4	0.01750	0.3330	0.493	102.86	14.81
		Max.	1.300	1.882	0.41	123.7	0.02695	0.3330	0.676	196.19	31.25
II	21	Min.	0.312	1.302	0.11	6.9	0.00105	0.1110	0.210	35.07	4.17
		25%	0.506	1.469	0.16	15.1	0.00511	0.1110	0.347	52.77	5.04
		50%	0.810	1.717	0.25	23.0	0.00809	0.1670	0.441	82.27	7.97
		75%	1.420	1.836	0.40	33.0	0.01022	0.1670	0.511	130.12	12.42
		Max.	2.080	2.167	0.48	98.6	0.01722	0.3330	0.613	157.33	18.69
III	26	Min.	0.498	1.541	0.15	12.3	0.00317	0.1110	0.372	36.47	3.83
		25%	0.810	1.723	0.22	17.4	0.00583	0.1670	0.486	55.21	4.90
		50%	1.020	1.884	0.29	25.6	0.01020	0.1670	0.583	72.45	7.04
		75%	1.562	1.931	0.41	68.8	0.01556	0.3330	0.688	101.92	9.05
		Max.	2.260	2.237	0.52	131.8	0.04195	0.3330	0.759	130.40	13.70







TABLE B-1 (Continued)

Bed Material	No. of Tests		Q (cfs)	V (fps)	h (ft)	Total Bed-Material Transport		S x 10 <sup>2</sup>	hS (ft x 10 <sup>3</sup> )	h/D <sub>50</sub>	b/h
						C <sub>tb</sub> (ppht)	G <sub>tb</sub> (lb/sec/ft)				
Chyn & Jorissen											
All Mtls.	58	Min.	0.116	0.866	0.07	9.6	0.00123	0.1100	0.222	30.48	5.81
		25%	0.522	1.329	0.18	16.9	0.00348	0.1450	0.290	71.26	8.06
		50%	0.661	1.446	0.22	26.4	0.00522	0.1650	0.351	86.90	9.35
		75%	0.783	1.589	0.25	35.8	0.00806	0.2000	0.422	113.88	11.30
		Max.	1.270	1.924	0.34	113.4	0.01511	0.3330	0.660	174.80	29.85
Chyn 1	12	Min.	0.434	1.226	0.15	13.8	0.00188	0.1200	0.248	60.97	6.06
		25%	0.530	1.352	0.18	19.3	0.00325	0.1570	0.290	71.26	10.00
		50%	0.541	1.454	0.19	29.2	0.00483	0.1810	0.344	73.63	10.81
		75%	0.555	1.561	0.21	47.6	0.00958	0.2000	0.422	81.95	11.30
		Max.	1.270	1.924	0.33	75.1	0.01367	0.3000	0.660	130.64	12.99
Chyn 2	10	Min.	0.443	1.334	0.17	12.3	0.00188	0.1100	0.264	60.96	6.85
		25%	0.661	1.404	0.21	16.6	0.00348	0.1500	0.311	75.65	8.30
		50%	0.668	1.498	0.23	24.9	0.00520	0.1680	0.377	84.47	8.97
		75%	0.682	1.589	0.24	31.7	0.00745	0.1780	0.430	88.51	9.71
		Max.	1.055	1.807	0.29	35.0	0.01000	0.2380	0.520	107.23	12.05
Chyn 3	9	Min.	0.447	1.355	0.16	9.9	0.00205	0.1110	0.264	86.71	8.10
		25%	0.661	1.421	0.20	18.7	0.00388	0.1450	0.302	104.57	8.55
		50%	0.671	1.485	0.22	27.7	0.00522	0.1610	0.328	114.56	9.17
		75%	0.674	1.579	0.23	32.7	0.00806	0.1630	0.403	122.96	10.05
		Max.	0.790	1.693	0.25	71.9	0.01511	0.2470	0.492	129.80	12.12
Jorissen I	13	Min.	0.116	0.866	0.07	9.6	0.00153	0.1120	0.222	34.04	5.81
		25%	0.384	1.246	0.15	14.7	0.00403	0.1130	0.314	76.73	6.60
		50%	0.653	1.446	0.25	26.4	0.00524	0.1660	0.384	126.02	8.06
		75%	1.026	1.618	0.30	58.8	0.00717	0.3310	0.464	156.59	13.25
		Max.	1.259	1.830	0.34	78.1	0.01103	0.3330	0.536	174.80	29.85
Jorissen II	14	Min.	0.161	0.925	0.09	9.6	0.00123	0.1110	0.245	30.48	6.15
		25%	0.348	1.212	0.15	14.7	0.00358	0.1120	0.290	51.16	7.52
		50%	0.679	1.414	0.24	33.6	0.00644	0.1670	0.358	84.09	9.05
		75%	0.789	1.644	0.27	77.9	0.00867	0.3310	0.398	93.20	13.70
		Max.	1.208	1.858	0.32	113.4	0.01086	0.3330	0.511	113.88	22.99
USWES - (Sands 1-10)											
All Mtls.	437	Min.	0.098	0.493	0.05	0.1	0.00000	0.1000	0.075	15.76	3.38
		25%	0.399	0.989	0.16	3.1	0.00044	0.1000	0.240	81.51	6.69
		50%	0.760	1.267	0.25	9.4	0.00177	0.1500	0.361	144.05	9.18
		75%	1.217	1.523	0.35	19.5	0.00497	0.2000	0.538	233.67	14.64
		Max.	2.267	2.406	0.68	143.2	0.04018	0.4500	1.800	1157.36	49.29
1	60	Min.	0.116	0.822	0.05	0.8	0.00003	0.1000	0.093	38.46	7.50
		25%	0.338	1.204	0.12	10.1	0.00097	0.1000	0.166	85.63	11.29
		50%	0.534	1.336	0.16	15.4	0.00258	0.1500	0.232	119.74	15.19
		75%	0.814	1.529	0.22	23.9	0.00431	0.2000	0.310	157.47	20.82
		Max.	1.260	1.801	0.32	40.5	0.00911	0.2000	0.440	233.67	45.57
2	40	Min.	0.150	0.863	0.07	0.7	0.00003	0.1000	0.119	49.32	5.85
		25%	0.412	1.201	0.15	11.6	0.00153	0.1000	0.206	100.00	8.44
		50%	0.820	1.441	0.23	19.8	0.00389	0.1500	0.321	160.27	10.83
		75%	1.087	1.589	0.29	27.4	0.00745	0.2000	0.446	196.58	17.25
		Max.	1.816	1.821	0.41	52.1	0.01842	0.2000	0.619	282.88	33.54
3	45	Min.	0.111	0.769	0.06	0.1	0.00001	0.1000	0.095	35.94	3.71
		25%	0.240	0.916	0.11	1.6	0.00014	0.1000	0.148	69.32	7.32
		50%	0.399	1.012	0.18	6.8	0.00072	0.1500	0.312	114.25	12.99
		75%	0.930	1.335	0.32	13.4	0.00333	0.2000	0.430	202.82	21.42
		Max.	2.267	1.775	0.62	42.5	0.01394	0.2000	0.661	399.87	41.30
4	42	Min.	0.130	0.721	0.07	0.3	0.00003	0.1000	0.099	46.58	4.39
		25%	0.280	0.910	0.11	2.2	0.00025	0.1000	0.156	79.75	7.32
		50%	0.516	1.043	0.24	6.6	0.00075	0.1500	0.354	170.08	9.60
		75%	0.970	1.224	0.32	12.3	0.00258	0.2000	0.482	223.01	20.47
		Max.	1.960	1.847	0.53	57.1	0.02264	0.2000	0.688	371.91	35.05



TABLE B-1 (Continued)

Bed Material	No. of Tests		Q (cfs)	V (fps)	h (ft)	Total Bed-Material Transport		S x 10 <sup>2</sup>	hS (ft x 10 <sup>3</sup> )	h/D <sub>50</sub>	b/h
						C <sub>tb</sub> (ppht)	G <sub>tb</sub> (lb/sec/ft)				
USWES Sands 1-10 (continued)											
5	32	Min.	0.128	0.789	0.06	0.1	0.00003	0.1000	0.106	46.49	4.14
		25%	0.319	0.962	0.13	3.0	0.00031	0.1000	0.151	99.85	5.96
		50%	0.800	1.071	0.32	6.9	0.00100	0.1500	0.446	246.19	7.81
		75%	1.225	1.309	0.40	12.4	0.00320	0.2000	0.559	307.16	19.27
		Max.	2.079	1.630	0.56	23.8	0.00906	0.2000	0.748	426.07	37.92
6	45	Min.	0.210	0.719	0.12	0.3	0.00003	0.1000	0.233	114.29	4.60
		25%	0.564	0.875	0.25	1.3	0.00022	0.1000	0.350	241.90	6.18
		50%	0.927	1.108	0.33	3.0	0.00064	0.1500	0.472	315.24	7.30
		75%	1.263	1.251	0.39	6.3	0.00175	0.2000	0.606	372.38	9.51
		Max.	1.645	1.562	0.52	15.6	0.00586	0.2000	0.770	500.00	20.12
7	32	Min.	0.098	0.493	0.05	0.3	0.00003	0.1000	0.087	52.24	6.08
		25%	0.263	0.695	0.16	0.9	0.00008	0.1000	0.246	175.91	7.92
		50%	0.473	0.878	0.24	2.1	0.00022	0.1500	0.340	259.06	10.02
		75%	0.755	0.988	0.31	4.9	0.00081	0.2000	0.450	329.42	16.21
		Max.	1.146	1.371	0.40	19.4	0.00575	0.2000	0.692	423.24	49.29
8	21	Min.	0.140	0.540	0.07	0.1	0.00000	0.1000	0.075	126.90	3.38
		25%	0.386	0.750	0.22	0.5	0.00003	0.1000	0.310	372.25	5.20
		50%	0.800	0.927	0.35	5.3	0.00091	0.1500	0.445	600.68	6.52
		75%	1.255	1.197	0.44	19.7	0.00588	0.2000	0.710	752.96	10.51
		Max.	2.238	1.708	0.68	79.3	0.03761	0.2000	1.026	1157.36	30.84
9	18	Min.	0.945	1.853	0.21	0.1	0.00003	0.3000	0.726	15.76	5.21
		25%	1.165	1.999	0.25	1.0	0.00046	0.3000	0.954	18.73	6.76
		50%	1.440	2.143	0.30	7.9	0.00305	0.4000	1.134	22.45	8.20
		75%	1.705	2.222	0.34	24.1	0.00987	0.4500	1.308	25.43	9.18
		Max.	2.226	2.406	0.44	143.2	0.04018	0.4500	1.800	33.01	10.91
10	102	Min.	0.243	1.118	0.09	0.6	0.00009	0.1000	0.186	29.84	3.59
		25%	0.733	1.393	0.23	8.2	0.00224	0.1000	0.316	73.47	5.40
		50%	1.145	1.500	0.32	16.3	0.00443	0.1500	0.442	101.38	7.34
		75%	1.692	1.639	0.43	23.3	0.00803	0.2000	0.621	137.31	10.10
		Max.	2.209	1.894	0.64	37.9	0.02006	0.2000	1.098	206.93	24.87
USWES - Turbidity Tests											
	217	Min.	0.232	1.160	0.20	5.6	0.00081	0.1000	0.200	125.47	2.00
		25%	0.232	1.160	0.20	7.5	0.00108	0.1000	0.200	125.47	2.00
		50%	0.843	1.686	0.50	12.7	0.00666	0.1000	0.500	313.68	2.00
		75%	0.843	1.686	0.50	21.1	0.01111	0.1000	0.500	313.68	5.00
		Max.	0.843	1.686	0.50	45.4	0.02389	0.1000	0.500	313.68	5.00
USWES - Synthetic Sands											
All Mtls.	312	Min.	0.306	0.903	0.24	0.3	0.00007	0.1000	0.240	68.59	1.08
		25%	0.306	1.249	0.25	4.3	0.00111	0.1000	0.250	113.16	1.32
		50%	0.827	1.557	0.52	7.4	0.00436	0.1000	0.524	193.98	1.91
		75%	1.369	1.654	0.76	10.2	0.00689	0.1000	0.757	266.72	4.00
		Max.	1.369	1.878	0.92	21.3	0.01347	0.1000	0.923	746.82	4.17
U.293	14	Min.	0.306	0.903	0.28	0.6	0.00011	0.1000	0.276	233.70	1.13
		25%	0.306	1.027	0.32	1.7	0.00036	0.1000	0.323	273.50	1.18
		50%	0.827	1.459	0.57	2.6	0.00200	0.1000	0.567	480.10	1.78
		75%	1.369	1.552	0.84	4.8	0.00247	0.1000	0.844	714.65	3.10
		Max.	1.369	1.622	0.88	6.9	0.00356	0.1000	0.882	746.82	3.62
U.417	15	Min.	0.306	1.191	0.24	3.7	0.00136	0.100	0.243	154.29	1.19
		25%	0.306	1.249	0.25	7.1	0.00158	0.100	0.251	159.37	1.25
		50%	0.827	1.543	0.54	8.0	0.00383	0.100	0.536	340.32	1.87
		75%	1.369	1.636	0.80	8.9	0.00561	0.100	0.801	508.57	3.98
		Max.	1.369	1.830	0.84	10.9	0.00923	0.100	0.843	535.24	4.12
U.589	14	Min.	0.306	1.214	0.25	3.8	0.00072	0.100	0.251	114.19	1.12
		25%	0.306	1.219	0.25	4.5	0.00089	0.100	0.252	114.65	1.17
		50%	0.827	1.490	0.57	7.5	0.00534	0.100	0.572	260.24	1.80
		75%	1.369	1.554	0.86	10.3	0.00645	0.100	0.858	390.35	3.97
		Max.	1.369	1.838	0.89	13.8	0.00867	0.100	0.889	404.46	3.98





TABLE B-1 (Continued)

Bed Material	No. of Tests		Q (cfs)	V (fps)	h (ft)	Total Bed-Material Transport		S x 10 <sup>2</sup>	hS (ft x 10 <sup>3</sup> )	h/D <sub>50</sub>	b/h
						C <sub>tb</sub> (ppht)	G <sub>tb</sub> (lb/sec/ft)				
USWES - Synthetic Sands (continued)											
U.833	16	Min.	0.306	1.224	0.25	1.9	0.00036	0.100	0.248	80.42	1.13
		25%	0.306	1.234	0.25	2.6	0.00050	0.100	0.250	81.06	1.35
		50%	0.827	1.472	0.56	5.4	0.00306	0.100	0.562	182.23	1.78
		75%	1.369	1.559	0.85	7.4	0.00492	0.100	0.853	276.59	4.00
		Max.	1.369	1.853	0.89	9.2	0.00648	0.100	0.888	287.94	4.03
A	18	Min.	0.306	1.244	0.24	3.4	0.00078	0.100	0.243	96.20	1.16
		25%	0.306	1.259	0.25	4.2	0.00118	0.100	0.246	97.39	1.32
		50%	0.829	1.576	0.53	7.9	0.00561	0.100	0.527	208.63	1.90
		75%	1.369	1.609	0.76	11.9	0.00719	0.100	0.757	299.68	4.07
		Max.	1.369	1.808	0.86	19.5	0.01011	0.100	0.859	340.06	4.12
B	14	Min.	0.306	1.229	0.24	2.9	0.00056	0.100	0.242	111.78	1.11
		25%	0.306	1.254	0.24	4.1	0.00079	0.100	0.245	113.16	1.17
		50%	0.827	1.524	0.55	8.1	0.00497	0.100	0.555	256.35	1.85
		75%	1.369	1.579	0.85	9.6	0.00633	0.100	0.855	394.92	4.08
		Max.	1.369	1.868	0.90	10.7	0.00845	0.100	0.898	414.78	4.13
C	14	Min.	0.306	1.259	0.24	4.2	0.00081	0.100	0.241	102.03	1.14
		25%	0.306	1.259	0.24	6.5	0.00150	0.100	0.243	102.88	1.37
		50%	0.827	1.555	0.53	9.9	0.00560	0.100	0.532	225.23	1.92
		75%	1.369	1.584	0.73	11.6	0.00675	0.100	0.729	308.64	4.12
		Max.	1.369	1.878	0.87	21.3	0.01100	0.100	0.874	370.03	4.15
D	16	Min.	0.306	1.234	0.24	0.3	0.00007	0.100	0.244	72.21	1.25
		25%	0.306	1.254	0.25	1.1	0.00021	0.100	0.248	73.39	1.33
		50%	0.827	1.634	0.51	5.9	0.00318	0.100	0.512	151.52	1.98
		75%	1.369	1.726	0.77	6.9	0.00510	0.100	0.768	227.29	4.03
		Max.	1.369	1.818	0.80	9.7	0.00708	0.100	0.800	236.76	4.10
E	30	Min.	0.306	1.224	0.25	1.7	0.00033	0.100	0.247	85.56	1.17
		25%	0.306	1.234	0.25	3.6	0.00069	0.100	0.249	86.25	1.34
		50%	0.827	1.593	0.52	6.3	0.00386	0.100	0.520	180.12	1.93
		75%	1.369	1.641	0.75	8.8	0.00544	0.100	0.747	258.75	4.02
		Max.	1.369	1.873	0.85	11.5	0.00982	0.100	0.855	296.16	4.05
F	15	Min.	0.306	1.239	0.24	1.7	0.00033	0.100	0.243	68.59	1.27
		25%	0.306	1.249	0.25	3.1	0.00058	0.100	0.247	69.71	1.31
		50%	0.827	1.603	0.52	9.4	0.00642	0.100	0.516	145.64	1.94
		75%	1.369	1.735	0.76	12.6	0.00767	0.100	0.763	215.35	4.05
		Max.	1.369	1.845	0.79	14.9	0.01161	0.100	0.789	222.69	4.12
G	15	Min.	0.306	1.234	0.25	1.2	0.00022	0.100	0.246	83.31	1.25
		25%	0.306	1.239	0.25	3.2	0.00061	0.100	0.247	83.64	1.30
		50%	0.827	1.549	0.53	7.4	0.00383	0.100	0.534	180.83	1.87
		75%	1.369	1.740	0.77	10.1	0.00664	0.100	0.767	259.74	4.05
		Max.	1.369	1.853	0.80	15.8	0.01347	0.100	0.797	269.90	4.07
H	29	Min.	0.306	1.209	0.25	1.7	0.00033	0.100	0.247	78.41	1.22
		25%	0.306	1.239	0.25	4.1	0.00078	0.100	0.251	79.68	1.33
		50%	0.827	1.563	0.52	8.0	0.00456	0.100	0.525	166.67	1.90
		75%	1.369	1.670	0.75	10.2	0.00625	0.100	0.752	238.73	3.98
		Max.	1.369	1.835	0.82	13.2	0.01125	0.100	0.820	260.32	4.05
I	15	Min.	0.306	1.234	0.25	1.2	0.00022	0.100	0.246	79.77	1.23
		25%	0.306	1.239	0.25	3.1	0.00058	0.100	0.247	80.09	1.32
		50%	0.827	1.641	0.50	7.8	0.00525	0.100	0.504	163.42	1.98
		75%	1.369	1.705	0.75	11.1	0.00667	0.100	0.755	244.81	4.05
		Max.	1.369	1.853	0.81	12.9	0.01081	0.100	0.812	263.29	4.07
J	29	Min.	0.306	1.219	0.25	1.9	0.00036	0.100	0.246	83.31	1.23
		25%	0.306	1.239	0.25	3.6	0.00070	0.100	0.250	84.66	1.32
		50%	0.827	1.628	0.51	8.0	0.00436	0.100	0.508	172.03	1.97
		75%	1.369	1.744	0.76	9.7	0.00756	0.100	0.757	256.35	4.00
		Max.	1.369	1.840	0.81	12.1	0.01034	0.100	0.814	275.65	4.07
K	15	Min.	0.306	1.209	0.25	5.8	0.00111	0.100	0.250	105.09	1.15
		25%	0.306	1.219	0.25	7.0	0.00145	0.100	0.253	106.35	1.29
		50%	0.827	1.482	0.56	8.8	0.00653	0.100	0.558	234.55	1.79
		75%	1.369	1.636	0.78	13.2	0.00728	0.100	0.777	326.61	3.95
		Max.	1.369	1.835	0.87	14.2	0.00983	0.100	0.867	364.44	4.00





TABLE B-1 (Continued)

Bed Material	No. of Tests	Q (cfs)	V (fps)	h (ft)	Total Bed-Material Transport		S  x 10 <sup>2</sup>	hS (ft x 10 <sup>3</sup> )	h/D <sub>50</sub>	b/h	
					C <sub>tb</sub> (ppht)	G <sub>tb</sub> (lb/sec/ft)					
USWES - Synthetic Sands (continued)											
L	14	Min.	0.306	1.249	0.24	5.4	0.00103	0.100	0.244	118.05	1.08
		25%	0.306	1.254	0.24	6.0	0.00114	0.100	0.245	118.53	1.35
		50%	0.827	1.543	0.53	9.7	0.00717	0.100	0.534	258.35	1.92
		75%	1.369	1.616	0.74	13.8	0.00778	0.100	0.739	357.52	4.08
		Max.	1.369	1.853	0.92	15.1	0.00847	0.100	0.923	446.54	4.10
M	14	Min.	0.306	1.209	0.25	5.2	0.00100	0.100	0.246	108.66	1.14
		25%	0.306	1.244	0.25	6.5	0.00125	0.100	0.252	111.31	1.25
		50%	0.827	1.504	0.56	8.9	0.00706	0.100	0.557	246.02	1.82
		75%	1.369	1.603	0.80	11.1	0.00847	0.100	0.797	352.03	3.97
		Max.	1.369	1.843	0.88	18.3	0.01034	0.100	0.878	387.81	4.07
Filter	14	Min.	0.306	1.254	0.24	5.5	0.00106	0.100	0.240	162.60	1.19
		25%	0.306	1.270	0.24	6.8	0.00131	0.100	0.243	164.63	1.36
		50%	0.827	1.600	0.52	9.2	0.00606	0.100	0.517	350.27	1.99
		75%	1.369	1.653	0.73	13.1	0.00881	0.100	0.733	496.61	4.12
		Max.	1.369	1.868	0.84	17.1	0.01122	0.100	0.842	570.46	4.17
T. Y. Liu											
All Mtls.	310	Min.	0.077	0.955	0.03	0.1	0.00003	0.060	0.212	6.18	6.17
		25%	0.533	1.639	0.11	1.3	0.00029	0.220	0.470	11.94	9.96
		50%	0.915	1.903	0.19	8.4	0.00170	0.350	0.640	20.20	14.30
		75%	1.530	2.167	0.27	29.0	0.00574	0.510	0.837	31.16	24.66
		Max.	2.750	2.856	0.44	236.2	0.01686	1.010	1.434	54.98	89.60
I	61	Min.	0.518	1.853	0.10	0.1	0.00003	0.060	0.212	7.02	6.17
		25%	0.895	2.163	0.14	0.5	0.00017	0.200	0.620	9.71	8.25
		50%	1.560	2.399	0.25	3.0	0.00108	0.380	0.756	17.72	10.75
		75%	2.087	2.614	0.33	12.7	0.00447	0.730	1.061	23.11	19.62
		Max.	2.750	2.856	0.44	66.7	0.01686	1.000	1.434	30.90	27.15
II	60	Min.	0.341	1.583	0.08	0.1	0.00003	0.125	0.327	7.50	6.70
		25%	0.681	1.864	0.12	0.9	0.00027	0.220	0.627	11.25	8.96
		50%	1.226	2.041	0.22	6.2	0.00147	0.420	0.783	20.35	12.39
		75%	1.720	2.226	0.30	24.2	0.00485	0.880	0.902	28.13	23.58
		Max.	2.576	2.677	0.40	73.0	0.01328	0.955	1.080	37.61	33.60
III	55	Min.	0.212	1.408	0.06	0.1	0.00003	0.155	0.363	7.55	7.09
		25%	0.490	1.639	0.11	3.1	0.00062	0.225	0.520	14.57	9.85
		50%	0.923	1.776	0.21	11.9	0.00267	0.260	0.609	28.05	12.92
		75%	1.487	1.955	0.27	32.0	0.00675	0.500	0.690	36.82	24.89
		Max.	2.310	2.269	0.38	148.8	0.01556	1.010	0.853	51.11	48.00
IV	47	Min.	0.077	0.955	0.03	0.3	0.00003	0.135	0.216	6.18	10.07
		25%	0.262	1.330	0.07	11.3	0.00083	0.190	0.336	15.03	14.00
		50%	0.516	1.492	0.14	33.4	0.00321	0.250	0.385	28.83	19.20
		75%	0.845	1.655	0.19	55.9	0.00785	0.500	0.471	39.54	36.82
		Max.	1.255	1.842	0.27	236.2	0.01329	1.000	0.572	54.98	89.60
V	41	Min.	0.385	1.726	0.08	0.1	0.00003	0.180	0.578	7.03	7.07
		25%	0.678	1.928	0.11	0.4	0.00013	0.270	0.805	9.65	9.02
		50%	1.151	2.105	0.21	2.6	0.00047	0.500	0.910	18.03	12.62
		75%	1.690	2.206	0.30	15.4	0.00319	1.000	1.090	25.23	23.58
		Max.	2.256	2.604	0.38	76.1	0.01336	1.000	1.300	32.17	32.39
VI	46	Min.	0.129	1.193	0.04	0.2	0.00003	0.165	0.297	6.99	8.93
		25%	0.310	1.396	0.08	3.4	0.00033	0.235	0.395	14.34	12.62
		50%	0.563	1.518	0.15	16.7	0.00199	0.250	0.500	27.25	19.20
		75%	0.969	1.705	0.21	39.1	0.00681	0.500	0.565	38.19	33.60
		Max.	1.440	1.903	0.30	222.8	0.01660	1.000	0.700	53.97	68.92



TABLE B-1 (Continued)

Bed Material	No. of Tests		Q (cfs)	V (fps)	h (ft)	Total Bed-Material Transport		S x 10 <sup>2</sup>	hS (ft x 10 <sup>3</sup> )	h/D <sub>50</sub>	b/h
						C <sub>tb</sub> (ppht)	G <sub>tb</sub> (lb/sec/ft)				
Bogard1 and Yen											
All Mtls.	48	Min.	0.553	2.226	0.11	0.7	0.00012	1.090	1.888	4.82	1.55
		25%	1.025	2.642	0.18	7.1	0.00256	1.530	3.115	6.04	3.64
		50%	1.465	2.752	0.24	11.2	0.00420	1.770	4.491	7.80	10.74
		75%	1.815	3.415	0.30	26.8	0.01325	2.020	5.257	9.05	15.62
		Max.	2.328	4.479	0.64	102.7	0.06201	2.480	7.353	13.11	23.91
1	20	Min.	0.700	2.545	0.17	1.4	0.00090	1.190	3.328	5.21	2.36
		25%	1.465	2.706	0.23	7.4	0.00349	1.750	4.389	7.04	9.11
		50%	1.922	2.753	0.27	12.2	0.00433	1.900	4.814	8.29	10.11
		75%	2.165	2.909	0.29	29.9	0.01206	2.180	5.285	8.96	13.35
		Max.	2.268	3.442	0.42	102.7	0.05095	2.480	5.965	12.92	16.08
2	18	Min.	0.553	2.226	0.11	0.7	0.00012	1.090	1.888	5.15	3.52
		25%	0.892	2.508	0.13	8.8	0.00179	1.480	2.581	5.87	13.61
		50%	1.076	2.588	0.17	12.2	0.00412	1.720	2.785	7.44	16.77
		75%	1.305	2.727	0.20	36.9	0.01455	1.990	3.131	9.05	20.99
		Max.	1.758	3.415	0.28	95.5	0.02789	2.290	3.509	12.73	23.91
3	10	Min.	0.884	3.609	0.24	0.7	0.00072	1.120	4.621	4.82	1.55
		25%	1.170	3.736	0.30	2.7	0.00202	1.250	5.227	6.04	2.24
		50%	1.610	4.024	0.38	8.1	0.00685	1.770	5.637	7.62	2.96
		75%	1.740	4.085	0.45	14.4	0.01389	1.860	6.458	9.09	3.37
		Max.	2.328	4.479	0.64	71.8	0.06201	2.090	7.353	13.11	4.22
M.B. O'Brien											
Columbia	83	Min.	0.670	0.703	0.29	0.2	0.00014	0.029	0.182	245.55	2.80
		25%	1.310	1.140	0.34	1.8	0.00121	0.057	0.453	292.12	2.88
		50%	3.510	1.309	0.53	6.6	0.00431	0.094	0.595	448.77	5.66
		75%	4.200	1.479	1.04	27.1	0.00742	0.167	0.836	881.46	8.70
		Max.	5.390	3.126	1.07	133.2	0.11668	0.323	1.466	908.55	10.34
H.J. Casey											
h & IIIa	92	Min.	0.028	0.711	0.03	0.0	0.0	0.119	0.125	7.62	1.82
		25%	0.218	1.347	0.12	3.0	0.00046	0.126	0.301	20.90	4.07
		50%	0.434	1.627	0.21	9.8	0.00178	0.249	0.528	36.95	6.50
		75%	0.798	1.882	0.32	26.0	0.00560	0.491	0.712	61.21	11.31
		Max.	2.041	2.459	0.72	272.2	0.05709	0.519	1.130	108.46	43.73
h	49	Min.	0.168	1.437	0.09	0.0	0.0	0.119	0.435	12.00	1.82
		25%	0.392	1.688	0.17	0.9	0.00047	0.129	0.591	23.47	2.88
		50%	0.706	1.847	0.29	8.0	0.00256	0.250	0.680	38.57	4.59
		75%	1.130	2.034	0.45	22.3	0.00797	0.494	0.794	61.36	7.54
		Max.	2.041	2.459	0.72	126.6	0.03999	0.509	1.130	96.97	14.74
III a	43	Min.	0.028	0.711	0.03	0.9	0.00003	0.119	0.125	7.62	3.07
		25%	0.119	1.121	0.08	4.3	0.00039	0.125	0.207	19.56	5.68
		50%	0.220	1.317	0.13	11.3	0.00122	0.248	0.289	32.26	10.33
		75%	0.431	1.545	0.23	32.2	0.00457	0.266	0.388	58.67	17.04
		Max.	1.056	2.062	0.43	272.2	0.05709	0.519	0.810	108.46	43.73
Ho, Pang-Yung											
All Mtls.	80	Min.	0.120	0.769	0.12	0.0	0.00001	0.099	0.119	16.71	1.52
		25%	0.837	1.575	0.35	0.5	0.00012	0.100	0.445	34.48	2.11
		50%	1.471	1.996	0.47	2.7	0.00131	0.128	0.818	58.02	2.79
		75%	1.903	2.403	0.63	13.0	0.00833	0.334	1.232	87.48	3.85
		Max.	2.426	3.348	0.86	54.3	0.05832	0.504	2.595	191.79	11.03
I	15	Min.	0.678	1.565	0.26	0.0	0.00001	0.105	0.583	26.52	1.52
		25%	1.181	1.932	0.46	0.1	0.00004	0.126	0.761	47.25	1.80
		50%	1.780	2.148	0.60	0.3	0.00038	0.165	0.904	60.86	2.19
		75%	2.278	2.442	0.73	2.7	0.00113	0.335	1.209	74.17	2.82
		Max.	2.426	2.936	0.86	54.3	0.05832	0.340	1.992	87.48	5.03





TABLE B-1 (Continued)

Bed Material	No. of Tests		Q (cfs)	V (fps)	h (ft)	Total Bed-Material Transport		S $\times 10^2$	hS (ft $\times 10^3$ )	h/D <sub>50</sub>	b/h
						$C_{tb}$ (ppht)	$G'_{tb}$ (lb/sec/ft)				
Ho, Pang-Yung (continued)											
II	11	Min.	0.570	1.810	0.24	0.0	0.00001	0.127	0.804	17.01	1.62
		25%	1.333	2.072	0.44	0.0	0.00002	0.167	0.923	31.47	1.83
		50%	1.919	2.276	0.58	0.2	0.00010	0.169	1.112	41.18	2.26
		75%	2.227	2.585	0.72	7.7	0.00549	0.335	1.487	50.89	2.95
		Max.	2.304	2.922	0.81	12.2	0.01293	0.336	1.952	57.27	5.47
III	8	Min.	1.068	2.339	0.33	0.0	0.00002	0.169	1.162	16.74	1.79
		25%	1.568	2.638	0.44	0.6	0.00032	0.334	1.518	22.19	2.48
		50%	1.903	2.742	0.52	0.8	0.00069	0.335	1.762	25.83	2.90
		75%	2.276	3.040	0.59	8.3	0.00819	0.502	2.238	29.48	3.77
		Max.	2.297	3.335	0.73	9.7	0.00892	0.504	2.595	36.58	3.92
IV	14	Min.	0.482	1.247	0.27	0.3	0.00007	0.100	0.316	63.31	1.60
		25%	0.901	1.613	0.39	1.6	0.00070	0.103	0.494	92.61	1.94
		50%	1.386	1.968	0.56	7.9	0.00523	0.126	0.697	132.00	2.41
		75%	1.843	2.089	0.68	13.4	0.01421	0.166	0.851	158.73	3.32
		Max.	2.230	2.303	0.82	23.1	0.02320	0.168	1.232	191.79	4.86
V	7	Min.	1.068	2.267	0.33	0.1	0.00007	0.333	1.195	16.71	2.30
		25%	1.167	2.539	0.36	0.7	0.00044	0.333	1.591	18.24	2.41
		50%	1.771	2.704	0.47	0.8	0.00070	0.335	1.817	24.13	2.76
		75%	2.262	3.066	0.54	12.8	0.01078	0.500	2.215	27.64	3.65
		Max.	2.297	3.348	0.57	18.9	0.02029	0.501	2.580	29.01	3.99
VI	25	Min.	0.120	0.769	0.12	0.7	0.00007	0.099	0.119	25.02	1.84
		25%	0.212	0.997	0.17	9.5	0.00131	0.100	0.173	36.37	3.14
		50%	0.453	1.265	0.28	13.0	0.00457	0.100	0.287	59.70	4.62
		75%	0.838	1.579	0.42	19.8	0.01062	0.100	0.426	87.87	7.58
		Max.	1.471	1.862	0.71	39.0	0.02728	0.102	0.714	150.09	11.03
Nomikos, Vanoni & Brooks											
All Mtls	63	Min.	0.170	0.767	0.15	0.3	0.00008	0.130	0.211	329.79	2.92
		25%	0.269	1.220	0.24	110.0	0.01840	0.201	0.506	482.97	3.60
		50%	0.387	1.438	0.24	200.0	0.05739	0.225	0.561	531.91	3.65
		75%	0.561	2.063	0.28	340.0	0.08472	0.260	0.651	818.79	5.13
		Max.	3.840	2.660	0.55	808.0	0.29330	0.390	0.940	1231.63	13.75
Nomikos Sand #6	5	Min.	0.306	1.231	0.24	338.0	0.07376	0.200	0.488	818.79	3.08
		25%	0.306	1.231	0.25	364.0	0.07943	0.206	0.525	855.70	3.08
		50%	0.433	2.028	0.26	460.0	0.14204	0.206	0.529	862.42	3.40
		75%	0.509	2.263	0.28	692.0	0.25119	0.245	0.696	953.02	3.43
		Max.	0.509	2.281	0.28	808.0	0.29330	0.250	0.710	953.02	3.59
Nomikos Sand #4	4	Min.	0.293	1.378	0.22	200.0	0.04179	0.225	0.502	496.66	3.60
		25%	0.293	1.413	0.23	200.0	0.04179	0.250	0.582	518.93	3.69
		50%	0.387	1.983	0.24	230.0	0.07151	0.275	0.652	527.84	3.76
		75%	0.436	2.139	0.24	330.0	0.09108	0.275	0.668	541.20	3.92
		Max.	0.436	2.139	0.24	330.0	0.09108	0.275	0.668	541.20	3.92
Nomikos Sand #5	12	Min.	0.170	0.806	0.24	30.0	0.00364	0.200	0.482	482.97	3.63
		25%	0.207	0.982	0.24	115.0	0.01698	0.210	0.506	482.97	3.63
		50%	0.292	1.385	0.24	290.0	0.06763	0.240	0.578	482.97	3.63
		75%	0.387	1.835	0.24	340.0	0.08832	0.270	0.651	482.97	3.63
		Max.	0.561	2.660	0.24	560.0	0.22404	0.390	0.940	482.97	3.63
Vanoni & Brooks Sand #4	16	Min.	0.510	0.767	0.20	0.3	0.00008	0.039	0.211	452.12	5.05
		25%	0.930	1.067	0.24	21.0	0.00330	0.107	0.496	534.52	5.21
		50%	1.210	1.405	0.30	115.0	0.03339	0.201	0.576	672.61	11.21
		75%	2.230	2.064	0.54	220.0	0.07711	0.276	0.654	1204.90	11.73
		Max.	3.840	2.528	0.55	300.0	0.09870	0.280	0.672	1231.63	13.75
Brooks Sand #1	12	Min.	0.200	0.914	0.15	20.0	0.00285	0.180	0.468	329.79	2.92
		25%	0.280	1.410	0.20	110.0	0.01900	0.220	0.511	419.15	3.57
		50%	0.370	1.786	0.24	190.0	0.03947	0.240	0.558	517.02	3.65
		75%	0.435	2.046	0.25	245.0	0.06049	0.310	0.637	531.91	4.49
		Max.	0.540	2.173	0.30	270.0	0.07513	0.350	0.689	638.30	5.65
Brooks Sand #2	10	Min.	0.200	0.819	0.17	19.0	0.00271	0.130	0.363	588.24	3.08
		25%	0.200	1.078	0.19	175.0	0.03307	0.185	0.518	653.98	3.12
		50%	0.265	1.340	0.24	400.0	0.08472	0.225	0.543	816.61	3.71
		75%	0.435	2.107	0.28	510.0	0.13229	0.245	0.617	968.86	4.63
		Max.	0.520	2.122	0.28	700.0	0.15201	0.330	0.682	982.70	5.15



TABLE B-1 (Continued)

Bed Material	No. of Tests	Q (cfs)	V (fps)	h (ft)	Total Bed-Material Transport		S $\times 10^2$	hS (ft $\times 10^3$ )	h/D <sub>50</sub>	b/h
					C <sub>tb</sub> (ppht)	G <sub>tb</sub> (lb/sec/ft)				
L.G. Straub										
18	Min.	0.283	1.132	0.11	41.7	0.00736	0.056	0.432	193.22	3.83
	25%	0.283	1.838	0.14	89.0	0.05563	0.108	0.608	237.29	4.13
	50%	0.849	2.300	0.24	496.1	0.11113	0.298	0.653	410.17	6.49
	75%	3.990	2.482	0.56	880.4	0.15547	0.462	0.748	954.24	8.26
	Max.	6.000	2.740	0.78	1340.0	1.11209	0.734	0.920	1327.12	21.90
R.A. Stein										
57	Min.	2.760	1.380	0.30	9.3	0.00801	0.061	0.404	229.01	3.33
	25%	6.420	2.326	0.50	188.5	0.18787	0.267	1.926	381.68	4.08
	50%	9.910	3.250	0.71	280.1	0.45152	0.321	2.384	541.98	5.63
	75%	11.600	4.419	0.98	689.0	0.99355	0.403	2.980	748.09	8.00
	Max.	17.000	6.043	1.20	3929.3	6.07454	1.079	6.474	916.03	13.33
Kalinske & Hsia										
9	Min.	0.700	0.841	0.35	640.0	0.12425	0.025	0.092	9722.21	3.41
	25%	1.260	1.247	0.37	1670.0	0.54621	0.025	0.165	10277.77	4.02
	50%	1.810	1.547	0.52	2240.0	1.12442	0.050	0.260	14444.44	4.33
	75%	2.600	1.806	0.56	3360.0	1.63682	0.100	0.350	15555.55	6.08
	Max.	3.200	2.735	0.66	11100.0	9.85087	0.130	0.676	18333.32	6.43
Barton & Lin										
31	Min.	0.900	0.708	0.30	1.9	0.00058	0.044	0.243	507.61	2.90
	25%	2.100	1.192	0.48	28.0	0.00799	0.086	0.526	812.18	5.33
	50%	4.200	1.500	0.63	57.1	0.03818	0.121	0.628	1065.99	6.35
	75%	7.200	2.596	0.75	164.1	0.19694	0.160	0.897	1269.04	8.33
	Max.	9.100	3.585	1.38	377.6	0.44768	0.210	1.292	4921.46	13.33
E.M. Laursen										
24	Min.	0.863	0.850	0.25	14.0	0.01078	0.043	0.296	692.52	3.02
	25%	2.111	1.330	0.47	131.0	0.06022	0.086	0.525	1434.90	4.23
	50%	3.064	1.700	0.56	305.0	0.17200	0.107	0.577	2094.18	5.54
	75%	4.424	2.130	0.72	5840.0	4.11390	0.144	0.696	3648.85	6.49
	Max.	6.424	3.360	0.99	9810.0	9.82083	0.210	0.936	5145.04	12.00
8	Min.	0.969	0.850	0.38	730.0	0.14713	0.078	0.296	2900.76	4.45
	25%	2.412	1.740	0.48	5840.0	4.11390	0.086	0.511	3648.85	5.30
	50%	3.175	1.910	0.56	8340.0	5.50773	0.101	0.572	4312.97	5.54
	75%	4.424	2.420	0.66	9700.0	7.67440	0.114	0.644	5061.07	6.49
	Max.	4.813	2.610	0.67	9810.0	9.82083	0.117	0.663	5145.04	7.89
16	Min.	0.863	1.070	0.25	14.0	0.01078	0.043	0.399	692.52	3.02
	25%	2.111	1.330	0.47	66.0	0.02898	0.092	0.565	1307.48	3.99
	50%	3.064	1.690	0.56	156.0	0.10025	0.120	0.580	1554.02	5.63
	75%	4.679	1.920	0.76	305.0	0.26114	0.152	0.746	2094.18	7.85
	Max.	6.424	3.360	0.99	515.0	0.50968	0.210	0.936	2756.23	12.00
B. Singh										
305	Min.	0.093	0.761	0.04	0.0	0.0	0.100	0.148	19.27	1.24
	25%	0.220	1.119	0.14	12.4	0.00161	0.150	0.320	69.71	3.79
	50%	0.406	1.327	0.21	25.2	0.00446	0.250	0.480	102.51	6.69
	75%	0.625	1.555	0.30	50.0	0.01142	0.350	0.708	148.97	13.19
	Max.	0.992	2.850	0.67	683.0	0.16842	1.400	2.300	329.30	63.01





B12

TABLE B-2  
DISTRIBUTION OF EXPERIMENTAL VALUES OF COMPUTED VARIABLES  
FOR DIFFERENT BED-MATERIALS AND DATA COLLECTIONS

Bed Material	Number of tests		$V^2/D_{50}$ (ft/sec <sup>2</sup> )	$V^2/h$ (ft/sec <sup>2</sup> )	$QS/b$ (ft <sup>2</sup> / sec x10 <sup>3</sup> )	$V D_{50}/\nu$	$\bar{C}/\sqrt{g}$	$f$	$n$	$V^2/D_{50}$ (ft/sec <sup>2</sup> )	$V D_{50}/\nu$
Colorado State University - B = 8.0 ft											
All Mtls.	239	Min.	292.6	0.59	0.037	45.92	7.02	0.0113	0.0083	1.386	2.42
		25%	1344.3	2.83	0.594	170.58	10.06	0.0357	0.0159	10.018	14.65
		50%	3183.5	5.30	2.530	280.71	11.80	0.0574	0.0207	32.165	25.13
		75%	12053.0	29.27	8.310	506.74	14.95	0.0790	0.0247	50.651	40.28
		Max.	36084.5	94.60	33.408	1851.88	26.55	0.1622	0.0374	319.157	128.91
.19 mm	40	Min.	872.0	0.59	0.037	45.92	8.87	0.0161	0.0104	2.429	2.42
		25%	1733.9	1.89	0.312	64.75	10.96	0.0263	0.0140	16.203	6.26
		50%	5245.2	4.64	1.382	112.62	12.64	0.0503	0.0204	40.986	9.96
		75%	23285.9	20.52	4.317	237.29	18.04	0.0732	0.0241	67.873	12.81
		Max.	36084.5	38.76	25.935	295.39	22.30	0.1015	0.0267	319.157	27.78
.27 mm	20	Min.	709.7	0.65	0.053	70.26	9.28	0.0235	0.0134	2.442	4.12
		25%	3782.5	3.60	1.430	162.20	10.14	0.0472	0.0183	28.391	14.05
		50%	4907.1	4.63	3.273	184.74	11.52	0.0631	0.0225	44.913	17.67
		75%	20680.8	29.67	7.626	379.26	15.02	0.0797	0.0255	64.109	21.12
		Max.	27477.7	44.26	27.275	437.16	18.43	0.0928	0.0284	222.856	39.37
.28 mm	37	Min.	728.2	0.66	0.058	75.18	8.86	0.0244	0.0133	2.477	4.38
		25%	3080.3	3.70	1.060	154.62	10.99	0.0319	0.0161	23.125	13.40
		50%	5074.6	5.58	2.598	198.46	11.42	0.0613	0.0213	41.520	17.95
		75%	13889.4	23.21	5.435	328.33	15.84	0.0662	0.0236	50.203	19.74
		Max.	26527.6	56.85	26.912	453.76	18.09	0.1019	0.0272	201.115	39.51
.45 mm	45	Min.	292.6	0.64	0.044	96.99	7.33	0.0113	0.0083	1.451	6.83
		25%	760.9	1.77	0.355	156.42	9.99	0.0288	0.0138	6.706	14.68
		50%	1940.8	5.00	1.964	249.81	11.80	0.0574	0.0213	24.150	27.87
		75%	9618.4	40.01	6.611	556.14	16.66	0.0800	0.0238	39.089	35.45
		Max.	26268.5	94.60	27.043	919.07	26.55	0.1486	0.0331	94.746	55.20
.93 mm	43	Min.	326.1	0.99	0.131	304.34	8.11	0.0324	0.0158	1.386	19.84
		25%	706.2	3.02	0.452	447.83	9.43	0.0389	0.0170	3.206	30.18
		50%	1344.3	5.83	2.359	617.90	13.16	0.0461	0.0192	12.293	59.09
		75%	3183.5	13.83	12.121	950.87	14.33	0.0899	0.0261	41.047	107.97
		Max.	12075.4	85.68	33.408	1851.88	15.70	0.1213	0.0329	58.511	128.91
.47 mm	54	Min.	840.1	1.66	0.398	175.50	7.02	0.0269	0.0130	6.578	15.53
		25%	1679.7	3.81	2.101	248.17	8.26	0.0381	0.0159	25.497	30.58
		50%	2920.8	5.56	4.608	327.25	11.17	0.0648	0.0225	40.093	38.34
		75%	13066.0	42.81	11.155	692.15	14.49	0.1171	0.0296	51.182	43.32
		Max.	18337.1	61.42	21.429	819.96	17.24	0.1622	0.0374	84.154	55.55
Colorado State University - B = 2.0 ft.											
All Mtls.	100	Min.	426.0	1.24	0.064	88.85	7.60	0.0222	0.0123	1.774	5.03
		25%	2798.2	5.24	1.759	206.38	9.92	0.0369	0.0161	23.871	17.40
		50%	5860.1	12.20	6.635	424.71	12.66	0.0499	0.0195	50.524	33.24
		75%	17347.2	37.60	19.222	583.28	14.74	0.0848	0.0240	93.693	53.15
		Max.	35626.2	74.20	75.770	1085.35	18.97	0.1382	0.0336	322.920	115.13
.32 mm	31	Min.	681.9	1.38	0.064	88.85	8.70	0.0231	0.0126	2.190	5.03
		25%	2683.4	4.98	1.307	176.25	9.92	0.0377	0.0165	23.871	16.62
		50%	5694.8	9.34	3.289	256.76	11.87	0.0567	0.0202	42.835	22.27
		75%	18578.0	32.53	16.969	463.75	14.56	0.0811	0.0239	120.735	37.39
		Max.	29761.9	51.23	54.351	586.97	18.62	0.1056	0.0283	322.920	61.14
.33(U) mm	14	Min.	923.4	2.00	0.140	108.30	8.45	0.0246	0.0130	3.717	6.87
		25%	1697.2	3.53	0.719	146.83	9.70	0.0302	0.0143	15.770	14.15
		50%	10406.7	23.00	4.441	363.58	13.30	0.0473	0.0180	43.974	23.63
		75%	18039.2	39.07	13.702	478.69	16.27	0.0848	0.0240	92.170	34.22
		Max.	31144.3	64.86	34.428	628.97	18.02	0.1118	0.0277	176.253	47.32
.33(G) mm	17	Min.	997.2	2.12	0.117	112.55	11.83	0.0222	0.0123	3.271	6.45
		25%	1819.7	3.79	0.460	152.04	13.67	0.0315	0.0148	9.740	11.12
		50%	4423.2	9.04	1.759	237.03	14.77	0.0366	0.0159	22.109	16.76
		75%	14200.1	30.15	8.660	424.71	15.92	0.0427	0.0172	65.123	28.76
		Max.	35626.2	74.20	29.596	672.71	18.97	0.0570	0.0198	148.602	43.45





TABLE B-2 (Continued)

Bed Material	Number of tests		$V^2/D_{50}$ (ft/sec <sup>2</sup> )	$V^2/h$ (ft/sec <sup>2</sup> )	$QS/b$ (ft <sup>2</sup> / sec x10 <sup>3</sup> )	$V D_{50}/\nu$	$\bar{C}/\sqrt{g}$	$f$	$n$	$V^2/D_{50}$ (ft/sec <sup>2</sup> )	$V D_{50}/\nu$
Colorado State University - B = 2.0 ft (Cont.)											
.54 mm	38	Min.	426.0	1.24	0.085	153.96	7.60	0.0317	0.0152	1.774	9.93
		25%	2917.7	6.16	5.630	402.92	8.49	0.0477	0.0193	44.222	49.60
		50%	6744.8	17.07	9.516	612.61	12.23	0.0551	0.0206	59.601	57.59
		75%	16586.8	41.99	28.723	960.68	12.95	0.1108	0.0301	92.108	71.59
		Max.	21171.4	58.62	75.770	1085.35	15.87	0.1382	0.0336	238.236	115.13
G.K. Gilbert											
All Mtls.	892	Min.	184.3	1.23	0.088	94.00	6.16	0.0094	0.0054	1.419	6.58
		25%	1458.7	31.03	2.287	335.82	10.51	0.0380	0.0132	13.866	25.90
		50%	3984.1	47.06	3.740	471.00	12.80	0.0487	0.0149	22.090	34.85
		75%	6311.7	73.79	6.160	788.33	14.50	0.0723	0.0190	30.784	61.04
		Max.	14404.3	402.66	40.691	11675.28	29.08	0.2107	0.0322	94.139	1163.64
A	61	Min.	980.9	5.25	0.674	99.04	6.16	0.0273	0.0107	15.578	12.48
		25%	4328.5	33.25	1.525	208.05	12.58	0.0357	0.0121	24.523	15.66
		50%	6070.1	45.06	2.227	246.38	13.85	0.0416	0.0134	29.125	17.07
		75%	7730.1	63.83	3.245	278.03	14.95	0.0505	0.0146	37.674	19.41
		Max.	11972.4	114.05	5.823	346.01	17.11	0.2107	0.0322	57.805	24.04
B	207	Min.	474.8	1.23	0.088	94.00	7.41	0.0094	0.0054	2.325	6.58
		25%	3926.2	29.96	1.860	270.30	11.86	0.0349	0.0120	20.734	19.64
		50%	5901.3	52.32	2.945	331.38	13.33	0.0450	0.0141	28.666	23.10
		75%	7541.4	85.15	4.400	374.61	15.13	0.0568	0.0164	39.792	27.21
		Max.	14404.3	402.66	12.265	517.73	29.08	0.1454	0.0298	94.139	41.85
C	236	Min.	746.9	2.78	0.653	184.84	7.21	0.0100	0.0065	10.632	22.05
		25%	2824.6	31.30	2.135	359.45	11.86	0.0380	0.0130	19.027	29.50
		50%	4487.5	47.01	3.426	453.07	13.34	0.0450	0.0144	24.043	33.16
		75%	6088.7	71.40	4.906	527.75	14.51	0.0573	0.0166	31.234	37.80
		Max.	13607.1	319.07	13.652	788.94	28.29	0.1536	0.0297	69.447	56.36
D	116	Min.	292.3	1.80	0.134	224.05	8.24	0.0330	0.0119	1.930	18.21
		25%	1735.9	26.82	2.359	546.00	10.99	0.0436	0.0136	13.912	48.88
		50%	2673.4	60.36	4.004	677.58	12.20	0.0544	0.0149	18.204	55.91
		75%	4246.3	94.54	6.287	853.95	13.62	0.0666	0.0180	23.682	63.77
		Max.	8436.0	140.00	16.350	1203.65	15.55	0.1177	0.0271	48.435	91.20
E	52	Min.	184.3	2.28	0.254	570.43	7.80	0.0450	0.0148	1.419	50.05
		25%	682.7	15.55	2.038	1097.87	9.84	0.0638	0.0179	5.989	102.83
		50%	1024.9	28.29	3.964	1345.22	10.57	0.0728	0.0193	9.769	131.33
		75%	1405.9	47.78	6.602	1575.51	11.20	0.0856	0.0218	13.698	155.51
		Max.	2746.3	91.32	12.122	2202.00	13.32	0.1313	0.0287	24.212	206.76
F	36	Min.	393.2	27.99	2.475	2103.11	8.80	0.0550	0.0161	3.790	206.47
		25%	559.5	32.17	4.615	2508.77	9.73	0.0684	0.0182	5.725	253.76
		50%	702.8	46.03	6.160	2811.65	10.47	0.0741	0.0193	7.137	283.34
		75%	939.0	57.35	8.786	3250.00	10.85	0.0875	0.0203	8.205	303.80
		Max.	1163.6	71.66	11.744	3617.82	12.05	0.1032	0.0225	10.527	344.11
G	69	Min.	353.0	16.55	4.560	3873.91	9.02	0.0616	0.0175	3.423	381.47
		25%	506.5	36.36	6.973	4640.62	9.61	0.0724	0.0193	4.781	450.84
		50%	609.7	47.01	10.010	5091.43	10.07	0.0787	0.0200	6.186	512.83
		75%	838.6	61.84	15.513	5970.95	10.50	0.0865	0.0210	8.479	600.42
		Max.	1416.0	94.02	40.691	7758.86	11.38	0.0982	0.0262	16.887	847.32
H	27	Min.	388.5	21.67	8.195	6875.00	8.57	0.0768	0.0197	3.838	683.37
		25%	451.8	30.38	12.233	7414.14	9.02	0.0836	0.0218	5.128	789.90
		50%	525.1	45.60	16.682	7993.37	9.24	0.0935	0.0234	6.553	892.95
		75%	789.0	58.42	27.466	9797.85	9.77	0.0983	0.0247	8.891	1040.05
		Max.	1120.3	79.16	40.352	11675.28	10.20	0.1087	0.0265	11.129	1163.64
I	88	Min.	3308.6	26.31	2.284	389.03	12.41	0.0247	0.0103	17.394	28.21
		25%	4312.8	34.87	3.093	444.16	13.90	0.0332	0.0126	22.245	31.90
		50%	6426.2	45.06	4.803	542.17	14.90	0.0366	0.0136	27.638	35.56
		75%	8222.3	77.23	6.378	613.28	15.51	0.0415	0.0148	33.915	39.39
		Max.	11237.0	118.79	10.210	716.95	18.00	0.0519	0.0165	49.264	47.47



TABLE B-2 (Continued)

Bed Material	Number of tests		$V^2/D_{50}$ (ft/sec <sup>2</sup> )	$V^2/h$ (ft/sec <sup>2</sup> )	QS/b (ft <sup>2</sup> / sec x10 <sup>3</sup> )	$V D_{50}/\nu$	$\bar{C}/\sqrt{g}$	f	n	$V^2/D_{50}$ (ft/sec <sup>2</sup> )	$V D_{50}/\nu$
Meyer-Peter											
All Mtls.	120	Min.	152.3	1.42	0.431	151.08	8.54	0.0297	0.0121	2.089	14.40
		25%	453.5	7.82	2.468	1306.77	9.57	0.0613	0.0202	4.135	112.41
		50%	608.9	16.05	5.393	3519.67	10.87	0.0677	0.0242	5.346	357.24
		75%	882.5	31.55	67.200	60521.86	11.43	0.0886	0.0264	6.968	5449.05
		Max.	2584.2	64.59	269.993	88806.06	16.41	0.1095	0.0313	19.732	9016.69
28.65 mm	34	Min.	373.5	13.33	49.585	55691.49	9.49	0.0599	0.0246	2.867	4879.48
		25%	485.3	19.58	80.408	63483.19	10.66	0.0645	0.0255	3.985	5753.09
		50%	577.0	27.47	101.828	69222.19	10.92	0.0671	0.0277	4.737	6271.96
		75%	710.0	34.87	149.371	76815.94	11.13	0.0703	0.0288	6.225	7189.87
		Max.	949.6	55.10	269.993	88806.06	11.55	0.0887	0.0313	9.790	9016.69
5.2 mm	20	Min.	395.4	11.54	4.583	4443.80	8.84	0.0596	0.0191	3.321	407.23
		25%	531.9	18.29	7.417	5154.00	10.28	0.0670	0.0205	4.521	475.15
		50%	657.3	28.92	11.512	5729.58	10.69	0.0708	0.0218	6.163	554.80
		75%	747.8	41.52	14.990	6111.26	10.99	0.0784	0.0226	8.096	635.88
		Max.	1028.7	64.59	24.566	7167.40	11.58	0.1023	0.0249	11.037	742.41
4.5 mm	7	Min.	444.0	25.60	4.371	3167.54	9.86	0.0484	0.0171	4.443	316.88
		25%	548.2	26.13	6.172	3519.67	10.00	0.0626	0.0193	5.647	357.24
		50%	794.9	32.10	8.534	4238.51	11.08	0.0651	0.0197	6.483	382.78
		75%	882.5	33.28	9.605	4465.96	11.29	0.0799	0.0204	6.925	395.60
		Max.	1139.8	42.98	10.902	5075.30	12.84	0.0822	0.0216	6.958	396.53
3.4 mm	24	Min.	152.3	6.47	0.902	1390.27	8.54	0.0873	0.0241	2.089	162.84
		25%	322.6	7.57	2.468	2092.60	9.27	0.0912	0.0249	3.751	225.01
		50%	427.0	7.64	3.545	2339.56	9.30	0.0923	0.0258	4.872	250.76
		75%	460.1	7.76	4.027	2628.47	9.36	0.0931	0.0264	5.366	283.40
		Max.	558.8	8.04	5.597	3295.42	9.57	0.1095	0.0273	6.521	355.54
22 mm	17	Min.	843.1	10.13	0.976	1002.37	11.37	0.0297	0.0121	3.135	61.12
		25%	932.2	11.44	1.938	1053.99	11.74	0.0468	0.0170	5.773	82.94
		50%	1236.7	12.24	2.931	1213.99	12.55	0.0507	0.0185	7.775	96.26
		75%	1433.0	14.01	4.281	1306.77	13.06	0.0580	0.0208	10.603	112.41
		Max.	1701.2	22.43	5.223	1423.82	16.41	0.0618	0.0215	11.812	118.64
1 mm	18	Min.	345.9	1.42	0.431	151.08	8.87	0.0471	0.0141	3.284	14.40
		25%	527.0	2.11	0.691	241.58	10.50	0.0578	0.0170	4.263	21.11
		50%	728.0	11.97	0.936	578.95	11.53	0.0609	0.0186	5.841	60.18
		75%	1113.6	14.22	1.441	782.09	11.76	0.0725	0.0238	11.906	69.21
		Max.	2584.2	56.93	3.944	1016.43	13.02	0.1015	0.0248	19.732	107.66
C.H. MacDougall											
All Mtls.	74	Min.	521.9	6.04	0.223	219.84	12.07	0.0273	0.0119	2.214	17.40
		25%	780.7	9.24	0.553	336.28	12.88	0.0355	0.0139	3.896	25.95
		50%	991.3	11.01	0.797	523.94	13.64	0.0431	0.0149	4.849	36.34
		75%	1170.7	17.33	1.059	707.65	14.99	0.0481	0.0158	5.920	50.09
		Max.	1686.2	21.94	1.698	895.41	17.12	0.0549	0.0174	10.365	62.59
I	27	Min.	521.9	6.04	0.223	219.84	12.58	0.0273	0.0119	3.268	17.40
		25%	993.5	9.85	0.376	303.33	12.73	0.0352	0.0129	4.357	20.09
		50%	1185.3	16.94	0.599	331.31	13.01	0.0472	0.0146	6.222	24.01
		75%	1332.1	17.41	0.793	351.23	15.07	0.0493	0.0153	7.557	26.45
		Max.	1686.2	18.85	1.272	395.17	17.12	0.0505	0.0174	10.365	30.98
II	21	Min.	555.3	7.42	0.273	397.11	13.24	0.0292	0.0125	2.214	25.08
		25%	707.3	8.24	0.519	448.20	13.85	0.0346	0.0137	3.666	32.27
		50%	966.6	9.91	0.788	523.94	14.76	0.0367	0.0140	4.651	36.34
		75%	1104.4	12.92	0.932	560.06	15.19	0.0416	0.0152	5.389	39.12
		Max.	1538.7	20.55	1.169	661.05	16.55	0.0456	0.0164	6.468	42.86
III	26	Min.	593.1	7.28	0.583	616.80	12.07	0.0308	0.0140	2.996	43.84
		25%	741.7	9.20	0.829	689.73	13.07	0.0391	0.0149	3.911	50.09
		50%	886.4	10.30	1.119	754.05	13.55	0.0441	0.0158	4.688	54.83
		75%	931.1	16.50	1.349	772.80	14.30	0.0467	0.0164	5.535	59.58
		Max.	1249.9	21.94	1.698	895.41	16.11	0.0549	0.0173	6.107	62.59







TABLE B-2 (Continued)

Bed Material	Number of tests		$V^2/D_{50}$ (ft/sec <sup>2</sup> )	$V^2/h$ (ft/sec <sup>2</sup> )	QS/b (ft <sup>2</sup> / sec x10 <sup>3</sup> )	$V D_{50}/\nu$	$\bar{C}/\sqrt{g}$	f	n	$V^2/D_{50}$ (ft/sec <sup>2</sup> )	$V D_{50}/\nu$
Chyn and Jorissen											
All Mtls.	58	Min.	300.0	5.92	0.193	170.36	9.42	0.0271	0.0126	2.767	16.66
		25%	700.4	8.63	0.379	286.09	13.18	0.0381	0.0140	3.759	21.89
		50%	884.2	10.53	0.499	358.98	13.77	0.0424	0.0149	4.589	25.86
		75%	1137.1	11.18	0.662	394.41	14.48	0.0460	0.0160	5.861	29.64
		Max.	1731.9	18.65	1.270	530.40	17.17	0.0900	0.0190	8.774	36.82
Chyn I	12	Min.	595.0	8.49	0.330	309.68	13.18	0.0356	0.0133	3.166	22.59
		25%	724.2	9.21	0.405	341.64	13.40	0.0408	0.0138	3.702	24.43
		50%	837.1	10.91	0.490	367.32	13.54	0.0437	0.0146	4.386	26.59
		75%	965.2	12.59	0.659	394.41	14.56	0.0452	0.0151	5.384	29.46
		Max.	1465.8	18.65	1.270	486.06	14.99	0.0460	0.0165	8.413	36.82
Chyn 2	10	Min.	653.9	7.97	0.352	363.34	13.10	0.0355	0.0134	3.121	25.10
		25%	723.7	9.09	0.446	382.25	13.53	0.0390	0.0139	3.682	27.26
		50%	823.8	10.73	0.564	407.84	13.88	0.0424	0.0150	4.457	30.00
		75%	927.2	11.18	0.681	432.67	14.31	0.0436	0.0153	5.086	32.04
		Max.	1198.5	13.30	0.939	491.91	15.01	0.0465	0.0160	6.146	35.23
Chyn 3	9	Min.	964.2	8.10	0.364	257.77	13.47	0.0352	0.0134	4.470	17.55
		25%	1061.0	9.75	0.429	270.40	14.05	0.0377	0.0137	5.108	18.76
		50%	1158.1	10.93	0.486	282.50	14.46	0.0382	0.0142	5.545	19.55
		75%	1310.9	11.12	0.644	300.57	14.56	0.0405	0.0147	6.812	21.67
		Max.	1507.0	14.41	0.832	322.27	15.06	0.0440	0.0149	8.317	23.94
Jorissen I	13	Min.	380.8	6.90	0.193	170.36	9.94	0.0296	0.0134	3.640	16.66
		25%	788.6	7.52	0.369	245.17	11.61	0.0416	0.0150	5.145	19.80
		50%	1061.8	9.68	0.532	248.48	12.46	0.0515	0.0163	6.285	21.89
		75%	1330.7	11.06	0.705	318.48	13.87	0.0592	0.0166	7.586	24.02
		Max.	1731.9	14.70	0.951	360.13	16.44	0.0808	0.0179	8.774	25.86
Jorissen II	14	Min.	300.0	5.92	0.268	264.08	9.42	0.0271	0.0126	2.767	25.36
		25%	514.4	9.48	0.334	345.82	10.77	0.0379	0.0142	3.269	27.57
		50%	700.4	10.62	0.533	403.50	13.65	0.0431	0.0148	4.044	30.66
		75%	946.7	11.12	0.661	469.13	14.52	0.0688	0.0173	4.495	32.33
		Max.	1210.2	12.58	0.812	530.40	17.17	0.0900	0.0190	5.768	36.62
USWES - (Sands 1-10)											
All Mtls.	437	Min.	255.2	1.60	0.061	31.94	5.71	0.0254	0.0093	1.738	2.90
		25%	636.5	4.04	0.242	128.88	9.42	0.0378	0.0134	3.626	10.71
		50%	859.7	7.18	0.454	175.41	12.30	0.0528	0.0179	6.696	15.03
		75%	1306.6	10.41	0.761	383.31	14.55	0.0899	0.0237	10.939	26.94
		Max.	4936.0	18.44	4.331	3236.26	17.75	0.2448	0.0369	55.900	323.83
I	60	Min.	489.8	7.67	0.083	113.21	12.90	0.0254	0.0100	2.173	7.54
		25%	1051.8	9.79	0.203	165.90	15.27	0.0302	0.0116	3.879	10.07
		50%	1294.8	11.54	0.316	184.06	15.57	0.0330	0.0124	5.421	11.91
		75%	1696.1	13.66	0.475	210.67	16.30	0.0344	0.0133	7.244	13.77
		Max.	2354.5	17.33	0.793	248.21	17.75	0.0480	0.0142	10.282	16.40
2	40	Min.	509.7	6.24	0.111	125.95	12.67	0.0339	0.0122	2.625	9.04
		25%	988.7	7.48	0.238	175.41	13.19	0.0363	0.0133	4.543	11.89
		50%	1421.4	9.56	0.455	210.33	13.93	0.0412	0.0145	7.080	14.84
		75%	1729.6	10.87	0.679	232.01	14.87	0.0462	0.0159	9.836	17.50
		Max.	2270.6	12.92	1.128	265.83	15.34	0.0497	0.0176	13.663	20.62
3	45	Min.	379.4	2.95	0.080	119.79	7.95	0.0308	0.0111	1.963	8.62
		25%	539.0	4.68	0.143	142.77	9.98	0.0392	0.0128	3.069	10.77
		50%	657.4	7.49	0.275	157.68	12.20	0.0537	0.0184	6.448	15.62
		75%	1144.2	9.06	0.558	208.02	14.28	0.0803	0.0212	8.887	18.33
		Max.	2023.0	14.63	1.168	276.60	16.11	0.1265	0.0251	13.672	22.74
4	42	Min.	366.4	2.63	0.084	102.10	7.18	0.0302	0.0110	2.250	8.00
		25%	583.8	3.45	0.164	128.88	9.04	0.0370	0.0118	3.545	10.04
		50%	767.0	5.28	0.311	147.72	11.35	0.0665	0.0200	8.044	15.13
		75%	1056.6	9.92	0.620	173.38	14.69	0.0977	0.0238	10.953	17.65
		Max.	2408.8	13.89	1.271	261.79	16.25	0.1549	0.0278	15.634	21.09



TABLE B-2 (Continued)

Bed Material	Number of tests		$V^2/D_{50}$ (ft/sec <sup>2</sup> )	$V^2/h$ (ft/sec <sup>2</sup> )	QS/b (ft <sup>2</sup> / sec x10 <sup>3</sup> )	$V \cdot D_{50}/\nu$	$\bar{C}/\sqrt{g}$	f	n	$V^2/D_{50}$ (ft/sec <sup>2</sup> )	$V \cdot D_{50}/\nu$
USWES - (Sands 1-10) Cont.											
5	32	Min.	474.7	2.60	0.091	103.54	7.16	0.0304	0.0111	2.614	7.68
		25%	705.3	3.30	0.161	126.21	8.99	0.0381	0.0118	3.718	9.16
		50%	874.0	4.63	0.471	140.49	10.02	0.0813	0.0232	10.946	15.72
		75%	1306.6	8.46	0.762	171.78	14.56	0.1061	0.0247	13.719	17.60
		Max.	2024.9	14.43	1.219	213.85	16.22	0.1560	0.0280	18.358	20.36
6	45	Min.	491.7	2.25	0.169	75.45	7.13	0.0764	0.0216	7.145	9.09
		25%	729.3	2.96	0.306	91.88	8.20	0.0868	0.0236	10.733	11.15
		50%	1168.7	3.47	0.504	116.31	9.07	0.0971	0.0242	14.475	12.94
		75%	1490.5	4.35	0.768	131.35	9.59	0.1188	0.0258	18.584	14.67
		Max.	2322.7	6.33	1.202	163.97	10.22	0.1573	0.0290	23.613	16.53
7	32	Min.	259.3	1.71	0.081	46.26	6.56	0.0260	0.0093	2.987	4.96
		25%	514.3	2.34	0.163	65.15	7.45	0.1069	0.0257	8.445	8.35
		50%	822.2	3.12	0.273	82.37	8.05	0.1237	0.0263	11.672	9.81
		75%	1040.1	4.47	0.461	92.65	8.74	0.1460	0.0272	15.448	11.29
		Max.	2005.3	14.85	0.949	128.65	17.54	0.1858	0.0303	23.755	14.00
8	21	Min.	494.2	1.60	0.061	31.94	5.71	0.0278	0.0102	4.086	2.90
		25%	952.1	2.33	0.218	44.33	7.05	0.0931	0.0256	16.890	5.90
		50%	1455.5	2.74	0.412	54.81	7.50	0.1421	0.0300	24.245	7.07
		75%	2426.0	2.93	0.814	70.77	9.26	0.1606	0.0317	38.684	8.94
		Max.	4936.0	9.23	1.520	100.94	16.94	0.2448	0.0369	55.900	10.74
9	18	Min.	255.2	10.52	1.349	2492.31	10.00	0.0528	0.0170	1.738	205.66
		25%	297.0	14.26	1.868	2688.46	10.85	0.0590	0.0184	2.284	235.75
		50%	341.3	15.85	2.374	2882.19	11.10	0.0660	0.0191	2.715	257.03
		75%	367.2	16.84	2.879	2989.23	11.64	0.0679	0.0198	3.131	276.05
		Max.	430.4	18.44	4.331	3236.26	12.30	0.0799	0.0225	4.309	323.83
10	102	Min.	400.8	3.38	0.210	348.38	9.22	0.0321	0.0118	1.921	24.12
		25%	622.8	5.96	0.441	434.30	11.82	0.0417	0.0149	3.264	31.44
		50%	722.0	7.00	0.657	467.59	12.92	0.0480	0.0164	4.566	37.19
		75%	862.1	9.47	1.018	510.95	13.85	0.0572	0.0195	6.415	44.08
		Max.	1150.5	14.59	1.910	590.26	15.78	0.0939	0.0257	11.343	58.61
USWES - Turbidity Tests											
	217	Min.	844.2	5.69	0.232	184.90	13.29	0.0382	0.0139	4.040	12.79
25%		844.2	5.69	0.232	184.90	13.29	0.0382	0.0139	4.040	12.79	
50%		1783.3	5.69	0.843	268.75	13.29	0.0452	0.0176	10.100	20.23	
75%		1783.3	6.73	0.843	268.75	14.46	0.0452	0.0176	10.100	20.23	
Max.		1783.3	6.73	0.843	268.75	14.46	0.0452	0.0176	10.100	20.23	
USWES - Synthetic Sands											
All Mtls.	312	Min.	433.2	2.38	0.306	106.60	8.61	0.0379	0.0143	2.208	11.13
		25%	682.6	3.87	0.306	315.49	10.97	0.0429	0.0153	3.644	25.80
		50%	900.6	4.75	0.827	382.07	12.16	0.0541	0.0195	6.246	31.60
		75%	1075.4	5.99	1.369	486.73	13.65	0.0667	0.0225	8.588	41.23
		Max.	2363.3	6.77	1.369	653.69	14.51	0.1078	0.0301	24.048	56.47
U.293	14	Min.	689.9	2.40	0.306	106.60	8.64	0.0577	0.0180	7.525	11.13
		25%	892.8	2.80	0.306	121.27	9.33	0.0685	0.0219	8.807	12.04
		50%	1801.3	3.54	0.827	172.26	10.49	0.0824	0.0224	15.459	15.96
		75%	2039.9	3.75	1.369	183.31	10.80	0.0919	0.0259	23.012	19.47
		Max.	2227.8	4.45	1.369	191.56	11.77	0.1069	0.0279	24.048	19.90
U.417	15	Min.	900.1	3.13	0.306	187.53	9.86	0.0394	0.0146	4.968	13.93
		25%	990.4	3.65	0.306	196.71	10.65	0.0434	0.0154	5.132	14.16
		50%	1511.5	4.48	0.827	243.01	11.80	0.0574	0.0201	10.958	20.69
		75%	1698.5	5.92	1.369	257.61	13.57	0.0705	0.0238	16.376	25.29
		Max.	2126.8	6.53	1.369	288.26	14.24	0.0822	0.0259	17.235	25.95
U.589	14	Min.	670.8	2.67	0.306	266.90	9.11	0.0434	0.0154	3.677	19.76
		25%	676.2	2.97	0.306	267.96	9.60	0.0439	0.0155	3.692	19.80
		50%	1010.2	4.53	0.827	327.52	11.87	0.0642	0.0214	8.380	29.83
		75%	1098.6	5.85	1.369	341.55	13.49	0.0866	0.0267	12.569	36.53
		Max.	1536.3	5.92	1.369	403.90	13.57	0.0963	0.0283	13.024	37.19





TABLE B-2 (Continued)

Bed Material	Number of tests		$V^2/D_{50}$ (ft/sec <sup>2</sup> )	$V^2/h$ (ft/sec <sup>2</sup> )	$QS/b$ (ft <sup>2</sup> / sec x10 <sup>3</sup> )	$V D_{50}/\nu$	$\bar{C}/\sqrt{g}$	$f$	$n$	$V^2/D_{50}$ (ft/sec <sup>2</sup> )	$V D_{50}/\nu$
USWES - Synthetic Sands (Cont.)											
U.833	16	Min.	485.8	2.68	0.306	377.48	9.12	0.0419	0.0151	2.589	27.56
		25%	493.7	3.69	0.306	380.53	10.71	0.0429	0.0153	2.610	27.67
		50%	702.1	3.89	0.827	453.82	11.00	0.0667	0.0218	5.868	41.49
		75%	788.3	5.99	1.369	480.86	13.65	0.0851	0.0264	8.906	51.11
		Max.	1112.8	6.14	1.369	571.31	13.81	0.0960	0.0282	9.272	42.15
A	18	Min.	612.5	2.96	0.306	314.21	9.59	0.0394	0.0146	3.098	22.34
		25%	627.8	4.32	0.306	318.09	11.59	0.0409	0.0149	3.136	22.48
		50%	983.3	4.72	0.829	398.11	12.12	0.0547	0.0195	6.718	32.91
		75%	1024.5	6.29	1.369	406.36	13.98	0.0595	0.0216	9.650	39.44
		Max.	1294.7	6.53	1.369	456.82	14.24	0.0869	0.0267	10.950	42.01
B	14	Min.	697.6	2.59	0.306	266.06	8.97	0.0389	0.0145	3.599	19.11
		25%	726.4	3.00	0.306	271.51	9.65	0.0404	0.0148	3.644	19.23
		50%	1073.5	4.76	0.827	330.04	12.16	0.0598	0.0205	8.254	28.94
		75%	1151.6	6.37	1.369	341.85	14.07	0.0857	0.0265	12.716	35.92
		Max.	1611.2	6.61	1.369	404.35	14.33	0.0993	0.0288	13.356	36.81
C	14	Min.	671.4	2.81	0.306	297.44	9.34	0.0384	0.0144	3.285	20.81
		25%	671.4	4.37	0.306	297.44	11.65	0.0394	0.0146	3.313	20.89
		50%	1023.1	4.84	0.827	367.18	12.26	0.0531	0.0199	7.252	30.91
		75%	1062.9	6.53	1.369	374.26	14.24	0.0588	0.0203	9.938	36.19
		Max.	1493.0	6.69	1.369	443.56	14.42	0.0916	0.0275	11.915	39.62
D	16	Min.	450.6	3.66	0.306	416.92	10.67	0.0399	0.0147	2.325	29.95
		25%	465.5	4.39	0.306	423.76	11.68	0.0419	0.0151	2.363	30.20
		50%	790.5	5.28	0.827	552.26	12.81	0.0504	0.0187	4.879	43.39
		75%	882.0	6.14	1.369	583.34	13.81	0.0621	0.0222	7.319	53.14
		Max.	978.2	6.45	1.369	614.32	14.16	0.0702	0.0237	7.624	54.23
E	30	Min.	518.9	3.00	0.306	353.37	9.65	0.0414	0.0150	2.755	25.75
		25%	527.3	4.41	0.306	356.22	11.70	0.0424	0.0152	2.777	25.85
		50%	879.5	4.89	0.827	460.03	12.33	0.0528	0.0192	5.800	37.36
		75%	933.3	6.07	1.369	473.90	13.73	0.0583	0.0212	8.332	44.77
		Max.	1214.9	6.21	1.369	540.67	13.90	0.0857	0.0265	9.536	47.90
F	15	Min.	433.2	3.82	0.306	438.93	10.89	0.0394	0.0146	2.208	31.34
		25%	440.3	4.22	0.306	442.51	11.45	0.0414	0.0150	2.245	31.60
		50%	725.0	4.98	0.827	567.84	12.44	0.0516	0.0189	4.690	45.67
		75%	849.7	6.21	1.369	614.75	13.90	0.0609	0.0219	6.934	55.53
		Max.	960.8	6.53	1.369	653.69	14.24	0.0674	0.0232	7.171	56.47
G	15	Min.	515.6	3.70	0.306	364.36	10.73	0.0409	0.0149	2.682	26.28
		25%	519.7	4.15	0.306	365.84	11.36	0.0414	0.0150	2.693	26.34
		50%	812.2	4.64	0.827	457.33	12.01	0.0553	0.0200	5.823	38.72
		75%	1024.7	6.21	1.369	513.68	13.90	0.0619	0.0221	8.363	46.41
		Max.	1162.1	6.29	1.369	547.04	13.98	0.0694	0.0236	8.691	47.31
H	29	Min.	464.4	3.40	0.306	380.99	10.28	0.0414	0.0150	2.525	28.09
		25%	487.2	4.41	0.306	390.24	11.70	0.0434	0.0154	2.566	28.32
		50%	775.9	4.73	0.827	492.45	12.12	0.0544	0.0195	5.367	40.96
		75%	884.8	5.92	1.369	525.90	13.57	0.0583	0.0214	7.687	49.02
		Max.	1069.1	6.21	1.369	578.06	13.90	0.0756	0.0247	8.382	51.19
I	15	Min.	493.7	3.50	0.306	380.53	10.43	0.0409	0.0149	2.568	27.45
		25%	497.7	4.35	0.306	382.07	11.63	0.0414	0.0150	2.579	27.50
		50%	873.0	5.34	0.827	506.05	12.89	0.0481	0.0182	5.262	39.29
		75%	942.5	6.21	1.369	525.78	13.90	0.0590	0.0215	7.883	48.09
		Max.	1112.8	6.29	1.369	571.31	13.98	0.0734	0.0243	8.478	49.87
J	29	Min.	503.3	3.47	0.306	360.01	10.39	0.0409	0.0149	2.682	26.28
		25%	519.7	4.32	0.306	365.84	11.59	0.0429	0.0153	2.726	26.49
		50%	897.5	5.22	0.827	480.73	12.73	0.0493	0.0184	5.539	37.77
		75%	1029.9	5.99	1.369	514.99	13.65	0.0595	0.0216	8.254	46.10
		Max.	1146.6	6.29	1.369	543.37	13.98	0.0740	0.0244	8.876	47.81





TABLE B-2 (Continued)

Bed Material	Number of tests		$V^2/D_{50}$ (ft/sec <sup>2</sup> )	$V^2/h$ (ft/sec <sup>2</sup> )	QS/b (ft <sup>2</sup> / sec x10 <sup>3</sup> )	$V D_{50}/\nu$	$\bar{C}/\sqrt{g}$	f	n	$V^2/D_{50}$ (ft/sec <sup>2</sup> )	$V D_{50}/\nu$
USWES - Synthetic Sands (Cont.)											
K	15	Min.	614.9	2.88	0.306	287.74	9.45	0.0429	0.0153	3.384	21.34
		25%	624.7	3.65	0.306	290.03	10.66	0.0444	0.0156	3.424	21.47
		50%	923.3	4.39	0.827	352.59	11.68	0.0585	0.0211	7.553	31.89
		75%	1124.5	5.78	1.369	389.11	13.41	0.0703	0.0226	10.517	37.63
		Max.	1415.6	5.99	1.369	436.57	13.65	0.0894	0.0271	11.735	39.75
L	14	Min.	754.7	2.38	0.306	258.16	8.61	0.0399	0.0147	3.801	18.32
		25%	760.9	4.42	0.306	259.22	11.72	0.0404	0.0148	3.817	18.36
		50%	1151.7	4.84	0.827	318.92	12.26	0.0553	0.0200	8.319	27.10
		75%	1263.9	6.37	1.369	334.09	14.07	0.0582	0.0208	11.512	31.89
		Max.	1660.3	6.45	1.369	382.91	14.16	0.1078	0.0301	14.379	35.63
M	14	Min.	646.1	2.77	0.306	273.83	9.28	0.0409	0.0149	3.499	20.15
		25%	683.4	3.58	0.306	281.62	10.55	0.0439	0.0155	3.584	20.39
		50%	998.6	4.57	0.827	340.42	11.92	0.0625	0.0210	7.922	30.32
		75%	1135.0	5.85	1.369	362.93	13.49	0.0718	0.0236	11.335	36.27
		Max.	1499.5	6.29	1.369	417.15	13.98	0.0928	0.0277	12.487	38.07
Filter	14	Min.	1065.6	3.14	0.306	185.10	9.88	0.0379	0.0143	5.236	12.98
		25%	1092.2	4.57	0.306	187.41	11.92	0.0394	0.0146	5.301	13.06
		50%	1733.6	5.37	0.827	236.10	12.92	0.0519	0.0190	11.279	19.04
		75%	1852.1	6.53	1.369	244.04	14.24	0.0563	0.0205	15.991	22.68
		Max.	2363.3	6.77	1.369	275.67	14.51	0.0819	0.0258	18.369	24.30
T.Y. Liu											
All Mtls.	310	Min.	187.8	9.00	0.259	463.68	9.63	0.0074	0.0064	0.484	40.50
		25%	339.1	14.03	0.796	928.09	12.10	0.0401	0.0140	2.020	73.03
		50%	409.6	21.75	1.234	1859.13	13.24	0.0456	0.0151	2.454	128.92
		75%	493.8	30.70	1.775	2601.70	14.12	0.0545	0.0160	2.903	193.90
		Max.	699.0	77.14	3.863	4028.68	32.81	0.0861	0.0190	4.042	303.20
I	61	Min.	243.5	11.42	0.554	2614.71	10.50	0.0074	0.0064	0.484	116.56
		25%	331.6	20.97	1.423	3051.63	12.72	0.0250	0.0115	1.415	199.34
		50%	408.1	23.69	1.936	3385.11	14.30	0.0391	0.0148	1.725	220.12
		75%	484.4	39.09	2.409	3688.14	17.87	0.0494	0.0160	2.421	260.74
		Max.	578.0	62.16	3.863	4028.68	32.81	0.0725	0.0182	3.274	303.20
II	60	Min.	235.1	11.30	0.570	1688.23	9.82	0.0241	0.0119	0.989	109.50
		25%	326.0	14.90	1.280	1987.95	11.74	0.0357	0.0143	1.893	151.51
		50%	390.8	20.02	1.624	2176.70	13.45	0.0453	0.0154	2.363	169.27
		75%	464.9	31.43	1.944	2374.00	15.07	0.0588	0.0162	2.724	181.73
		Max.	672.0	43.56	2.726	2854.39	18.22	0.0829	0.0178	3.261	198.85
III	55	Min.	267.5	9.76	0.554	1044.31	9.84	0.0338	0.0127	1.576	80.17
		25%	362.2	13.57	0.874	1215.26	12.68	0.0427	0.0145	2.258	95.95
		50%	425.3	15.93	1.129	1316.78	13.29	0.0452	0.0152	2.645	103.84
		75%	515.5	27.41	1.332	1449.71	13.67	0.0497	0.0158	2.996	110.53
		Max.	694.4	39.02	1.934	1682.57	15.37	0.0825	0.0171	3.703	122.87
IV	47	Min.	187.8	9.00	0.259	463.68	9.72	0.0306	0.0095	1.432	40.50
		25%	364.4	11.76	0.426	645.98	12.32	0.0403	0.0132	2.228	50.51
		50%	458.6	15.86	0.591	724.67	13.75	0.0422	0.0139	2.553	54.07
		75%	563.8	30.39	0.780	803.48	14.09	0.0526	0.0145	3.125	59.81
		Max.	699.0	77.14	0.967	894.67	16.14	0.0846	0.0155	3.795	65.92
V	41	Min.	252.1	11.00	1.022	2038.17	10.56	0.0362	0.0151	1.575	161.10
		25%	314.8	15.48	1.648	2277.40	11.20	0.0466	0.0157	2.195	190.16
		50%	375.0	25.63	1.845	2485.73	12.30	0.0528	0.0163	2.481	202.18
		75%	412.0	37.32	2.317	2605.34	13.10	0.0637	0.0166	2.972	221.27
		Max.	574.2	44.48	3.125	3075.78	14.85	0.0716	0.0190	3.544	241.65
VI	46	Min.	255.4	9.66	0.392	665.55	9.63	0.0385	0.0132	1.715	54.54
		25%	349.5	12.25	0.577	778.65	11.97	0.0449	0.0145	2.281	62.90
		50%	413.1	16.02	0.732	846.51	12.72	0.0495	0.0149	2.887	70.76
		75%	521.1	26.04	0.969	950.77	13.34	0.0558	0.0155	3.262	75.22
		Max.	649.3	47.41	1.234	1061.29	14.40	0.0861	0.0176	4.042	83.73



TABLE B-2 (Continued)

Bed Material	Number of tests		$V^2/D_{50}$ (ft/sec <sup>2</sup> )	$V^2/h$ (ft/sec <sup>2</sup> )	QS/b (ft <sup>2</sup> / sec x10 <sup>3</sup> )	$V D_{50}/\nu$	$\overline{C}/\sqrt{g}$	f	n	$V^2/\nu_{50}$ (ft/sec <sup>2</sup> )	$V D_{50}/\nu$
Bogardi & Yen											
1	20	Min.	197.5	22.71	9.086	8351.12	6.28	0.0910	0.0220	3.266	1073.99
		25%	223.2	26.02	12.604	8878.73	6.68	0.1364	0.0264	4.308	1233.36
		50%	231.1	29.12	13.777	9032.85	7.12	0.1607	0.0288	4.725	1291.75
		75%	257.9	40.40	14.515	9544.14	7.89	0.1792	0.0320	5.187	1353.41
		Max.	361.0	59.03	18.744	11291.07	9.37	0.2025	0.0340	5.855	1437.91
2	18	Min.	222.1	28.84	4.202	4965.97	7.86	0.0682	0.0194	2.724	550.02
		25%	282.0	36.11	6.505	5595.70	8.44	0.1044	0.0214	3.725	643.13
		50%	300.2	41.92	7.644	5773.24	8.56	0.1095	0.0222	4.019	668.05
		75%	333.4	48.52	8.817	6084.54	8.75	0.1120	0.0234	4.519	708.38
		Max.	522.9	53.77	10.573	7619.96	10.82	0.1292	0.0264	5.065	749.93
3	10	Min.	264.7	20.20	17.238	17762.09	7.42	0.0735	0.0214	3.024	1898.41
		25%	283.6	35.91	20.665	18385.68	9.06	0.0854	0.0220	3.420	2018.87
		50%	329.1	49.15	22.687	19804.82	9.64	0.0871	0.0227	3.689	2096.73
		75%	339.0	55.63	26.539	20100.67	9.67	0.0972	0.0246	4.226	2244.15
		Max.	407.6	64.92	29.946	22041.87	10.43	0.1451	0.0329	4.811	2394.59
M.B. O'Brien											
Columbia River	83	Min.	418.6	1.18	0.128	83.04	5.00	0.0279	0.0141	4.973	9.05
		25%	1101.1	1.65	0.553	134.68	7.74	0.0688	0.0227	12.345	14.26
		50%	1451.3	2.64	0.774	154.61	9.36	0.0912	0.0269	16.219	16.35
		75%	1852.9	4.21	1.166	174.70	10.78	0.1335	0.0299	22.791	19.38
		Max.	8273.8	21.71	3.953	369.17	16.91	0.3198	0.0446	39.971	25.66
H.J. Casey											
h & IIIa	92	Min.	128.5	5.64	0.109	280.07	10.15	0.0295	0.0107	1.021	24.96
		25%	357.1	7.77	0.409	530.43	12.17	0.0427	0.0144	2.231	38.78
		50%	460.1	12.60	0.838	1105.25	12.68	0.0502	0.0160	2.692	92.13
		75%	568.3	19.62	1.353	1375.52	13.75	0.0540	0.0173	3.396	110.72
		Max.	1080.1	26.09	2.778	1823.04	16.45	0.0775	0.0203	6.626	141.44
h	49	Min.	278.4	5.64	0.625	1065.37	11.05	0.0411	0.0145	1.889	87.76
		25%	384.3	7.45	1.007	1251.70	12.09	0.0492	0.0162	2.569	102.33
		50%	460.1	12.45	1.234	1369.60	12.48	0.0513	0.0171	2.951	109.68
		75%	558.0	20.91	1.572	1508.28	12.75	0.0547	0.0179	3.447	118.55
		Max.	815.2	25.30	2.778	1823.04	13.95	0.0654	0.0203	4.907	141.44
IIIa	43	Min.	128.5	6.43	0.109	280.07	10.15	0.0295	0.0107	1.021	24.96
		25%	319.1	8.21	0.228	441.29	12.47	0.0373	0.0127	1.689	32.11
		50%	440.2	13.25	0.381	518.31	13.63	0.0430	0.0141	2.362	37.96
		75%	606.6	18.55	0.589	608.40	14.64	0.0514	0.0150	3.174	44.01
		Max.	1080.1	26.09	1.671	811.86	16.45	0.0775	0.0193	6.626	63.59
Ho, Pang-Yung											
All Mtls.	80	Min.	124.2	3.45	0.091	365.62	10.36	0.0391	0.0139	0.806	29.45
		25%	329.0	5.69	0.651	746.99	11.77	0.0468	0.0175	2.107	54.53
		50%	461.8	6.90	1.689	1763.26	12.38	0.0522	0.0190	2.834	135.18
		75%	605.0	14.13	2.932	3224.30	13.08	0.0578	0.0203	4.088	272.15
		Max.	1243.7	22.22	8.655	6673.91	14.29	0.0744	0.0240	9.305	578.54
I	15	Min.	248.7	5.06	0.912	1539.90	11.42	0.0469	0.0177	1.908	134.86
		25%	379.1	6.31	1.500	1901.14	12.00	0.0504	0.0187	2.489	154.04
		50%	468.6	7.75	1.942	2113.67	12.18	0.0539	0.0196	2.958	167.92
		75%	605.8	14.71	3.029	2403.23	12.59	0.0555	0.0204	3.954	194.16
		Max.	875.6	16.55	5.849	2889.24	13.05	0.0612	0.0207	6.519	249.29







TABLE B-2 (Continued)

Bed Material	Number of tests		$V^2/D_{50}$ (ft/sec <sup>2</sup> )	$V^2/h$ (ft/sec <sup>2</sup> )	QS/b (ft <sup>2</sup> / sec x10 <sup>3</sup> )	$V/D_{50/\nu}$	$\bar{C}/\sqrt{g}$	f	n	$V^2/D_{50}$ (ft/sec <sup>2</sup> )	$V/D_{50/\nu}$
Ho, Pang-Yung (Cont.)											
II	11	Min.	232.3	5.85	1.455	2553.85	11.26	0.0534	0.0184	1.835	227.00
		25%	304.2	7.83	1.913	2922.70	11.66	0.0548	0.0194	2.107	243.26
		50%	367.0	8.04	2.542	3210.38	11.92	0.0563	0.0203	2.539	266.99
		75%	473.8	14.69	3.845	3647.32	12.07	0.0588	0.0206	3.395	308.75
		Max.	605.0	15.05	5.703	4121.69	12.24	0.0631	0.0213	4.456	353.71
III	8	Min.	273.4	7.67	2.719	4681.34	11.33	0.0546	0.0182	1.870	387.17
		25%	347.8	14.92	4.004	5279.90	11.52	0.0566	0.0193	2.442	442.40
		50%	375.7	15.72	4.830	5487.33	11.77	0.0600	0.0204	2.834	476.64
		75%	461.8	21.04	6.803	6084.34	11.94	0.0613	0.0205	3.600	537.21
		Max.	555.7	21.51	8.655	6673.91	12.10	0.0622	0.0210	4.176	578.54
IV	14	Min.	364.6	4.92	0.394	531.85	11.30	0.0454	0.0174	2.386	43.02
		25%	610.1	5.69	0.796	688.01	12.22	0.0467	0.0180	3.728	53.78
		50%	908.1	6.86	1.372	839.34	12.80	0.0510	0.0187	5.265	63.91
		75%	1023.6	7.19	1.760	891.12	13.08	0.0535	0.0195	6.423	70.59
		Max.	1243.7	8.96	2.838	982.28	13.27	0.0626	0.0216	9.305	84.96
V	7	Min.	261.2	12.97	2.711	4463.53	10.99	0.0520	0.0186	1.956	386.22
		25%	327.4	13.57	4.039	4997.06	11.22	0.0578	0.0191	2.603	445.59
		50%	371.3	16.46	4.827	5322.02	11.56	0.0598	0.0201	2.972	476.14
		75%	477.6	21.76	6.749	6035.68	11.75	0.0635	0.0207	3.623	525.71
		Max.	569.3	22.22	8.638	6590.02	12.40	0.0662	0.0216	4.221	567.40
VI	25	Min.	124.2	3.45	0.091	365.62	10.36	0.0391	0.0139	0.806	29.45
		25%	209.0	5.32	0.162	474.31	12.85	0.0434	0.0156	1.171	35.50
		50%	336.2	5.61	0.349	601.61	13.20	0.0458	0.0164	1.942	45.72
		75%	524.2	5.92	0.651	751.18	13.56	0.0483	0.0174	2.886	55.74
		Max.	729.2	6.50	1.121	885.96	14.29	0.0744	0.0240	4.833	72.13
Nomicos, Vanoni & Brooks											
All Mtls	63	Min.	1302.4	1.19	0.169	23.68	6.47	0.0234	0.0119	15.131	3.12
		25%	3314.8	4.48	0.717	45.67	8.29	0.0327	0.0132	35.023	4.51
		50%	5088.3	7.99	0.885	62.30	10.15	0.0775	0.0212	41.744	6.12
		75%	9225.7	17.56	1.044	89.05	15.62	0.1162	0.0259	48.192	6.58
		Max.	17463.1	29.37	2.500	132.75	18.48	0.1906	0.0320	76.718	8.68
Nomicos Sand #6	5	Min.	5088.3	5.34	0.857	36.70	8.15	0.0259	0.0119	52.730	3.74
		25%	5088.3	5.34	0.874	36.70	8.23	0.0266	0.0121	56.761	3.88
		50%	13802.7	16.86	0.990	60.44	16.19	0.0305	0.0128	57.206	3.89
		75%	17192.4	19.94	1.198	67.45	17.34	0.1179	0.0259	75.184	4.46
		Max.	17463.1	20.41	1.198	67.98	17.55	0.1203	0.0261	76.718	4.51
Nomicos Sand #4	4	Min.	4229.2	7.81	0.921	61.87	9.40	0.0327	0.0131	35.983	5.71
		25%	4446.1	8.42	0.921	63.44	9.76	0.0328	0.0132	41.774	6.15
		50%	8760.9	17.64	0.995	89.05	15.61	0.0839	0.0212	46.740	6.50
		75%	10185.9	19.63	1.246	96.02	15.62	0.0904	0.0221	47.923	6.59
		Max.	10185.9	19.63	1.246	96.02	15.62	0.0904	0.0221	47.923	6.59
Nomicos Sand #5	12	Min.	1302.4	2.70	0.389	40.23	6.47	0.0327	0.0133	31.103	6.22
		25%	1931.0	4.00	0.615	48.98	6.91	0.0451	0.0156	32.658	6.37
		50%	3842.5	7.96	0.801	69.10	10.15	0.1162	0.0250	37.324	6.81
		75%	6749.5	13.98	0.885	91.58	14.74	0.1775	0.0309	41.989	7.22
		Max.	14183.2	29.37	2.500	132.75	15.62	0.1906	0.0320	60.651	8.68
Vanoni & Brooks Sand #4	16	Min.	1311.9	1.19	0.169	34.46	7.18	0.0234	0.0120	15.131	3.70
		25%	2535.8	3.38	0.703	47.91	8.96	0.0492	0.0187	35.551	5.67
		50%	4399.4	6.38	0.881	63.11	9.93	0.0845	0.0230	41.340	6.12
		75%	9490.8	10.92	1.013	92.69	15.38	0.1053	0.0265	46.896	6.52
		Max.	14236.0	20.99	1.472	113.52	18.48	0.1550	0.0289	48.192	6.60
Brooks Sand #1	12	Min.	1778.5	3.34	0.457	42.97	7.21	0.0278	0.0121	32.063	5.77
		25%	4227.1	7.90	0.860	66.25	9.67	0.0336	0.0134	35.023	6.03
		50%	6784.6	16.63	0.986	83.93	13.40	0.0454	0.0154	38.229	6.30
		75%	8905.4	17.56	1.111	96.16	15.97	0.0926	0.0224	43.641	6.73
		Max.	10047.0	20.97	1.243	102.13	16.95	0.1537	0.0289	47.238	7.00
Brooks Sand #2	10	Min.	2322.4	2.41	0.297	23.68	7.49	0.0296	0.0124	40.412	3.12
		25%	4019.4	4.24	0.651	31.15	7.73	0.0308	0.0128	57.715	3.73
		50%	6213.8	7.99	0.905	38.73	9.39	0.0993	0.0229	60.484	3.82
		75%	15354.7	18.80	1.094	60.88	16.12	0.1337	0.0275	68.756	4.07
		Max.	15587.5	20.43	1.119	61.34	16.44	0.1425	0.0280	75.943	4.28



TABLE B-2 (Continued)

Bed Material	Number of tests	$V^2/D_{50}$ (ft/sec <sup>2</sup> )	$V^2/h$ (ft/sec <sup>2</sup> )	QS/b (ft <sup>2</sup> / sec x10 <sup>3</sup> )	$V D_{50}/\nu$	$\bar{C}/\sqrt{g}$	f	n	$V^2/D_{50}$ (ft/sec <sup>2</sup> )	$V D_{50}/\nu$	
L. G. Straub											
18	Min.	2171.9	5.13	0.718	66.79	7.77	0.0166	0.0115	34.594	6.96	
	25%	5723.7	9.03	1.120	108.42	11.75	0.0267	0.0128	33.198	8.26	
	50%	8966.1	18.24	1.543	135.70	14.92	0.0364	0.0138	35.643	8.56	
	75%	10445.1	29.19	1.667	146.46	17.30	0.0579	0.0161	40.797	9.15	
	Max.	12722.2	54.06	2.079	161.64	21.97	0.1325	0.0268	50.230	10.16	
R. A. Stein											
57	Min.	1453.7	1.90	0.842	180.78	7.19	0.0042	0.0051	9.930	14.94	
	25%	4130.3	7.92	4.717	304.72	8.57	0.0363	0.0166	47.341	32.62	
	50%	8063.0	16.00	7.118	425.75	11.87	0.0567	0.0203	58.599	36.30	
	75%	14904.8	33.99	11.135	578.86	14.83	0.1088	0.0282	73.249	40.58	
	Max.	27873.3	89.06	35.067	791.59	43.80	0.1543	0.0370	159.132	59.81	
Kalinske & Hsia											
9	Min.	19639.3	1.91	0.078	3.03	15.41	0.0232	0.0127	82.736	0.20	
	25%	43188.6	2.67	0.217	4.49	15.97	0.0246	0.0135	147.583	0.26	
	50%	66478.7	4.60	0.402	5.57	16.92	0.0279	0.0137	232.556	0.33	
	75%	90556.4	8.03	0.587	6.50	18.02	0.0313	0.0140	313.055	0.38	
	Max.	207790.7	14.39	1.849	9.85	18.55	0.0336	0.0149	604.644	0.53	
Barton & Lin											
31	Min.	849.0	0.84	0.172	29.46	6.04	0.0207	0.0115	13.240	2.48	
	25%	2405.4	2.41	0.645	70.18	9.16	0.0369	0.0168	28.817	7.70	
	50%	3807.1	3.20	0.979	85.65	10.48	0.0727	0.0226	34.434	8.41	
	75%	12163.5	10.42	2.511	153.43	14.72	0.0952	0.0271	52.697	10.04	
	Max.	21745.4	24.25	3.990	211.87	19.63	0.2193	0.0356	87.951	12.05	
E.M. Laursen											
All Mtls	24	Min.	3169.5	1.90	0.252	11.14	8.45	0.0129	0.0093	35.593	1.28
		25%	5515.3	3.68	0.733	31.70	10.35	0.0420	0.0176	51.110	1.89
		50%	8292.1	5.41	1.089	48.02	11.80	0.0580	0.0212	66.534	4.87
		75%	26689.5	6.83	1.500	61.37	13.99	0.0758	0.0229	125.718	5.40
		Max.	52001.9	23.92	2.163	121.30	24.89	0.1118	0.0257	162.966	6.27
8	Min.	5515.3	1.90	0.252	11.14	8.70	0.0243	0.0132	72.856	1.28	
	25%	23118.3	5.41	0.941	22.80	13.20	0.0291	0.0148	125.718	1.68	
	50%	27847.8	6.56	1.089	25.02	13.99	0.0420	0.0175	140.515	1.78	
	75%	44698.3	9.49	1.604	31.70	16.60	0.0746	0.0229	158.321	1.89	
	Max.	52001.9	12.06	1.681	34.19	18.13	0.1054	0.0257	162.966	1.91	
16	Min.	3169.5	1.91	0.531	38.61	8.45	0.0129	0.0093	35.593	4.09	
	25%	4900.7	3.68	0.733	48.02	10.27	0.0545	0.0201	50.394	4.87	
	50%	7910.1	5.09	1.099	61.00	11.67	0.0597	0.0217	51.734	4.93	
	75%	10214.1	6.31	1.500	69.32	12.37	0.0833	0.0235	66.534	5.59	
	Max.	31276.3	23.92	2.163	121.30	24.89	0.1118	0.0256	83.512	6.27	
B. Singh											
305	Min.	284.9	3.17	0.135	154.83	8.08	0.0382	0.0116	2.343	14.04	
	25%	615.5	5.80	0.354	227.58	9.90	0.0595	0.0166	5.065	20.65	
	50%	865.4	8.85	0.614	269.86	10.64	0.0705	0.0191	7.599	25.29	
	75%	1189.1	13.23	1.090	316.32	11.59	0.0815	0.0216	11.208	30.71	
	Max.	3992.4	49.72	6.554	579.62	14.46	0.1225	0.0290	36.411	55.35	



## A P P E N D I X      C

Joint Distribution Between Experimental Values  
of Pairs of the Parameters in the  
Mathematical Model





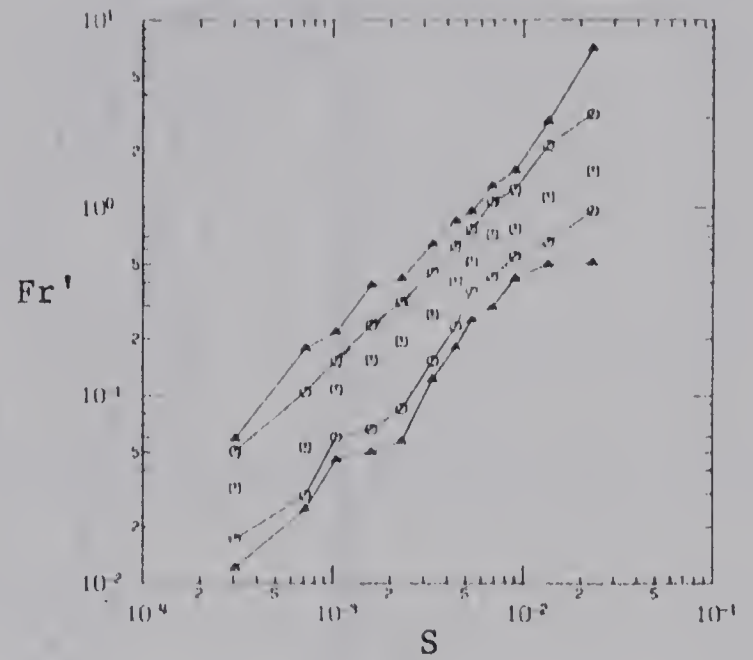
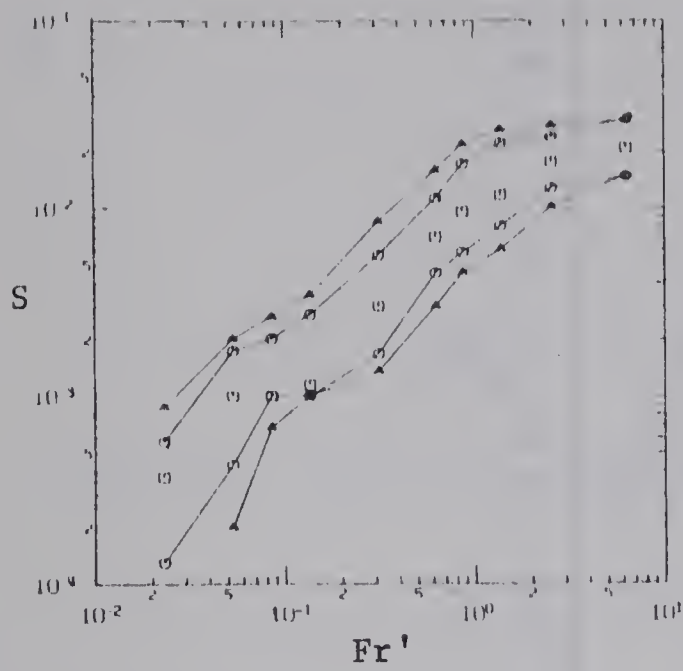


Figure C-1. Joint Distribution Between Experimental Values of  $Fr'$  and  $S$

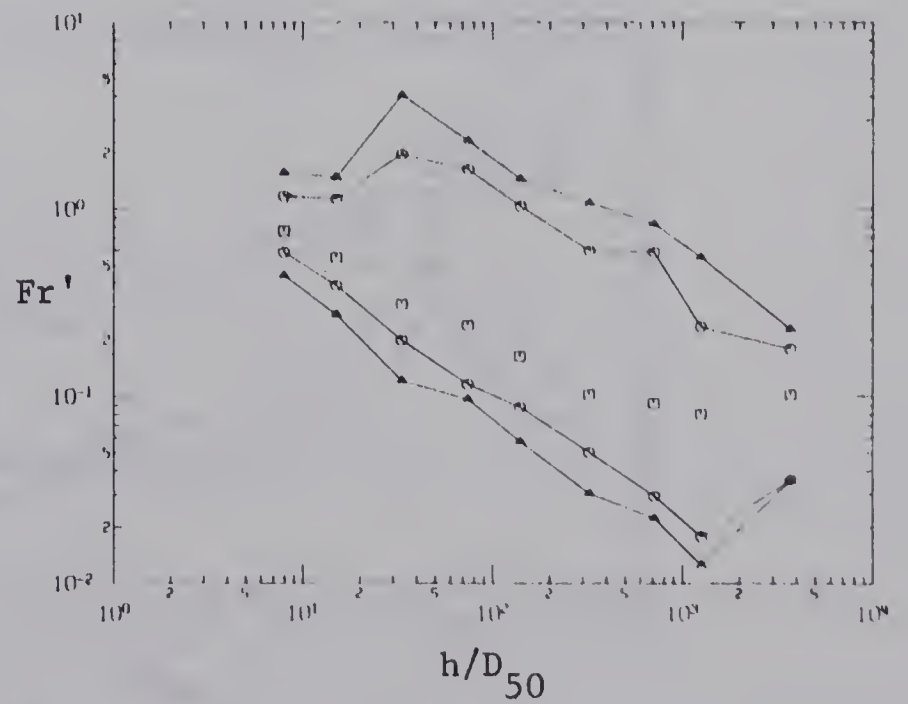
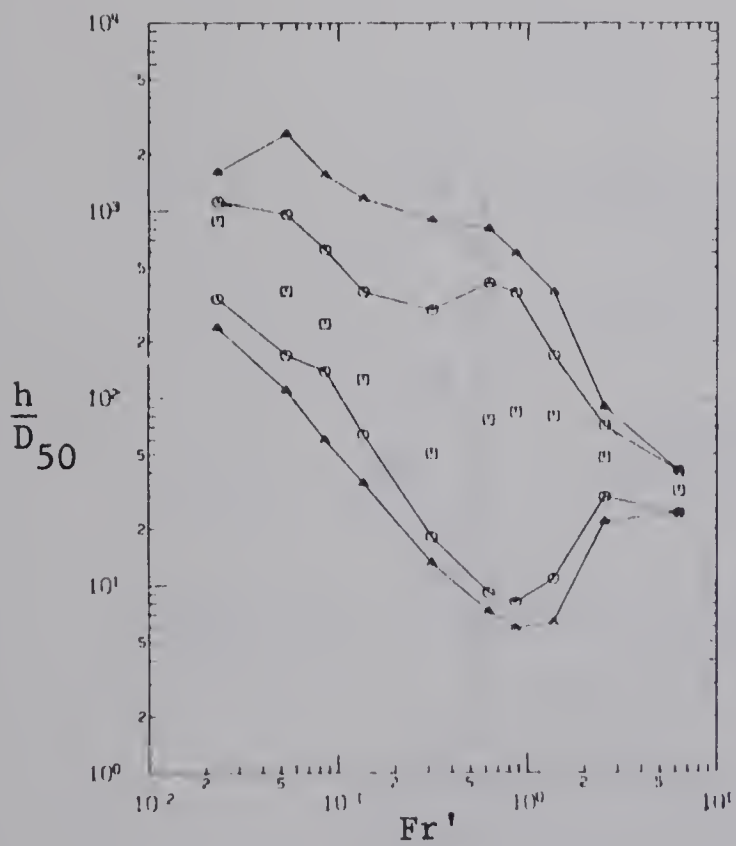


Figure C-2 Joint Distribution Between Experimental Values of  $Fr'$  and  $h/D_{50}$



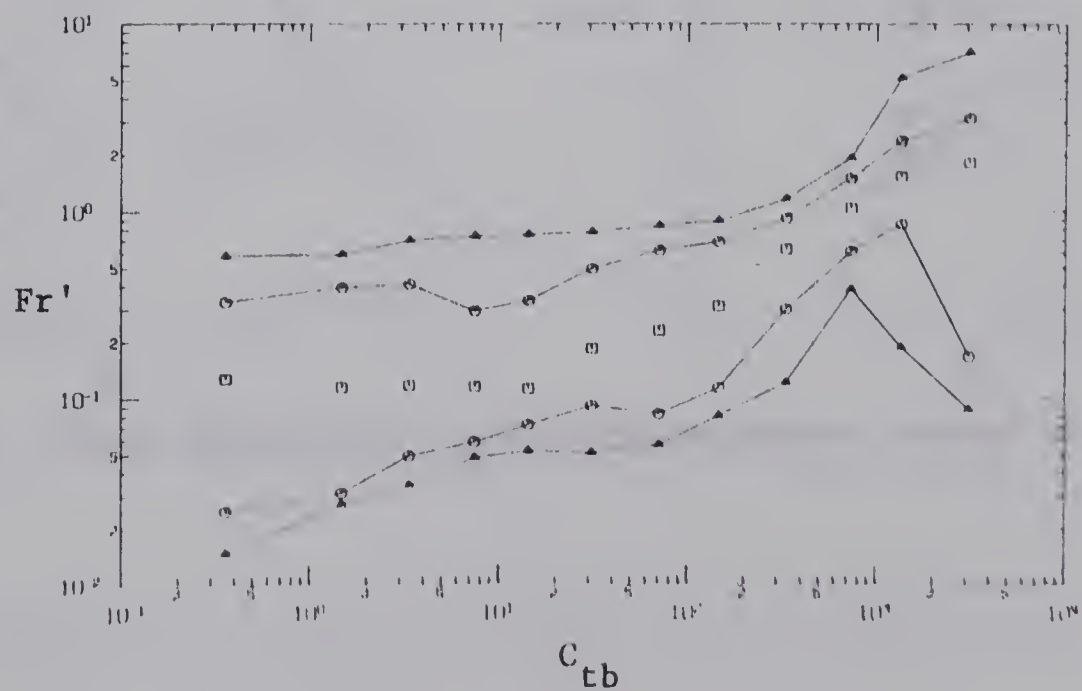
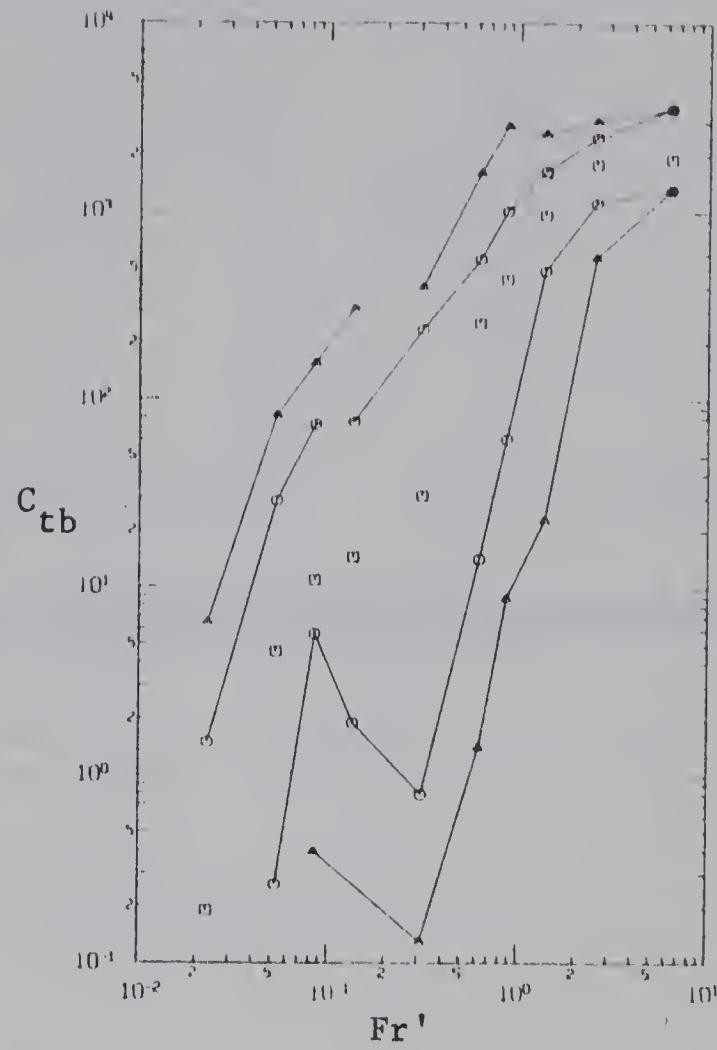


Figure C-3. Joint Distribution Between Experimental Values of  $Fr'$  and  $C_{tb}$





C4

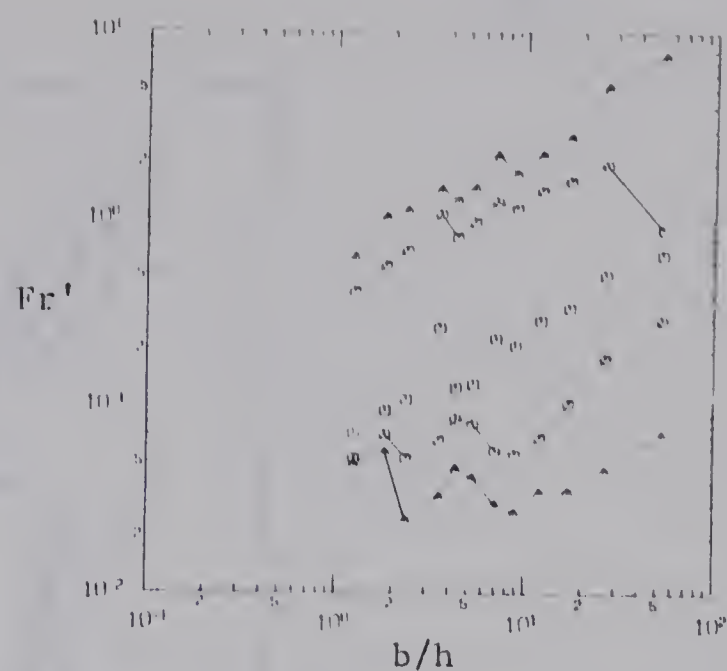
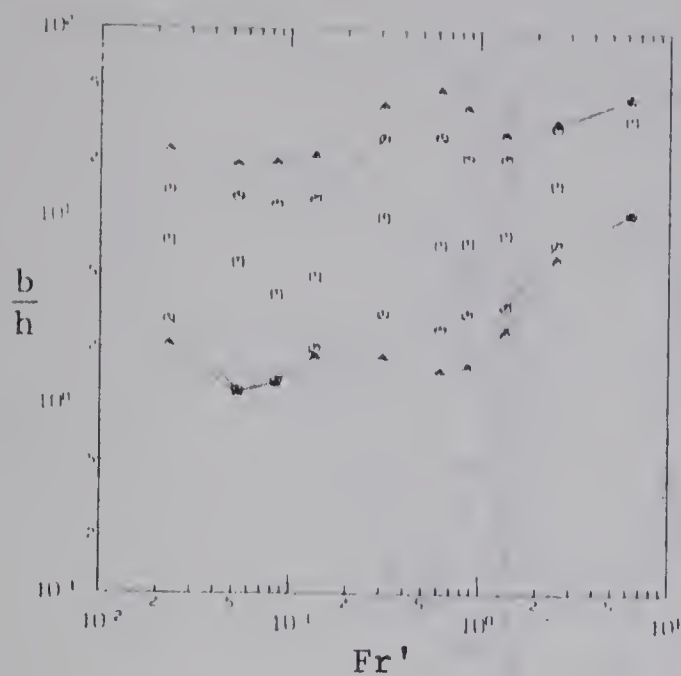


Figure C-4. Joint Distribution Between Experimental Values of  $Fr'$  and  $b/h$

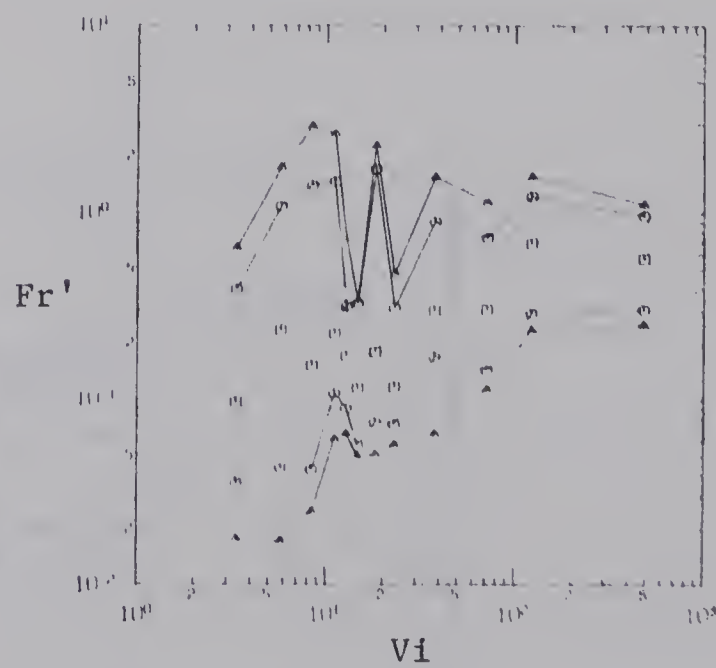
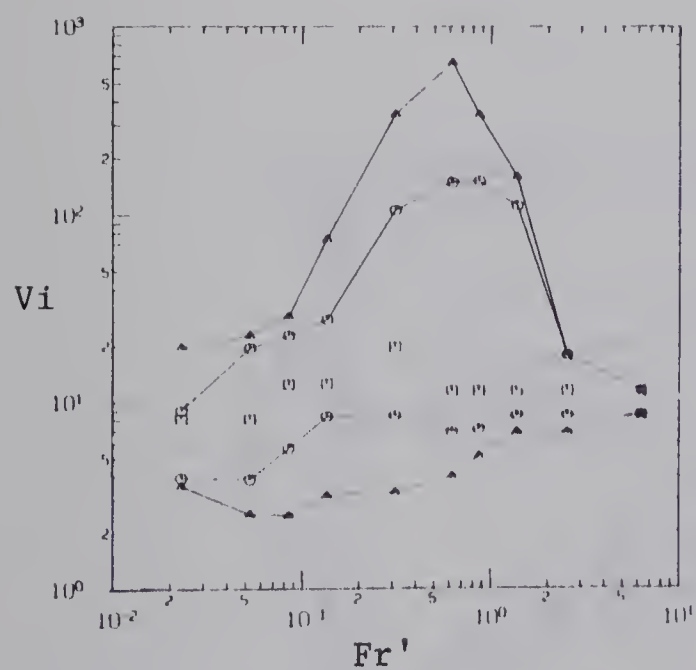


Figure C-5. Joint Distribution Between Experimental Values of  $Fr'$  and  $Vi$



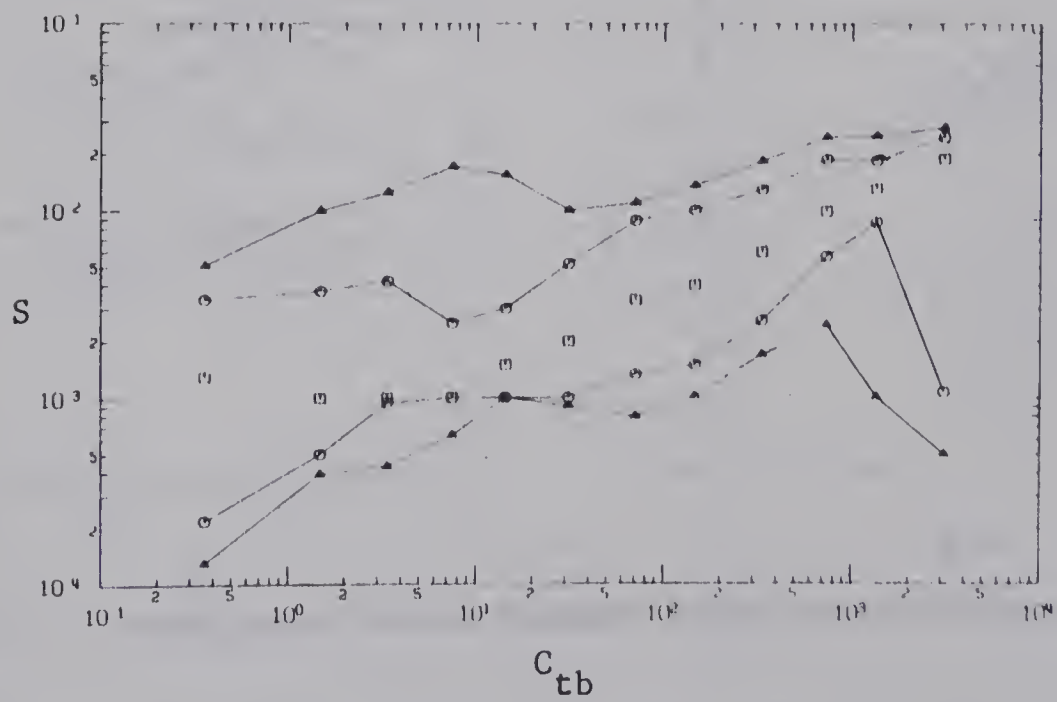
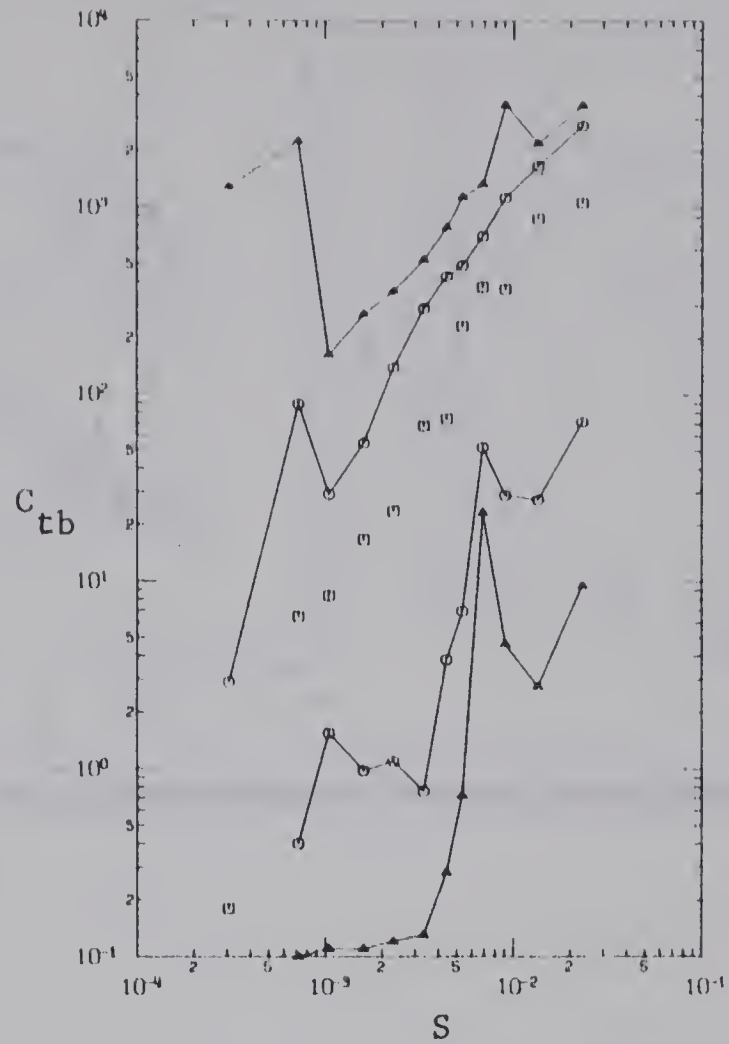


Figure C-6. Joint Distribution Between Experimental Values of  $S$  and  $C_{tb}$



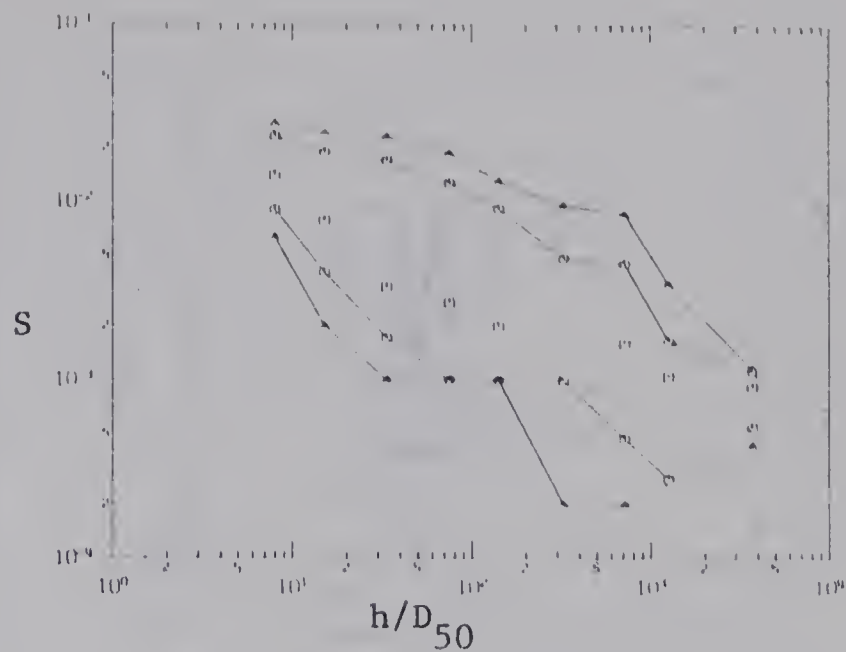
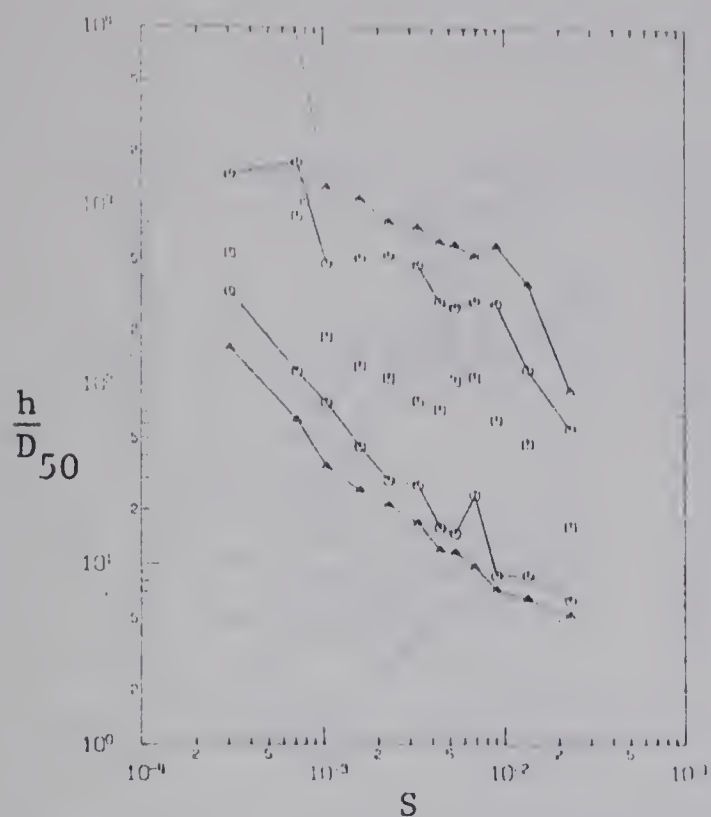


Figure C-7. Joint Distribution Between Experimental Values of  $S$  and  $h/D_{50}$

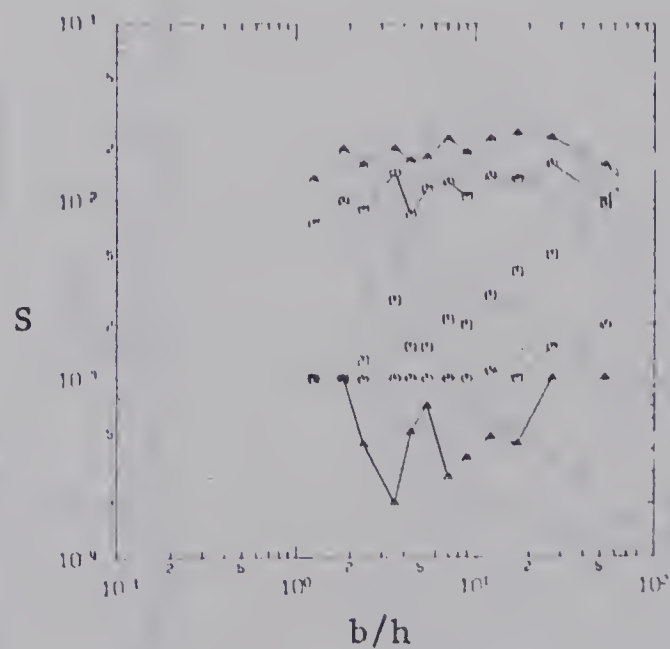
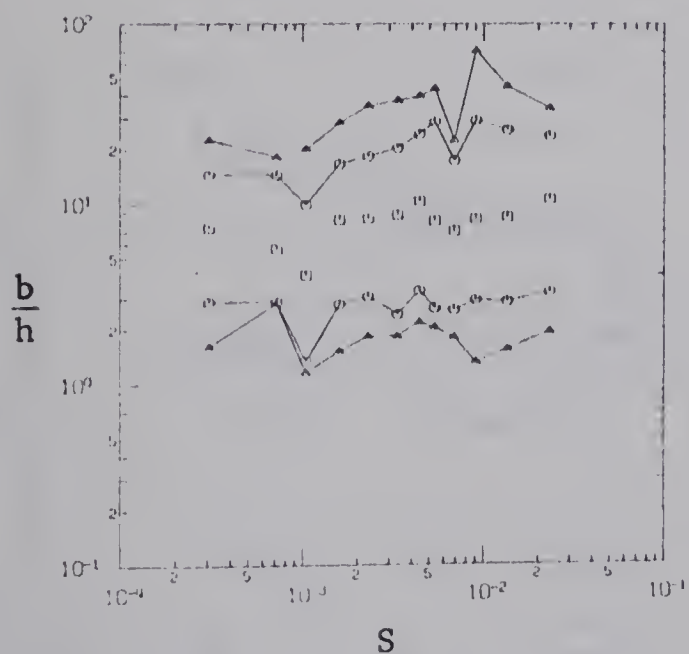


Figure C-8. Joint Distribution Between Experimental Values of  $S$  and  $b/h$





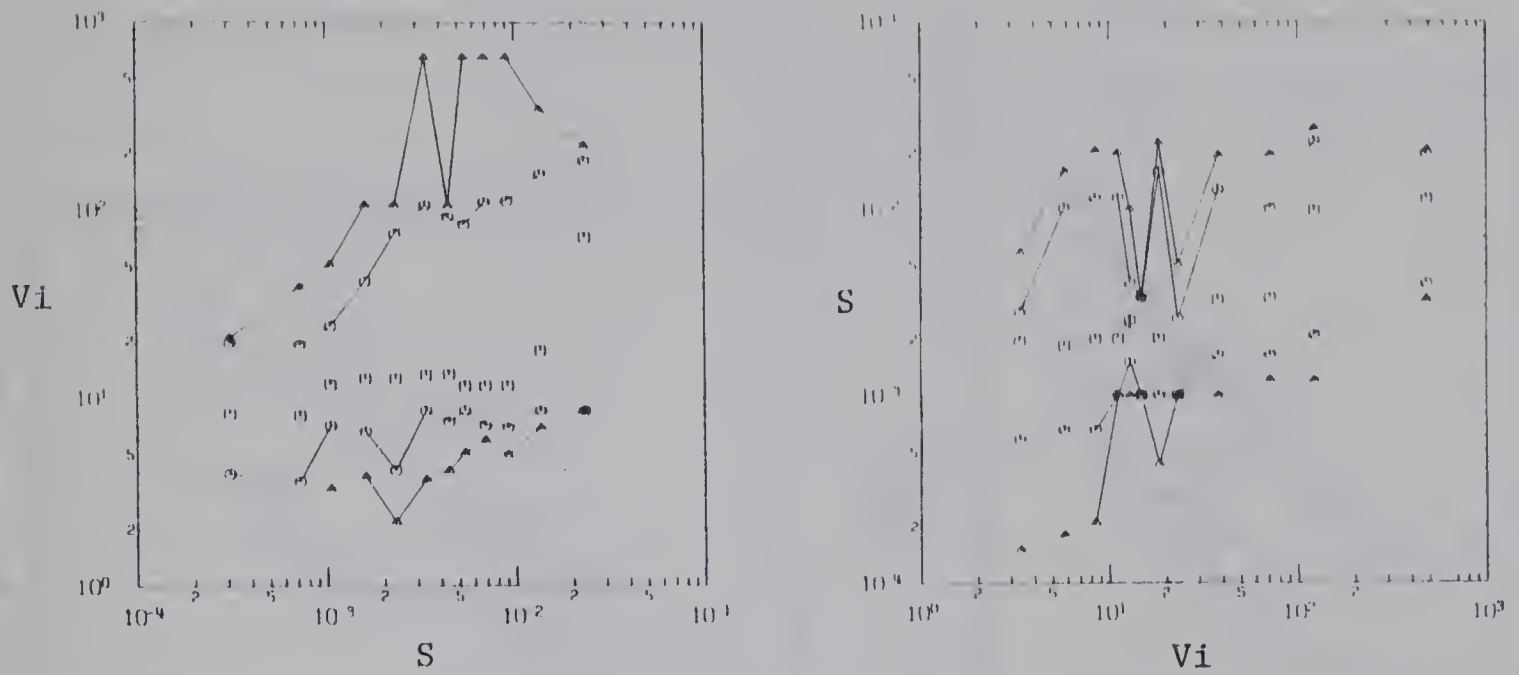


Figure C-9. Joint Distribution Between Experimental Values of  $S$  and  $V_i$

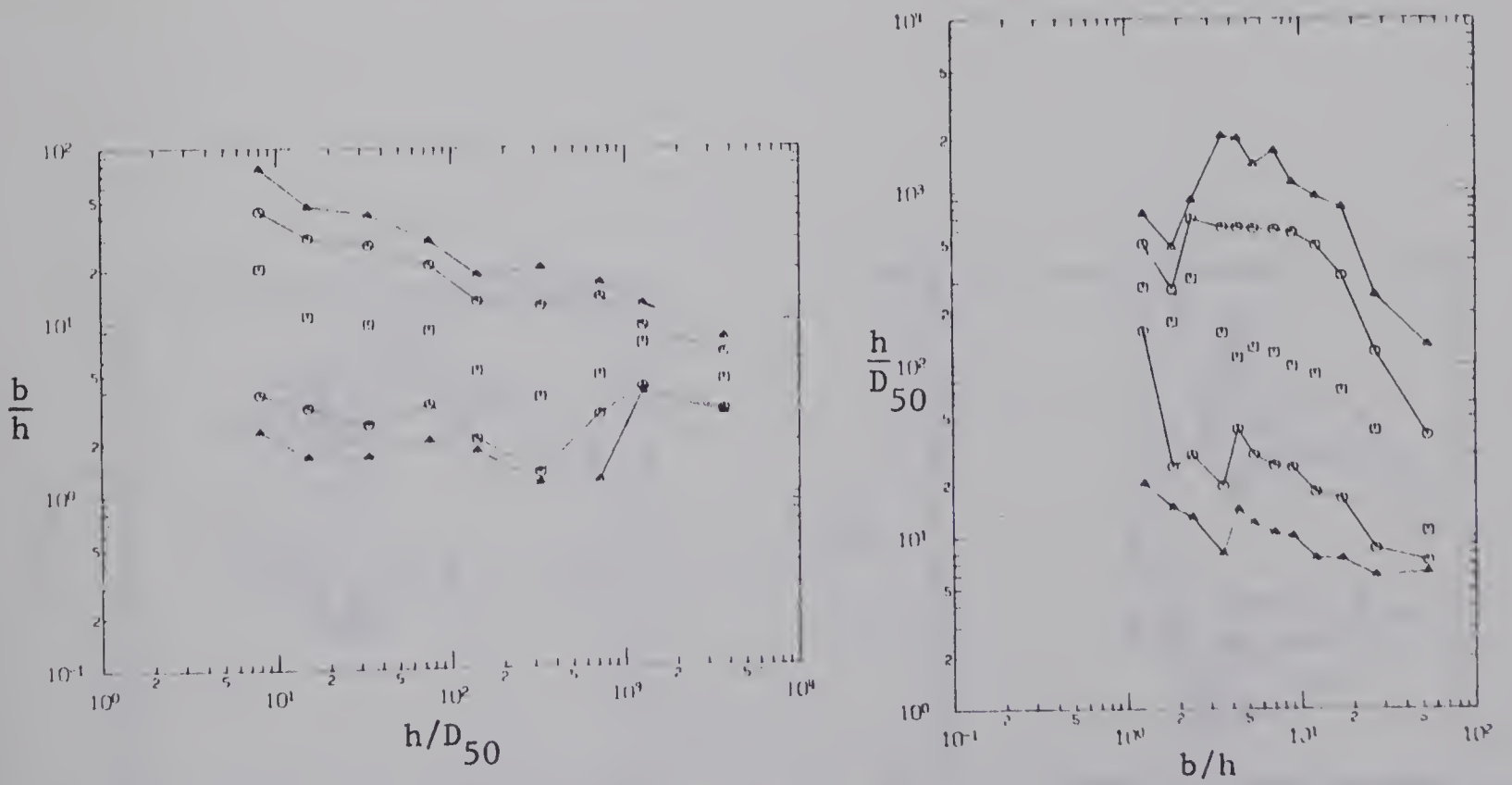


Figure C-10. Joint Distribution Between Experimental Values of  $h/D_{50}$  and  $b/h$



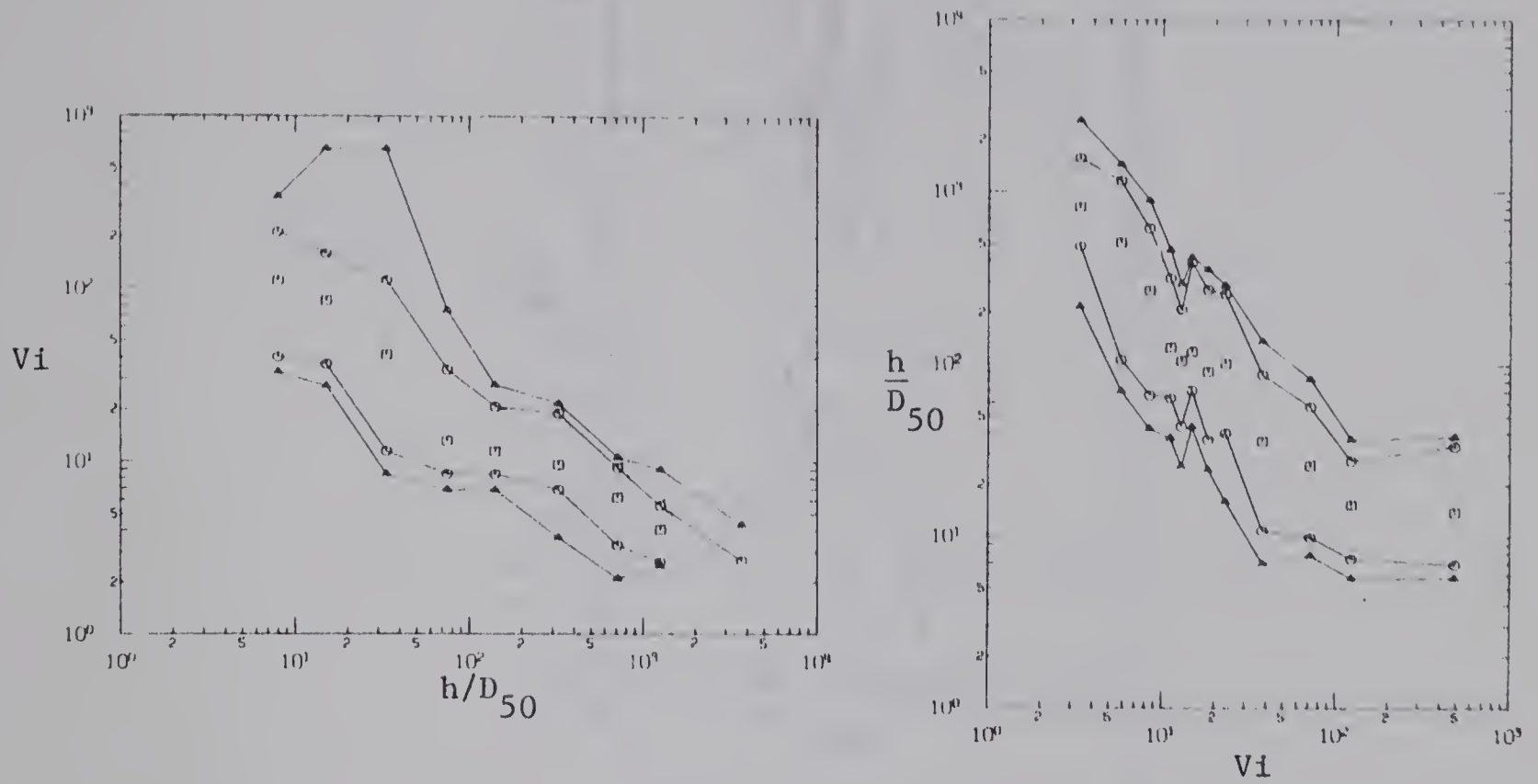


Figure C-11. Joint Distribution Between Experimental Values of  $h/D_{50}$  and  $Vi$

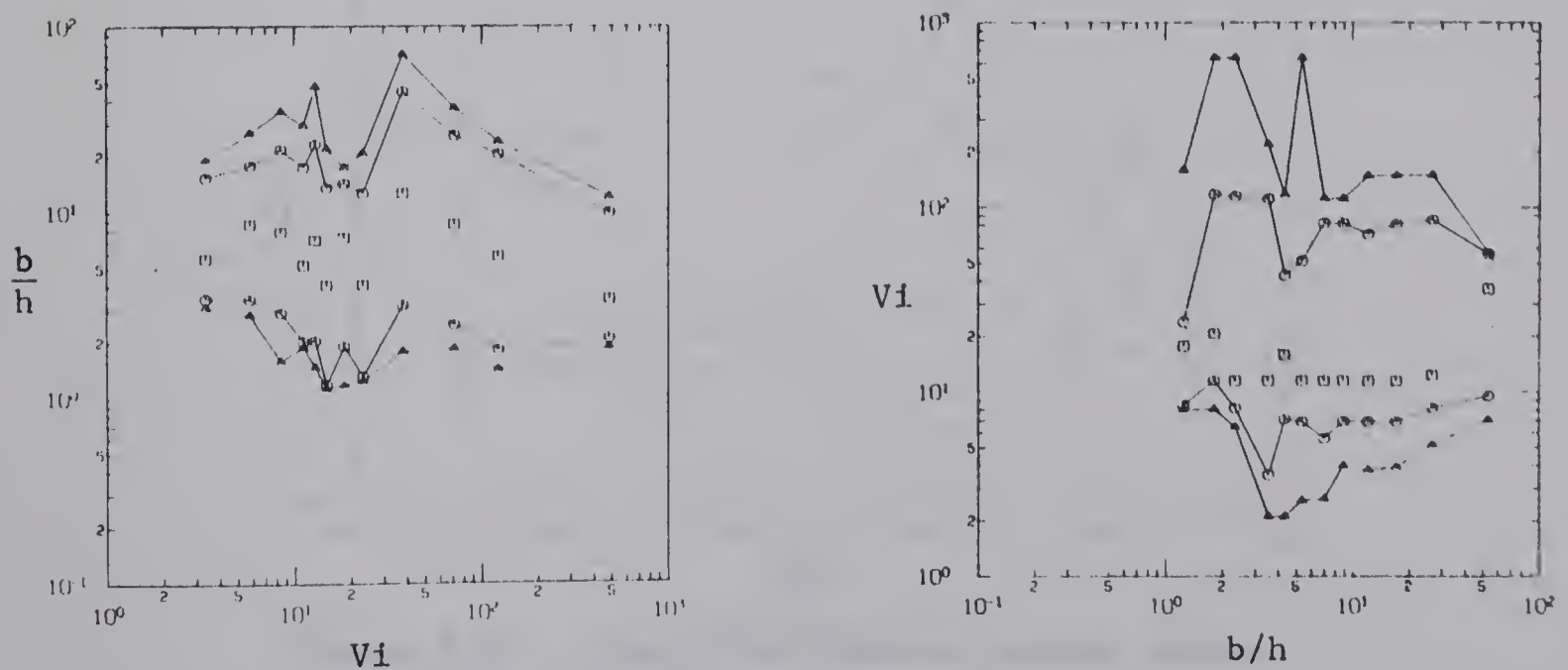


Figure C-12. Joint Distribution Between Experimental Values of  $Vi$  and  $b/h$





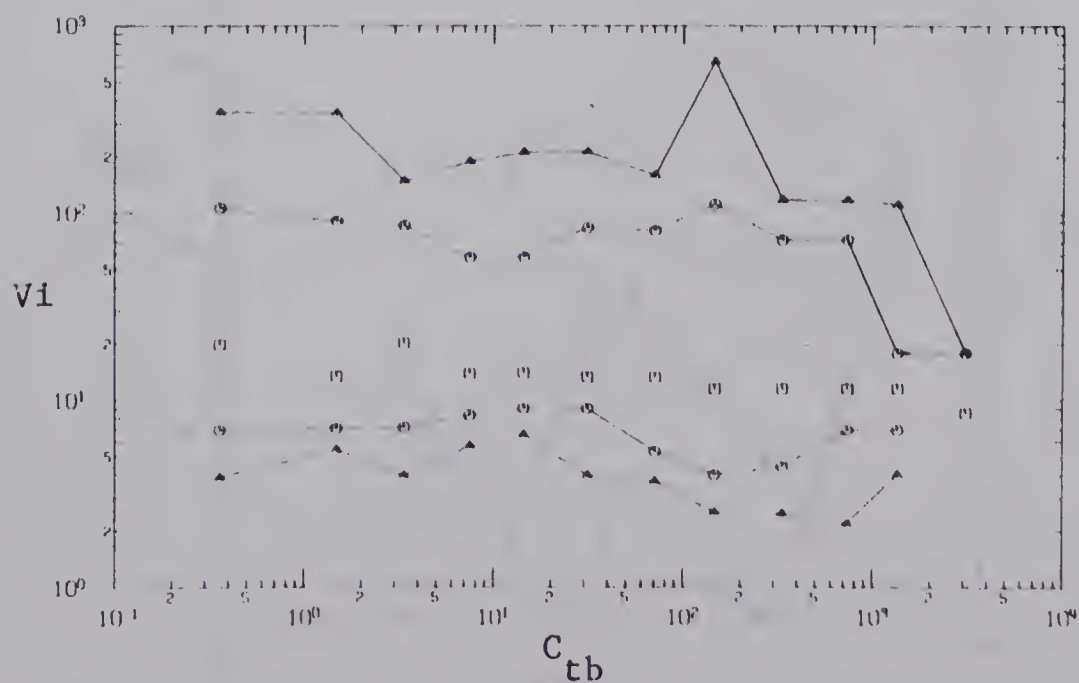
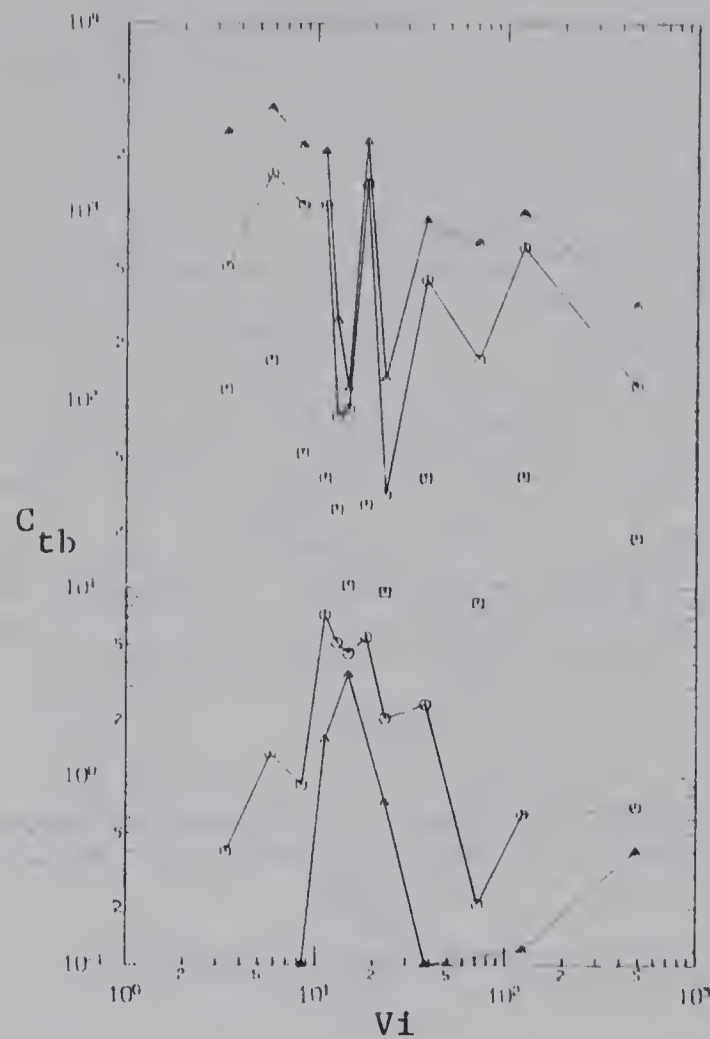


Figure C-13. Joint Distribution Between Experimental Values of  $V_1$  and  $C_{tb}$



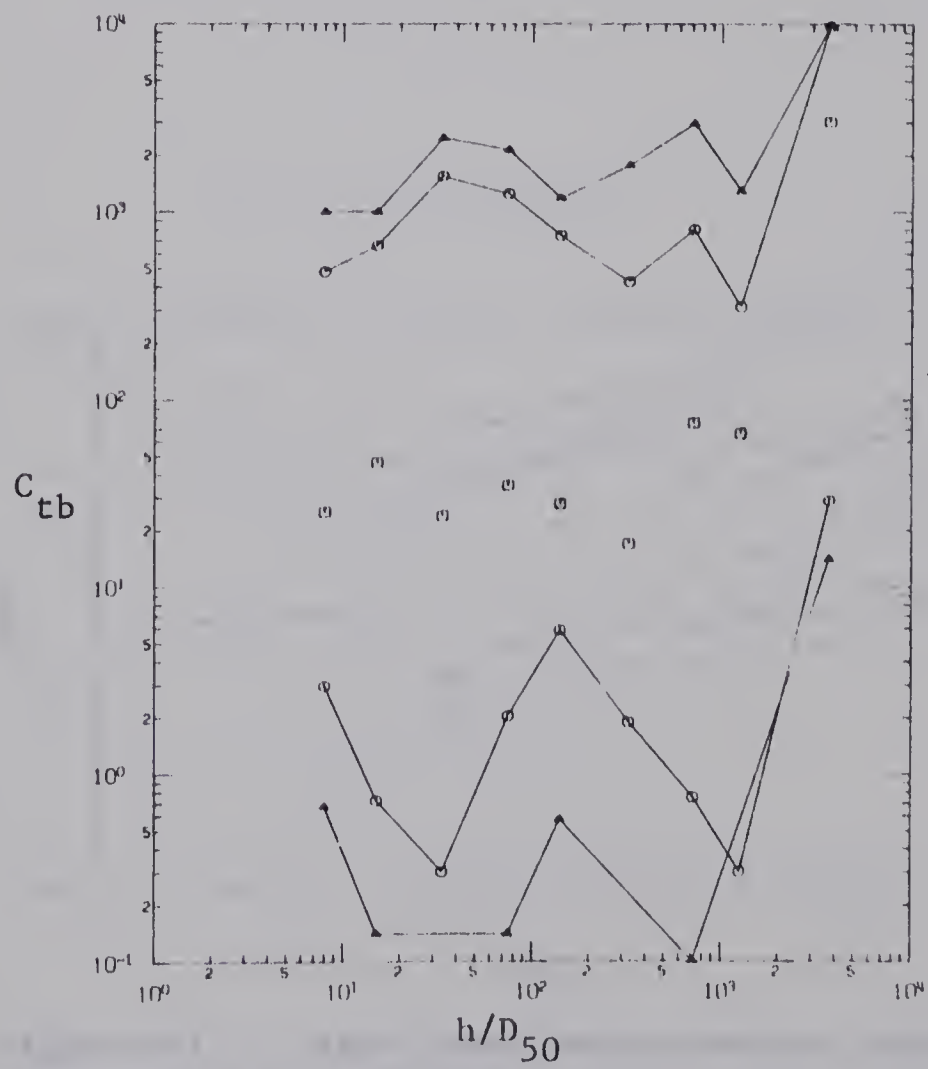
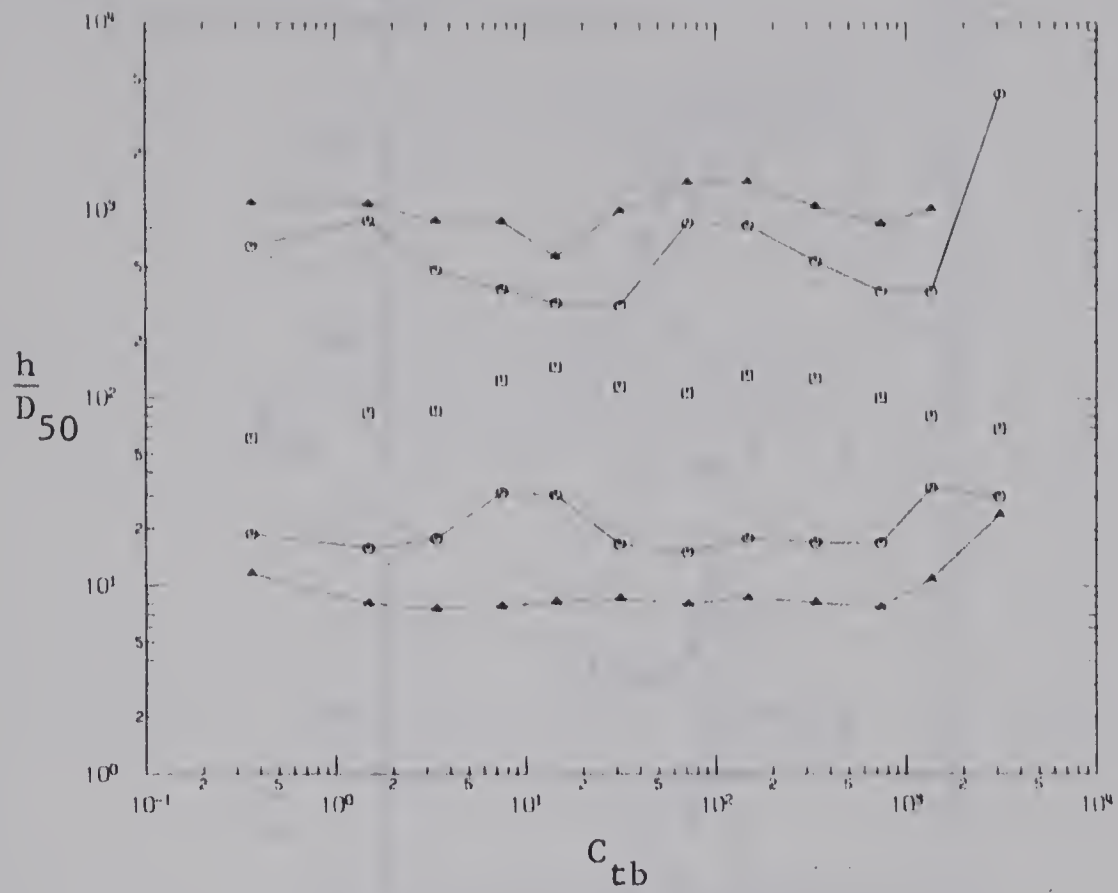


Figure 6-14. Joint Distribution Between Experimental Values of  $C_{tb}$  and  $h/D_{50}$



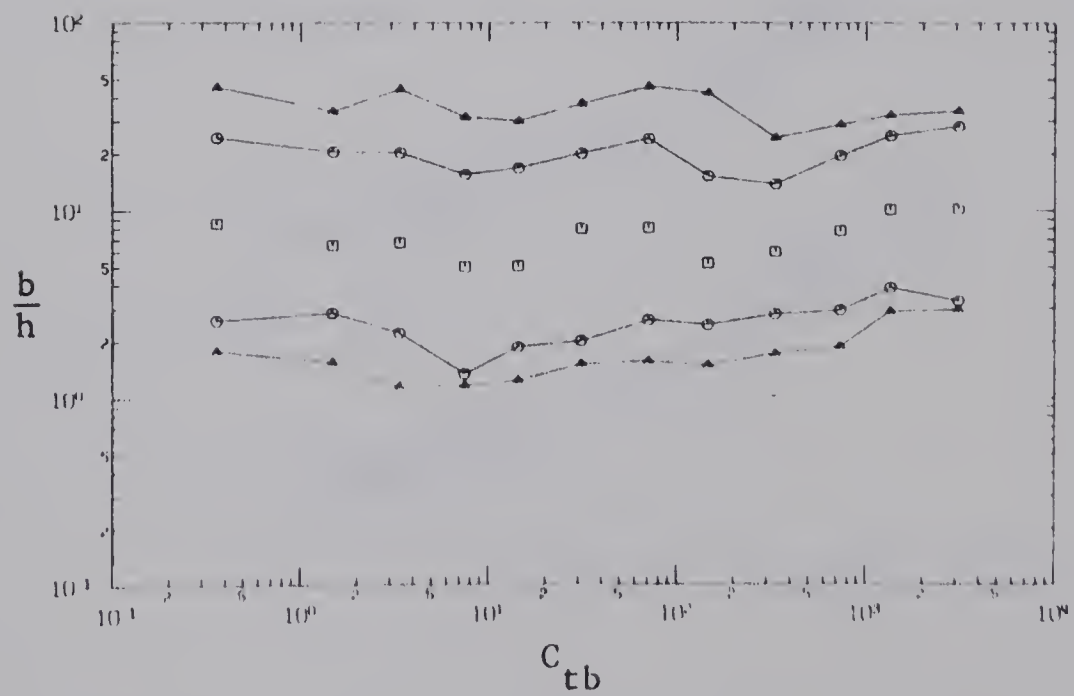
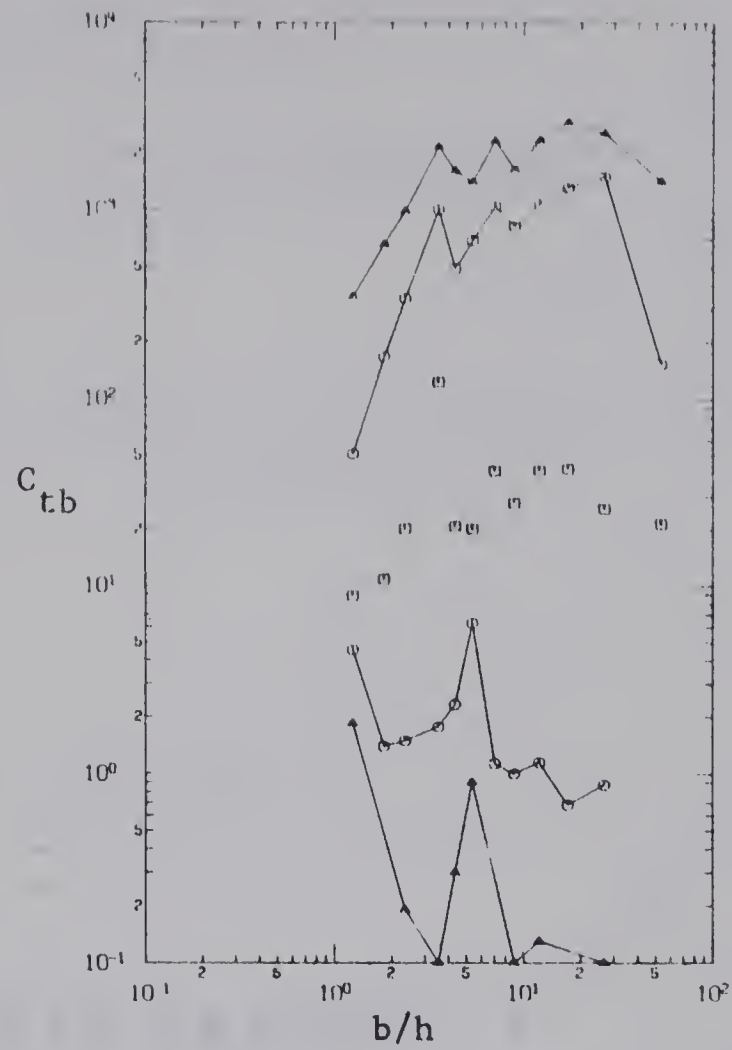


Figure 6-15. Joint Distribution Between Experimental Values of  $C_{tb}$  and  $b/h$





## A P P E N D I X     D

### Scatter Diagrams



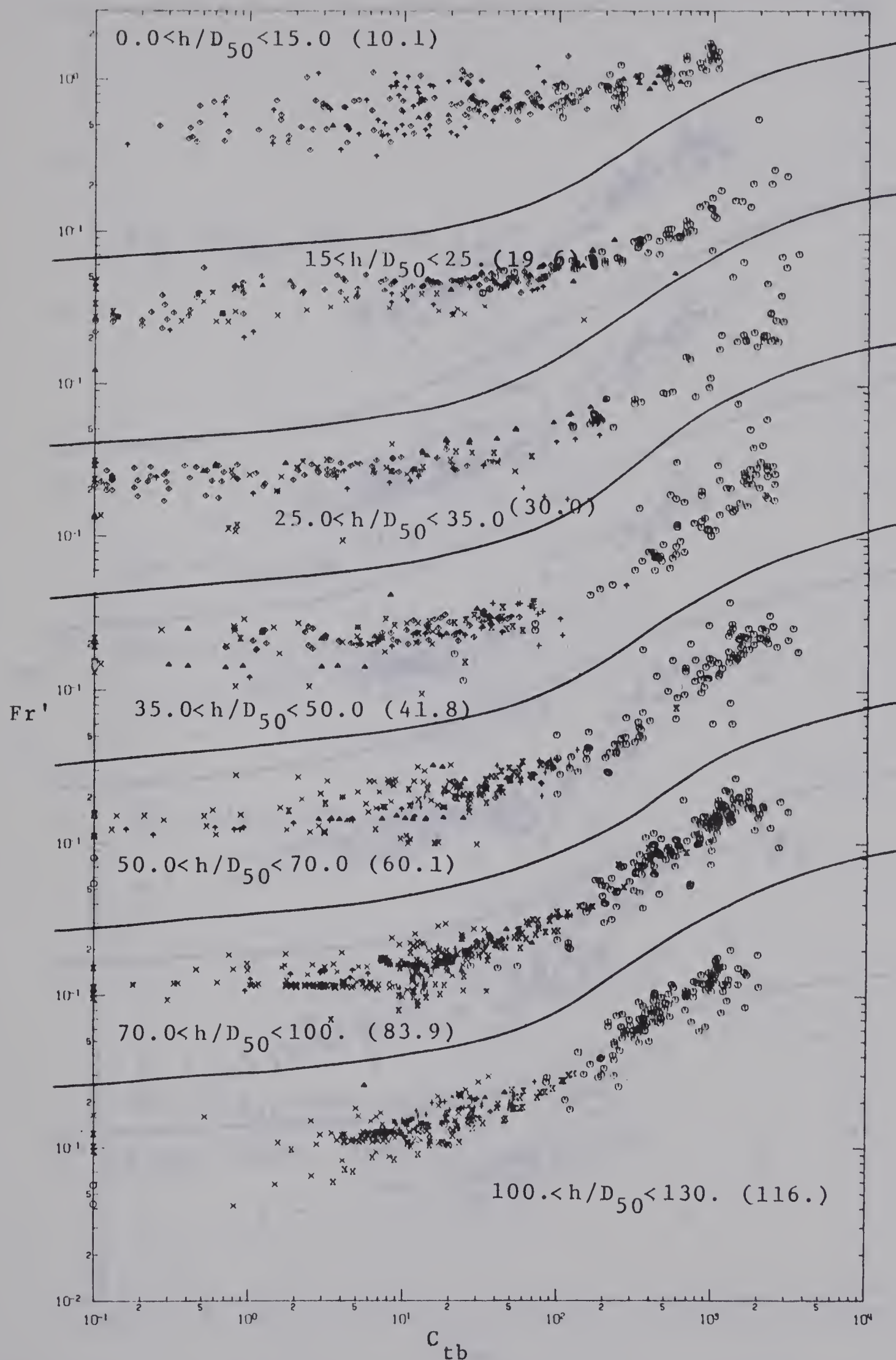


Figure D-1. Variation of  $C_{tb}$  with  $Fr'$  at Different Levels of  $h/D_{50}$





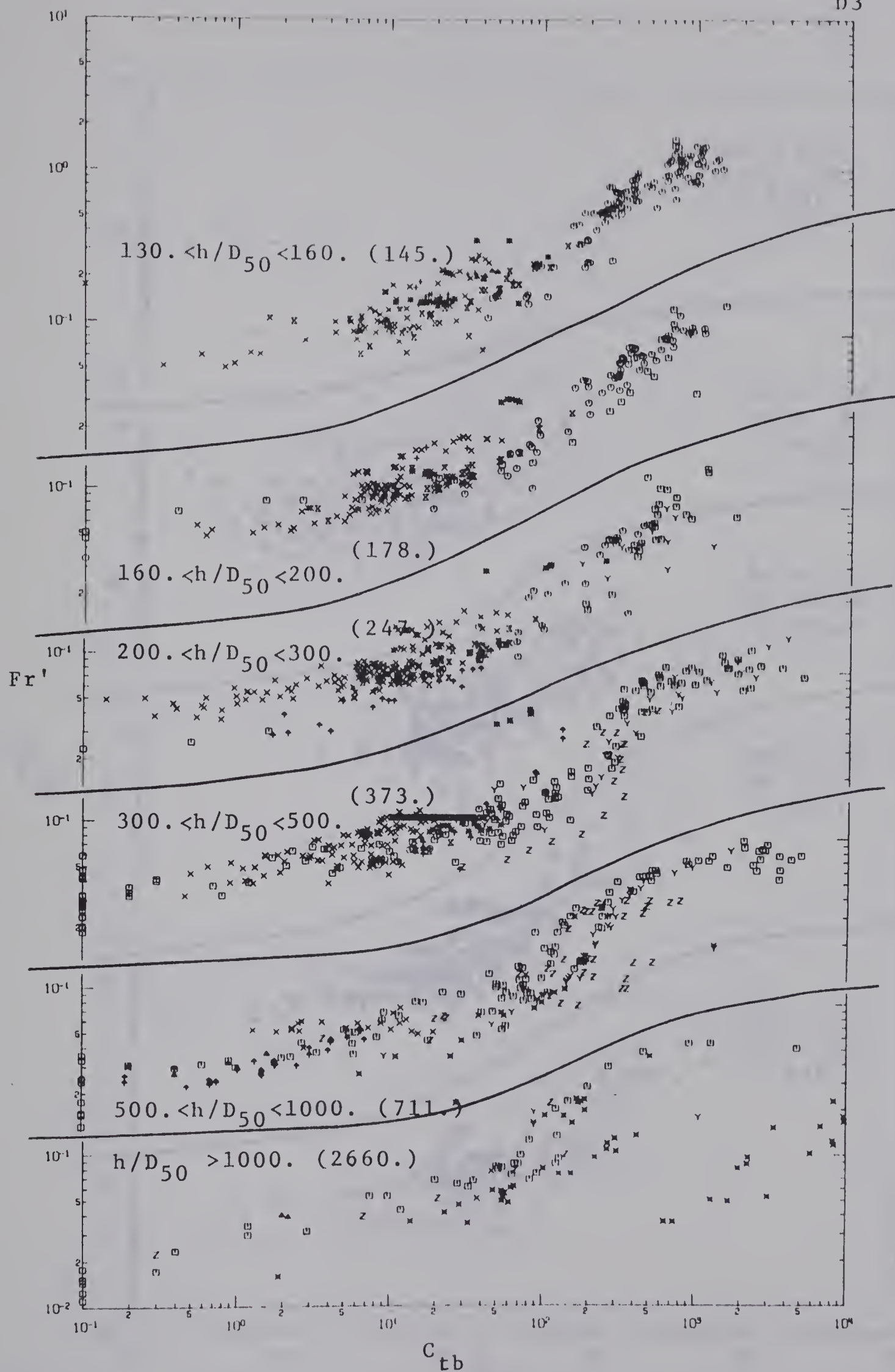


Figure D-1 (Continued)



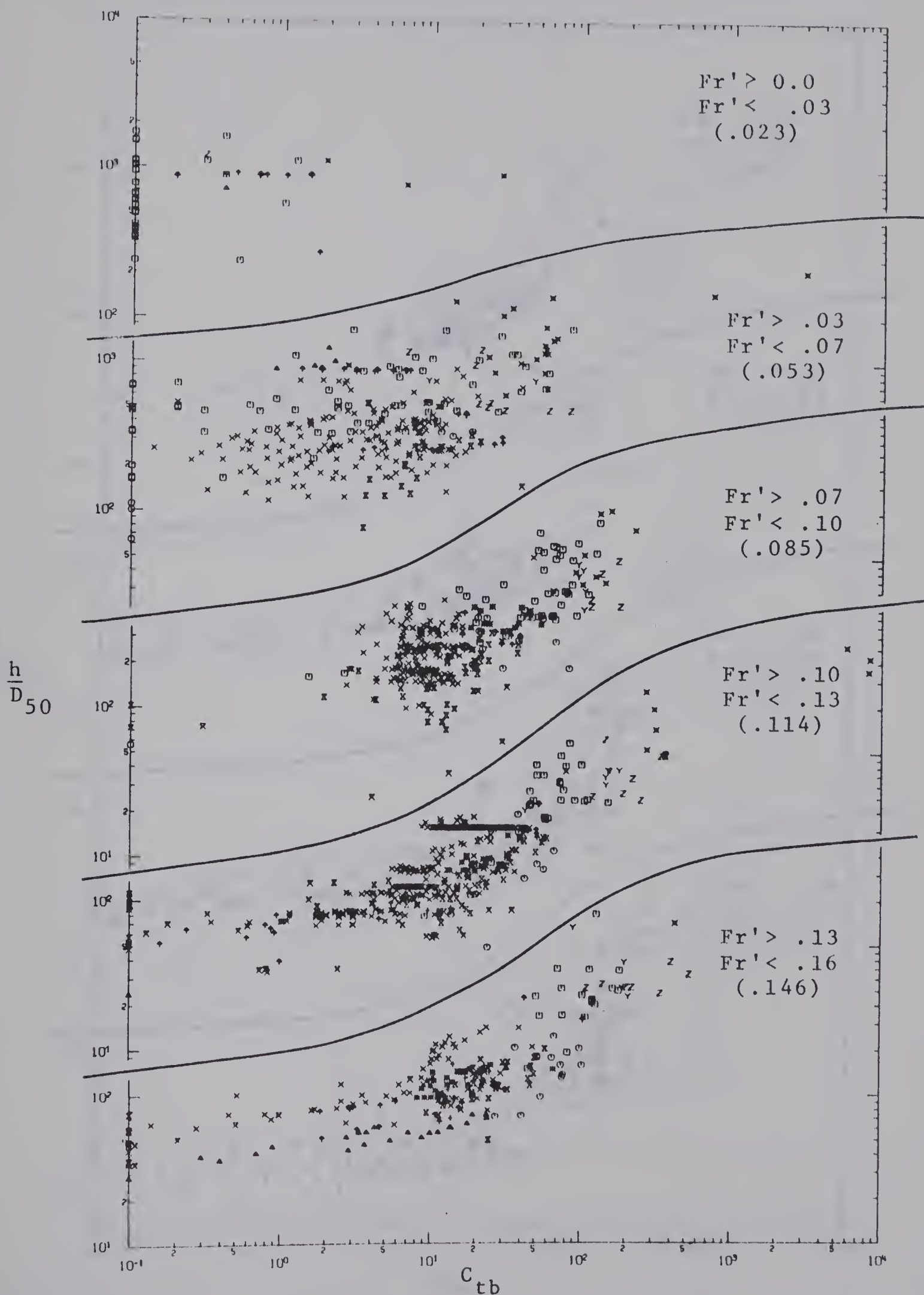


Figure D-2. Variation of  $C_{tb}$  with  $h/D_{50}$  at Different Levels of  $Fr'$





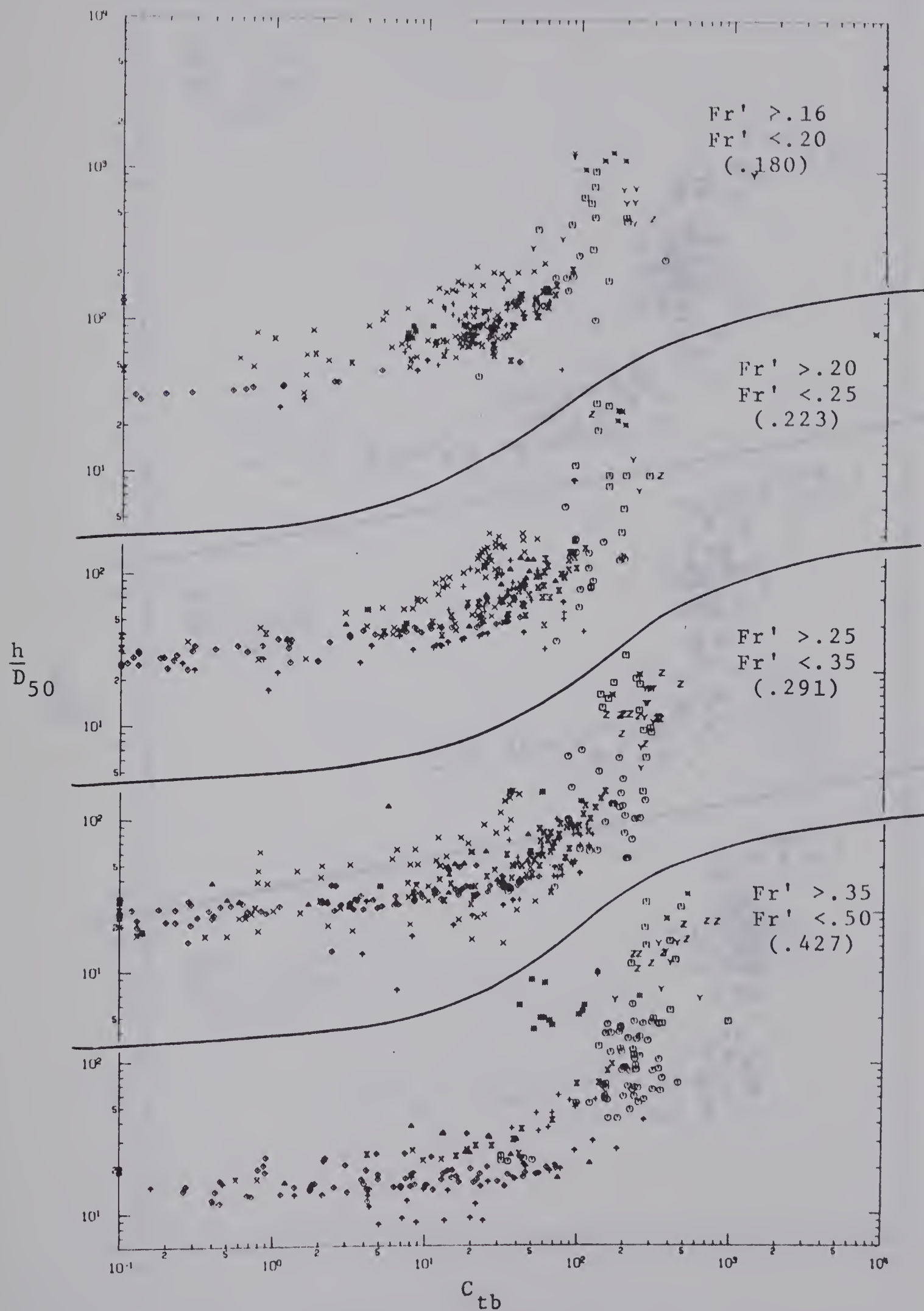


Figure D-2 (Continued)





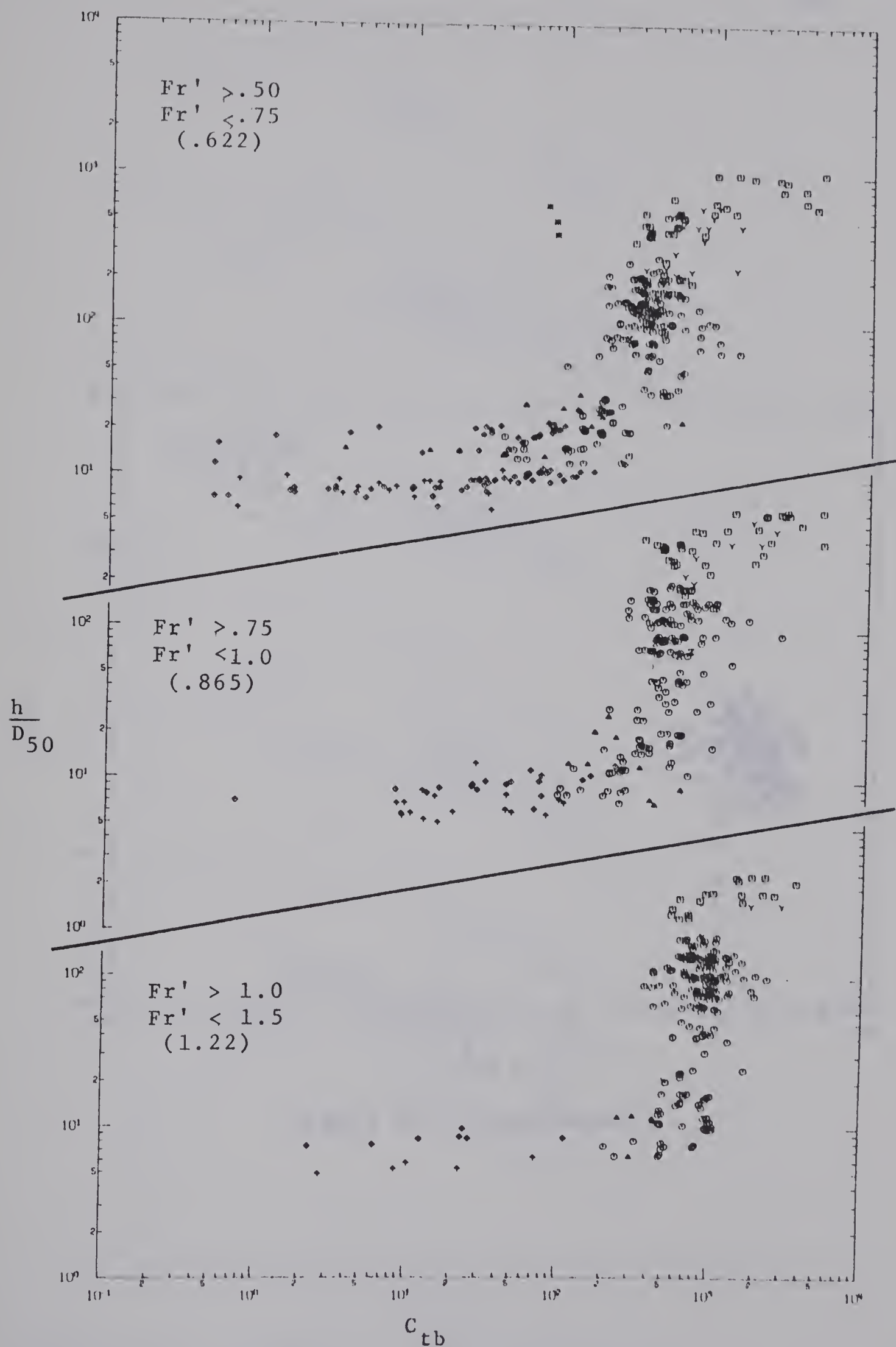


Figure D-2 (Continued)



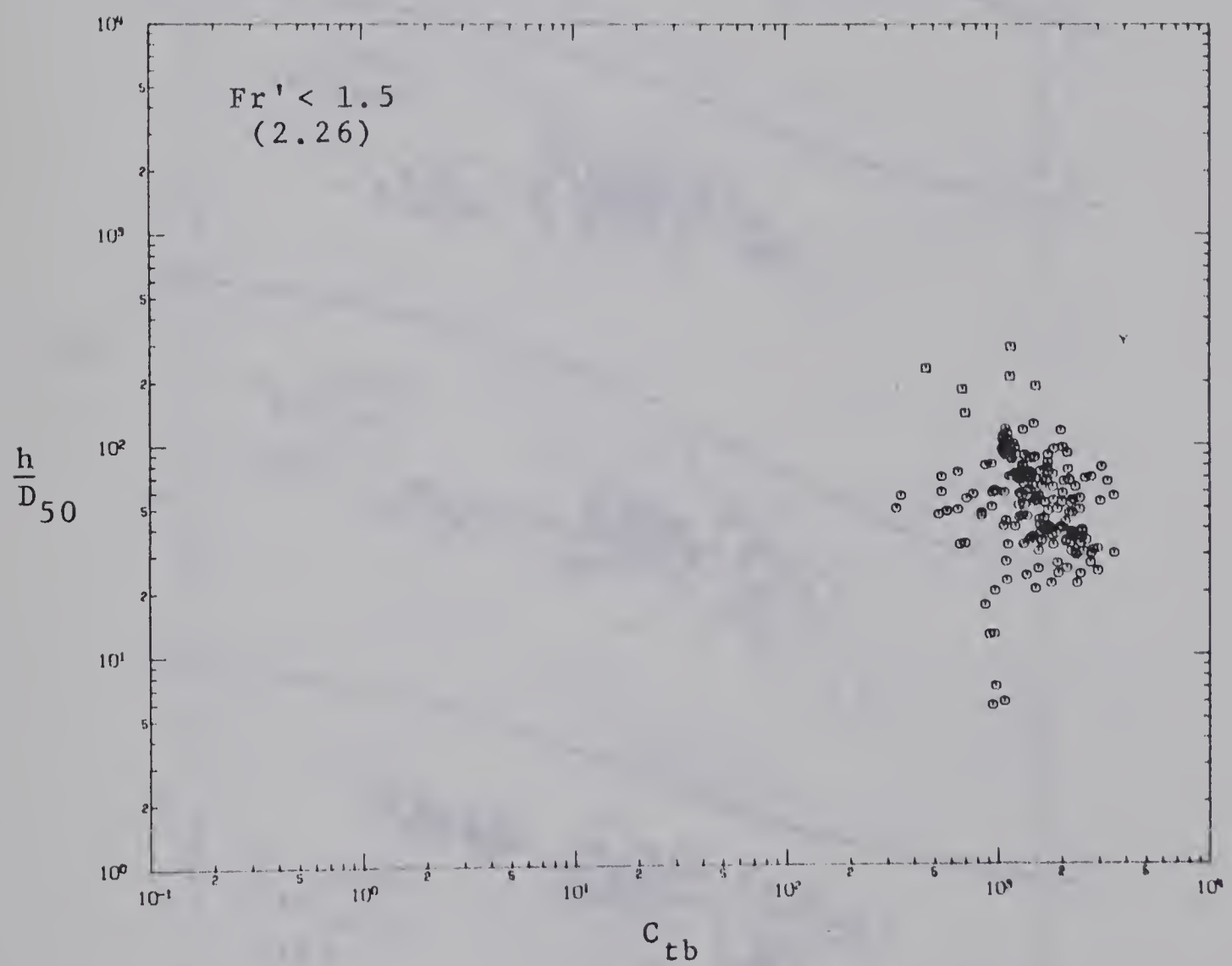


Figure D-2 (Continued)





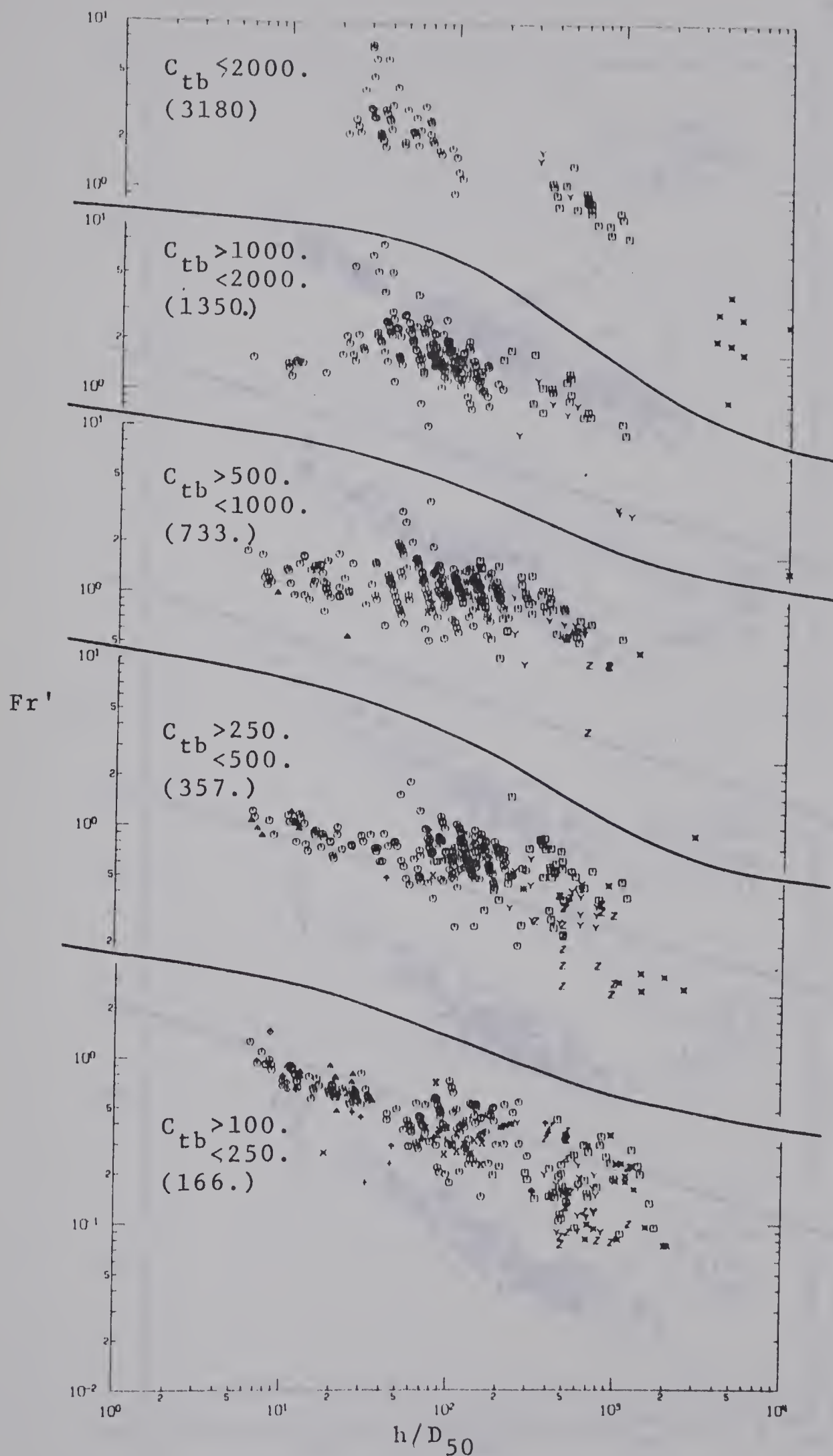


Figure D-3. Variation of  $h/D_{50}$  with  $Fr'$  at Different Levels of  $C_{tb}$



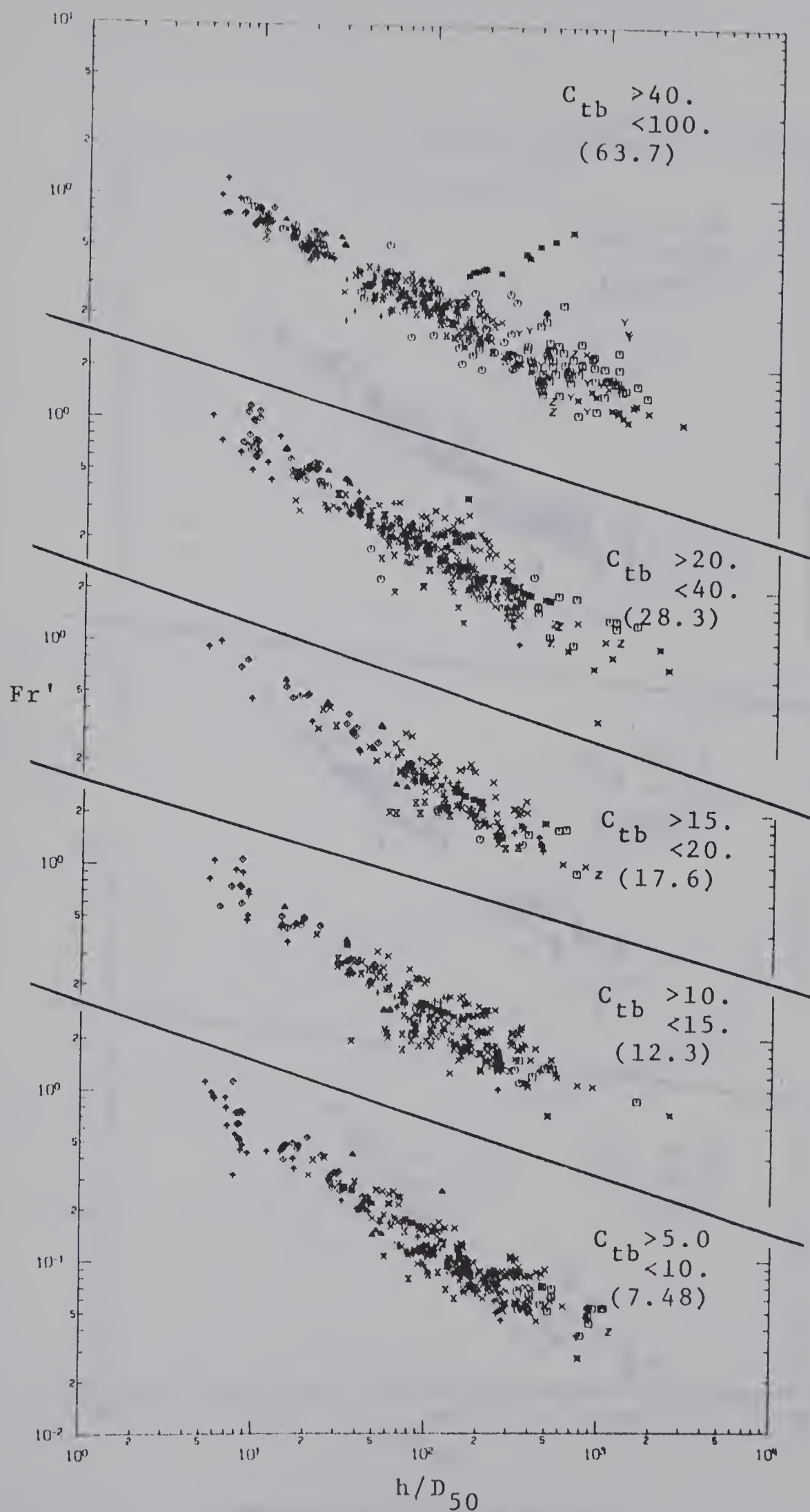


Figure D-3 (Continued)



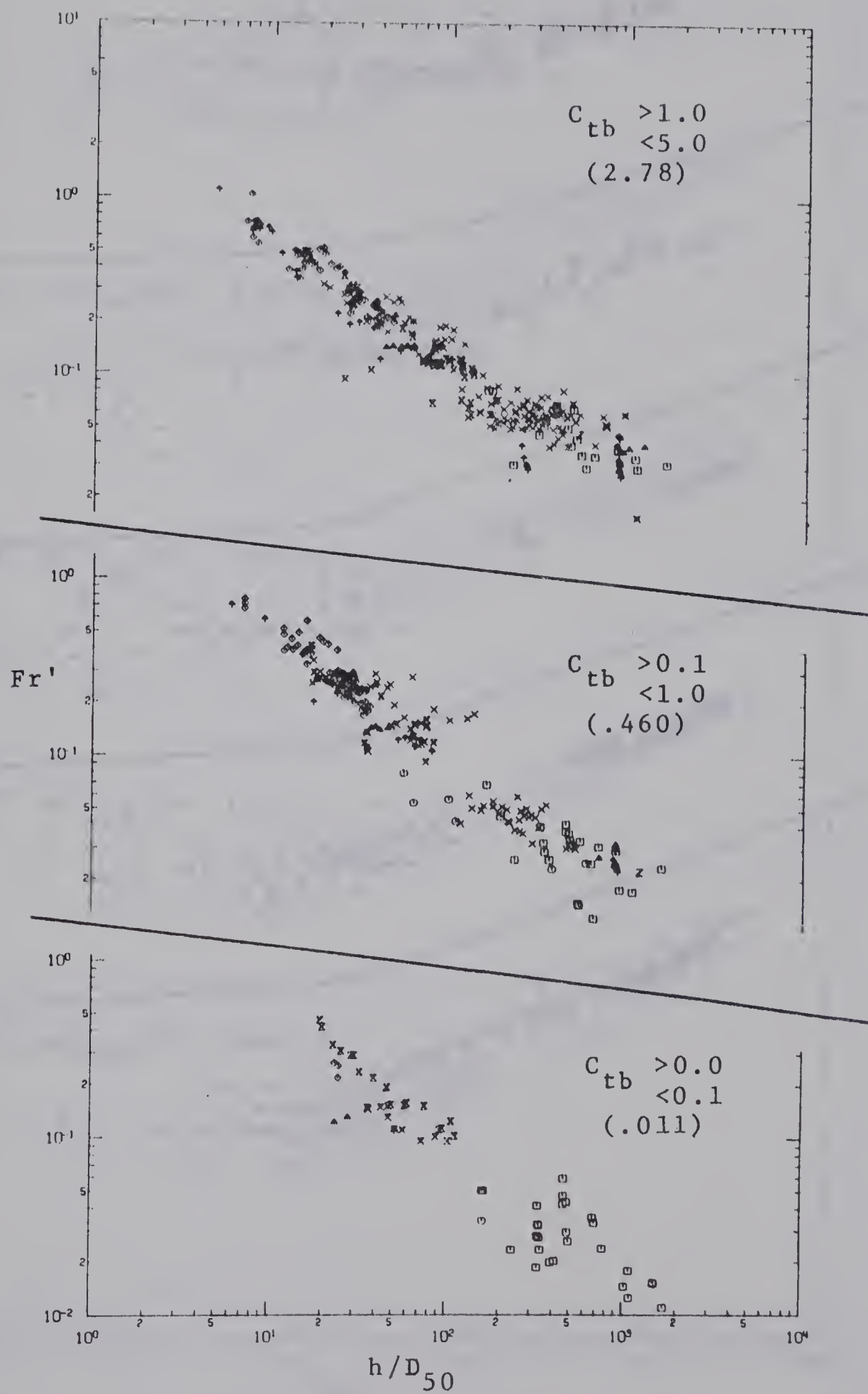


Figure D-3 (Continued)





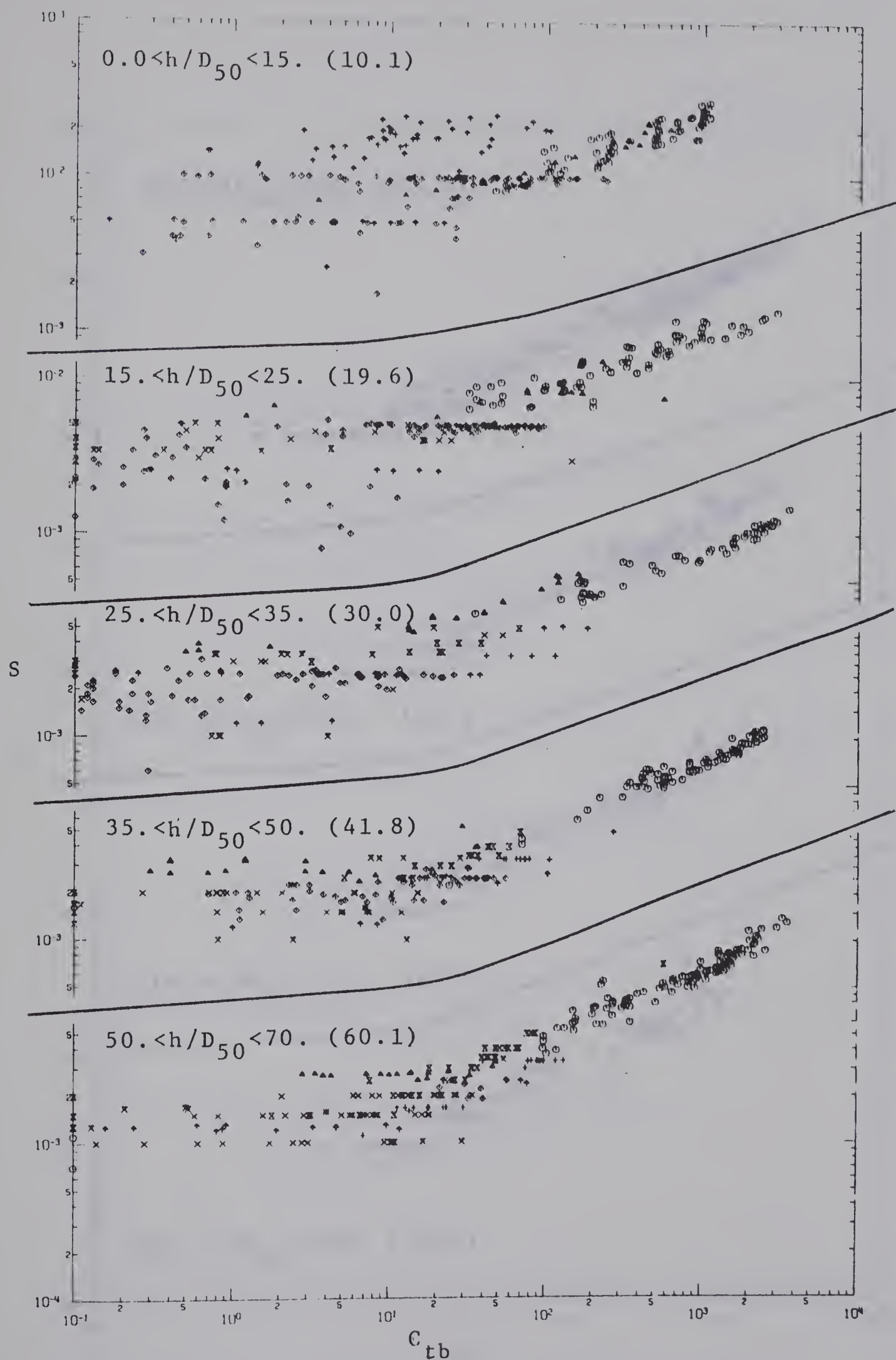


Figure D-4. Variation of  $C_{tb}$  with  $S$  at Different Levels of  $h/D_{50}$



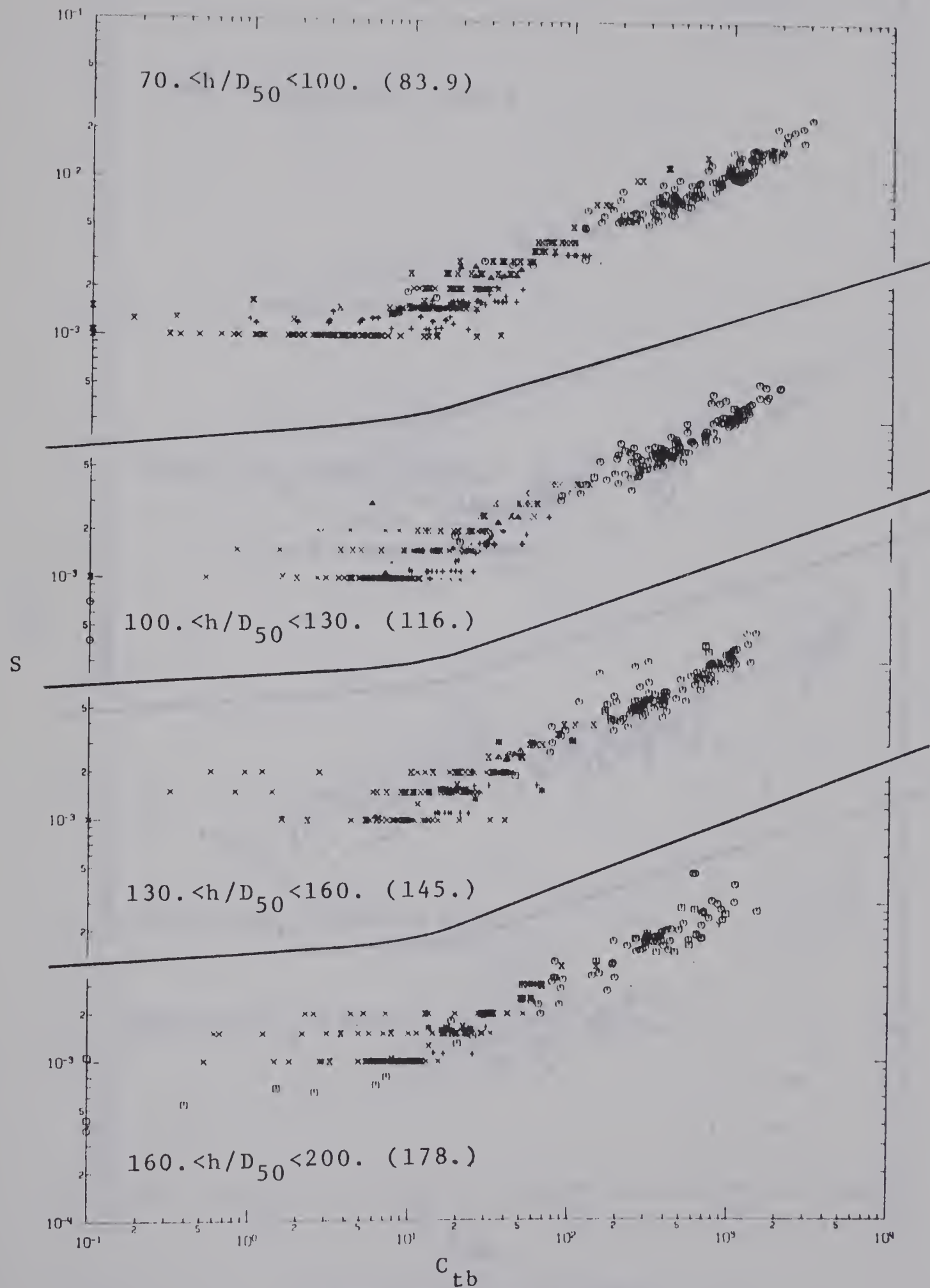


Figure D-4 (Continued)





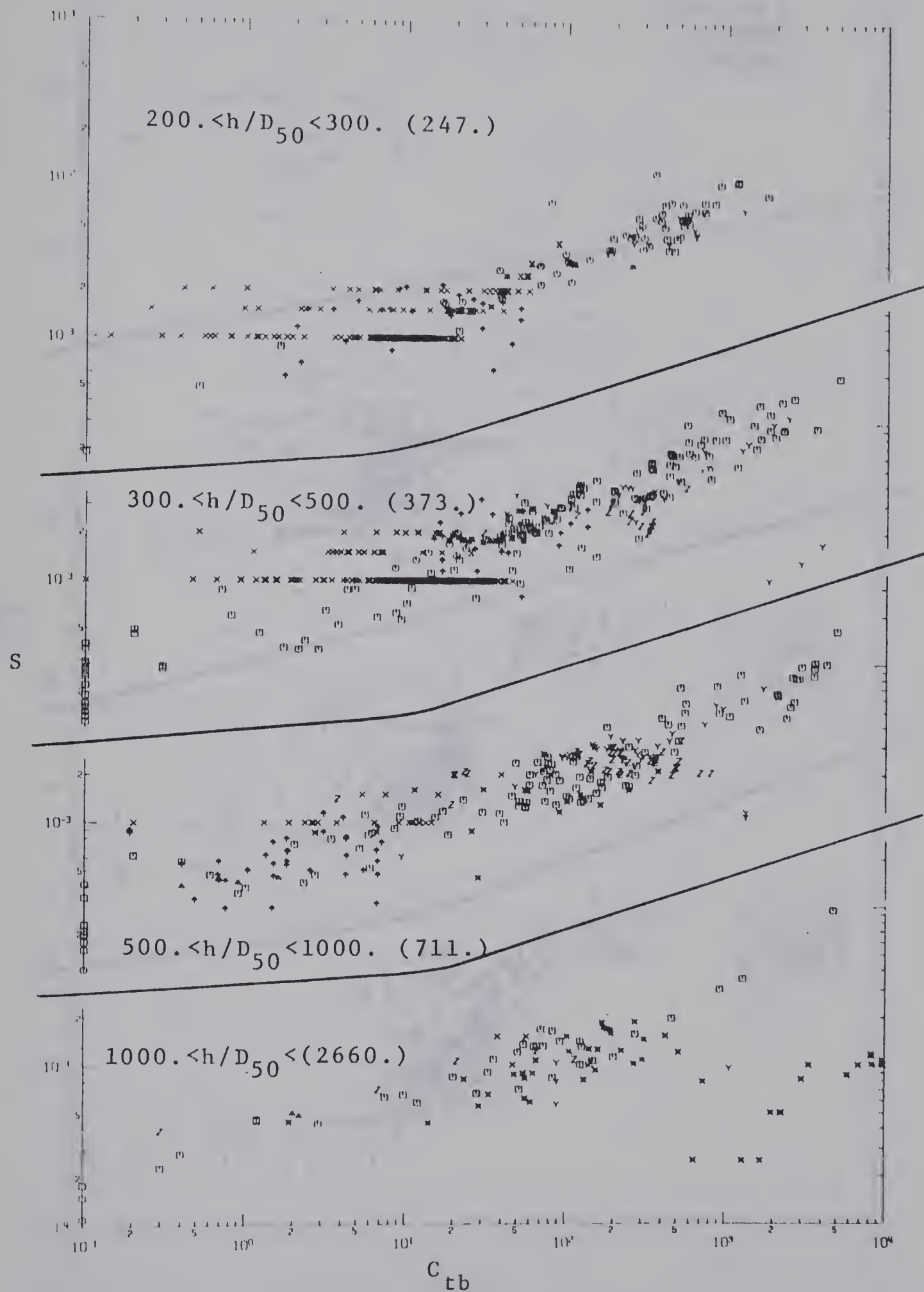


Figure D-4 (Continued)



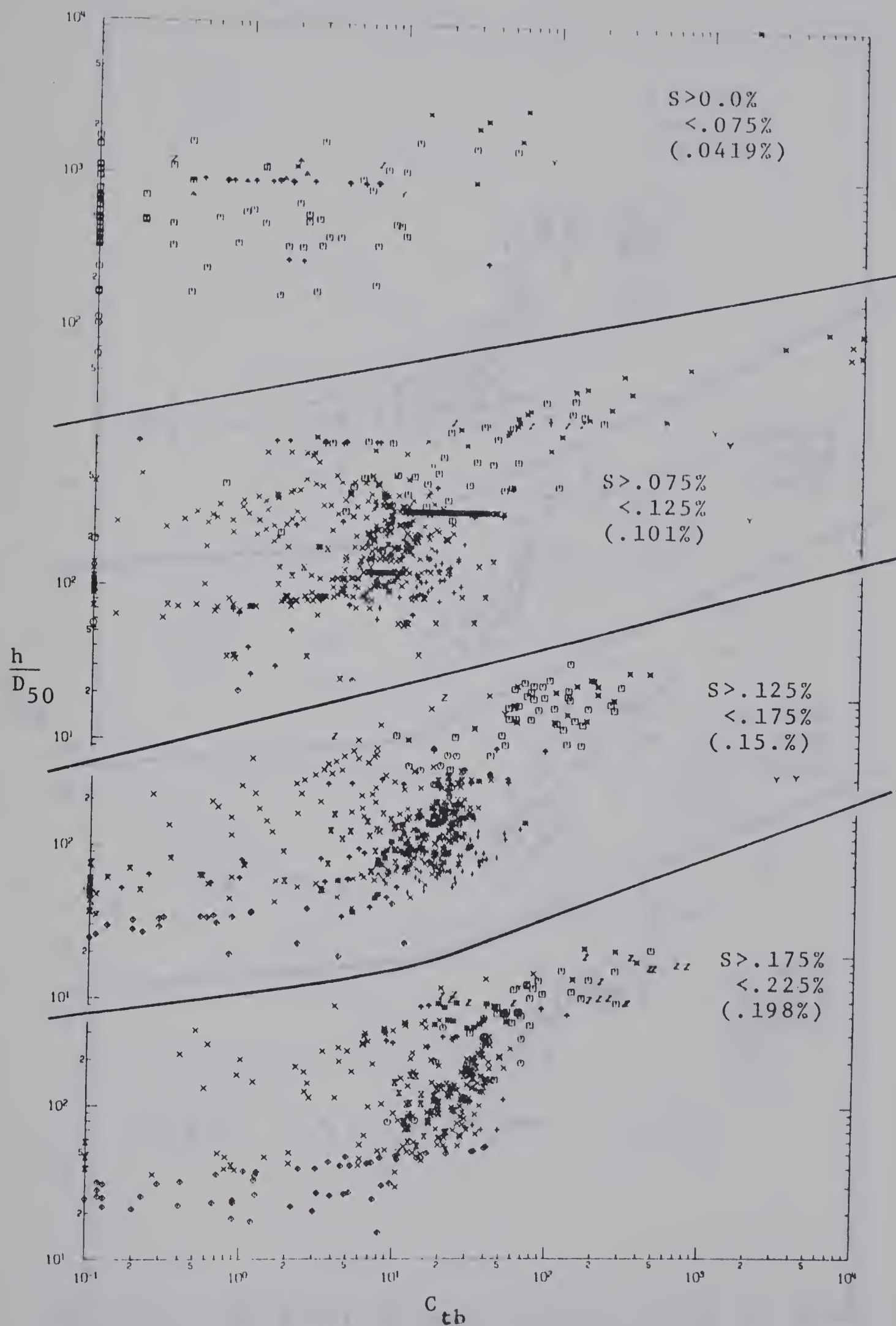


Figure D-5. Variation of  $C_{tb}$  with  $h/D_{50}$  at Different Levels of  $S$



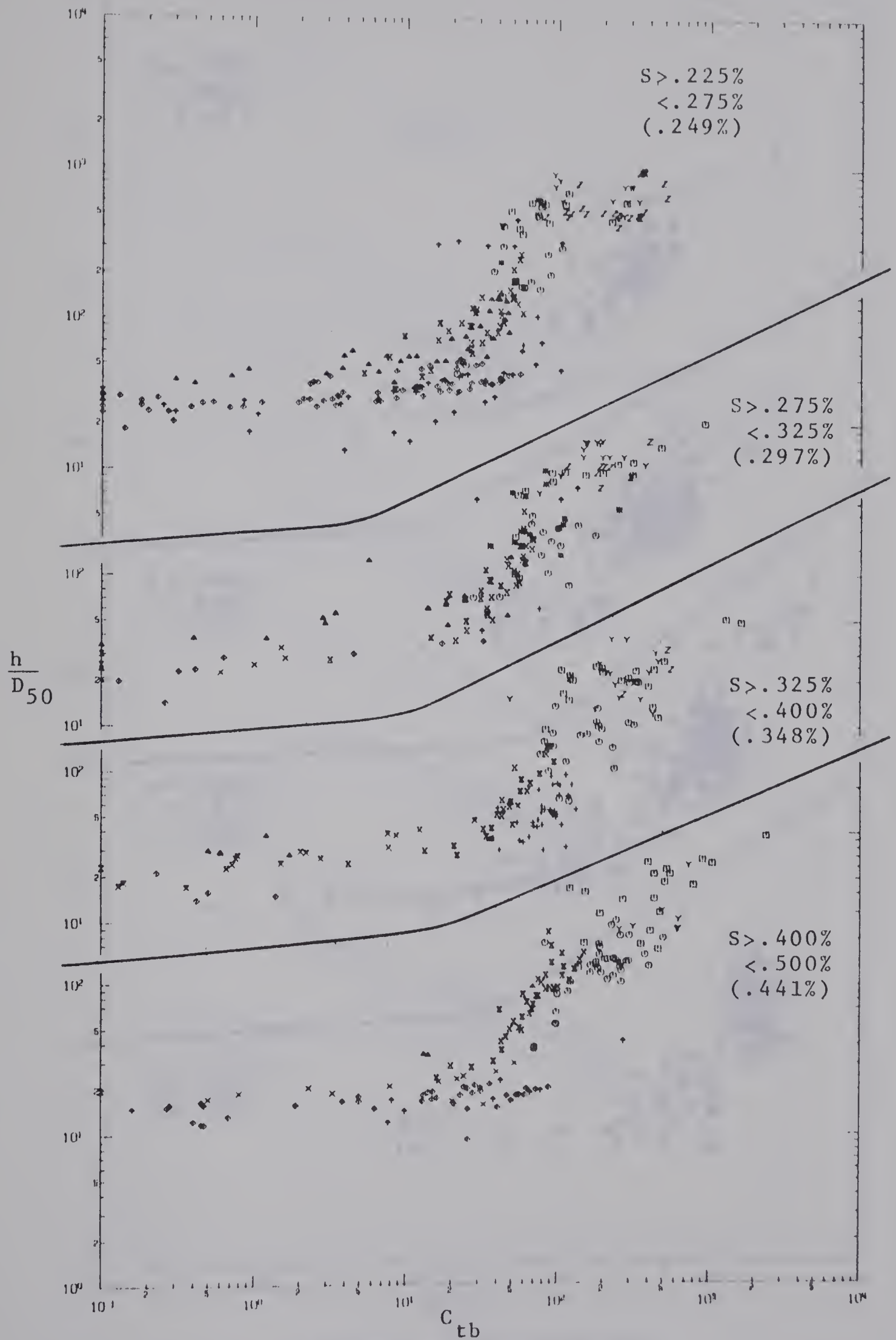


Figure D-5 (Continued)





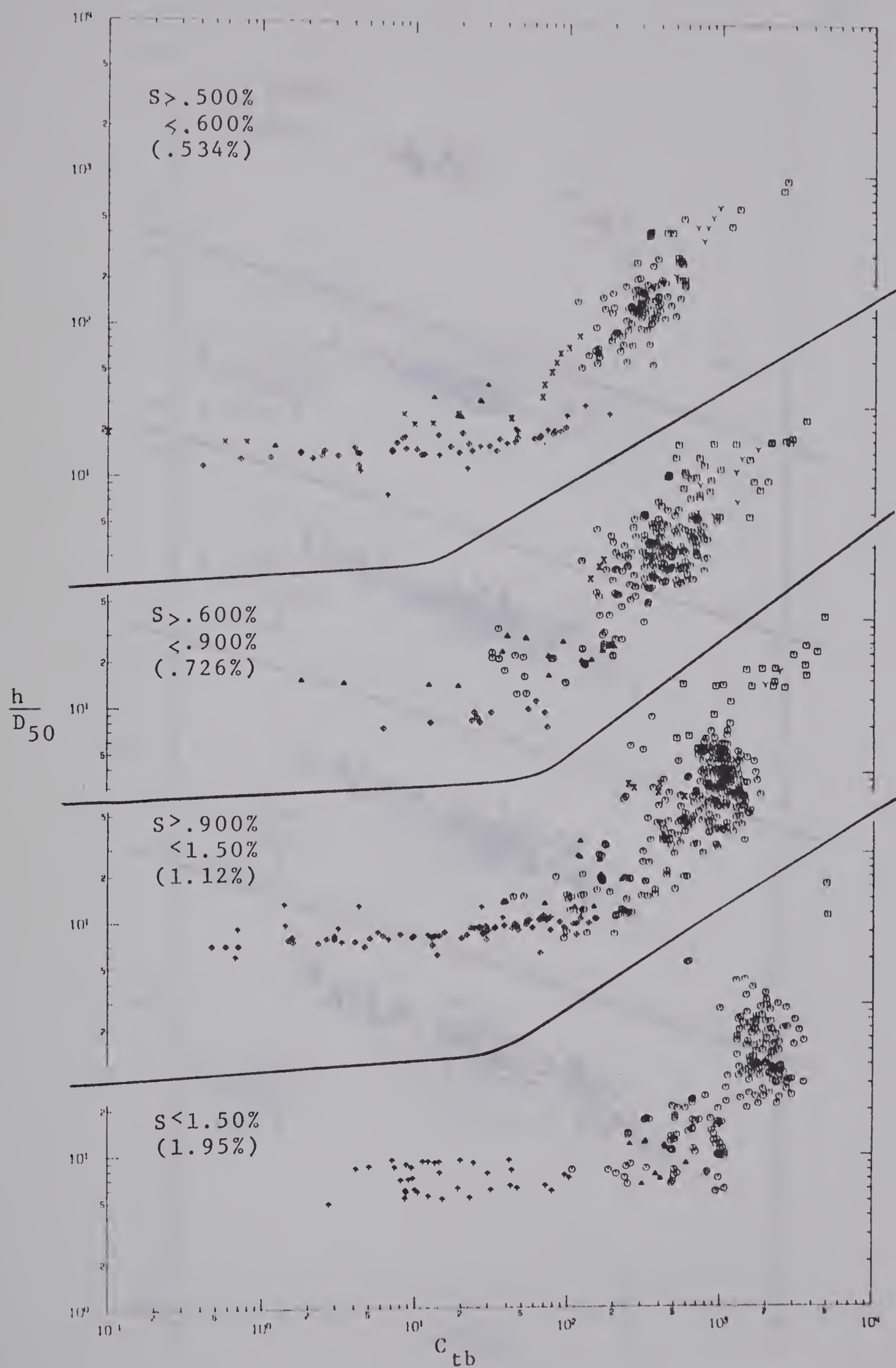


Figure D-5 (Continued)



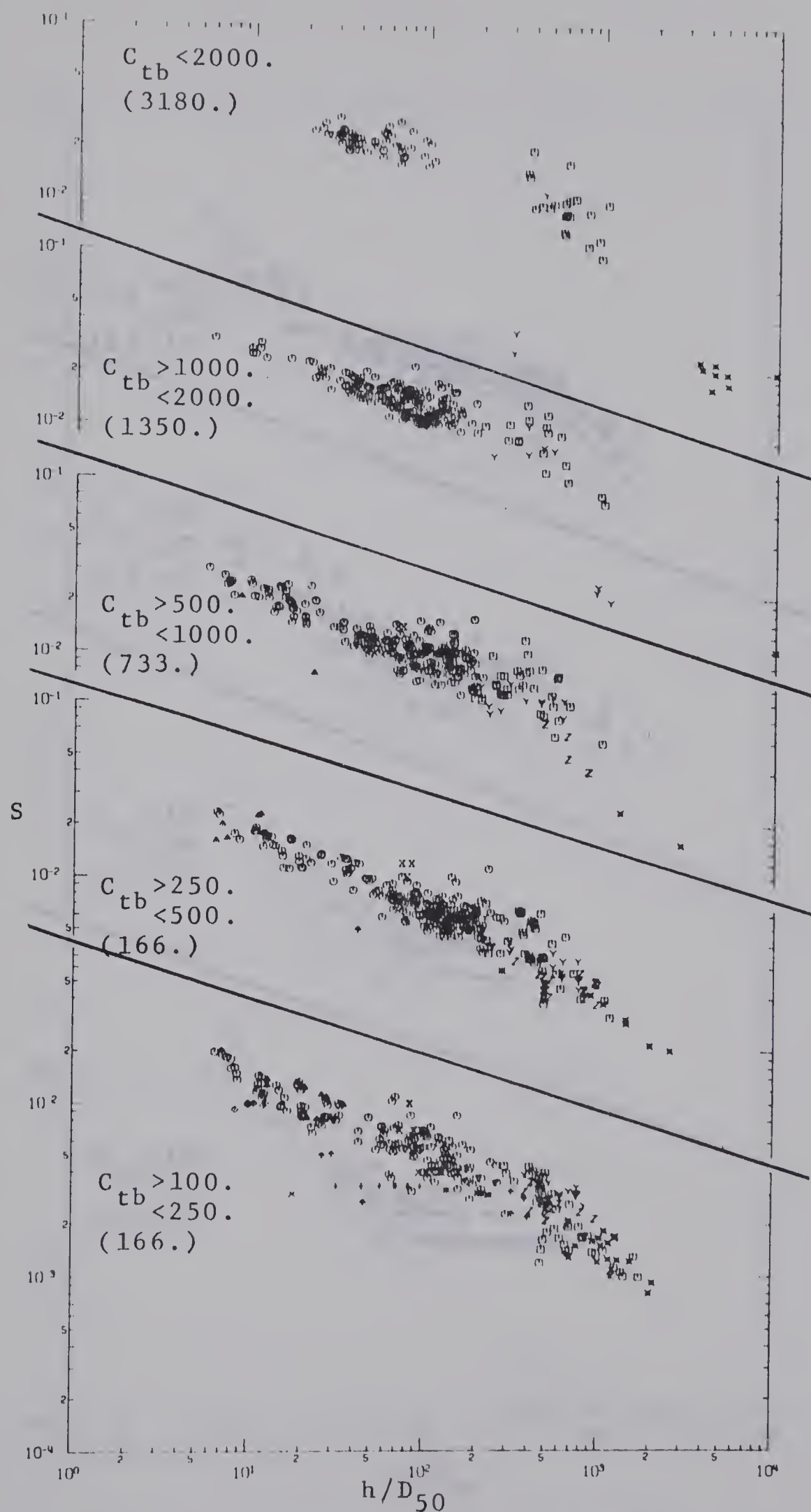


Figure D-6. Variation of  $h/D_{50}$  with  $S$  at Different Level of  $C_{tb}$





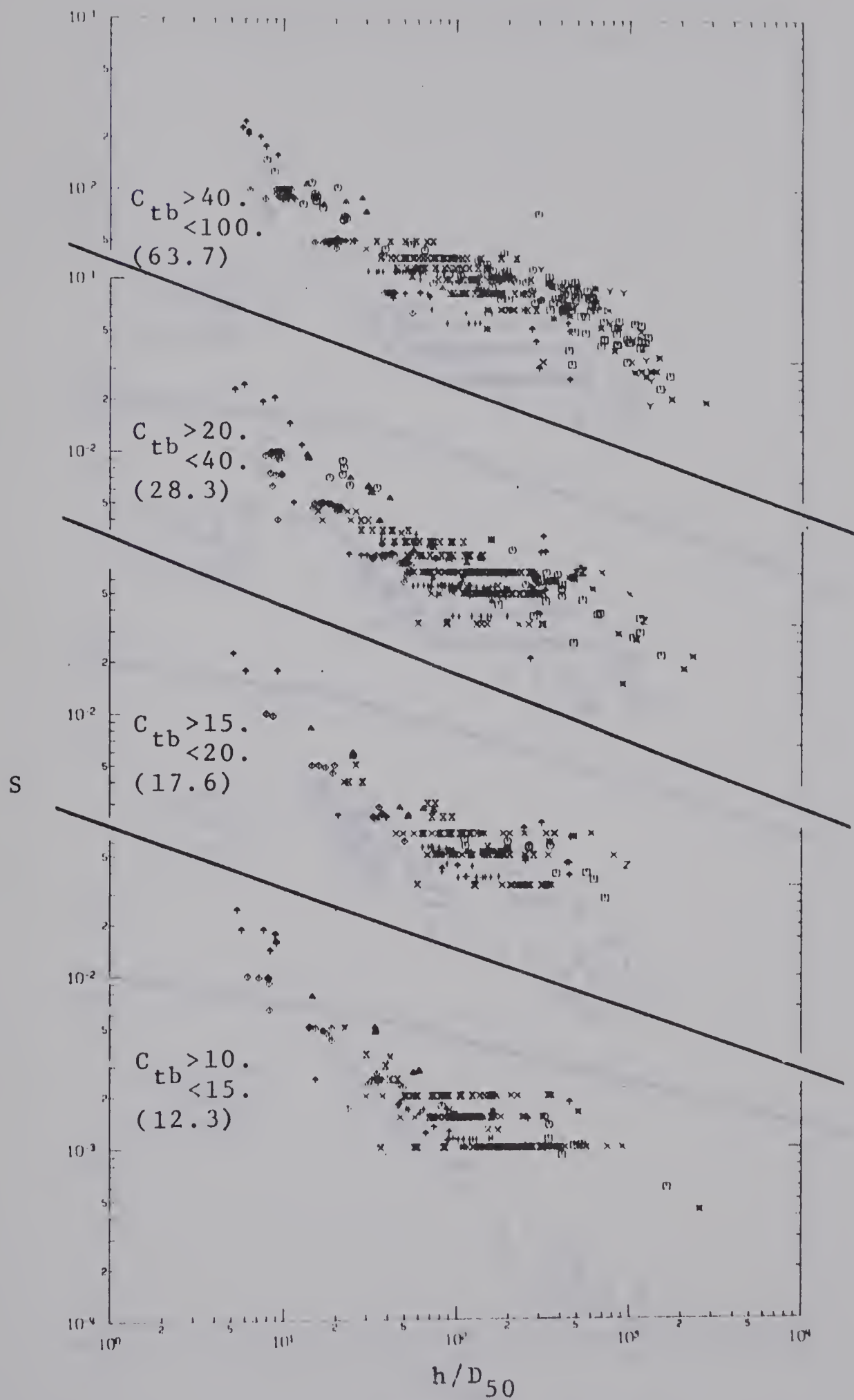


Figure D-6 (Continued)



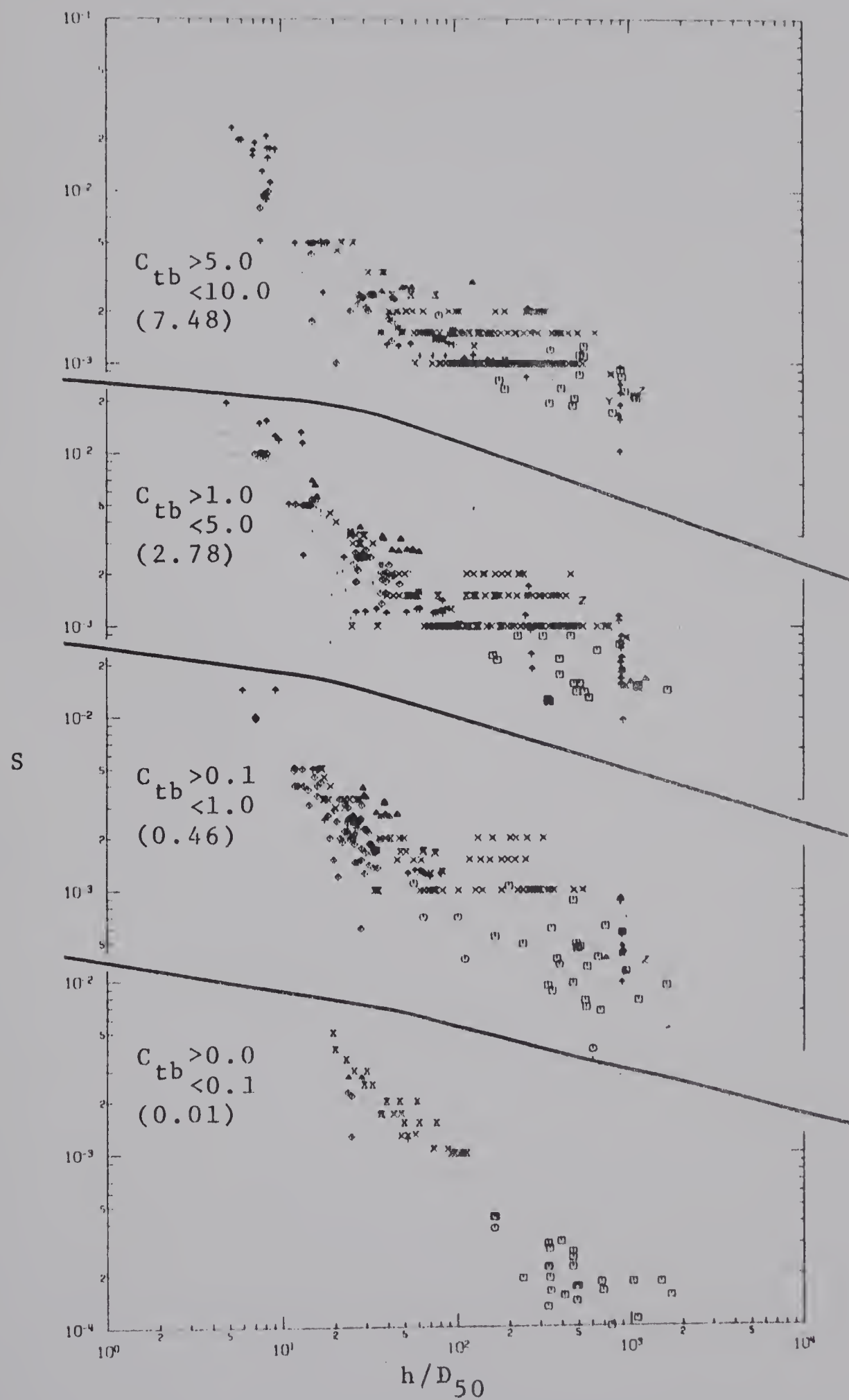


Figure D-6 (Continued)







**B29944**